UNCLOGGING THE ZINC SINK: EXAMINING THE ROLE OF ZINC TRAFFICKING IN MUCOLIPIDOSIS TYPE IV AND LYSOSOMES

by

Ira Kukic

B.S., University of Virginia, 2009

Submitted to the Graduate Faculty of

the Dietrich School of Arts and Sciences in partial fulfillment

of the requirements for the degree of

Doctor of Philosophy

University of Pittsburgh

2014

UNIVERSITY OF PITTSBURGH

DIETRICK SCHOOL OF ARTS AND SCIENCES

This dissertation was presented

by

Ira Kukic

It was defended on

April 4th, 2014

and approved by

Paula Grabowski, Professor and Chair, Department of Biological Sciences

Jon P. Boyle, Assistant Professor, Department of Biological Sciences

Michael Grabe, Assistant Professor, Department of Biological Sciences

Patrick H. Thibodeau, Assistant Professor, Department of Cell Biology

Dissertation Advisor: Kirill Kiselyov, Associate Professor, Department of Biological Sciences

UNCLOGGING THE ZINC SINK: EXAMINING THE ROLE OF ZINC TRAFFICKING IN MUCOLIPIDOSIS TYPE IV AND LYSOSOMES

Ira Kukic, PhD

University of Pittsburgh, 2014

Zinc is an essential micronutrient that regulates many cellular processes. Deficits or excessive abundance in zinc concentration have catastrophic consequences for organisms and have been linked to many human diseases. Consequently, intracellular zinc levels are kept within narrow limits by an orchestrated network of zinc binding proteins and transporters. Within the cell, zinc accumulates in virtually all organelles, including lysosomes, which break down cellular waste materials. Lysosomes have recently become the focus of zinc regulation, as they have been shown to absorb zinc from the cytoplasm and contribute to zinc-induced toxicity. Additionally, recent evidence of zinc permeability of the lysosomal ion channel TRPML1, and the evidence of abnormal zinc levels in cells deficient in TRPML1, suggested a role for TRPML1 in zinc transport. Mutations in TRPML1 in humans result in a neurodegenerative lysosomal storage disorder called Mucolipidosis type IV (MLIV) characterized by psychomotor and mental retardation.

I have found that an siRNA-driven TRPML1 knockdown in HeLa cells leads to the buildup of enlarged cytoplasmic and lysosomal vesicles filled with zinc via live cell confocal imaging. Also, lysosomal enlargement and zinc buildup in TRPML1-deficient cells exposed to zinc are ameliorated by knocking down the lysosomal zinc importer ZnT4. This data provides important insights into the function of TRPML1 and the role of zinc in MLIV and other neurodegenerative diseases. Moreover, I have found that lysosomes, generally, play a

cytoprotective role during exposure to extracellular zinc, which requires lysosomal acidification and exocytosis. Specifically, inhibition of lysosomal function with bafilomycin redistributed zinc pools to other organelles and increased cell death. Furthermore, inhibition of lysosomal exocytosis through knockdown of lysosomal SNARE proteins VAMP7 and SYT7 suppressed zinc secretion. VAMP7 knockdown increased apoptosis. Interestingly however, the overexpression of the lysosomal biogenesis transcription factor TFEB increased zinc secretion, suggesting that zinc secretion correlates with lysosomal function. Overall, these data underscore a role for TRPML1 and lysosomes in zinc metabolism and suggest that lysosomes form a "zinc sink" to dynamically buffer and counteract high zinc levels. This is a novel paradigm that implicates lysosomes in an entirely new function and identifies a completely new zinc detoxification pathway.

TABLE OF CONTENTS

LIST OF FIGURES

PREFACE

I would first and foremost like to thank my thesis advisor, Dr. Kirill Kiselyov, for his guidance and support throughout my graduate years. Thank you for believing in me and pushing me to grow as a scientist and person. I am also extremely thankful to my committee members for being so generous with their time, advice and guidance. I would also like to thank past and current members of the Kiselyov lab for interesting conversations and assistance with experiments, especially Grace Farber who was instrumental in setting me up when I joined the lab. Additionally, I would like to thank everyone in the Biological Sciences department: the main office staff (especially Cathy Barr), the fiscal office staff, Tom Harper, my teaching mentors (Drs. Alison Slinskey Legg and Valerie Oke), and my fellow graduate students who have made grad school bearable, fun and an adventure (sometimes literally)!

Most importantly, I would like to thank my parents and sister for their unwavering love, support and encouragement. None of my accomplishments could have been possible if it were not for your sacrifices, your happiness for me and the knowledge that my success is your success. Lastly, I would especially like to thank my better half. Thank you for sharing the highs and lows with me, for your laughter, love and encouragement and for making me a better person.

I could not have done it without you! Thank you!

1.0 INTRODUCTION

1.1 OVERVIEW

Zinc is an essential nutrient for all organisms and is required for almost all aspects of cell physiology. Deficits in zinc content or excessive abundance in zinc concentration have catastrophic consequences for organisms and have been linked to many human diseases. Thus, cells maintain zinc concentrations within very narrow limits through a precise and highly regulated system that controls zinc abundance and distribution. The vast number of zinc-binding proteins reflects the complexity of zinc homeostasis and transporters found in every cell compartment. However, given its physiological importance, it is surprising that many aspects of zinc function and regulation are still not very well understood. For example, it is still not known why or how zinc enters and leaves certain cell compartments such as the mitochondria or lysosomes, and whether this transport is physiologically important. Moreover, the lysosome is generally depicted as the degradative compartment of the cell, and yet there are a large number of metal transporters found on the lysosomal membrane, suggesting that they also regulate metal homeostasis. What remains puzzling is why lysosomes have been shown to take up large quantities of zinc. My thesis research investigates the role of lysosomes, and specifically, the lysosomal protein TRPML1, in regulating cellular zinc levels. As such, this chapter focuses on the current knowledge of zinc homeostasis, lysosomal functions, and TRPML1 function.

1.2 ZINC REGULATION AND PHYSIOLOGICAL REQUIREMENTS

Zinc (Zn^{2+}) is an essential micronutrient and the most abundant trace element in cells. It is required for many different processes including transcription, enzymatic activity, and cell signaling. However, excess Zn^{2+} is also toxic and has been associated with many pathological conditions, thus necessitating careful regulation of Zn^{2+} levels for proper cell function. Additionally, a growing body of evidence indicates that just like Ca^{2+}, Zn^{2+} pools are redistributed for cellular needs, identifying Zn^{2+} as "the Ca^{2+} of the twenty-first century" [1]. Here I will briefly describe the orchestrated network responsible for regulating Zn^{2+} homeostasis as well as why this is important.

1.2.1 Cellular zinc levels.

A bioinformatics study on the human genome showed that roughly 10% of proteins (about 2800 gene products) bind Zn^{2+} [2]. Zn^{2+} binds to and is required for the function of many proteins including enzymes, transcription factors, receptors, growth factors and cytokines, emphasizing its broad physiological relevance [3]. For example, Zn^{2+} is required in the nucleus for gene transcription, where it forms a "zinc finger" DNA binding motif in TFIIIA, by arranging in a tetrahedral coordination complex with the conserved cysteine and histidine residues [4]. Zn^{2+} is also required in the mitochondria for ATP production [5], in the Golgi for enzyme activation [6], and in the lysosome for enzyme maturation [7]. Interestingly, free or labile Zn^{2+} is also critical for cellular response and acts as modulator of synaptic transmission [1] and as a signaling molecule, much like Ca^{2+}, that mediates intracellular communication [8]. So, since many proteins can interact with it, control of Zn^{2+} concentration and localization is critical for

physiological responses and because of this, compartmentalized cells need Zn^{2+} transport mechanisms to accumulate and dissipate Zn^{2+} in various organelles such as the nucleus, ER, Golgi, mitochondria and lysosome. These transport mechanisms are discussed in section 1.2.2.

Although it varies from cell type to cell type, mammalian cells need a total cellular Zn^{2+} concentration of 0.1 – 0.5 mM to maintain proper functions. This concentration represents the total calculated Zn^{2+} cellular concentration, which is much higher than the one calculated for extracellular physiological content [9] (blood plasma has a free Zn^{2+} concentration of 20 pM [10]), further supporting the role and need for intracellular Zn^{2+}. Inside cells, the majority of this Zn^{2+} is bound to proteins, keeping free intracellular Zn^{2+} levels within the pM range [11]. Thus, optimal cell health and function are possible only within a very narrow range of intracellular Zn^{2+} free concentrations. More importantly, even though Zn^{2+} is the only essential transition metal to not have redox activity [12], more Zn^{2+} is prevalent in cells than any other transition metal. This poses a problem for cells since metal binding to proteins follows the Irving-Williams series for metal ion complex stability and, except for Cu^{2+}, Zn^{2+} is highly preferred over other metals [13]. This means that if intracellular Zn^{2+} concentrations are not tightly regulated, then unspecific Zn^{2+} binding would permanently take place. Not surprisingly, uncontrolled Zn^{2+} access to metalloproteins is deleterious and likely results in cell death. In sum, cytosolic free Zn^{2+} concentrations are kept within a narrow range that is optimal for proper Zn^{2+} functions, but below a threshold that would result in unspecific interactions with metalloproteins. To achieve this, cells use a combination of cytosolic Zn^{2+}–binding proteins called metallothioneins and Zn^{2+} transporters that sequester Zn^{2+} in organelles. Perturbations in this delicate balance are associated with many pathologic conditions. For example, Zn^{2+} deficiency has been associated with hormonal imbalance, immune deficiency, impaired synaptogenesis, impaired vision, learning and

memory, and seizure susceptibility, while Zn^{2+} overload has been associated with ischemic cell death, immune deficiency, oxidative stress, excitotoxicity, apoptosis and amyloid plaque formation (Alzheimer's disease) [14]. Thus, a careful Zn^{2+} balance must be achieved to maintain homeostasis.

1.2.2 Zinc transporters and metallothioneins.

Zn^{2+} uptake into cells as well as its transport into and out of intracellular organelles is orchestrated by a network of transmembrane proteins that facilitate its movement. The first Zn^{2+} transporter was identified in 1995 [15]. Since then, 24 such proteins have been described in mammalian cells, and they can be divided into two distinct families: the Zn^{2+} Transporter (ZnT, SLC30A) family and Zrt-, irt-like protein (ZIP or SLC39A) family named after the yeast Zrt1 and *Arabidopsis* Irt1 proteins. The 14 identified ZIPs control Zn^{2+} influx by importing Zn^{2+} into the cell across the plasma membrane, or by transporting it out of organelles and into the cytoplasm. The 10 identified ZnTs, on the other hand, control Zn^{2+} efflux by either transporting Zn^{2+} into organelles or exporting it out of the cell across the plasma membrane.

Most ZIPs are predicted to have eight transmembrane domains with N- and C-termini within the noncytoplasmic face of the membrane (Figure 1). ZnTs, on the other hand, are predicted to have six transmembrane domains (with the exception of ZnT5 which has nine) and N- and C- termini within the cytoplasm. Both families have a long cytoplasmic loop with a histidine-rich domain thought to facilitate Zn^{2+} binding, which is present between transmembrane domains 3-4 in ZIPs and 4-5 in ZnTs [16, 17]. A recent crystal structure of the *Escherichia coli* ZnT homologue, YiiP, confirmed these topological predictions for ZnTs and shed light on the transport mechanisms (Figure 2) [18, 19]. YiiP was found to be a Y-shaped homodimer held

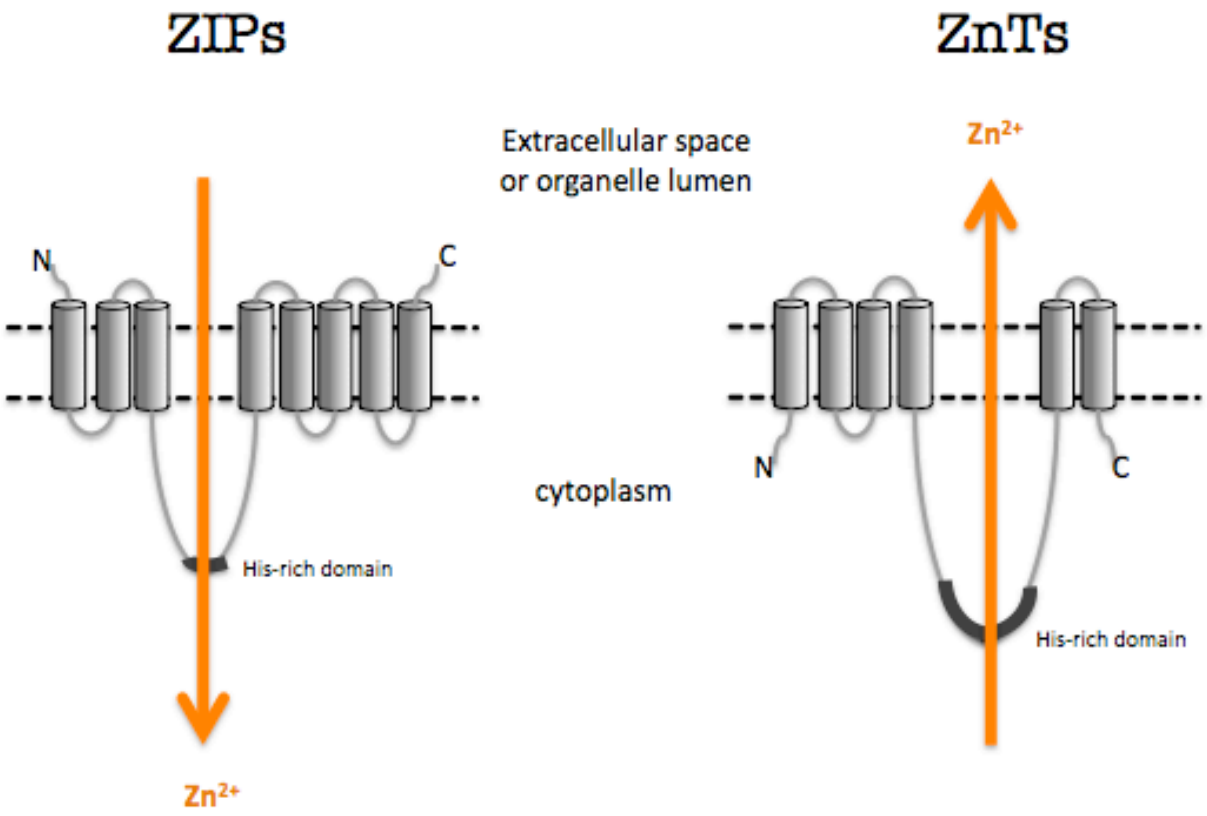

Figure 1. Predicted structures and transport mechanisms of ZIP and ZnT transporters.

Predicted topologies of ZIP (left) and ZnT (right) are shown. The histidine –rich cluster of ZIPs and the histidine-rich loop of ZnTs are indicated by the bold lines. ZIPs transport zinc from the extracellular space or intracellular compartments into the cytoplasm through an unknown mechanism. ZnTs, on the other hand, transport zinc from the cytoplasm into intracellular compartments or into the extracellular space through a Zn^{2+} / H^{+} exchange mechanism. Figure adapted from [17].

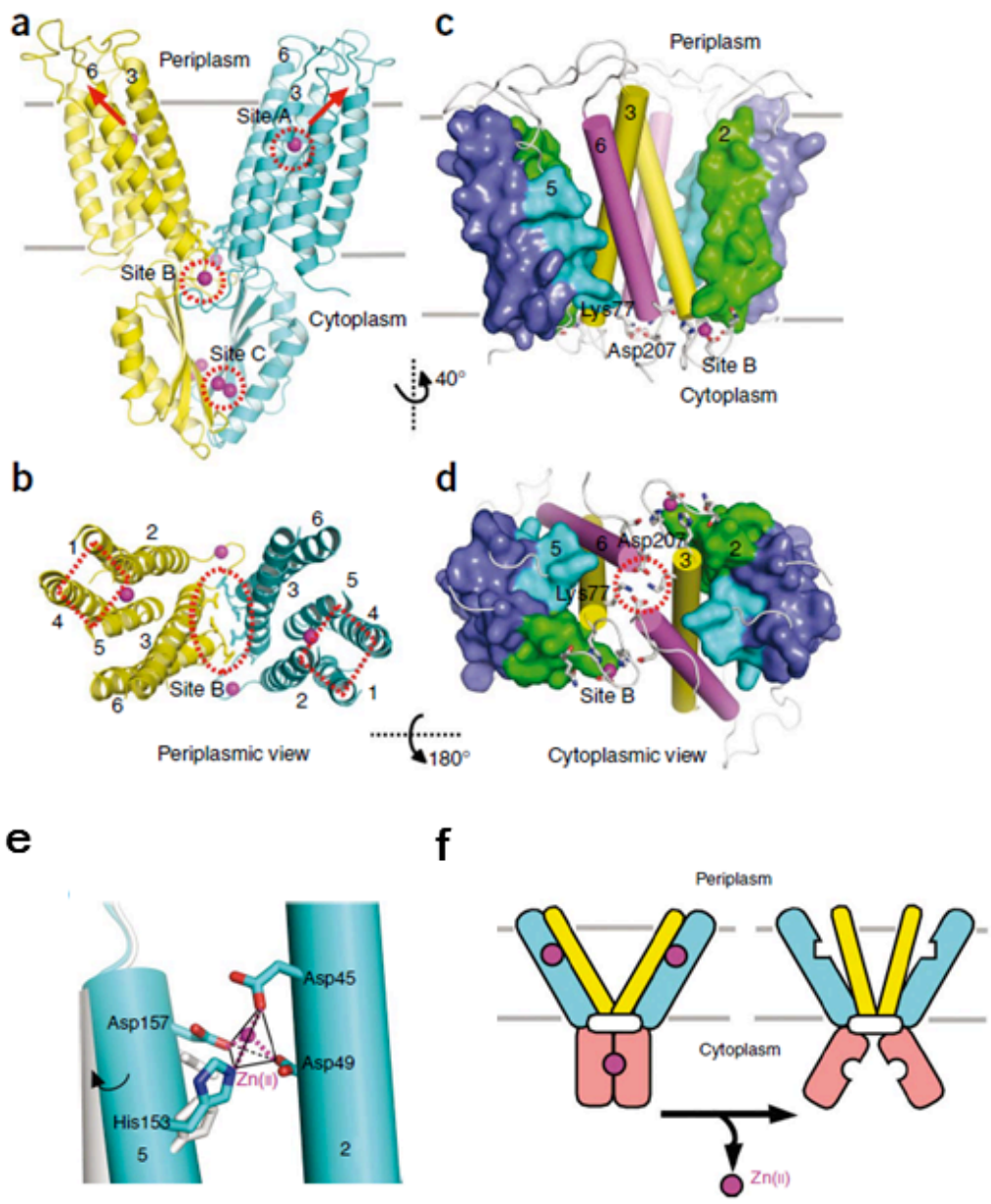

Figure 2. YiiP structure and helix packing in the TMD.

(a) Ribbon representation of the YiiP homodimer (yellow and cyan for each protomer) viewed from the membrane plane. Magenta spheres represent bound zinc ions in zinc-binding sites, which are marked by red circles. Grey lines indicate the possible membrane boundaries. Red arrows indicate the directions of Zn(II) exit from the two active sites. Conserved hydrophobic residues involved in the TMD-TMD contacts are shown as sticks. (b) The YiiP homodimer viewed from the periplasm with the extracellular loops. The red oval marks hydrophobic interactions at

the TMD-TMD interface, and red diamonds highlight the four-helix bundles. (c) Packing of the TM3-TM6 pairs in the membrane. TMDs are viewed from the membrane plane and are related to a with a 40° rotation about the dimer two-fold axis. TM3-TM6 pairs are shown in cylinder representation, whereas the four-helix bundle is shown in solvent-accessible surface. (d) The charge interlock at the dimer interface is highlighted with a red circle and viewed from the cytoplasm. (e) Regulation of coordination geometry. A close-up view of site A situated between TM2 and TM5 (cyan cylinders) with four coordinating residues (cyan sticks) in a tetrahedral arrangement (shown as a tetrahedron). The black arrow indicates a hypothesized TM5 movement (shown as a gray cylinder) with respect to TM2. (f) Schematic model for autoregulation. TM3-TM6 pairs and four-helix bundles are colored in yellow and cyan, respectively. Open boxes represent the charge interlock located at the pivotal point of the hinge-like motions. Figure adapted from [19].

together through the tetrahedral binding of four Zn^{2+} ions at the interface of the cytoplasmic domains (Figure 2) [18, 19]. Dax Fu and colleagues found that Zn^{2+} binding triggers hinge movements of two electrically repulsive cytoplasmic domains pivoting around four salt bridges located at the intersection of the cytoplasmic and transmembrane domains (TMDs) [19]. These salt bridges then interlock transmembrane helices so that they can coordinate the active site of Zn^{2+} transport [19]. Also, the cytoplasmic domain of YiiP was found to mimic the metal-binding domains of the metal-transporting P-type ATPases, which might be a modular regulatory element for transport activity [19]. Similarly, even though the exact function of the histidine-rich loop has not yet been determined, mutagenesis of the histidine residues has been shown to abolish Zn^{2+} transport activity [20, 21]. It has also been shown that the histidine residues confer metal ion selectivity [22], such as selectively transporting Zn^{2+} over cadmium (Cd^{2+}) (mammalian ZnTs have been shown to mobilize iron (Fe^{2+}), manganese (Zn^{2+}), and Cd^{2+} [16]). Nonetheless, both ZIPs and ZnTs have a histidine-rich domain that allows them pump Zn^{2+} either out of (in the case of ZIPs) or into (in the case of ZnTs) organelles. Not surprisingly then,

because of their function, most ZIPs are found on the plasma membrane while most ZnTs are found in intracellular compartments [23]. Subsequently, ZnTs are known to function as Zn^{2+}/ H^{+} exchangers, and when reconstituted into proteoliposomes, the bacterial ZnT homologue, ZitB, confirms this mechanism [24]. Additionally, many ZnTs localize to acidic vesicular compartments [16] and there is some evidence that the low pH is necessary for Zn^{2+} binding and transport activity [24, 25]. At the same time, while the transport mechanism for ZIPs has not yet been clarified and structural data are lacking, it has been proposed that they function either as electrodiffusion channels, or HCO_3^- symporters [16]. One recent study using the *Bordatella bronchiseptica* ZIP homologue, ZIPB, showed that ZIPB is a selective electrodiffusion channel with an unsaturable Zn^{2+} flux (no evidence of saturation up to an extracellular Zn^{2+} concentration of 2mM) [26], but whether this applies to other ZIPs remains to be seen.

In addition to Zn^{2+} transporters, intracellular and specifically, cytoplasmic Zn^2 levels are also controlled by metallothioneins (MTs). MTs are small, cysteine rich proteins that bind Zn^{2+} with high affinity. They were first discovered in 1957 as cadmium (Cd^{2+})-binding proteins from horse kidney samples that were high in metal and sulfur content [27]. Since then, MTs have been shown to be instrumental in metal ion homeostasis, detoxification of toxic metals, and protection against allergic inflammation and oxidative stress [11]. Mammalian MTs are encoded by a multigene family that consists of 10 functional genes including 7 MT-1 genes (MT-1A, -B, -E, -F, -G, -H, and –X) in addition to the MT-2A, MT-3 and MT-4 genes [28-31]. MT-1 and MT-2 are ubiquitously expressed [32, 33], MT-3 is primarily expressed in the central nervous tissue [1, 34], and MT-4 is expressed in stratified squamous epithelial tissues [30]. In addition to Cd^{2+} and Zn^{2+}, MTs have binding affinities for other metals as follows: $Hg^{2+} > Cu^{2+} > Cd^{2+} > Zn^{2+}$ [35, 36]. Mammalian MTs have a dumbbell-shaped conformation consisting of two structural

domains: an α–domain that has 11 cysteine residues and can bind 4 Cd^{2+} or Zn^{2+}, or 6 Cu^{2+} ions, and a β–domain that has 9 cysteine residues and can bind 3 Cd^{2+} or Zn^{2+}, or 6 Cu^{2+} ions [11]. Of the 61-68 amino acids that make up MTs, 20 are highly conserved cysteines that allow them to bind up to 7 Zn^{2+} atoms per molecule, with an overall binding affinity of up to 10^{-13} M [11, 37]. It has also been shown that MTs assume a donor/ acceptor role for other Zn^{2+} binding proteins in order to influence key cellular processes such as transcription, proliferation, differentiation, signal transduction and apoptosis [38, 39].

Mouse knockout studies have demonstrated the importance of MTs in Zn^{2+} homeostasis. For example, MT-null mice lacking the MT-1 and MT-2 genes fed Zn^{2+} deficient diets had delayed kidney development compared to their wild-type littermates, likely due to a decreased hepatic reservoir of Zn^{2+} needed for development [40]. At the same time, MT-null adult mice exposed to increased Zn^{2+} were predisposed to pancreatic acinar cell degeneration [40]. These data demonstrate that MTs are critical for protecting organisms against both Zn^{2+} deficiency and excess, and necessary for accommodating Zn^{2+} influx. These results are not entirely surprising since the expression of MT-1 and MT-2 is ubiquitous, but exceptionally high in the intestine, pancreas, kidney and liver [40]. However, the most widely studied role of MTs is their ability to protect *in vitro* and *in vivo* against reactive oxygen species (ROS) due to their high thiol content. For example, in mouse models where MT is overexpressed in cardiac tissue, MT inhibits ischemia-reperfusion induced myocardial injury and apoptosis [41, 42]. It has also been shown that MT expression is upregulated by ROS through antioxidant response elements (AREs) within their promoter region [43]. Additionally, MTs have been shown to act as reducing agents and antioxidants. It is proposed that ROS oxidizes the normally Zn^{2+}–bound MT, causing it to release Zn^{2+} [44, 45]. Evidence from this comes from nitric oxide studies. Nitric oxide increases

intracellular Zn^{2+} levels through the oxidation of Zn^{2+}–MT in mouse lung fibroblasts [46]. Further supporting this idea, H_20_2 exposure has also been shown to release Zn^{2+} in cell free and cell culture studies [47-49]. The released Zn^{2+} then binds to MTF-1, which will upregulate MTs and ZnTs, and restart the cycle (see below). Lastly, through their antioxidant activity, MTs may also protect cells against allergic inflammation by suppressing inflammatory cytokines [50], which, if impaired, cause severe inflammatory responses in multiple sclerosis and *Helicobacter*-induced gastritis [51-53]. Together, these data highlight the importance of MT function in many different biological processes and disorders.

1.2.3 Transcriptional regulation of ZnTs and ZIPs.

The expression of many ZnT and ZIP transporters is regulated transcriptionally as well as postranscriptionally. In higher eukaryotes ranging from insects to mammals, some transporters and MTs are transcriptional targets of the Zn^{2+}–sensing, metal-response-element-binding transcription factor-1 (MTF-1). MTF-1 regulates the metal-dependent induction of gene expression in response to heavy metal toxicity, ionizing radiation and oxidative stress [54-58]. Often times, MTF-1 is referred as a Zn^{2+} sensor because of its nanomolar affinity for Zn^{2+} [59]. The reason behind this high affinity is that MTF-1 has a metalloregulatory DNA-binding domain that has 6 Cys_2His_2 zinc fingers that allow it to bind to Zn^{2+} with very high affinity [60, 61]. Under basal conditions, MTF-1 is localized within the cytoplasm, however, upon a transient increase in cytoplasmic Zn^{2+}, MTF-1 binds to Zn^{2+} and translocates to the nucleus to activate the expression of Zn^{2+}–responsive genes [62-65]. For example, in mammals, MTF-1 protects against Zn^{2+} toxicity by increasing the expression of MT-1 and MT-2 [66] as well as lowering cytoplasmic Zn^{2+} levels by upregulating the expression of ZnT1, the Zn^{2+} efflux transporter

localized to the plasma membrane [57]. Thus far, MTF-1 inducible targets include MT genes, ZnT1, and the glutamate-cysteine ligase heavy chain (γGCS_{hc}) that codes for an oxidative stress protein [67], but MT induction is the best studied. Some of the stimuli that induce MT gene induction include: metal ions Zn^{2+}, Cd^{2+}, and Cu^{2+}, and chemical agents diethylmaleate, paraquat, nitric oxide, hydrogen peroxide and cytokines [68-75]. The transcriptional induction of MT and other MTF-1 target genes depends on the highly conserved metal response element (MRE) consensus sequence (5'-TGCRCnCGGCCC-3') found within the promoters of such genes [76-80]. Interestingly, although MTF-1 knockout in mice is lethal, it has not been shown that MTF-1 regulates the expression of other ZnTs or ZIPs, potentially due to a redundant pathway. Multiple levels of MTF-1 functional regulation have been found; including nuclear translocation, DNA-binding, posttranslational modification through phosphorylation, and interactions with other factors. Additionally, a recent report showed that a single-nucleotide within the MRE consensus sequence can affect MTF-1 transcriptional activation. For example, given that the core (Zn^{2+}) MRE is TGCRCNC, the Cu^{2+} MRE is TGCACRCG, while the Cd^{2+} MRE is TGCACYCG [81], indicating that the cells can sense the specific challenge they are exposed to and can respond accordingly.

To date, the transcription factor regulating ZIP expression, that responds to Zn^{2+} deficiency, has not yet been identified in mammals. However, it has been identified in *S. cerevisiae*, as Zn^{2+} -responsive activator protein-1 (Zap1) [82-84]. Under Zn^{2+} deficient conditions, Zap1 upregulates the expression of 3 ZIPs: ZRT1, ZRT2, and FET4 [82-84]. Zap1 also induces Zn^{2+} release from vacuolar stores by activating the expression of the vacuolar ZIP, ZRT3 [85]. Lastly, Zap1 has also been shown have some features in common with MTF-1 (such as transactivating domains, and DNA-binding domains with Cys_2His_2 zinc finger motifs) as well

as to induce the expression of 43 other genes, some of which also participate in Zn^{2+} homeostasis [86]. While a homologue for Zap1 has not yet been identified for multi-cellular organisms, some Zn^{2+} transporters, such as ZIP6 and ZnT2, have been shown to be regulated by signal transducers and activators of transcription 3 (STAT3) [87] and STAT5 [88], respectively, suggesting that different signaling cascades converge on the transcriptional control of Zn^{2+} transporters. These transcriptional control mechanisms likely reflect cell type-specific functions and signaling events.

1.2.4 Subcellular localization of zinc transporters.

To understand metal ion homeostasis, one first has to understand how the subcellular localization of the transport machinery. The first Zn^{2+} transporter identified was ZnT1. It was cloned in 1995 and identified in baby hamster kidney (BHK) cells that were growing in very high (300 μM) extracellular Zn^{2+} concentrations [15]. When normal BHK cells were transfected with ZnT1 cDNA, they grew in high Zn^{2+} concentrations, all the while keeping intracellular Zn^{2+} concentrations low [15]. Another study found that the mRNA expression of ZnT1 was upregulated in response to high Zn^{2+} exposure in rat hippocampal neurons that this upregulation is often associated with neuronal death [89] (discussed further in section 1.3). From these and other studies, ZnT1 was identified as a Zn^{2+} efflux transporter that localizes to the plasma membrane and mediates Zn^{2+} efflux from the cytoplasm to prevent toxic accumulation of Zn^{2+} (Figure 3). Similarly, the primary uptake system for cellular Zn^{2+} is the ZIP family of transporters. Of the 14 ZIPs identified, ZIP1 is ubiquitously expressed and upregulated by Zn^{2+} deficiency [90]. In basal conditions, ZIP1 has been shown to localize to intracellular compartments, but in Zn^{2+}-deficient conditions, ZIP1 has been shown to migrate to the plasma

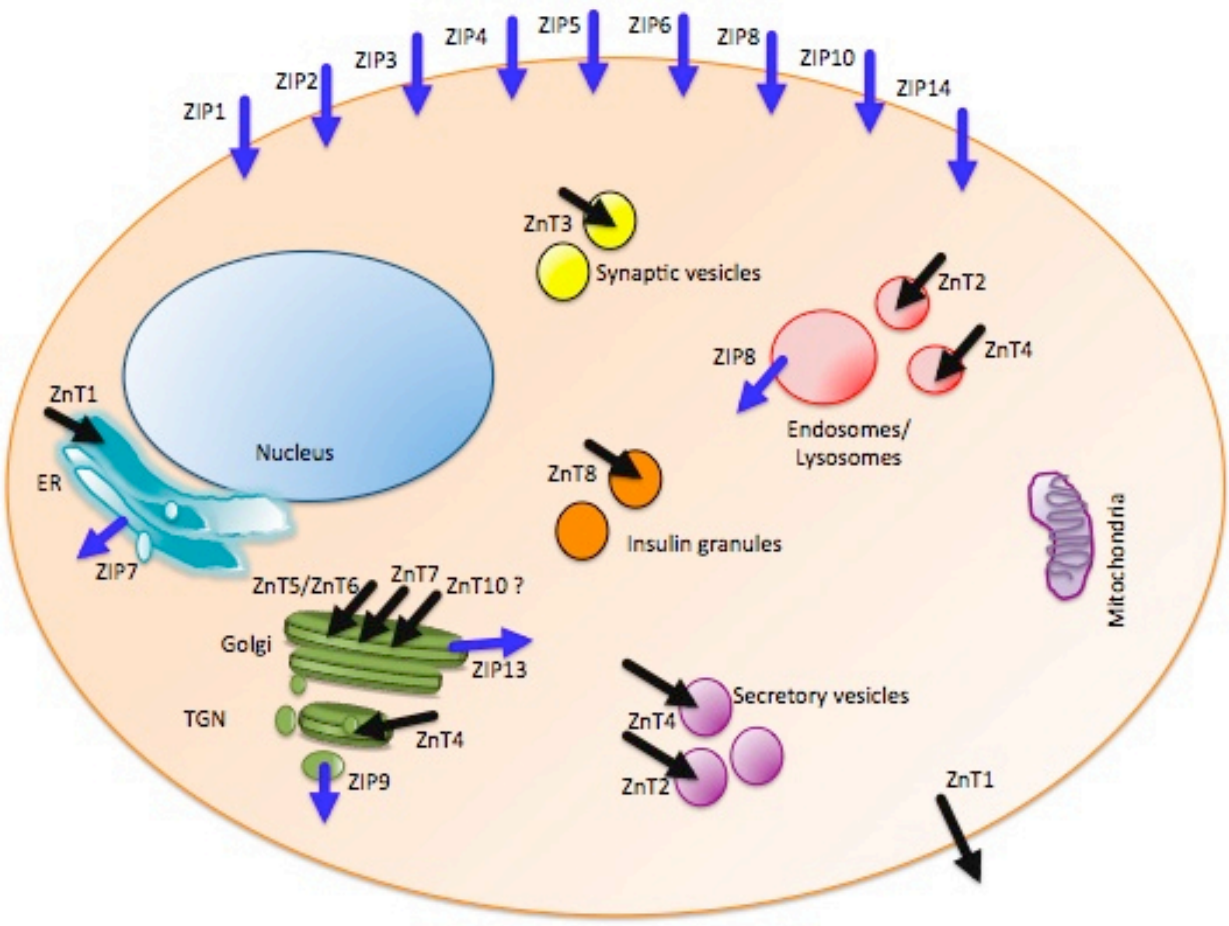

Figure 3. Subcellular localization of ZIP and ZnT transporters.

The localization and direction of zinc mobilization by ZIPs (blue arrows) and ZnTs (black arrows) are shown according to current information available. Extracellular zinc is taken up by ZIP transporters localized at the plasma membrane, while cytoplasmic zinc is transported by ZnTs into the secretory compartments such as the ER and the Golgi, endosomes/ lysosomes, synaptic vesicles in the brain or insulin granules of pancreatic β-cells. This diagram depicts a static view of ZIP and ZnT localization, as they have been shown to change their subcellular localization in a cell-specific, developmentally regulated, and zinc-dependent manner. Additionally, in polarized epithelial cells, ZIP4, ZIP8, and ZIP14 localize to the plasma membrane, while ZIP5 has been shown to localize to the basolateral membrane. TGN, trans-Golgi network. To this date, the subcellular localization of ZnT9, ZIP11 and ZIP12 has not been identified. Figure adapted from [91].

membrane to mediate Zn^{2+} uptake [92]. Since then, other ZIPs were also found to be important for Zn^{2+} uptake. ZIP3 has been shown to be important for Zn^{2+} uptake in mammary epithelial cells [93]. ZIP4 has been found to regulate dietary Zn^{2+} absorption and is mutated in acrodermatitis enteropathica (AE) [94], a recessive disorder characterized by dermatitis, hair loss and diarrhea. Additionally, ZIP5 has been implicated in Zn^{2+} transport from the bloodstream into enterocytes [95], and ZIP14 has been associated with Zn^{2+} uptake in the liver in response to acute inflammation and infection [96]. Notably, most knock out models of ZIPs have abnormal embryonic development [16].

The Zn^{2+} transporters mediating Zn^{2+} transport into and out of organelles vary from cell type to cell type, but I will briefly present the most notable cases, which are summarized in Figure 3. Many organelle specific functions depend on Zn^{2+}. For example, processing of the Alzheimer's Aβ protein depends on a Zn^{2+} metalloprotease in the Golgi [97], and the packaging of insulin into secretory vesicles also depends on Zn^{2+} in the Golgi [98]. Similarly, in the ER, glycosylphosphatidylinositol phosphoethanolamine transferase (GPI-PET) depends on Zn^{2+} for its function in the biosynthesis of GPI anchors [99]. In vertebrates, ZnT5 and ZnT6 form a complex and localize to the Golgi to transport Zn^{2+} into the Golgi [100]. ZnT7 homoligomers and ZIP7 also localize to the Golgi and regulate Zn^{2+} trafficking [101, 102]. Finally, mutations in or knock out of the Golgi ZIP13 protein show delayed growth and abnormalities in hard and connective tissue development, characteristic of the Ehlers-Danlos syndrome in humans [103]. Other transporters involved in packaging Zn^{2+} into vesicles include ZnT3 in synaptic vesicles [104] (discussed further in section 1.3), ZnT8 in pancreatic β-cells [105], and ZnT4 and ZnT2 in endosomes and lysosomes. Notably, mutations in ZnT4 result in the *lethal milk (lm)* syndrome where mouse pups do not survive when nursed by lactating dams harboring mutations in ZnT4

[106]. When nursed by wild-type dams or given oral Zn^{2+} supplements, these pups do survive [107], suggesting that ZnT4 is important for Zn^{2+} secretion into milk. In sum, the complement of Zn^{2+} transporters expressed within each cell type reflects its specific function.

It is likely that these 24 Zn^{2+} transporters do not represent a complete list, since some organelles such as the mitochondria have not yet been associated with specific transporters. It is known that Zn^{2+} is required in the matrix of the mitochondria for proper function, and that labile Zn^{2+} can be detect in the mitochondria of neurons by the Zn^{2+}–responsive fluorophore, RhodZin-3 [108]. How Zn^{2+} gets in the mitochondria is not known. It was previously thought that Zn^{2+} enters the mitochondria through the Ca^{2+} uniporter system. However, recent studies in rat brain samples have shown mitochondrial Zn^{2+} accumulation that is both Ca^{2+} uniporter-dependent and Ca^{2+} uniporter-independent [109]. This suggests that there are other unidentified Zn^{2+} transporters, and/ or mechanisms for Zn^{2+} trafficking in cells.

1.3 ZINC HOMEOSTASIS AND NEURODEGENERATIVE DISORDERS

In 1955, Maske discovered Zn^{2+} -dithizonate staining in rat hippocampal slices [110]. Since then, it has been well established that Zn^{2+} is selectively stored in and released from presynaptic vesicles within neurons of the cerebral cortex [1]. The concentration of Zn^{2+} within these vesicles can reach millimolar levels [111-113]. The term “gluzinergic” has been used to describe these neurons because in addition to Zn^{2+}, they also release glutamate [114]. Since 1955, our knowledge of the neurobiology of Zn^{2+} has vastly expanded. Overall, through its effects on glutamate and γ–aminobutyric acid (GABA) receptors, Zn^{2+} has been found to modulate the excitability of neurons and to play a key role in synaptic plasticity [14, 115]. Here I will briefly

describe Zn^{2+} signaling in normal function as well as in pathophysiology of acute brain damage and neurodegenerative diseases.

1.3.1 Gluzinergic neurons and synaptic zinc release.

Due to the prevalence of gluzinergic neurons, synaptically released Zn^{2+} has been implicated in neurogenesis, neuronal migration, synatogenesis, motor coordination, memory formation, and olfactory and vision processing [14]. Consistent with its essential role, Zn^{2+} deficiency, chelation, or genetic Zn^{2+} absorption disorders have been associated with pain, impaired vision and spatial learning, memory deficits and loss of taste and smell [14]. These studies emphasize the necessary levels of Zn^{2+} that are needed for normal brain function.

Zn^{2+} entry into neuronal somata and dendrites occurs through the Zn^{2+}–permeable, gated channels such as the *N*-methyl-D-aspartate (NMDA) channels and the voltage-gated, Ca^{2+}-permeable α–amino-3-hydroxy-5-methyl-4-isoxazole propionic acid (AMPA) channels [116, 117]. In the presynaptc terminal, Zn^{2+} is packaged into synaptic vesicles through ZnT3 along with glutamate and is released into the synaptic cleft through exocytosis. Once at the postsynaptic terminal, Zn^{2+} can enter cells through Zn^{2+}–permeable glutamate transporters and channels. Zn^{2+} has been shown to inhibit both the NMDA-type glutamate ionophore [118] and the GABA type A ($GABA_A$) receptor [119]. Not surprisingly then, this high amount of Zn^{2+} translocation has been associated with excitotoxic, Zn^{2+}–induced cell injury [120]. One of the major reasons for this cell injury is the Zn^{2+} released from MT-3 due to nitrosylation of oxidation of the thiol ligands [121, 122]. In fact, MT-3 knockout mice have significantly reduced cell injury in the thalamus and hippocampal field CA1 [120]. However, at the same time, lack of

MT-3 in hippocampal field CA3, increased cell death after excitotoxic injury, suggesting that postsynaptic MT-3 functions as a both a cytoprotective Zn^{2+} sink and a source of toxic free Zn^{2+}.

Although Zn^{2+} lacks redox activity, it has been shown that free ionic Zn^{2+} is toxic. Neuronal injury and death have been observed after a 15-minute exposure to 300 – 600 μM Zn^{2+} in cortical cell culture [123], as well as after a 5-minute exposure to 100 μM Zn^{2+} following depolarization with high potassium [124]. This neurotoxicity likely results from Zn^{2+} and Ca^{2+} influx through L-type, NMDA and AMPA/kainite channels. Subsequently, Zn^{2+} toxicity has also been observed *in vivo* following seizures or transient cerebral ischemia [125], focal ischemia [126], and traumatic brain injury [127]. Nevertheless, the source of the toxic Zn^{2+} in degenerating neurons is still debated. Even neurons from ZnT3 knockout mice had extensive Zn^{2+} accumulation [128], indicating that other sources beside presynaptic Zn^{2+} affect toxicity. For example, other sources of Zn^{2+} contributing to toxicity could come from Zn^{2+} mobilized from MT-3, or from the mitochondria [129].

Several lines of evidence indicate that Zn^{2+} toxicity is largely due to oxidative stress. Zn^{2+}-induced cell death is often associated with the production of superoxides and lipoperoxides [130], and attenuated with antioxidants [131]. The exact mechanism of Zn^{2+}–induced cell death is not entirely clear and varies depending on Zn^{2+} concentration and cell type used, but a few pathways have been identified. When cells are treated with lower Zn^{2+} concentrations, DNA fragmentation and caspase activation, indicative of apoptosis, have been observed [131, 132]. However, when cells are treated with higher Zn^{2+} concentrations, cell body swelling, and organelle destruction have been observed, indicative of necrosis [130]. Apoptotic cell death seems to involve induction of the neutrophin receptor $p75^{NTR}$ and $p75^{NTR}$-associated death executor (NADE), as well as the release of cytochrome C and apoptosis-inducing factor (AIF)

from the mitochondria [133, 134]. While necrotic cell death involves the activation of the poly-ADP-ribose polymerase-1 (PARP-1) pathway [135].

1.3.2 Zinc and neurodegenerative disorders.

Zn^{2+} has been both directly and indirectly implicated in many neurological diseases including Alzheimer's disease, amyotrophic lateral sclerosis (ALS), depression, epilepsy, ischemia and schizophrenia [14]. Here I will briefly review Zn^{2+} dysregulation in Alzheimer's and ALS, as well as discuss therapeutic strategies.

Aberrant homeostasis has been linked to β–amyloid aggregation, characteristic of Alzheimer's disease (AD). Presenilin, the enzyme responsible for cleaving β–amyloid precursor protein (APP), and the enzyme mutated in Alzheimer's has been implicated in Zn^{2+} clearance [136]. Other AD-associated enzymes such as APP, tau and BACE have metal-binding properties, suggesting that metal homeostasis might be the key mechanism driving AD [137]. Moreover, neuritic plaques and cerebrovascular amyloid deposits from AD patients were found to have high Zn^{2+} concentrations [138] and Zn^{2+} co-purifies with β–amyloid from post-mortem brains [139]. Interestingly, Zn^{2+} and Cu^{2+} chelators reversed synthetic Aβ aggregation *in vitro* [140] and reduced amyloid deposits in post-mortem brain tissue from patients [141]. Furthermore, evidence from ZnT3 knock down in a mouse model of Alzheimer's disease showed that synaptic Zn^{2+} release is one of the major insults leading to pathology. Specifically, mice lacking ZnT3 and therefore synaptic vesicle Zn^{2+}, had fewer β–amyloid plaques [142].

Mutations in the Cu^{2+}/ Zn^{2+} superoxide dismutase (SOD1) enzyme are associated with familial amyotrophic lateral sclerosis (ALS, also known as Lou Gehrig's disease). SOD1 is a

ubiquitously expressed enzyme that binds Zn^{2+} [143]. Gain of function mutations in SOD1 have been associated with motor neuron injury due to increased peroxidase activity and aberrant free radical handling, leading to excitotoxicity [144, 145]. Additionally, some SOD1 mutant proteins have decreased Zn^{2+}, but increased Cu^{2+} affinity, leading to the generation of peroxynitrate and toxicity-induced neuronal death [146, 147]. Furthermore, metallothionein expression is upregulated in brain and liver tissue of ALS patients. Specifically, MT-1, MT-2 and MT-3 expression is increased in astrocytes, and MT-3 in neurons [148]. Lack of MT-1, MT-2 or MT-3 has been shown to accelerate the onset of symptoms and to shorten life time, consistent with MTs' protective role in preventing the buildup to toxic levels [149].

Clearly then, Zn^{2+} homeostasis is an integral part of normal brain function. The therapeutic strategies employed in treating excess free Zn^{2+}, such as in Alzheimer's or ALS, have to maintain physiological Zn^{2+} concentrations in order to maintain proper function. Any therapies leading to too much or not enough intracellular Zn^{2+}, will likely result in devastating cell death. As such, metal chelating drugs have been used, but more knowledge on Zn^{2+} homeostasis is needed to fully develop therapeutic approaches. For example, the quinoline compound, clioquinol has been shown to bind Zn^{2+} in the mid-nanomloar range and has been used to reduce amyloid plaques and slow cognitive decline in Alzheimer's patients [150]. Another therapeutic agent used was pyruvate. Pyruvate has been shown to protect against Zn^{2+}–induced cell death in cortical and oligodendrocyte progenitor cultures, in addition to preventing Zn^{2+} accumulation in the brain [89, 151]. It is likely that studying Zn^{2+} release, channels and transport will prove important in designing new drug targets for treating many neurological disorders.

1.4 LYSOSOMAL BIOGENESIS AND FUNCTION

With the exception of erythrocytes, lysosomes are found in all eukaryotic cells and are the major digestive compartment within cells. Lysosomes are intracellular organelles with an acidic interior, which contains roughly 25 specific membrane proteins [152] and 60 resident hydrolases [153]. Christian de Duve first described lysosomes in a series of centrifugal fractionation experiments in the 1950s [154-156] that resulted in a Nobel Prize. Since then, lysosomes have been recognized as advanced organelles that are involved in many cellular processes and crucial regulators of cell homeostasis.

Insides cells, lysosomes appear as dense bodies in the cytoplasm [157], most often in a perinuclear pattern that constitutes up to 5% of the intracellular volume. Lysosomal size and number can vary drastically due to undigested material, for example, lysosomes are typically 1 μm in diameter [157, 158]. They are enclosed by a single 7-10 nm phospholipid-bilayer [159], high in carbohydrate content due to the heavily glycosylated lysosomal membrane proteins [160], lysosomes have a pH of 4.5-5.0 [161]. Although this provides an optimal condition for the multitude of resident hydrolases and the degradation of all types of macromolecules, it also creates a challenge for lysosomal membrane proteins to not be degraded. To protect the membrane from the lytic enzymes found within, lysosomal membrane proteins are heavily glycosylated at their luminal domains to form a glycocalyx [160], and the inner membrane is rich in phospholipid bis(monacylglycero)-phosphate (BMP), also known as lyso-bis-phosphatidic acid (LBPA) [162]. This regulation and maintenance of this special lysosomal environment is necessary for cell survival. Yet, when this environment is perturbed, it results in several diseases called lysosomal storage disorders. The following sections will discuss the transcriptional control

of lysosomal genes, biosynthesis and delivery of lysosomal proteins, and how lysosomes attain, degrade and expel material.

1.4.1 Regulation of lysosomal biogenesis.

Until recently, the molecular machinery regulating lysosomal biogenesis remained unknown. However, in 2009, Sardiello et al. discovered that genes encoding lysosomal proteins had a GTCACGTGAC sequence within their promoters that they called the coordinated lysosomal expression and regulation (CLEAR) sequence [163]. They showed that transcription factor EB (TFEB), a member of the microphatalmia and basic helix-loop-helix leucine-zipper family of transcription factors, directly binds to CLEAR elements in lysosomal genes, thereby promoting their expression [164, 165]. Cells overexpressing TFEB showed that TFEB translocates to the nucleus after lysosomal stress, binds to CLEAR sequences, and leads to the generation of more lysosomes which can more effectively degrade lysosomal and autophagy substrates [163, 166]. Furthermore, TFEB regulates the biogenesis of autophagosomes, the fusion of autophagososmes with lysosomes, and autophagic flux. More recently, Palmieri et al, were able to combine microarray, deep sequencing of TFEB chromatin immunoprecipitate, genomic and expression data to identify over 500 TFEB target genes, solidifying TFEB's role as a master regulator of lysosomal function [164, 165]. More recently, Martina et al., discovered that another transcription factor, transcription factor E3 (TFE3), also induces the expression of genes involved in autophagy and lysosomal biogenesis, but in response to nutrient status [167], indicating that cells are able to actively monitor lysosomal function and respond to degradative as well as environmental needs.

Once lysosomal genes are transcribed, the sorting of lysosomal proteins requires the integration of the biosynthetic and endocytic pathways. Newly translated lysosomal proteins are synthesized as N-glycosylated precursors and most soluble acid hydrolases obtain a mannose-6-phosphate (M6P) recognition marker in the *cis*-Golgi which is recognized by the mannose-6-phosphate receptor (M6PR) in the trans-Golgi network (TGN) [168, 169]. The M6PR-bound hydrolases are first delivered to endosomes [170, 171] where due to the slightly acidic luminal pH, they dissociate from the receptors, allowing the receptors to recycle back to the TGN [172, 173] and the hydrolases to continue on to be delivered to lysosomes. Newly synthesized lysosomal membrane proteins (unlike soluble hydrolases) can either be directly transported to lysosomes through the TGN and clathrin-dependent transport of lysosomal hydrolases [174, 175], or indirectly by following the constitutive secretory pathway where they are first transported to the plasma membrane and then, through endocytosis, delivered to lysosomes.

Endocytosis starts at the plasma membrane and ends in lysosomes, with many intermediate "stations" distinguished by their molecular content, morphology and pH (Figure 4). Early endosomes (EEs) receive endogenous proteins such as M6PRs carrying lysosomal hydrolases from the TGN [170, 171], which they then sort for either recycling or degradation. Cargo without a specific targeting signal enters tubular sorting endosomes (TSEs) for recycling, while lysosomal cargo remains in the EEs [176, 177]. Cargo receptors and lysosomal transmembrane proteins require sorting signals in their cytosolic domains. As a result, lysosomal proteins have dileucine-based motifs DXXLL or [DE]XXXL[LI] [178, 179] and tyrosine-based motifs YXX∅ [180, 181] that interact with the clathrin machinery and adaptor protein complexes. For example, the adaptor protein complex protein AP3 is required for transport of lysosomal proteins from TSEs to lysosomes [176, 182]. This complex combination of luminal

and cytosolic signals with recognition proteins ensures specific and proper transport of lysosomal proteins. The intricate and critical nature of these pathways are evident in many human diseases. For example, mutations affecting the function of AP3 in humans result in a pigmentation and bleeding disorder called Hermansky-Pudlak syndrome [183-185] where patients have an inappropriate redistribution of lysosomal membrane proteins to the plasma membrane. These patients have impaired formation of lysosomes and lysosomal related organelles (LROs) such as melanosomes and platelet-dense granules. Similarly, M6PR knockout mice and human patients with I-cell disease (also known as Mucolipidosis type II), lack the M6P recognition tag because of a deficiency in *N*-acetylglucosamine (GlcNAc) phosphotransferase activity and as a result, secrete lysosomal enzymes from cells [186-188]. This is an oversimplification of the trafficking and regulated transport of lysosomal proteins (for a more detailed review, please see [189]).

1.4.2 Lysosomal function.

The lysosome gets its name from the Greek words *lysis,* meaning digestion, and *soma,* meaning body. The major function of lysosomes is degradation of intra- and extracellular macromolecules. While extracellular material is ingested by cells through endocytosis and delivered to the lysosomes through many different compartments, intracellular material reaches the lysosome through different forms of autophagy. After digestion, certain products can either be reused by the cell as building blocks for anabolic processes, or be expelled into the extracellular environment through lysosomal exocytosis (Figure 4). In this section, I will briefly discuss lysosomal function and its role in endocytosis, autophagy, and exocytosis.

The unique and highly acidic (pH 4.5 -5.0) environment of the lysosomal lumen is maintained by the action of the vacuolar H^+-ATPase; a transmembrane multimeric protein

complex that pumps protons from the cytosol against the electrochemical gradient into the lysosomal lumen through ATP hydrolysis [190, 191]. Lysosomal transporters such as the Cl^-/H^+ antiporter, anion transporter chloride channel 7 (CIC-7), have been shown to regulate the activity of this pump [191-194]. Additionally, lyosomal function depends on proper lysosomal ion concentrations facilitated by channels such as the cation transporter mucolipin 1 (TRPML1), two pore calcium channel 1 (TPC) [191, 195-197], solute carrier family 11, member 2 (Slc11a2) (also known as divalent metal transporter 1 (DMT1) or natural resistance-associated macrophage protein 2 (NRAMP2)) [198], and the zinc transporter ZnT4 (Figure 5).

The low pH of the lysosomal lumen facilitates both the action of over 50 resident proteolytic enzymes (proteases, nucleases, lipases, phosphatases, peptidases, glycosidases and sulfatases) and the degradation process by loosening the structures of macromolecules [199, 200]. This combination ensures lysosomal degradation of all kinds of cellular macromolecules.

Of the lysosomal hydrolases, the cathepsin family of proteases is the best characterized and is categorized into three groups based on the amino acid within the active site: aspartic cathepsins (D and E), cysteine cathepsins (B, C, F, H, K, L, O, S, V, W, and X) and serine cathepsins (A and G) [201]. Interestingly, while the activity of most lysosomal hydrolases depends on the lysosomal environment, some hydrolases, such as Cathepsin B, can function in a wider pH range and play a critical role in cell death mechanism, discussed later in this chapter, by cleaving cytosolic proapoptotic substrates [202-204].

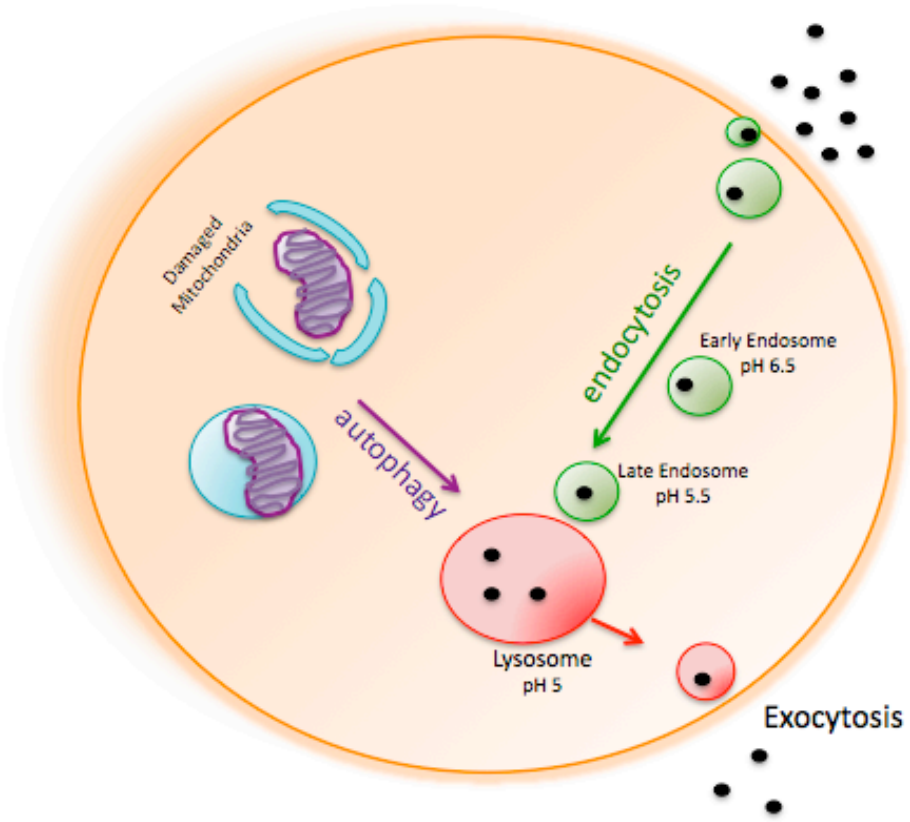

Figure 4. Lysosomal function in endocytosis, autophagy and exocytosis.

Lysosomes are responsible for the degradation of macromolecules in cells and have distinct morphology and function. Endocytosis (right side) is a process where cells absorb extracellular material (black dots) by engulfing them. Often, this material travels through several intermediate compartments, with decreasing pH environments, before reaching the lysosome for degradation. In the opposite process, lysosomes can expel material outside of the cell through docking and fusion of lysosomes with the plasma membrane in a process called lysosomal exocytosis (bottom). Another function of lysosomes involves autophagy (left side). During autophagy, sequestration of proteins or damaged organelles begins with the formation of the phagophore, a double membrane autophagosome that can engulf parts of the cytoplasm as well. The autophagosome can then fuse with a lysosome to obtain acid hydrolases, or to form an autolysosome in order to degrade cargo.

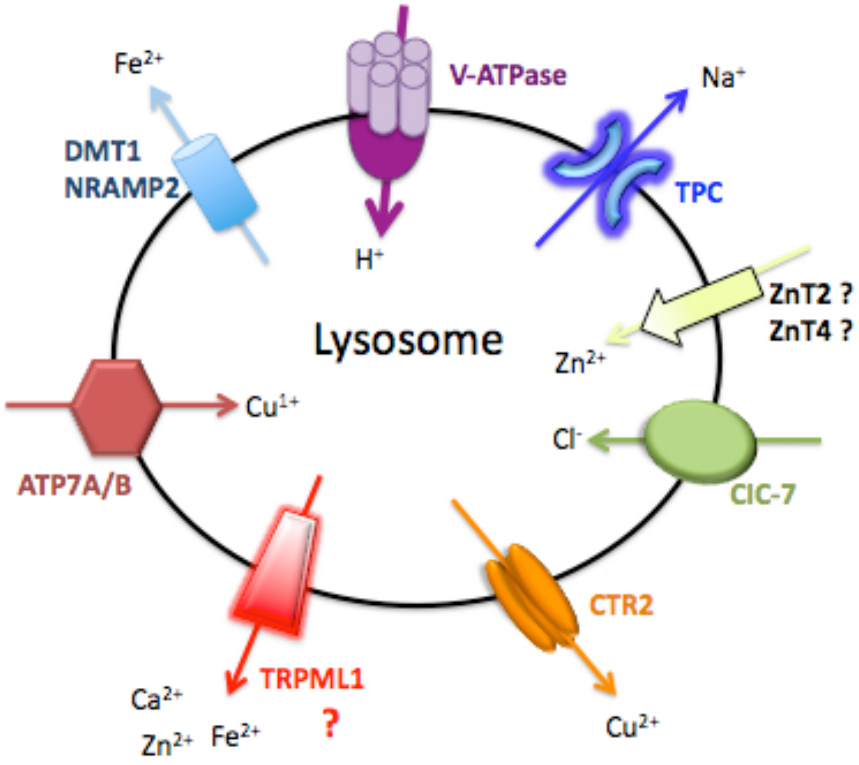

Figure 5. Lysosomal metal transporters.

Model illustrating the transport direction of the identified lysosomal metal transporters. Lysosomal function depends on the correct ion concentration regulated by these transporters.

Extracellular material is internalized from the plasma membrane as endocytic cargo in early endosomes (EEs) and then to late endosomes (LEs), which eventually fuse with lysosomes to degrade the cargo. This transfer from EE to lysosomes usually takes less than an hour. During this time, the various compartments undergo many changes including exchanging material and membrane components, decreasing luminal pH, forming intraluminal vesicles (ILVs), changing morphology (losing EE tubular extensions), and gathering lysosomal components [205]. However, how this cargo is exactly delivered from LEs to lysosomes is still not entirely understood and multiple models have been proposed. In the maturation model, LEs gradually mature into lysosomes by gradually obtaining lysosomal components and shedding endosomal components [206]. In contrast, the vesicular model proposes that the mode of delivery is through vesicles that form and bud from LEs and then fuse with lysosomes [207]. Alternatively, the "Kiss and run" model postulates that the membranes of LEs and lysosomes transiently fuse (kiss), exchanging contents, before separating (run). Lastly, the hybrid model suggests that LEs and lysosomes permanently fuse to form a hybrid organelle containing both endosomal and lysosomal components, where LE components are later selectively retrieved and lysosomes re-formed. Because of this continuous exchange of contents between the intermediate compartments of the endocytic pathway, the use of terms such as EE, LE and lysosomes is an oversimplification of the complexity found within the system. Nonetheless, markers used to distinguish between these different compartments are widely used. For example, the early endosomal antigen 1 (EEA1) and Rab5 GTPase are used to identify EE [208], while lysosomes can be distinguished from LE because they lack M6PR receptors [209]. Current evidence suggests that LE directly fuse with lysosomes, requiring N-ethylmaleimide sensitive factor (NSF), soluble NSF attachment proteins (SNAPs) and small GTPases such as Rab7 [210].

Similar to other membrane trafficking events, this process has three sequential steps: tethering, the formation of a trans-SNAP receptor (SNARE) complex, and the fusion of membranes from two different organelles. Tethering appears to be regulated by the homotypic fusion and vacuole protein sorting (HOPS) complex (VPS18 and VPS39, in particular), that is recruited by Rab7 [211, 212]. While membrane fusion requires syntaxin-7, VTI1B, syntaxin-8 [213-215], and the release of lumenal calcium (Ca^{2+}) necessary for phospholipid bilayer fusion [216]. At the end of this process, lysosomes are reformed from the hybrid organelle through the loss of M6PRs, endosomal SNAREs and the condensation of luminal content [217]. Defects in lysosomal reformation have been linked to lysosomal storage disorders such as Mucolipidosis type IV [218] (discussed further in section 1.5.2).

Similarly, during autophagy, intracellular components such as damaged proteins, or entire organelles are degraded and recycled. In mammalian cells, autophagy begins with autophagosomes forming double membranes around cytosolic proteins or effete organelles such as dysfunctional mitochondria, and then either fusing with the lysosome to either create an autolysosome or briefly interacting with the lysosome to transfter the autophagic content for degradation. Moreover, autophagy can be classified into three categories: chaperone-mediated autophagy, microautophagy and macroautophagy. In chaperone-mediated autophagy, cytosolic proteins with specific motifs are delivered to lysosomes via LAMP-2A and Hcs70 [219]. Very little is known about microautophagy where macromolecules are directly translocated to the lysosomal lumen for degradation [220]. Macroautophagy, on the other hand, engulfs cytoplasm, along with soluble materials and organelles within a double membrane called the phagophore to form the autophagosome, which subsequently fuses with lysosomes to degrade and recycle material [221]. Mammalian target of rapamycin complex 1 (mTORC1) is a kinase that is central

for regulating autophagy and detecting the cell's energy status by responding to signals from amino acids, growth factors and glucose [222]. A basal rate of autophagy is necessary for homeostasis, but can be strongly upregulated to various physiological stresses such as the presence of aggregated proteins or during starvation [223]. Under basal conditions, mTORC1 associates with the lysosomal membrane and interacts with and phosphorylates TFEB to prevent TFEB nuclear translocation [224]. Upon starvation, mTORC1 is inhibited, allowing unphosphorylated TFEB to upregulate the expression of genes coding for lysosomes and autophagosomes. Nutrient stress also changes lysosomal localization from peripheral to perinuclear clustering [225]. Thus, lysosomal localization regulates mTORC1 signaling. Curiously, the reverse is not true. mTORC1 activity does not influence lysosomal localization. This implicates lysosomes as key players in the control of the cellular response to nutrient stress.

For many years, it was thought that only specialized secretory cells undergo a process called lysosomal exocytosis where lysosomes fuse with the plasma membrane in order to secrete material. However, over the last decade or so, it has been recognized that all cell types are capable of lysosomal exocytosis [226]. Lysosomal exocytosis is a Ca^{2+}-regulated mechanism that leads to the release of lysosomal contents into the extracellular matrix. This mechanism is important for many physiological processes such as plasma membrane wound repair [227, 228], platelet function in coagulation [229], melanocyte derived pigmentation [230], degranulation in cytotoxic T lymphocytes [231], bone resorption by osteoclasts [232], bacterial defense by mast cells [233], and parasitophorous vacuole formation by *Trypanosoma cruzi* [234]. Lysosomal exocytosis is a two-part process where lysosomes first relocate from their perinuclear localization closer to the plasma membrane [235], and then fuse with the plasma membrane in response to a transient increase in intracellular Ca^{2+} [226]. In cytotoxic T lymphocytes, for

example, once a foreign antigen is detected, lytic granules (LROs) are delivered to the immunological synapse via microtubules [236] between the lymphocyte and the target cell to induce apoptosis of the foreign cell. Fusion of the lytic granule to the plasma membrane depends on priming by Munc-13-4 [237] while docking is Rab27a dependent [238]. Although cell-type specific SNARE proteins for this process have not been identified, evidence suggests that VAMP7 is required in eosinophils and neutrophils [239, 240] and VAMP8 is required in platelets [241]. Defects in the biogenesis, movement and exocytosis of these LROs cause albinism, bleeding disorders and immunodeficiency in several syndromes including; Griscelli, Chediak Higashi and Hermansky-Pudlak syndromes [242-244].

In addition to lysosomal exocytosis, autophagy also plays an important role in the host defense mechanism against intracellular pathogens [245]. In animals, macroautophagy facilitates the recognition of infected cells by innate immune effectors, initiating an elaborate inflammatory or immune response [246, 247]. Not surprisingly then, bacteria and viruses have developed strategies for either subverting or manipulating autophagic pathways [248, 249]. Beyond influencing cell-intrinsic immune responses, autophagy has also been shown to be important for the antigenic profile of antigen-donor cells and their ability to release immunogenic signals [250, 251], as well as the survival, differentiation and function of antigen-presenting cells and T lymphocytes [252-255]. Specifically, recent evidence indicates that in antigen-donor cells, autophagy affects the release of cytokines [256-259]. Moreover, mutations in autophagy-related genes have been associated with immune diseases [245, 260], and an increase in tumor development due to depressed immunosurveillance [261, 262]. Thus, autophagy and thereby lysosomes have a critical role in cellular immune responses.

Lysosomal exocytosis is not only important for secreting lysosomal content, but also has an essential role in plasma membrane repair. Injury of the plasma membrane occurs frequently in cells infected with pathogens [263], or in muscle and skin cells exposed to mechanical stress [264]. Lysosomal exocytosis is thought to be the primary source of membrane for resealing [265]. Restoring plasma membrane integrity is essential for cell survival and occurs within seconds to a minute timeframe [266, 267]. Soon after plasma membrane disruption, lysosomal markers such as LAMP1 appear at the cell surface due to the elevation in cytosolic Ca^{2+} [228]. Ca^{2+}-regulated exocytosis is modulated by the vesicle SNARE (v-SNARE) TI-VAMP/VAMP7, the Ca^{2+} sensor synaptotagmin VII (SYT7) on lysosomes, the target SNAREs (t-SNAREs) SNAP23 and syntaxin 4 on the plasma membrane [268], along with many Rab proteins on the lysosomal membrane [269-271]. TRPML1, a Ca^{2+} lysosomal channel has also been shown to mediate lysosomal exocytosis [272, 273] (discussed further in section 1.5.2). Defects in resealing the plasma membrane lead to bacterial infection [274] and muscular dystrophy [275], which is characterized by impaired muscle fiber repair. Intriguingly, TFEB overexpression has been shown to increase lysosomal exocytosis through TRPML1 upregulation [273], and play an important role in osteoclast differentiation and bone resorption [276]. Additionally, once lysosomes fuse with the plasma membrane and plasma membrane integrity has been restored, the lesion is removed through endocytosis to promote wound resealing [277]. One of the lysosomal enzymes released extracellularly through lysosomal exocytosis, acid sphingomyelinase (aSMase) [278], promotes endocytosis by making ceramide. High ceramide content in the plasma membrane induces inward bending of the membrane and facilitates endocytosis [279]. Finally, lysosomes contain an abundance of ATP that is released with lysosomal exocytosis [280] that can be used for cell communication by binding to ATP binding receptors [281].

1.4.3 Signaling from lysosomes.

Given the abundance of their hydrolytic enzymes, lysosomes were coined “suicide bags” by Christian de Duve [155], since they could be quite harmful to cells if not controlled. Damage or compromise of the lysosomal membrane results in the release of lysosomal content into the cytoplasm, which indiscriminately degrades cellular material. While partial and selective lysosomal membrane permeabilization (LMP) induces apoptosis, a complete rupture induces cytosolic acidification and necrosis [282]. Specifically, LMP induces the translocation of lysosomal proteases such as cathepsin B, CD, and L into the cytoplasm, where they remain active even at neutral pH [283]. Cytoplasmic cathepsins trigger signaling cascades that either activate proapoptotic effectors such as caspases and mitochondria, or amplify the cell death signal [283, 284]. Depending on LMP activation and the cell type, post LMP signaling often activates either the caspase cascade through the intrinsic pathway, or the caspase-independent pathway of cell death [285, 286]. For example, the leak of cathepsin B into the cytoplasm has been shown to induce apoptosis through chromatin condensation, DNA fragmentation, plasma membrane blebbing, and phosphatidylserine exposure to the outer plasma membrane [287, 288]. In addition to the cathepsin leak, LMP also releases Ca^{2+}. Lysosomes have a Ca^{2+} content that is similar to the endoplasmic reticulum (ER), of up to 600 μM [289, 290]. Lysosomal Ca^{2+} is released through the TPC via nicotinic acid adenine dinucleotide phosphate (NAADP) [291]. LMP induced increases in Ca^{2+} cause the externalization of phosphatidylserine [292], effectively marking that cell for cell death via phagocytosis. There is a growing list of events that trigger LMP. Most of the agents that induce LMP affect the integrity of the lysosomal membrane such as lysomotropic agents like Leu-Leu-O-Me and hydixychloroquine. But other apoptotic stimuli such as photodamage, p53 activation, and the generation of reactive oxygen species (ROS) also

induce LMP [293-295]. Lysosomal cell death pathways are also important physiologically in mammary gland regression [296] (discussed further below) and embryonic development [297].

It is not clear how cathepsins translocate from the lysosome into the cytosol. Current paradigms propose either pore formation or simple membrane damage. One study suggests that there is a size-selectivity in the content released from lysosomes of up to 40 kDa [202]. Yet, another study showed the release of β–*N*-acetylglucosaminidase, a 150 kDa lysosomal hydrolase [298, 299]. Also unclear are the signaling pathways that induce LMP. One recent study dissected the signaling pathway involved in the tumor necrosis factor-related apoptosis-inducing ligand (TRAIL) induced LMP. TRAIL is normally expressed in immune effector cells, and induces apoptosis in target cells by binding to the death receptor 5 (DR5) [300]. This ligand-receptor complex is then internalized through endocytosis and recruits the phosphofurin acidic cluster sorting protein (PACS2), which then forms a complex with Bim and Bax to induce LMP [301]. Regardless of the exact signaling cascade, maintenance of lysosomal membrane integrity is essential for cell survival and evidence suggests that LMP susceptibility is related to the stability of lysosomal membranes. Susceptibility to LMP varies depending on cholesterol content [302], lysosomal size or lysosomal ion content such as iron [303] or zinc [304], which make lysosomes more prone to LMP. Other factors that determine the extent of LMP are endogenous inhibitors. For example, the Hsp70 family of chaperones, cannot only protect lysosomal membranes against permeabilization, but can also reverse Niemann-Pick disease A phenotypes, where lysosomal stability is chronically decreased [305]. Furthermore, endogenous cysteine cathepsin inhibitors, such as stefin, in the cytosol inhibit the activity of accidentally released cathepsins [306]. Another interesting regulatory step is that, except for cathepsin B, C, D, and L that remain active even at neutral pH [283, 307], most cathepsins are inactivated by the neutral pH in the

cytoplasm. This inactivation has been linked to either unfolding or deprotonation [308, 309], but the proteolytic activity of cathepsins can be stabilized through either substrate binding [307], or LMP induced cytosolic acidification. Once in the cytoplasm, cathepsins cleave several known substrates that induce the mitochondrial cell death pathways. For example, cathepsins B, D, H, K, L and S have been shown to activate the pro-apoptotic Bcl-2 family member, Bid [310, 311], and a recent study suggests that cathepsins also target XIAP and anti-apoptotic Bcl-2 proteins [312]. Moreover, LMP induced cell death requires Bax/Bak [313], and cytochrome C release [314]. Other cathepsin substrates include sphingosine kinase-1 [315], and membrane-associated guanylate kinases [316], implicating LMP control in cell-cell contacts, proliferation and tumor necrosis factor (TNFα) signaling.

LMP-induced cell death has been implicated in post-lactation mammary gland involution. Decreased suckling triggers a weaning signaling cascade that involves the controlled elimination of the milk secreting mammary gland epithelial cells through necrosis and glandular involution. In the first phase of postlactation, the expression of lysosomal membrane proteins LAMP1 and LAMP2 decreases, making the lysosomes more leaky, leading to the translocation of cathepsins B and L into the cytoplasm and activating caspase-independent cell death [296]. At the same time, the expression of cathepsin B and L increases, but the expression of the intracellular cysteine peptidase inhibitor serpin *Spi2A* decreases. Accompanying these events are calpain activation and increased intracellular Ca^{2+} levels. These events lead to increased plasma membrane permeability and lysosomal-mediated necrotic cell death. Kreuzaler et al. recently showed that the transcription factor STAT3 controls the expression of these proteins and when deleted, delays mammary gland cell death and involution [296]. These data link STAT3 and LMP in a physiologically relevant cell death model that could potentially be used for mammary

tumor therapies or drug targets. On the other hand, studies in bovine mammary gland remodeling have implicated autophagic cell death and the formation of autophagosomes as a cell death mechanism [317]. Thus, it is unclear whether autophagy also contributes to remodeling of the mammary gland during involution, as it could either be activated as a cytoprotective measure to prevent cell death, or as a consequence of cell starvation.

Lysosomes are no longer regarded as "waste" or "suicide" bags, but are now recognized as advanced organelles that are involved in many cellular processes and are crucial for regulating cell homeostasis. Consequently, it has also become increasingly evident that lysosomes are pivotal in nutrient sensing and integrating signaling pathways important for metabolism and growth. In fact, mTORC1 localizes to the lysosome and is activated upon nutrient starvation. Under basal conditions when nutrients are present, mTORC1 phosphorylates the kinase complex ULK1-ATG13-FIP200 (unc-51-like kinase 1-autophagy-related 13-focal adhesion kinase family-interacting protein of 200 kDa) [318], which suppresses its activity and prevents autophagosome formation [319-321]. Under starvation, or pharmacologically induced mTORC1 inhibition, ULK1-ATG13-FIP200 is activated, and autophagy takes place, suggesting that lysosomes act as sensors, rather than just effectors of these cellular pathways. Moreover, amino acids must build up inside the lysosomal lumen for mTORC1 activation [322], and under starvation conditions, mTORC1 has been shown to interact with lysoNa$_{ATP}$, an endolysosomal ATP-sensitive Na^+-permeable channel, to regulate lysosomal pH stability and amino acid homeostasis. During starvation, mTORC1 dissociates from the lysosomes, allowing lysoNa$_{ATP}$ to open and control lyosomal membrane potential in response to ATP levels [323]. Intriguingly, prolonged starvation leads to lysosomal reformation that requires the kinase activity of phosphatidylinositol 4-kinase IIIβ (PI4KIIIβ) [324] and mTORC1 reactivation [325, 326].

1.5 LYSOSOMAL DYSFUNCTION IN HUMAN DISEASES

Given the vast range of cellular functions that converge on the lysosomal compartment, it is not surprising that disruptions of this compartment have a profound impact on cell homeostasis. Lysosomal dysfunction has been associated with several human diseases, in addition to the process of aging. Over time, lysosomal function decreases and a progressive accumulation of undigested material occurs [327]. In fact, one of the main reasons why caloric restriction prolongs life spans is by enhancing the autophagic-lysosomal pathways [328]. Unfortunately, 1 in 5000 births worldwide are affected by lysosomal storage disorders (LSDs) in which a lysosomal defect creates intra-lysosomal accumulations of undigested material [329, 330]. Even though lysosomes are centrally implicated in LSDs, they have also been shown to be involved in many more widespread diseases such as cancer, Alzheimer's disease, amyotrophic lateral sclerosis and Parkinson's disease. In this section, I will discuss many of the LSD pathologies as well as the neurodegenerative diseases associated with lysosomal and autophagic dysfunction.

1.5.1 Lysosomal storage disorders.

Lysosomal storage disorders (LSDs) are a class of genetic pathologies characterized by the accumulation of material inside lysosomes. To date, over 50 human diseases associated with lysosomal dysfunction have been identified. The majority of these diseases are autosomal recessive and monogenic, although multiple mutations have been found in the same gene for each disorder. Unfortunately, identifying the genetic mutation has not led to new therapies as the underlying molecular and cellular events are highly complex and remain elusive [331]. The key question within the field is to address how endosomal-lysosomal storage leads to pathogenesis.

Nonetheless, LSDs provide a wealth of information about the normal functions of lysosomal proteins. The most common mutations causing LSDs occur in lysosomal enzymes, nonenzymatic lysosomal proteins, and nonlysosomal proteins that regulate lysosomal functions [331]. The degree of penetrance depends on the severity of the mutation; null mutations develop symptoms *in utero* or early on in childhood, while milder mutations can develop later in adulthood [331].

Some of the first LSDs to be clinically characterized were Gaucher disease and Tay-Sachs disease in the 1880s [332]. Both Gaucher disease and Tay-Sachs disease are now classified as sphingolipidoses. In general, LSDs have distinct clinical and biochemical features, but are often classified based on the storage material that accumulates; mucopolysaccharidoses (MPS) accumulate mucopolysaccharides, sphingolipidoses accumulate sphingolipids, and oligosaccharidoses accumulate oligosaccharides. It is important to note that some LSDs have an accumulation of multiple substrates due to a deficiency in a single enzyme, largely due to the dysfunction in some of the common substrates. Additionally, LSDs are identified at a cellular level by the primary defect in the clearance of autophagic and endocytic substrates that lead to the formation of dense cellular inclusions filled with undigested material [333-335]. This undigested material seems to also lead to many secondary defects shared by many LSDs such as reduced autophagic flux, insufficient metabolic function, perturbed Ca^{2+} homeostasis in the ER and the mitochondria, increased reactive oxygen species, and impaired inflammatory and apoptotic signaling [336-339]. These secondary defects complicate matters for researchers trying to identify the root cause of each LSD and make it difficult to interpret the causative and underlying insults from the genetic mutation. These secondary defects also make it difficult to study LSDs in patient fibroblasts since they already have developed inclusions and secondary

defects, thereby obscuring the model system. Even with these chronic complications, the patient fibroblasts cells are nonetheless, indispensable for finding treatments.

Strikingly, most LSDs are characteristically neurodegenerative in nature (except for Gaucher and Pompe diseases), resulting in mental retardation, progressive motor degeneration, retinopathies and shortened life spans. Lysosomal dysfunctions could arise from genetic mutations, lack of or mislocalized protein delivery, or misfolding. In some LSDs, a genetic mutation directly affects the activity of one lysosomal enzyme, such as glucocerebrosidase/ β-glucosidase in Gaucher disease [340], β-hexosaminidase A in GM2 gangliosidosis (Tay-Sachs), α-glucosidase in Pompe disease, or α–galactosidase A in Fabry disease [332]. While in other LSDs, a defect in a critical processing step can affect multiple enzymes, such as in multiple sulphatase deficiency (MSD), where a defect in the sulphatase-modifying factor- 1 gene (*SUMF1*) results in a defective enzyme responsible for generating the Cα-formylglycine residue that is the critical catalytic center of all sulphatases [341, 342]. In the same way, improper trafficking of lysosomal enzymes causes other LSDs. For example, in Mucolipidosis II and III, a mutation in the *GNPTA* (MGC4170) gene coding for the GlcNAc-1-phosphotransferase results in a defect in the M6P tag from the Golgi, and instead of lysosomal localization, the hydrolases are secreted out of the cell [343, 344]. LSDs are not exclusively due to defects in lysosomal enzymes, but can also arise from defects in lysosomal membrane proteins, such as in Mucolipidosis type IV (discussed in section 1.5.2), neuronal ceroid lipofuscinosis (NCLs, also known as Batten disease), cystinosis and Niemann-Pick C (NPC). NPC, for example, is caused by a defect in the cholesterol transporter NPC1, or by defects in the soluble lysosomal cholesterol binding protein NPC2 and is characterized by impaired sphingolipid and cholesterol levels [345]. Cystinosis, on the other hand, results due to a mutation in cystinon, a cystine

transporter, which subsequently leads to the buildup of the amino acid cystine inside lysosomes [346]. In these diseases, mutations in lysosomal membrane proteins have demonstrated the importance of maintaining the lysosomal environment, and have added complexity to the dynamics of how we look at lysosomes and LSDs.

1.5.2 Mucolipidosis type IV.

Unlike most other LSDs that arise from lysosomal enzyme deficiencies, Mucolipidosis type IV (MLIV) occurs from loss-of-function mutations in *MCOLN1*, a gene encoding the lysosomal ion channel transient receptor potential mucolipin 1 (TRPML1). MLIV was first described in 1974 [347]. It was subsequently found to be autosomal recessive, and to predominantly occur among the Ashkenazi Jewish population with a carrier frequency of 1 in 100 [348, 349], but it has also been reported in non-Jewish populations [350, 351]. As of 2014, over 20 different TRPML1 mutations have been identified, but the two founder mutations account for over 95% of MLIV cases [352, 353]. Most of the mutations result in loss of TRPML1 channel, but a few affect channel localization or function [354, 355]. Some splice variants have been reported, but their function or regulation is uncharacterized [356, 357]. MLIV is a developmental and degenerative disorder with the onset beginning within a year of birth and patients presenting with severe motor and mental impairment, corneal clouding and progressive retinal degeneration, achlorhydria (low production of gastric acid, but elevated plasma gastrin levels), anemia, and a thin corpus collosum [355]. Most MLIV patients are unable to walk by their early teens, have limited or no ability to speak, and have severe vision loss or blindness.

Electron microscopy of patient fibroblasts showed enlarged vacuolar structures, or inclusions, that accumulate mucopolysaccharides, sphingolipids and phospholipids in

multiconcentric lamellae [347, 358, 359]. This suggests that the loss of TRPML1 affects many different lysosomal hydrolases and likely affects the lysosomal environment. It is difficult to reach conclusions about the pathology from these inclusions since it has been reported that they vary from tissue to tissue [360, 361]. This variation could be due to cell type specific transcriptional profiles, and/ or to cell type specific reactions to TRPML1 loss. The presence of these inclusions or vacuoles in parietal cells, for example, could explain the achlorhydria seen in MLIV patients. Parietal cells normally produce gastric acid in the stomach epithelium, but TRPML1 loss could result in defects in the endocytic pathway or exocytosis, and lead to decreased gastric acid secretion [362]. Similarly, in retinal epithelial cells these vacuoles or inclusions could be causing the vision loss or be a factor in neurodegeneration in neurons. However, no correlation between the number of inclusions and the severity of the MLIV symptoms has been observed. Thus, it is unclear whether the formation of these inclusions and vacuoles is the primary insult as a result of TRPML1 loss, or a secondary defect. Delineating cell type specific responses and understanding TRPML1 function will provide insights into TRPML1 cell type-specific roles and an understanding of how cells respond to different endocytic loads and insults.

The *MCOLN1* gene, coding for the TRPML1 channel, was cloned by three labs in 2000 [363-366]. Since then, several orthologues have been discovered in *Drosophila* (trpml), *C. elegans* (cup-5) and mice. In humans, TRPML1 is predicted to roughly be 65 kDa. Although no crystal structure of TRPML1 exists, it is predicted to have 6 transmembrane domains, a putative transient receptor potential (TRP) channel pore domain between the fifth and sixth transmembrane domains, an N- and C- terminus orientated towards the cytosol [355], and a

large, highly *N*-glycosylated loop between the first and second transmembrane domains in the lysosomal lumen that gets cleaved by Cathepsin B (Figure 6) [367].

The TRP family of ion channels includes TRPA, TRPC, TRPM, TRPML, TRPV and TRPP [368]. Most TRP channels respond to extracellular stimuli such as temperature, light, mechanical stress, and osmolarity, but a few respond to intracellular stimuli such as pH or ion concentrations [369]. Several TRP channels localize to endosomal compartments, but *TRPML1 is the first member of the TRP superfamily to localize to late endosomes and lysosomes* [367, 370]. Trafficking of TRPML1 requires two acidic di-leucine motifs at the N- and C- terminus of the protein. The E^{11}TERLL motif at the N-terminus interacts with the clathrin adaptors AP1 and AP3 to sort TRPML1 directly from the TGN to the lysosomes. However, TRPML1 is also sorted indirectly from the TGN to the plasma membrane, and then to the lysosome through endocytosis and AP2 binding to the E^{573}EHSLL motif within the C-terminus [371]. TRPML1 also has two proline-rich regions (aa 28-36, and 197-205), and a lipase serine active site domain (aa 104-114). Additionally, TRPML1 does not seem to have ankyrin repeats like other TRP channels, but it has been shown to be phosphorylated by PKA-domains [372]. Lastly, TRPML1 has been reported to homo- and hetero-multimerize with its two homologues TRPML2 and TRPML3 [373, 374]. TRPML2 and TRPML3 also localize to endosomes and lysosomes. It is not known whether any of the MLIV symptoms might be due a mislocalization of TRPML3, for example, instead of just TRPML1 loss. There is very little evidence from co-localization studies of the native protein, possibly due to a short-half life in the lysosome, or a lack of good antibodies. Further work on the structural determinants of TRPML1 will fully explain TRPML1 function.

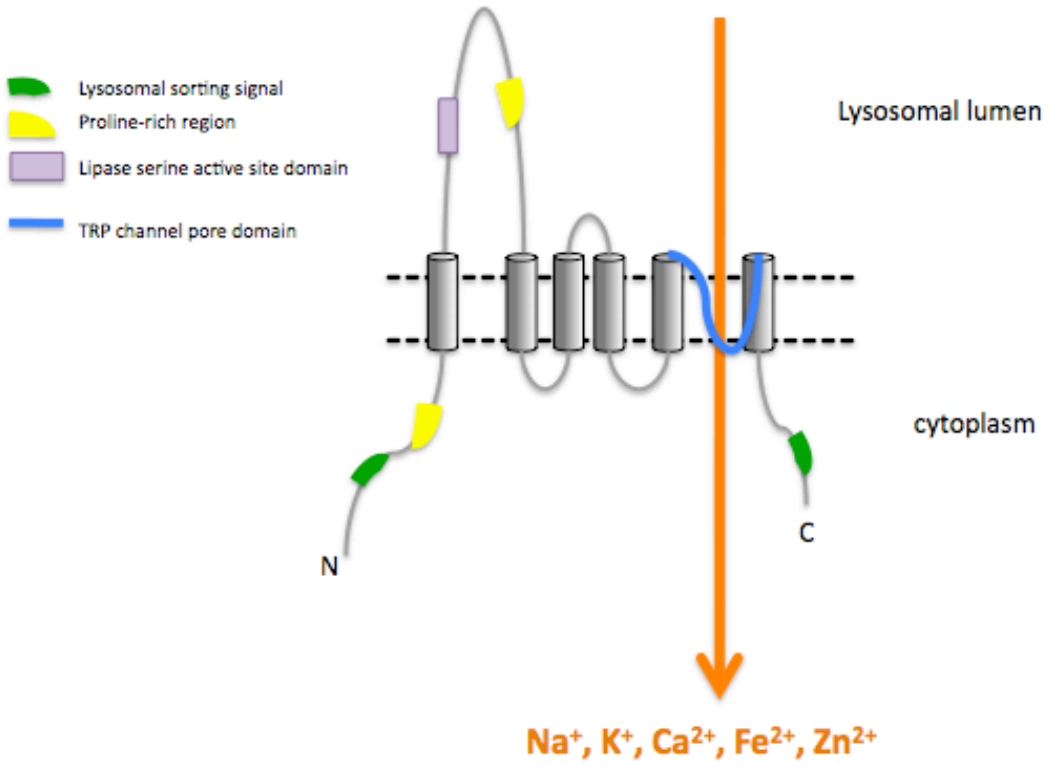

Figure 6. TRPML1 predicted structure.

Model illustrating TRPML1 topology and some of the identified structural features. TRPML1 localizes to late endosomes and lysosomes and has been shown to be permeable to Na^{+}, K^{+}, Ca^{2+}, Fe^{2+} /Mn^{2+}, and potentially Zn^{2+}. Mutations in TRPML1 cause MLIV.

Even with the severe pathology of MLIV, TRPML1 functions remain unclear. The first study on the cation-selective channel activity by TRPML1 was published in 2002 and examined the activity of a *MCON1* cDNA transfected into either *Xenopus* oocytes or HEK-293 cells [375]. In both cases, the study confirmed permeability to Na^+, K^+, and Ca^{2+} [375]. Two years later, another group showed that in a lipid bilayer system, TRPML1 is a pH-dependent cation channel and postulated that TRPML1 regulates the vesicular membrane potential by switching off at low pH and thus, it was concluded that mutated TRPML1 cannot shut off at low pH [354]. Since then, TRPML1 channel activity has been recorded on native endolysosomal membranes by direct lysosomal patch-clamp studies of enlarged (vacuolin-treated) lysosomes. These studies made use of a constitutive active TRPML1 mutant (V432P) to show that TRPML1 is an inwardly rectifying (from the lysosomal lumen to the cytoplasm) channel permeable to Na^+, K^+, Ca^{2+}, Fe^{2+} /Mn^{2+}, and potentially Zn^{2+} [376]. This 2008 study identified TRPML1 as an endolysosomal iron release channel, whose activity may be potentiated by low pH.

Since TRPML1 function is so poorly understood. At first, the main physiological function of TRPML1 was thought to facilitate Ca^{2+} efflux necessary for SNARE-mediated endo-lysosomal membrane fusion. This "traffic-," or "biogenesis" model for TRPML1 function proposes that TRPML1 directly regulates membrane traffic and in the absence of TRPML1, endocytic material (lipids and proteins) targeted for degradation accumulate. Several studies have shown delays in lipid trafficking in MLIV models ranging from MLIV fibroblasts [370, 377] to *C. elegans* [218, 378]. Support for this model is based on the observation that TRPML1-deficient cells delay trafficking of a fluorescent BODIPY conjugate, C5-lactosylceramide (LacCer) [370, 379, 380], as well as defects in lysosomal biogenesis, increased colocalization of endosomal and lysosomal markers, and the accumulation of vacuolar structures in CUP-5

knockout *C. elegans* [378, 381]. TRPML1 loss has been also associated with lipofuscin accumulation [382, 383], decreased lysosomal exocytosis [272], and deficient autophagy [372]. Additionally, MLIV fibroblasts, mouse neurons, and *Drosophila* knockouts have defective chaperone-mediated as well as macro-autophagy and accumulate autophagososmes, effete mitochondria, ubiquitinated aggregates, and p62 protein inclusions [372, 382-385]. It is not clear whether these defects in membrane trafficking and lipid metabolism are the primary cause of MLIV, or an added complexity due to secondary effects of undigested material. It is likely that the buildup of undigested material prevents the delivery of trafficking markers into lysosomal compartments by "clogging" membrane traffic and appears as defects in membrane traffic, clouding the possible primary cause of MLIV pathogenesis. An example of this occurred in sphingolipidoses where a metabolic defect had multiple membrane traffic delays similar to the ones observed in MLIV [386]. Thus, to fully understand MLIV pathogenesis and TRPML1 function, it is imperative to distinguish the acute primary deficits from the more chronic, secondary compensatory side effects. To directly address this problem, two labs at the University of Pittsburgh, led by Drs. Ora Weisz and Kirill Kiselyov, utilized an siRNA-driven TRPML1 knockdown system in HeLa cells in 2008 to determine the immediate effects of TRPML1 loss [387]. Interestingly, they confirmed the accumulation of inclusions and decreased lysosomal pH in this system, but *found no trafficking delays* [387].

Thus the second "metabolic," model prevailed. This model suggests that TRPML1 regulates ion homeostasis and directly impacts the activity of lysosomal enzymes. Under this paradigm, loss of TRPML1 decreases lysosomal digestive function by affecting lysosomal ion concentrations. Support for this model comes from several key observations made over the last couple of years. To begin with, Dong et al. recently showed that TRPML1 directly binds and is

activated by $PI(3,5)P_2$ [388, 389], an endolysosomal specific phosphoinositide. This suggested that TRPML1 is active in the lysosome and provided insight into the spatial and mechanistic regulation of endolysosomal dynamics as well as of TRPML1 Ca^{2+} release. Additiomal details were revealed when the penta-EH-hand protein ALG-2 has been found to bind both $PI(3,5)P_2$ and TRPML1 only when Ca^{2+} is present [390]. The current hypothesis is that ALG-2 acts as a Ca^{2+} sensor to modulate trafficking events through TRPML1. Moreover, TRPML1 might regulate the activity of other lysosomal transporters such as the two-pore family of ion channels (TPC). TPCs are Na^{+} channels in endosomes and lysosomes. Pharmacological inhibition of TPC activity has been shown to rescue enlarged lysososmes in TRPML1-deficient cells, further implicating TRPML1 as a regulator of TPCs [197, 290, 391, 392]. More support for the "metabolic" model of TRPML1 function comes from the observation that TRPML1-deficient cells buildup Zn^{2+} inside lysosomes [393]. Eicheisdoerfer et al. showed that an RNA interference model of MLIV in HEK-293 cells leads to chelatable Zn^{2+} inside the lysosomes of TRPML1-deficient cells [393]. They also showed that MLIV patient fibroblast cells had increased levels of Zn^{2+}.

In sum, TRPML1 is a lysosomal divalent metal transporter that seems to modulate key lysosomal functions. TRPML1 regulates the ionic environment within the lysosomal lumen and in doing so, affects lysosomal acidification and the delivery and activation of lysosomal enzymes. Due to its permeability, TRPML1 may also regulate membrane fusion events and key aspects of transition metal trafficking from lysosomes into the cytoplasm. The latter has gained a lot of attention in the recent years.

Transition metal toxicity has been linked to lysosomal storage phenotypes [394, 395] and LMP [396]. Transition metals such as Zn^{2+}, Ni^{2+}, Cu^{2+}, Co^{2+}, Fe^{2+}, and Fe^{3+} can be delivered to

lysosomes either from the cytoplasm through lysosomal transporters, or as byproducts through the endocytic pathway. During endocytosis, cells engulf extracellular content as well as transition metal-bound proteins that are degraded along the way to the lysosome, releasing the potentially toxic metals. Some transition metals such as Fe^{3+} can undergo Fenton-like reactions and produce free radicals that can lead to LMP [397, 398]. It is tempting to hypothesize that TRPML1 might have a role in dissipating transition metal buildup in lysosomes. There are several well-known transporters with this activity. SLC11A1 (NRAMP1) and SLC11A2 (NRAMP2, also known as DMT-1) are divalent cation transporters implicated in lysosomal metal trafficking [399, 400] (Figure 5). However, based on the recent findings by Eicheisdoerfer et al. and Dong et al., it is likely that there are other metal export mechanisms and unidentified channels maintaining lysosomal ion homeostasis. As intriguing as this possibility is, it still leaves many questions to be answered. The role of TRPML1 in transition metal toxicity will need to be further dissected, and it would be interesting to see the relative contribution of TRPML1 compared to the known metal transporters such as DMT-1 and TPCs. How are their localization and/or activation affected by TRPML1 loss? What activates the TRPML1 transport activity and what structural determinants are important for this activity? Is there a TRPML1 dependent correlation between inclusion bodies and transition metal toxicity? Addressing these and other questions will greatly expand the current knowledge of lysosomal function and lysosomal ion transport pathways.

1.5.3 Lysosomal dysfunction and neurodegenerative diseases.

Many of the pathologies associated with LSDs, such as defects in autophagy, intracellular substrate aggregation and inflammation, also occur in neurodegenerative diseases such as

Alzheimer's, Parkinson's and Huntington's [401]. In fact, recent evidence shows that neurodegeneration is often associated with lysosomal dysfunction [402, 403]. Neurons in particular, are especially sensitive to perturbations in lysosomal function or autophagy, and it has been shown that suppression of basal autophagy in mice leads to neurodegeneration [404, 405].

Alzheimer's disease (AD) is one of the most common forms of dementia. Sadly, it is progressive with age, results in death, and there is currently no cure. Recent observations have implicated lysosomal function in this disease [406]. In AD, amyloid-β peptides aggregate in and affect the function of neurons [407]. Recent work by Li et al., showed that endocytic trafficking of amyloid-β to lysosomes for degradation is a major clearance pathway [408]. Furthermore, presenilin 1 (PS1), the transmembrane protein mutated in AD, has been shown to be essential for v-ATPase delivery to lysosomes, and consequently, essential for lysosomal acidification and proteolysis during autophagy [409]. PS1 was found to be required for *N*-glycosylation of the V0a1 subunit of the v-ATPase. Mutations in PS1 lead to defective lysosomal and autophagic degradation, and early-onset AD [410, 411]. However, another study recently showed that PS1 mutations affect lysosomal function not by changing lysosomal acidification per se, but rather by disrupting Ca^{2+} homeostasis, and thereby lysosomal fusion [412]. Lastly, cystatin B is an endogenous inhibitor of lysosomal cystein proteases, and cystatin B knockout mice rescue amyloid-β aggregation, accumulation of ubiquitinated proteins and other autophagic substrates, and reverse the learning and memory defects seen in AD [413], further supporting the role of lysosomal function in neurodegeneration.

Lysosomal dysfunction is also associated with Parkinson's disease (PD) where dopaminergic cell death and autophagosome accumulation are prevalent. One of the earliest insults in PD is a drastic decrease in the expression of the lysosomal proteins LAMP1 and

LAMP2 and lysosomes [414, 415]. This results in lysosomal membrane permabilization, likely induced by the accumulation of ROS generated by mitochondria, and results in the accumulation of autophagosomes, as well as cell death due to the release of lysosomal proteases into the cytoplasm [414]. Strikingly, both genetic, and pharmacological induction of lysosomal biogenesis through TFEB activation attenuates cell death by increasing lysosomal function and autophagic clearance [414]. Another characteristic feature of PD is the accumulation of α–synuclein. α–synuclein is normally degraded by chaperone-mediated autophagy [416], but accumulates in PD. It was recently found that reduced expression and activity of glucocerebrosidase (the enzyme mutated in Gaucher's disease), lead to α–synuclein accumulation [417], providing a link between LSDs and PD. These findings further emphasize the key role of lysosomal enzymes in the pathology of neurodegenerative disorders.

1.5.4 Therapeutic strategies for lysosomal dysfunctions.

There is currently no treatment for MLIV. Individuals are diagnosed by a blood test to confirm elevated gastrin levels (the cause of which still remains unknown) and mutations in *MCOLN1* [334]. Some symptoms may be alleviated through iron supplements to treat anemia, or corneal transplants to temporarily correct corneal clouding. Intensive physical therapy as well as occupational, speech and vision therapies are recommended to help with life skills and ataxia.

The search for therapies for lysosomal storage disorders is ongoing, disease specific, and difficult given that the biochemical and molecular basis for the diseases are still being discovered. Several attempts were made to treat animal models of LSD and neurodegenerative diseases by enhancing lysosomal and autophagic function [413, 414, 418, 419]. An exciting and promising recent therapeutic avenue became available with the discovery of TFEB. The

possibility to enhance cellular clearance by inducing TFEB function is very appealing. Indeed, TFEB overexpression has been shown to effectively clear storage material in cell models of Pompe's, Batten, MSD, and MLIV disease [273]. TFEB also cleared storage material in i*n vivo* mouse models of MSD and Pompe's disease [273, 420] and has been used to promote clearance in neurodegenerative diseases such as Parkinson's [414] and Huntington's disease [421]. It is not exactly clear how TFEB is able to do this. TFEB mediated rescue of LSDs occurs even with lysosomal enzyme deficiency. The current evidence indicates that TFEB activates lysosomal exocytosis [273], thereby secreting the stored material out of the cells. It is likely that TFEB rescue is achieved through a combination of lysosomal biogenesis, autophagy and lysosomal excoytosis. As enticing as pharmacological manipulation of TFEB seems for therapeutics, long-term studies will need to be done to fully understand the effects of TFEB overexpression. Furthermore, since the stored material is secreted out of the cell, its toxicity within circulating blood and their effects on the brain will clearly need to be addressed. A greater understanding of the molecular details in disease pathogenesis will lead to better diagnostic and therapeutic tools. As such, lysosomes are attractive targets because of their emerging roles in nutrient sensing, signaling, metabolism, and transition metal toxicity.

1.6 DISSERTATION AIMS

In the above sections, I have described the current state-of-knowledge of lysosomal and cellular zinc homeostasis. From these descriptions, it is clear that several questions have been raised but remain unanswered. For example, what is the function of TRPML1 and what does its zinc-permeability have to do with lysosomal function or MLIV pathogenesis? Is the zinc

dyshomeostasis a secondary defect due to endocytosis and autophagy, or is it directly related to TRPML1 function? Could this zinc dyshomeostasis be related to MLIV pathogenesis? What signals modulate TRPML1 function? Furthermore, if lysosomes are the main degradative compartment of the cell, then why and how do they regulate cellular metal ion homeostasis? My research has provided insights into these questions and a broader understanding of TRPML1 and lysosomal function.

The first aim of my research was to determine the role of TRPML1 in zinc homeostasis. To this end, I have used the now well-established model system from our lab of siRNA-mediated knockdown of TRPML1 to address this question. These studies revealed that in the absence of TRPML1, lysosomes expand in size and accumulate zinc. The source of this zinc appears cytoplasmic and not endocytic or autophagic, since the zinc accumulation and lysosomal enlargement are dependent on the lysosomal zinc transporter ZnT4. Furthermore, TRPML1 appears to be a zinc leak pathway, transporting zinc from the lysosome into the cytoplasm. Reassuringly, the zinc dyshomeostasis observed in TRPML1 knockdown cells also occurs in MLIV patient fibroblasts, and these studies have begun to establish the zinc-binding protein, metallothionein 2A, as a biomarker for MLIV.

The second aim of my research was to understand why zinc accumulates in lysosomes. Many published studies have shown Zn^{2+} buildup in lysosomes and some have even identified the molecular machinery that transports zinc in and out of lysosomes. But, given the susceptibility of lysosomal damage and the grave consequences that this would ensue for cells, it was unclear why lysosomal zinc accumulation occurred in cells. I was able to address this question through the use of pharmacological and siRNA-mediated knockdown of the molecular machinery regulating these processes. These studies provided not only a novel zinc

detoxification pathway, as well as a toolbox for zinc secretion research, but also uncovered a deeper understanding and a new role for lysosomal exocytosis. Specifically, my analysis revealed that under moderate zinc exposure, lysosomes function as zinc sinks, temporarily sequestering higher zinc levels from the cytoplasm in order to avoid apoptosis. This zinc is then expelled out of the lysosomes through an excocytosis mechanism that is dependent on the lysosomal SNAREs VAMP7 and SYT7. However, under higher zinc loads, lysosomal zinc sequestration is overloaded, leading to lysosomal membrane permeabilization and cell death. Cumulatively, my thesis research has provided a detailed characterization of a number of factors involved in lysosomal zinc homeostasis.

2.0 ZINC-DEPENDENT LYSOSOMAL ENLARGEMENT IN TRPML1-DEFICIENT CELLS INVOLVES THE MTF-1 TRANSCRIPTION FACTOR AND ZNT4 (SLC30A4) TRANSPORTER

The work discussed in this Chapter has been adapted from published material and is reprinted, with alterations, by permission from the Biochemical Journal.:

Ira Kukic, Jeffrey K. Lee, Jessica Coblentz, Shannon L. Kelleher, and Kirill Kiselyov, "Zinc-dependent lysosomal enlargement in TRPML1-deficient cells involves the MTF-1 transcription factor and ZnT4 (Slc30a4) transporter." Biochemical Journal. 2013; 451: 155-163 © the Biochemical Society.

2.1 INTRODUCTION

Transition metals, including Zn^{2+}, are widely recognized for their toxic effects caused by acute and chronic exposures, albeit most of the transition metals are indispensable for proper cell function. Zn^{2+} has the widest repertoire of known biological roles, which include a cofactor in several enzymes and DNA-interacting proteins [12, 422]. Zn^{2+} deficiency, as well as excess, has been shown to be deleterious for cells [423, 424], prompting the need for tight regulation of its cellular levels. Such regulation is carried out by a system of transporters, chelating proteins and Zn^{2+} -sensitive transcriptional responses [91, 425, 426].

Zn^{2+} enters the body through enterocytes, primarily through Zip4, a member of the Zip (Slc39a) family of Zn^{2+} transporters [427, 428]. From the enterocyte cytoplasm, Zn^{2+} moves into the bloodstream through a series of transporters including those belonging to the ZnT (Slc30a) family [91, 429]. In general, Zip transporters are responsible for influx of Zn^{2+} into the cytoplasm, while ZnT transporters for its efflux. In the bloodstream, Zn^{2+} is taken up by cells via Zip transporters, and by the endocytosis of Zn^{2+} bound to plasma proteins. After entering the cytoplasm, Zn^{2+} is chelated by cytoplasmic proteins, such as metallothioneins (MTs) [430], and extracted into organelles or across the cell membrane by ZnT transporters. For example, ZnT2 and ZnT4 transporters are localized in intracellular vesicular compartments, including lysosomes. They play important roles in vesicular Zn^{2+} accumulation [431-433]. The reason for Zn^{2+} chelation and extraction is twofold. First, high levels of Zn^{2+} are damaging to cells [423, 424]. Second, a number of biological processes requiring Zn^{2+} take place inside organelles, necessitating Zn^{2+} transport across the organellar membranes [91, 434]. MTs also serve as Zn^{2+} reservoirs, releasing chelated Zn^{2+} under low- Zn^{2+} conditions [425].

The balance between ZnTs, Zips and MTs is responsible for the net Zn^{2+} flux and for the free cytoplasmic Zn^{2+} concentration in the given cell type. Zn^{2+} spikes, driven by variations in dietary Zn^{2+} uptake, are read by Zn^{2+}-responsive transcription factors including MTF-1, which binds cytoplasmic Zn^{2+} through its Zn^{2+}-finger motifs leading to its nuclear translocation [435]. Upon activation by cytoplasmic Zn^{2+}, MTF-1 induces the transcription of genes coding for MTs and some ZnTs, such as ZnT1 and ZnT2 [88, 436]. This feedback system allows cells to rapidly quench spikes in free cytoplasmic Zn^{2+}. The combined activity of Zn^{2+} transporters and chelators keeps free Zn^{2+} concentration in the nanomolar range.

The recent identification of Zn^{2+} permeability through the lysosomal ion channel TRPML1 [376] raised the possibility that this ion channel is involved in Zn^{2+} transport. This notion was later supported by the finding that Zn^{2+} builds up in the lysosomes of TRPML1-knockdown (KD) cells [393]. TRPML1 is an ion channel residing in the later portions of the endocytic pathway due to the presence of lysosomal localization signals on its C- and N-terminals [437, 438]. TRPML1 is encoded by the *MCOLN1* gene, which was identified as the gene mutated in the lysosomal storage disease mucolipidosis type IV (MLIV) [439, 440]. MLIV is associated with the buildup of cytoplasmic storage bodies, motor dysfunction and developmental delays [355, 441, 442]. The recent characterization of TRPML1 activation by $PI(3,5)P_2$ [388] suggested its activation by delivery to the $PI(3,5)P_2$-rich lysosomes and late endosomes [440]. The discussion of TRPML1 function has been focused on its role in the fusion of vesicles in the endocytic pathway (reviewed in [440]), and, recently, lysosomal secretion [273]. At the same time, the evidence of Fe^{2+} and Zn^{2+} permeability through TRPML1 [376] raises an interesting possibility that it plays a role in regulating cellular transition metal levels.

Here, we sought to delineate the mechanism through which TRPML1 participates in cellular Zn^{2+} homeostasis. We based our search on the assumption that if TRPML1 is directly involved in the regulation of Zn^{2+} transport, then, cellular Zn^{2+} trafficking and Zn^{2+} dependent processes should change as a function of TRPML1 status. Our assays show that both of these assumptions are true, strongly suggesting that TRPML1 is involved in the regulation of cellular Zn^{2+} homeostasis. We found that the effects of Zn^{2+} in TRPML1 KD cells included a characteristic lysosomal enlargement. The Zn^{2+}-sensing cytoplasmic transcription factor MTF-1 plays a key role in this process, as MTF-1 KD reversed Zn^{2+}-dependent lysosomal enlargement in TRPML1 KD cells. Suppressing the expression of the vesicular Zn^{2+} transporter ZnT4

eliminated the Zn-induced lysosomal enlargement and Zn^{2+} retention in TRPML1-deficient cells. Pulse-chase experiments with extracellular Zn^{2+} show that Zn^{2+} clearing from vesicular structures including lysosomes is delayed in TRPML1 KD cell. However, Zn^{2+} secretion was not decreased in these cells; instead, it was somewhat increased. We conclude that TRPML1 works in concert with ZnT4, to regulate lysosomal Zn^{2+} trafficking, perhaps by providing a lysosomal Zn^{2+} leak pathway. This is supporting evidence of the novel role of TRPML1 in regulating cellular transition metals and TRPML1 as a new target in transition metals toxicity.

2.2 EXPERIMENTAL METHODS

2.2.1 Cell Culture

HeLa cells were maintained in DMEM (Sigma-Aldrich, St Louis, MO) supplemented with 7% FBS, 100 μg/ml penicillin/streptomycin, and 5 μg/ml Plasmocin prophylactic (Invivogen, San Diego, CA). For siRNA and cDNA transfection, antibiotic free media was used. Metals were added directly to the DMEM. Zn^{2+} (100 μM) was added to antibiotic free medium, containing serum, 24 hrs after transfection, for 48 hrs.

2.2.2 siRNA-mediated KD and plasmid transfection

ON-TARGET plus siRNA were designed as described previously [387, 443] and synthesized by Dharmacon (Lafayette, CO). The TRPML1 siRNA probe targeting the sequence 5'-CCCACATCCAGGAGTGTAA-3' in *MCOLN1* was used for all TRPML1 KDs. The MTF-1

siRNA (Cat number SASI_Hs01_00177112), ZnT2 siRNA (Cat number SASI_Hs01_00055662), and ZnT4 siRNA (Cat number SASI_Hs00225995) were from Sigma. Non-targeting control siRNA#1 (Sigma) was used as a negative control. Cells were transfected using Lipofectamine 2000 (Invitrogen, Carlsbag, CA) as described by manufacturer's protocol using 600 nM siRNA per 35 mm well. All KDs were confirmed using SYBR-green based qPCR. For DNA transfections, 2 μg of HA-tagged human ZnT2 or ZnT4 were used in parallel with 1 μg of GFP tagged TRPML1 constructs.

2.2.3 Reverse Transcriptase and Quantitative qPCR

RNA was isolated from cells using Trizol (Invitrogen) according to the manufacturer's protocol. cDNA was synthesized using the GeneAmp RNA PCR system (Applied Biosystems, Carlsbad, CA) with oligo dT priming. qPCR was performed SYBR green (Fermentas, Glen Burnie, MD). The amount of cDNA loaded was normalized to starting RNA concentrations, with a final concentration of 9 ng (40 ng in ZnT experiments) of RNA loaded per experimental well. Six-point standard curves were generated for each primer using 1:2 dilutions of cDNA. cDNA for the following genes were amplified using the indicated primers (IDT, Coralville, IA).

MCOLN1: forward: 5'-TCTTCCAGCACGGAGACAAC-3',

reverse: 5'-AACTCGTTCTGCAGCAGGAAGC-3'.

MT2a: forward: 5'-AAGTCCCAGCGAACCCGCGT-3',

reverse: 5'-CAGCAGCTGCACTTGTCCGACGC-3'.

MTF-1: forward: 5'-GCCATTTCGGTGCGATCACGAT-3',

reverse: 5'-TTTCACCAGTATGTGTACGAACGTGAGT-3'.

ZnT2 (SLC30A2): forward: 5'-GCAATCCGGTCATACACGGGAT-3',

reverse: 5'- CAGCTCAATGGCCTGCAAGT-3'.

ZnT4 (SLC30A4): forward: 5'- CACATACAGCTAATTCCTGGAAGTTCATCT-3',

reverse: 5'- GCCTGTAACTCTGAAGCTGAATAGTACAT-3'.

All primers were designed to span exons and negative RT controls were tested to ensure amplification of cDNA only. qPCR was performed using the Standard Curve method on the 7300 Real Time System (Applied Biosystems). Reactions were run on the following parameters: 2 min at 50°C, 10 min at 95°C, and 40 cycles at 95°C for 15 sec followed by 60°C for 1 min. All experimental samples were run in triplicate and normalized to a β-actin endogenous control.

2.2.4 Microscopy

Cells were seeded on glass coverslips and loaded with dyes for 15 min at 37ºC in buffer containing, in mM: 150 NaCl, 5 KCl, 1 $CaCl_2$, 1 $MgCl_2$, 10 HEPES, pH 7.4, 1 g/L glucose. The loading was followed by 15 min washout in all cases except TSQ. Lysotracker Red DND-99, FluoZin-3,AM, TSQ (Sigma) were used at 0.1, 0.1, and 150 μM respectively. Confocal microscopy was performed using Leica TCS SP5 and BioRad 3000 confocal microscopes. Live cells were treated as above. For colocalization experiments, cells were fixed for 5 min in 4% paraformaldehyde at room temperature and permeabilized using 0.1% Triton X100 for 5 min on ice. Following washout and blocking in BSA and goat serum, cells were treated with primary anti-HA antibody (Roche, 12CA5) overnight. Cells were then incubated in fluorescent-tagged secondary antibodies for 1 hr. Images were analyzed using ImageJ (Bethesda, MD).

2.2.5 β-Hexosamindase activity assay

Untreated control and TRPML1 siRNA-transfected cells were washed with 37ºC PBS and 1 mL 37ºC serum-free DMEM was added to each 35mm dish. For each sample, 100 µl of the supernatant was incubated with 400 µl 1mM 4-nitrophenyl N-acetyl-β-D-glucosaminide (Sigma, N9376) for 1 hour at 37ºC in 0.1M citrate buffer (pH 4.5) (Sigma, C2488). This volume was replaced with fresh 37ºC 100 µl of DMEM to the dish. Samples were collected every hour for 4 hours. Reactions were stopped by adding 500 µl borate buffer (100 mM boric acid, 75 mM NaCl, 25 mM sodium borate, pH 9.8) and the absorbance was measured in a spectrophotometer at 405 nm. To determine total cellular content of β-hexosamindase, cells were lysed with 1mL 1% Triton X-100 and after a 10000g spin for 5 minutes at 4ºC, 100 µl of the cell extracts were used for the enzyme activity reaction. Enzyme activity was determined as the amount of 4-nitrophenol produced per mg of protein (Bradford method). Absorbance was calibrated with different amounts of 4-nitrophenol (Sigma, N7660) in 0.1 M citrate buffer.

2.2.6 Zinc secretion assay

Control, TRPML1 and MTF1 siRNA-transfected cells were plated on a 12 well plate and after 48 hours, pulsed with 100 µM Zn for 3 hours, washed twice with warm PBS, and chased in 1mL DMEM per well. Duplicate time-points were collected for 0, 5, 15, 30 or 60 minutes. For each sample, 50 µl of supernatant was placed in a 96-well plate. Zn content was measured by incubating the supernatants with 10 µM cell-impermeant FluoZin-3 tetrapotassium salt (Molecular Probes, Invitrogen F-24194) for 15 minutes at 37^{o}C. The 96-well plate was read via a FujiFilm FLA-5100 fluorescent image analyzer. After the last time point, cells were washed with

PBS, 200 µl detergent solution was added to lyse the cells and fluorescence was normalized to total protein in each sample.

Statistical significance was calculated using a one-tailed, unpaired t-test with $p \leq 0.05$ considered significant. Data are presented as mean±S.E.M.

2.3 RESULTS

2.3.1 Zinc-dependent lysosomal enlargement in TRPML1 KD cells

Since Zn^{2+} dyshomeostasis has been reported in TRPML1-KD cells [393], we sought to delineate mechanisms linking TRPML1 loss, Zn^{2+} dysregulation, and vacuolar enlargement in TRPML1-KD cells. In order to test how TRPML1 loss affects cells exposed to Zn^{2+}, we used TRPML1-specific siRNA described before [387, 443]. The siRNA-mediated KD resulted in more than 85% KD of TRPML1 mRNA, as confirmed by qPCR with TRPML1 specific primers (Figure 7). In the previous studies utilizing the same system, the same siRNA resulted in almost complete elimination of TRPML1 protein, within the same time scale [387, 443].

TRPML1 KD cells were previously reported to contain enlarged Zn^{2+}-positive organelles [393]. We performed live-cell confocal analysis of control and TRPML1-KD HeLa cells stained with the Zn^{2+} selective dyes TSQ and FluoZin-3,AM, in conjunction with the lysosomal dye Lysotracker. Figure 8 A shows that, while Zn^{2+} is barely detectable in Lysotracker-positive compartments in untreated control cells, such compartments displayed TSQ fluorescence in cells treated with 100 µM Zn^{2+} for 48 hrs. We did not consistently detect enlarged Lysotracker-positive compartments in TRPML1-KD cells until these cells were treated with Zn^{2+}. Following

Zn^{2+} treatment, large compartments positive for Zn^{2+} (TSQ) and Lysotracker were abundant in TRPML1 KD cells (Figure 8A). Figure 8B shows similar analysis of Zn^{2+} in control and TRPML1-KD cells, performed using Lysotracker and another Zn dye, FluoZin-3,AM. The enlarged Lysotracker-positive vesicles in Zn^{2+} treated TRPML1-KD cells also displayed bright FluoZin-3 fluorescence, consistent with high concentrations of Zn^{2+}. Interestingly, FluoZin-3 signal was also detected in Lysotracker-negative vesicles, consistent with our previous observations of non-lysosomal Zn^{2+} pools in mammary cells [444, 445], which was more commonly observed in Zn^{2+}-treated TRPML1-KD cells than in Zn^{2+}-treated control cells (Figure 7B). The lysosomal enlargement trend in Zn^{2+}-treated TRPML1-KD cells persisted over 96-hr period (not shown).

The fact that TRPML1-KD cells treated with Zn^{2+} and stained with TSQ show cytoplasmic fluorescence (Figure 8A), while FluoZin-3,AM-stained cells do not (Figure 8B), can be explained by the nature of these dyes' fluorescence and interaction with Zn^{2+}. In the cytoplasm, Zn^{2+} is bound to proteins such as MTs and very little Zn^{2+} is present in free ion form. MTs bind large amounts of Zn^{2+} (up to 7 ions per molecule), with very high affinity (pM range) [446]. Both TSQ and FluoZin-3 are sensitive to Zn^{2+} in mid- to high-nanomolar range. However, unlike FluoZin-3, which only fluoresces when bound to more labile Zn^{2+}, TSQ fluoresces even when in a complex with metalloproteins such as MT-Zn [447, 448]. Therefore, the difference between TSQ and FluoZin-3 stains may reflect large amounts of Zn^{2+} ions bound in Zn^{2+}-treated TRPML1-KD cells to cytoplasmic proteins such as metallothionein 2a (MT2a).

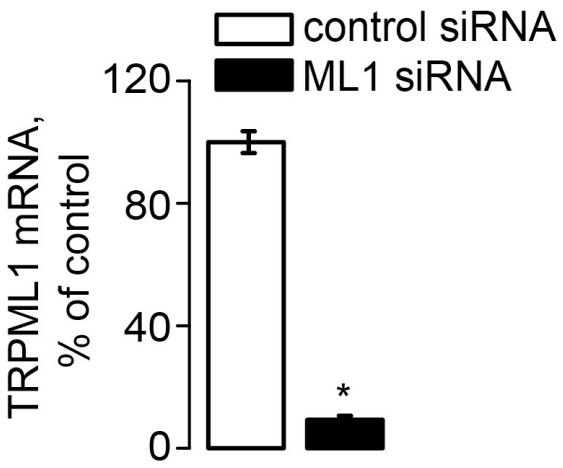

Figure 7. siRNA-mediated TRPML1 KD.

qPCR results demonstrating TRPML1 KD. mRNA levels are expressed as percentile of control levels. Represents 6 experiments. * represents $p<0.05$.

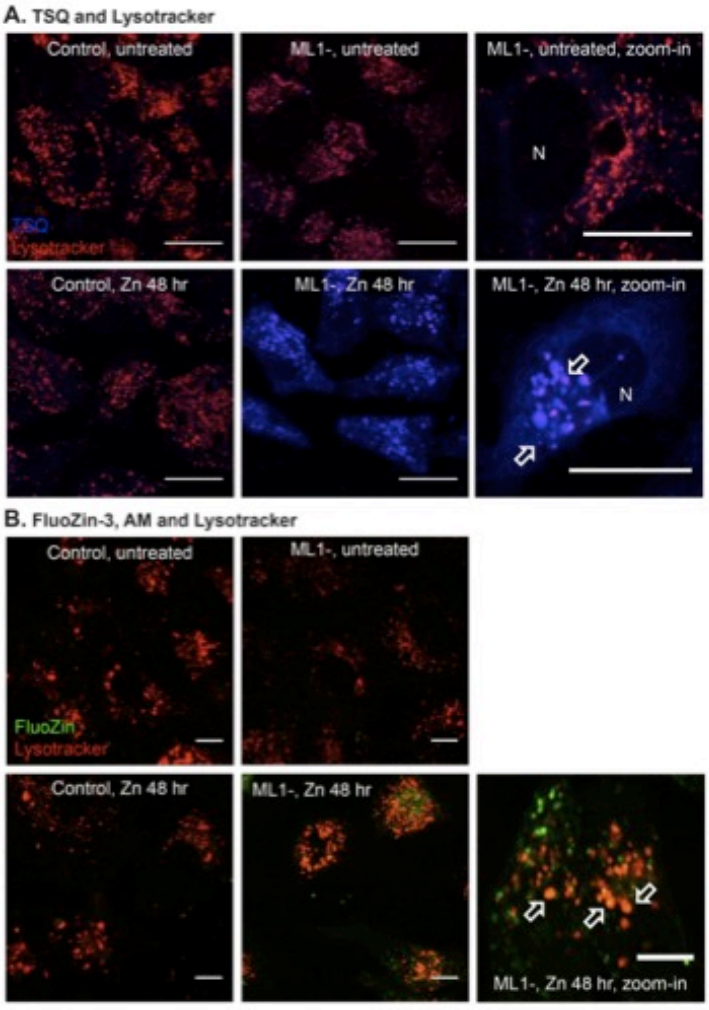

Figure 8. Zn^{2+} accumulation and enlargement of Lysotracker positive compartments in TRPML1-deficient Zn^{2+} treated cells.

Confocal images of HeLa cells stained with Lysotracker and with TSQ (A) or FluoZin-3,AM (B). **A**. Cells costained with Lysotracker and TSQ. Control cells were transfected with scrambled siRNA. TRPML1 KD cells (ML1-) were transfected with TRPML1 siRNA, and treated with Zn^{2+} 24 hrs later. Zn^{2+} treatment took place over 48-hr period. N indicates nuclei; arrows point to enlarged Lysotracker and TSQ-positive compartments. Note enlargement of Lysotracker-positive compartments and presence of bright TSQ fluorescence inside them. **B**. Similarly treated cells costained with Lysotracker and FluoZin-3,AM. Each panel represents 3-5 individual experiments. Arrows point to Lysotracker positive compartments showing bright FluoZin-3 fluorescence. Scale bars are 20 μm.

Using Lysotracker fluorescence images, we calculated the average gain in the lysosomal size in Zn^{2+}-treated TRPML1-KD cells. The same Lysotracker concentration, laser intensity, pinhole and gain values were used throughout the experiments. The grey-scale Lysotracker images were filtered using 50% intensity threshold yielding binary black-and-white images, which were then treated using Watershed segmentation algorithm implemented as an ImageJ plugin (Figure 9A). Large clusters of signal not resolved using this algorithm were manually eliminated (Figure 9B). Next, the ImageJ "Analyze particles" algorithm was used, which yielded numbers and sizes of Lysotracker-positive particles in each image (Figure 9C). For particle counting the following options were used: minimal size 0.09 μm^2, minimal circularity was 0.5. The same algorithm was used in all subsequent analysis in this paper.

Zn^{2+}-treated TRPML1-KD cells showed a tendency towards increasing the number of larger Lysotracker-positive particles (Figure 10). In Zn^{2+}-exposed TRPML1-KD cells, lysosomes were approximately 80% larger than in Zn^{2+}-exposed control cells or in untreated TRPML1-KD cells (Figure 11). Lysotracker-positive particles in Zn^{2+}-treated TRPML1-KD cells averaged 176.15±12.50% (8 independent experiments, 3-5 images each, 1-3 cells on each image, 214 to 573 Lysotracker-positive particles in each experiment, $p<0.05$ relative to control) of the average size of individual lysosomal areas in Zn^{2+}-treated control siRNA-transfected cells (100±4%, 8 independent experiments, 3-5 images each, 1-3 cells on each image, 99 to 1100 Lysotracker-positive particles in each experiment). The use of threshold preserves the relative sizes of compartments, but makes evaluation of their absolute sizes unreliable. With this reservation in mind, the average size of Lysotracker-positive compartment in Zn^{2+}-treated control cells was 2.09±0.30 μm^2 (statistics as above; two experiments were omitted from this analysis due to different microscope settings). In TRPML1-KD Zn^{2+}-treated cell it was 3.56±0.51 μm^2. Beyond

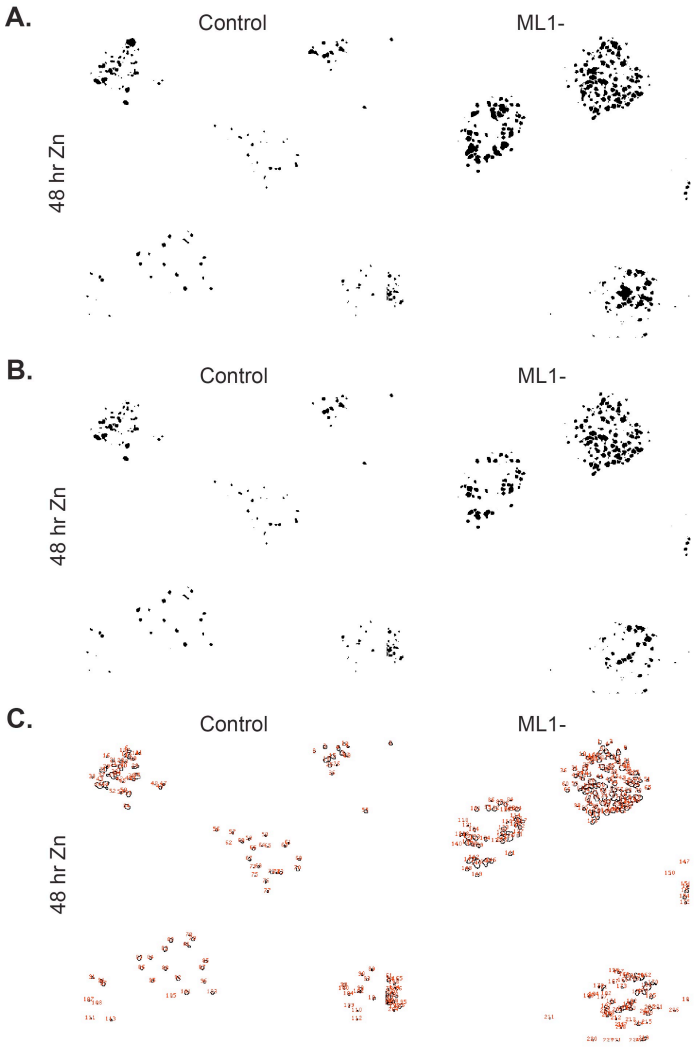

Figure 9. Analysis of lysosomal enlargement in TRPML-KD cells exposed to Zn^{2+}.

Image analysis of lysosomal sizes. **A.** Confocal images of Lysostracker-stained cells from Fig 7B were subjected to 50% maximal integrity threshold in ImageJ yielding black-and-white binary images. Next, the ImageJ watershed function was used. **B.** The binary images were compared to the original images and areas containing unresolved clumps of lysosomes were eliminated. **C.** The images were analyzed using "Analyze particles" function with 0.09 μm^2 minimal area threshold and the minimal circularity threshold of 0.5. Red characters represent numbering of the individual particles.

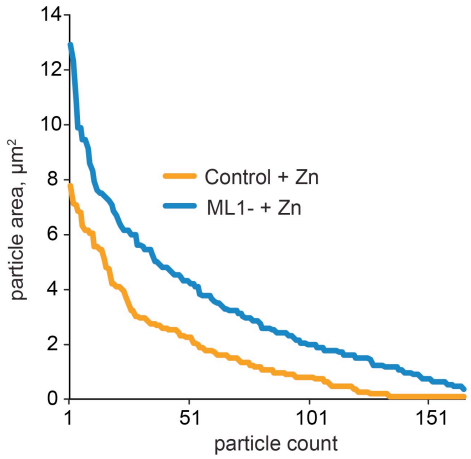

Figure 10. An example of lysosomal enlargement in Zn^{2+}-treated TRPML1-KD cells.

Confocal images of HeLa cells stained with Lysotracker and analyzed as in Fig 8. Particle area sizes (in μm^2) were calculated, sorted in descending order and plotted against number corresponding to each particle. Note an increase in number of larger particles in TRPML1-KD cells exposed to Zn^{2+}.

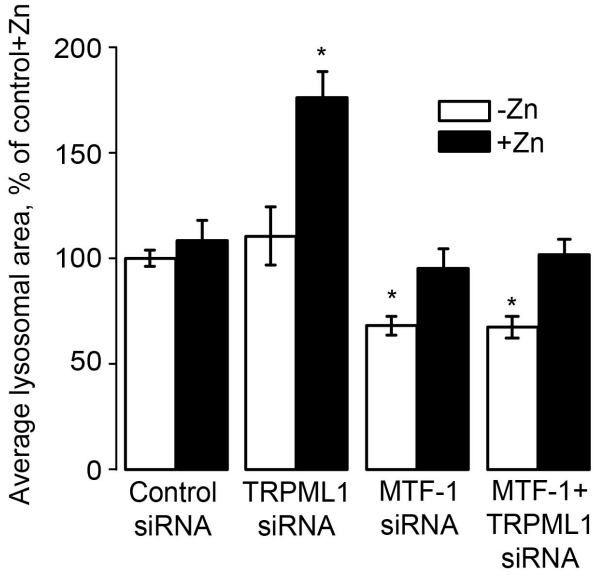

Figure 11. Statistical analysis of lysosomal enlargement in TRPML1-deficient, Zn^{2+}-treated cells.

Average lysosomal particle area in control, MTF-1 siRNA-transfected and TRPML1 siRNA-transfected cells under untreated (hollow) and 48 hr Zn^{2+}-treated (shaded) conditions. Lysotracker confocal images of Fluozin-3,AM experiments were thresholded at 50% and particle size area calculated for each experiment using ImageJ. Represents 3-5 separate experiments. See main text for details of analysis and statistics. * represents $p<0.05$ relative to control sample. MTF-1+TRPML1 siRNA denotes cells transfected with mixture of MTF-1 and TRPML1 siRNA.

agreeing with the previous report on Zn^{2+} buildup in TRPML1-KD cells [393], these data suggest that in the absence of TRPML1, a Zn^{2+}-dependent process leads to the enlargement of Lysotracker-positive (ostensibly lysosomal) compartments. Ni^{2+}, used at the same concentration, did not induce lysosomal enlargement (Figure 12), suggesting that this aspect of TRPML1 KD phenotype is Zn^{2+}-specific.

These data confirm, in a different system, the previous findings on lysosomal enlargement and Zn^{2+} retention in TRPML1-KD cells [393]. A logical question following observation of this phenomenon is the source and means of Zn^{2+} buildup in the lysosomes of TRPML1-KD cells. Since Zn^{2+} is retained by the lysosomes in TRPML1-KD cells, TRPML1 must be involved in the clearance of Zn^{2+} from the lysosomes. Where does the Zn^{2+} retained in TRPML1-KD cells come from? Zn^{2+} retained by the lysosomes 1) may come through endocytosis, or 2) may be taken up by cells through cell membrane transporters and then exported into lysosomes across their membranes. In both cases TRPML1 dissipates Zn^{2+} accumulation. The difference between the two scenarios is that the latter entails 1) a lysosomal Zn^{2+} transporter that works in concert with TRPML1 to regulate Zn^{2+} traffic between cytoplasm and lysosomes, and 2) dependence of the lysosomal Zn^{2+} accumulation in TRPML1-KD cells on a cytoplasmic step.

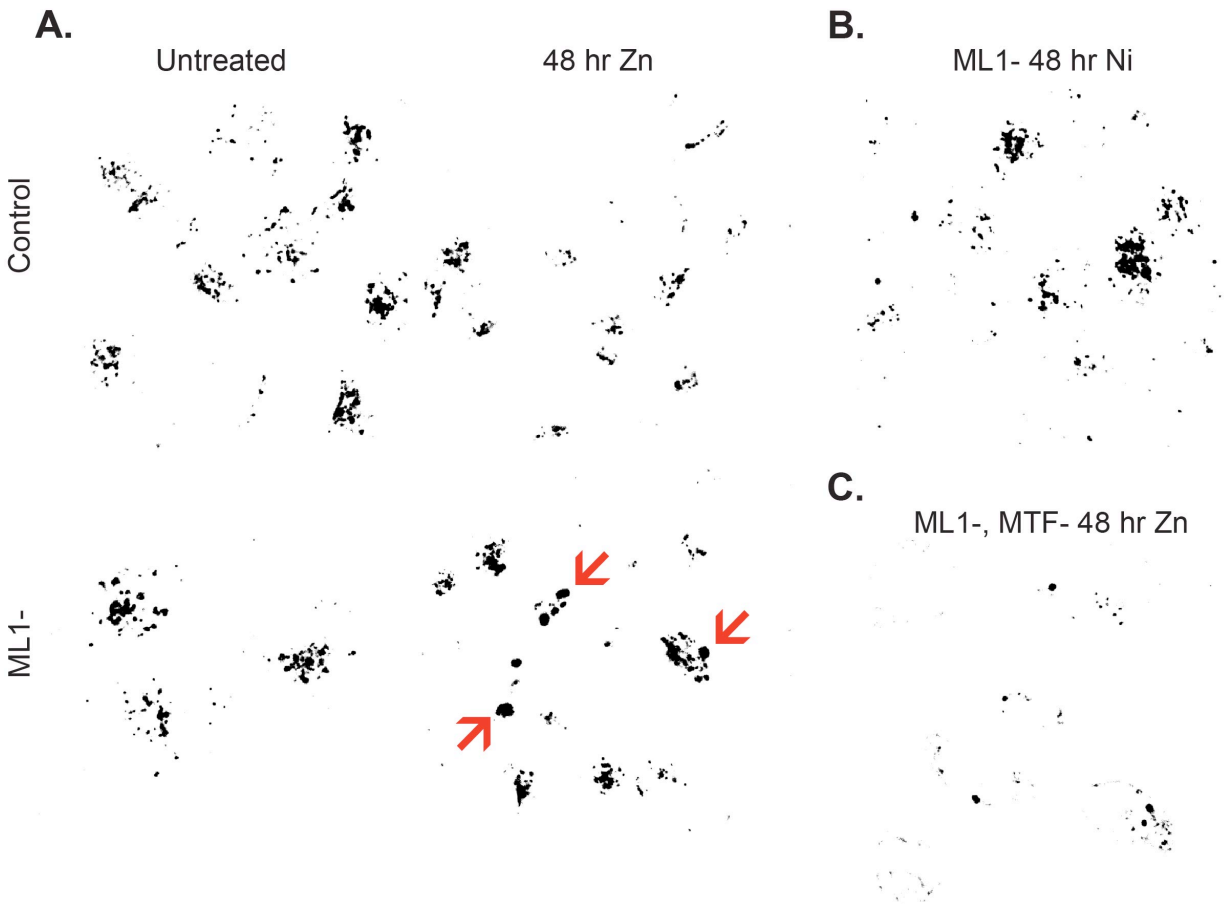

Figure 12. Lysosomal enlargement is Zn^{2+}- and MTF-1–specific.

Confocal images of HeLa cells stained with Lysotracker, thresholded at 70% of maximal pixel intensity value. Cells not completely present within the field of view were removed from the image. Each image represents 3 experiments, 3-5 images per experiment per condition. **A.** Lysosomes in control and TRPML1 siRNA-transfected cells under untreated (left) and 48 hr Zn^{2+} treated (right) conditions. **B.** TRPML1 siRNA transfected cells treated with 100 μM Ni^{2+} for 48 hrs. **C**. TRPML1 and MTF1 siRNA transfected cells treated with Zn^{2+}.

2.3.2 The role of MTF-1 in lysosomal enlargement

Cytoplasmic Zn^{2+} is tightly regulated, and therefore, the expression of proteins involved in Zn^{2+} maintenance is managed by Zn^{2+}-dependent transcription factors such as MTF-1. Zn^{2+} binding to MTF-1, followed by MTF-1 nuclear import leads to the expression of proteins involved in Zn^{2+} handling, such as MTs. Their mRNA levels can thus be used to monitor cytoplasmic Zn^{2+} levels.

Figure 13A shows a successful siRNA mediated knockdown of over 90% of MTF-1 mRNA in untreated cells. This effect had a clear physiological significance, as MTF-1 KD severely suppressed mRNA levels of MT2a, which is the most ubiquitous and best described MT, well known to be regulated by MTF-1 (Figure 13B). In unstimulated cells, MTF-1 siRNA decreased MT2a mRNA levels to 19.12±5.71% of control levels ($n=3$, $p<0.05$). This established a toolkit for testing the role of MTF-1 in TRPML1-dependent effects of Zn^{2+}.

MTF-1 suppression eliminated the buildup of enlarged vacuoles in TRPML1 KD cells (Figures 11, 12, and 13C). In the double TRPML1/MTF-1–KD Zn^{2+}-treated cells, the average lysosomal area was 101.78±7.06% (3 independent experiments, 3-4 images each, 1-3 cells on each image, 127 to 1035 Lysotracker-positive particles in each experiment) of its value in Zn^{2+}-treated control cells, a statistically indistinguishable value. These data suggest that these TRPML1-dependent aspects of Zn^{2+} phenotype in HeLa cells are mediated by MTF-1. The fact that suppression of a Zn^{2+}-dependent step in the cytoplasm eliminates lysosomal enlargement and Zn^{2+} retention in TRPML1-KD cells strongly suggests that the source of Zn^{2+} retained in TRPML1-deficient lysosomes is not mediated through endocytosis, but is derived directly from a cytoplasmic route. This route is discussed below. We asked whether dysregulation of this route affects cytoplasmic Zn^{2+} and which Zn^{2+} transporters are involved in this process.

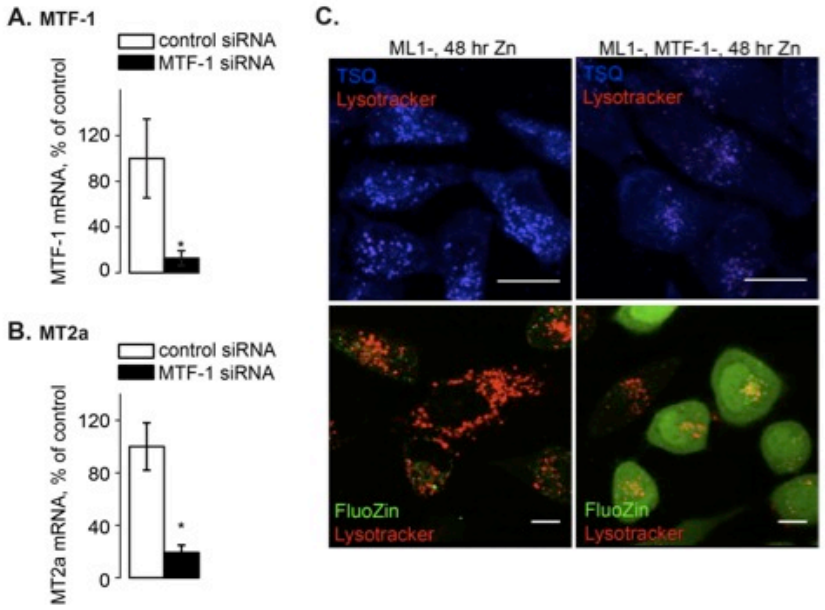

Figure 13. MTF-1 is involved in the enlargement of Lysotracker positive compartments in Zn^{2+}-treated TRPML1 deficient cells.

A. qPCR results demonstrating MTF-1 KD by siRNA**. B**. qPCR results showing MT2a suppression in cells treated with MTF-1 siRNA. Data points in Panels A and B represent 3 individual experiments, each performed in triplicate. * represents $p<0.05$. **C**. Confocal images of cells costained with Lysotracker and TSQ (top panels) or FluoZin-3 showing that Lysotracker positive compartments are no longer enlarged in Zn^{2+}-treated cells when MTF-1 is suppressed alongside TRPML1. Represents 3 experiments. Scale bars are 20 μm.

2.3.3 The MT2a mRNA response in TRPML1 KD cells

As discussed above, the presence of a cytoplasmic Zn^{2+}- and TRPML1-dependent process suggests that the expression of Zn^{2+}-dependent genes in cells exposed to Zn^{2+} is also affected by TRPML1 activity. In this regard, MTF-1/ Zn^{2+}–dependent genes can be used as cytoplasmic Zn^{2+} reporters. In order to test this idea, we first screened mRNA levels of a well-known MTF-1-

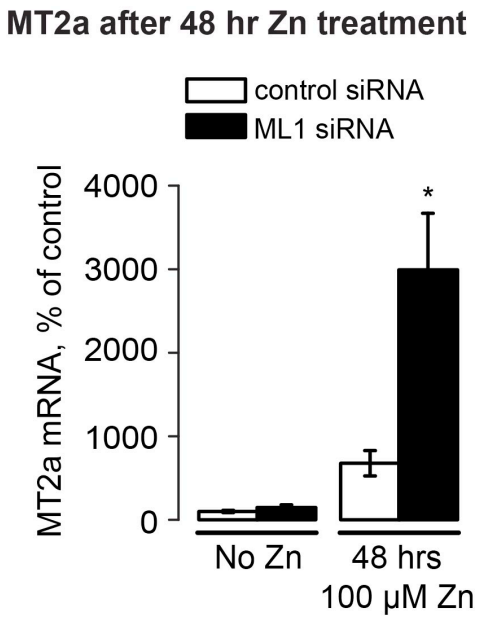

Figure 14. MTF-1 is involved in the enlargement of Lysotracker positive compartments in Zn^{2+}-treated TRPML1 deficient cells.

MT2a response to Zn^{2+} changes is amplified in TRPML1-deficient cells. qPCR results showing augmented MT2a mRNA response to 48-hr long treatment with Zn^{2+} in TRPML1 KD HeLa cells, compared to HeLa cells transfected with scrambled siRNA. Represents 3 individual experiments, each performed in triplicate. * represents $p<0.05$.

dependent gene product, MT2a. Figure 14 shows that upregulation of MT2a mRNA in response to Zn^{2+} is significantly augmented in TRPML1-KD cells, compared to cells transfected with control siRNA. In control cells, 48-h stimulation with Zn^{2+} increased MT2a mRNA levels to 676.8±152.3% of control levels ($n=3$, $p<0.05$), while in TRPML1-KD cells, the response to Zn^{2+} was significantly greater (2992.7±678.5% of control levels; $n=3$, $p<0.05$). We conclude that a Zn^{2+} handling deficit in TRPML1-KD cells leads to a persistent dysregulation of Zn^{2+} management.

It should be noted that, in our system, the difference in MT2a mRNA response is only seen under Zn^{2+} exposure (Figure 14) and not under the basal conditions. Therefore, the upregulation of MT2a mRNA is a reaction to the change in cytoplasmic Zn^{2+} buffering in the absence of TRPML1. Together with the MTF-1 KD assays, these experiments established that the lysosomal Zn buildup and enlargement in TRPML1-KD cells depend on a cytoplasmic step, and that TRPML1 loss increases cytoplasmic Zn^{2+} (also consistent with the data shown in Figure 8). We propose that TRPML1 works in concert with a lysosomal Zn^{2+} transporter to maintain normal Zn^{2+} levels in the cytoplasm and in the lysosomes. The loss of such concerted activity leads to cytoplasmic and lysosomal Zn^{2+} buildup. Next, we set out to identify such a transporter.

2.3.4 ZnT4 KD rescues zinc-dependent lysosomal enlargement in TRPML1 KD cells

Of the Slc30 (ZnT) family, ZnT2, ZnT3, ZnT4 and ZnT8 have been implicated in Zn^{2+} loading within endocytic compartments [449-451]. However, ZnT3 and ZnT8 expression seems to be restricted to brain and pancreas [104, 452]. For this reason, ZnT2 and ZnT4 became the first target of our investigation. Recombinant ZnT2 and ZnT4 both partially colocalized with TRPML1 (Figure 15), indicating that they might work in concert with TRPML1. If either ZnT2 or ZnT4 are necessary for the TRPML1-dependent aspect of Zn^{2+} homeostasis, then KD should affect the Zn^{2+} phenotype in TRPML1-KD cells. The predicted direction of Zn^{2+} transport through ZnT transporters is into the lysosomes. Therefore, a ZnT KD should negate the effects of TRPML1 KD. We chose to modulate ZnT levels using siRNA.

Figure 16A shows a qPCR confirmation of ZnT2 and ZnT4 KD (over 70% and 95% control mRNA levels in untreated cells, respectively). ZnT2 siRNA decreased ZnT2 mRNA

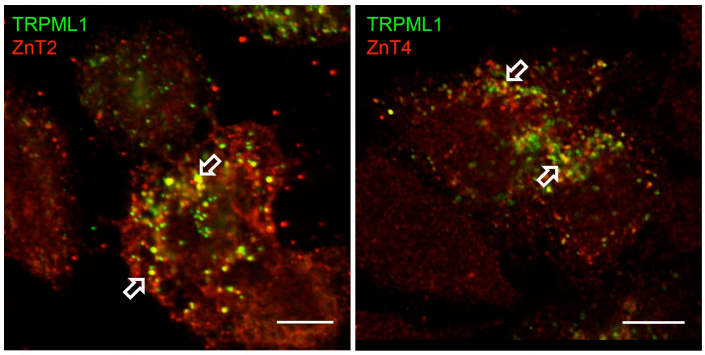

Figure 15. ZnT2 and ZnT4 colocalize with TRPML1

Confocal images of HeLa cells transfected with HA-tagged ZnT2 or ZnT4 constructs (in red) in parallel with a GFP-tagged TRPML1 construct (in green). Panel represents 3 separate experiments, 3 images per experiment, per condition. Merged images showing colocalization (yellow) of the HA- and GFP-tagged constructs. Cells were transfected for 24 hrs and not treated with Zn^{2+}.

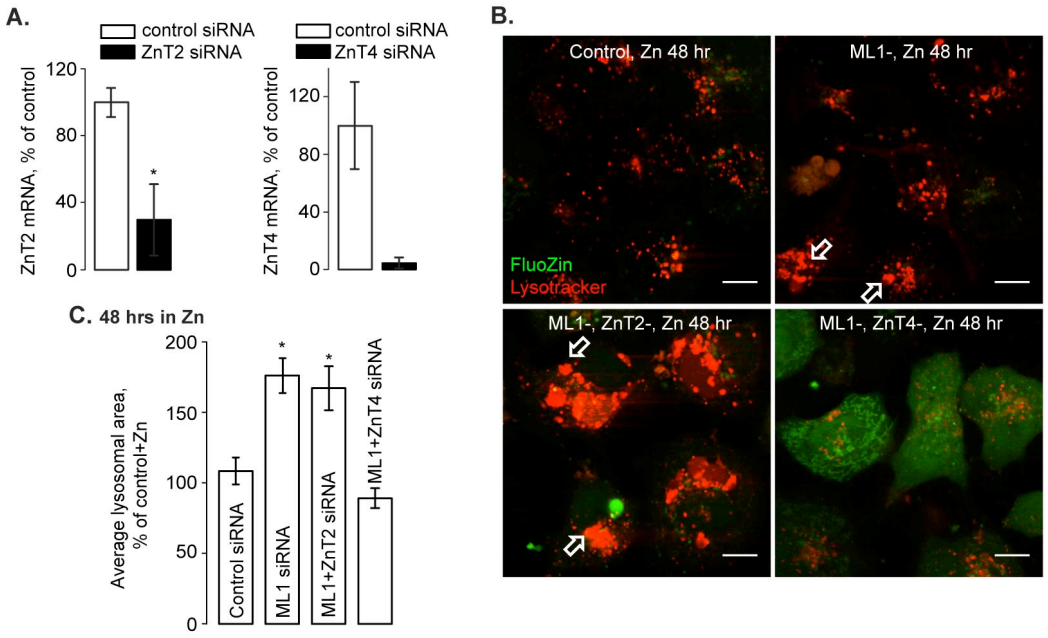

Figure 16. ZnT4 knockdown rescues enlarged lysosomes under TRPML1 suppression.

A. qPCR results showing ZnT2 and ZnT4 KD by siRNA. Data points represent 3 individual experiments, each performed in triplicate. * represents $p<0.05$. **B**. Confocal images of HeLa cells treated with 100 μM Zn^{2+} for 48 hrs,

and stained with Lysotracker (red) and FluoZin-3,AM (green). Cells were transfected with different siRNA constructs and treated with Zn^{2+} 24 hrs later. Merged confocal images show localization of Zn^{2+} and lysosomes in cells transfected with control siRNA, TRPML1 siRNA (ML1-), TRPML1 and ZnT2 siRNA, or TRPML1 and ZnT4 siRNA. Represents 3 individual experiments, 3 images per experiment, per condition. Note enlarged lysosomes present in Zn^{2+} treated TRPML1-deficient cells with and without ZnT2. Note the marked reduced size of lysosomes in ZnT4 KD cells, even under TRPML1 suppression. Scale bars are 20 μm.

levels to 29.88±21.31% of control levels (n=3, $p<0.05$), while ZnT4 siRNA decreased ZnT4 mRNA levels to 4.36±3.73% of control levels (n=3, $p<0.05$). siRNA-mediated KD of ZnT4, but not ZnT2 rescued lysosomal swelling and lysosomal Zn^{2+} buildup in Zn^{2+}-treated TRPML1 KD cells (Figure 16 B,C). In the double TRPML1/ZnT4–KD cells exposed to Zn^{2+}, the average lysosomal area fell to about 50% of the value reported in TRPML1-KD cells. It averaged 89.06±7.08% of the lysosomal size in control, untreated cells (4 independent experiments). In double TRPML1/ZnT2–KD cells, it remained largely the same as in TRPML1-KD cells exposed to Zn^{2+} (167.22±15.71% of control cells, 4 independent experiments, $p<0.05$). The fact that ZnT4 KD abolished lysosomal enlargement under TRPML1 suppression has a clear physiological significance because it identifies the lysosomal Zn^{2+} transporter that, in concert with TRPML1, forms a lysosomal "Zn^{2+} sink," which absorbs the cytoplasmic Zn^{2+} (Figure 17). In direct agreement with this, Zn^{2+}-treated TRPML1- and ZnT4-KD cells have large amounts of Zn^{2+} within the cytoplasm compared to ZnT2 KD (Figure 16B). Whether or not this phenomenon is specific to HeLa cells remains to be established, but this is consistent with Zn^{2+} accumulation in lysosomes in ZnT4-overexpressing mammary cells [444]. We would like to note that the triple TRPML1/ZnT2/ZnT4 KD was extremely cytotoxic even at the control conditions, which precluded its analysis.

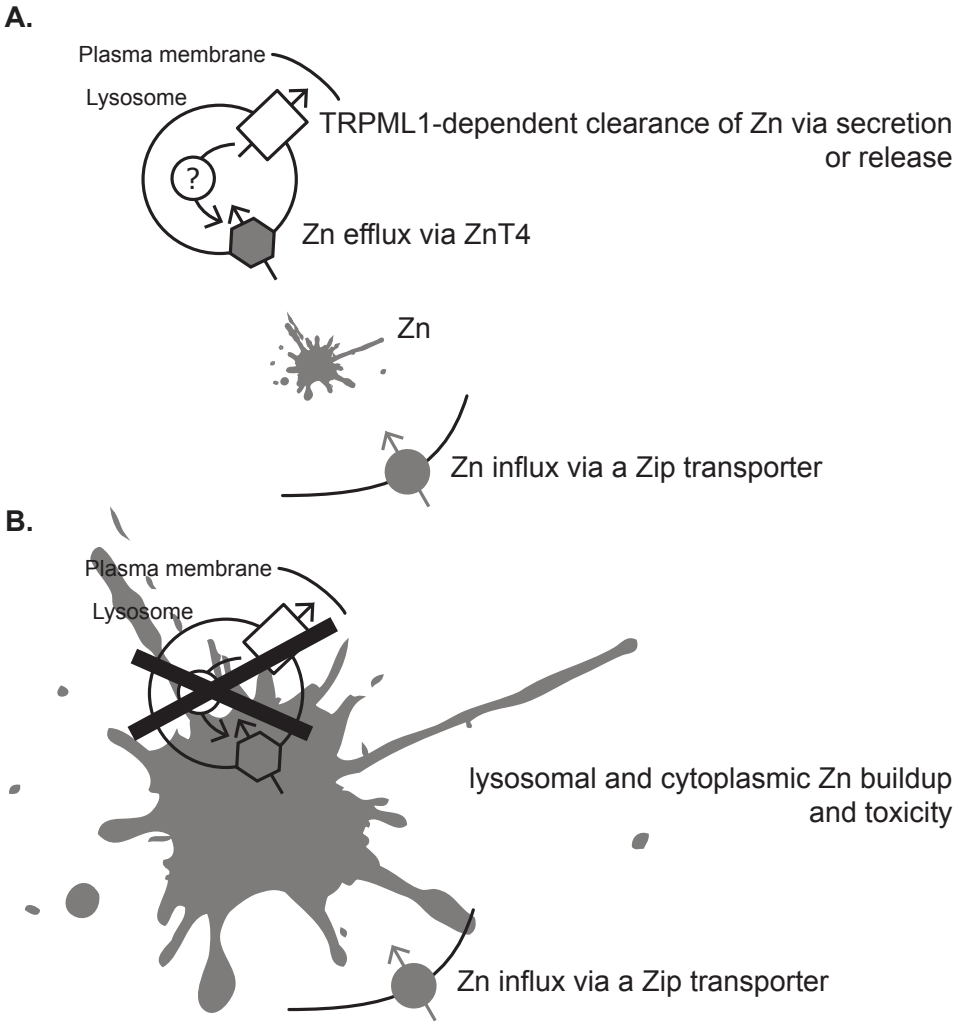

Figure 17. **A model of "Zn^{2+} sink".**

A. Under the normal conditions, Zn^{2+} entering the cytoplasm is sequestered into lysosomes by ZnT4 (and perhaps ZnT2 in some tissues). Lysosomal Zn^{2+} is released or secreted via a TRPML1-dependent process. TRPML1 may also regulate ZnT activity (denoted by "?"). **B**. The loss of "Zn^{2+} sink" function leads to lysosomal and cytoplasmic Zn^{2+} buildup.

2.3.5 Zinc secretion and lysosomal zinc leak in TRPML1 KD cells

The data described above suggest that ZnT4 loads lysosomes with Zn^{2+} and that in the absence of TRPML1, Zn^{2+} is trapped in the lysosomes. Furthermore, clearance of Zn^{2+} from the lysosomes in TRPML1-KD cells was delayed, compared to control cells (Figure 18). The reason for Zn^{2+} retention in TRPML1-deficient lysosomes was the subject of our next set of experiments.

TRPML1 has been implicated in lysosomal secretion. Therefore, it is possible that suppression of the lysosomal secretion due to TRPML1 loss traps Zn^{2+} in the lysosomes. Alternatively, it is possible that TRPML1 is lysosomal Zn^{2+} channel, responsible for the Zn^{2+} leak from lysosomes into the cytoplasm. The role of TRPML1 in Zn^{2+} secretion was analyzed using two assays. The premise of this experiment was: if Zn^{2+} retention in the TRPML1-KD cells is due to retarded secretion, then Zn^{2+} secretion in TRPML1-KD cell will be significantly lower than in control cells. This is directly addressed in Figure 19A. We measured Zn^{2+} release from Zn^{2+}-preloaded control and TRPML1 KD-cells using FluoZin-3 tetrapotassium salt. Cells, grown on 12-well plates, were incubated in culture medium with 100 μM Zn^{2+} for 3 hr (pulse). Next they were washed in PBS and placed into fresh culture medium (chase), whose samples were taken 0, 5, 15 and 60 min later. Samples were analyzed using FluoZin-3 (cell impermeable salt) fluorescence, which was normalized to the total protein content of the well containing the given sample of cells. Figure 19A shows that Zn^{2+} content of the medium during the chase phase was not lower, but indeed higher in TRPML1-KD than in control cells.

Next, total constitutive lysosomal secretion was recorded using ß-hexosaminidase release over four-hour time interval. The previously described protocol was used [453]. Figure 19B shows that there was no detectable difference in constitutive exocytosis of ß- hexosaminidase

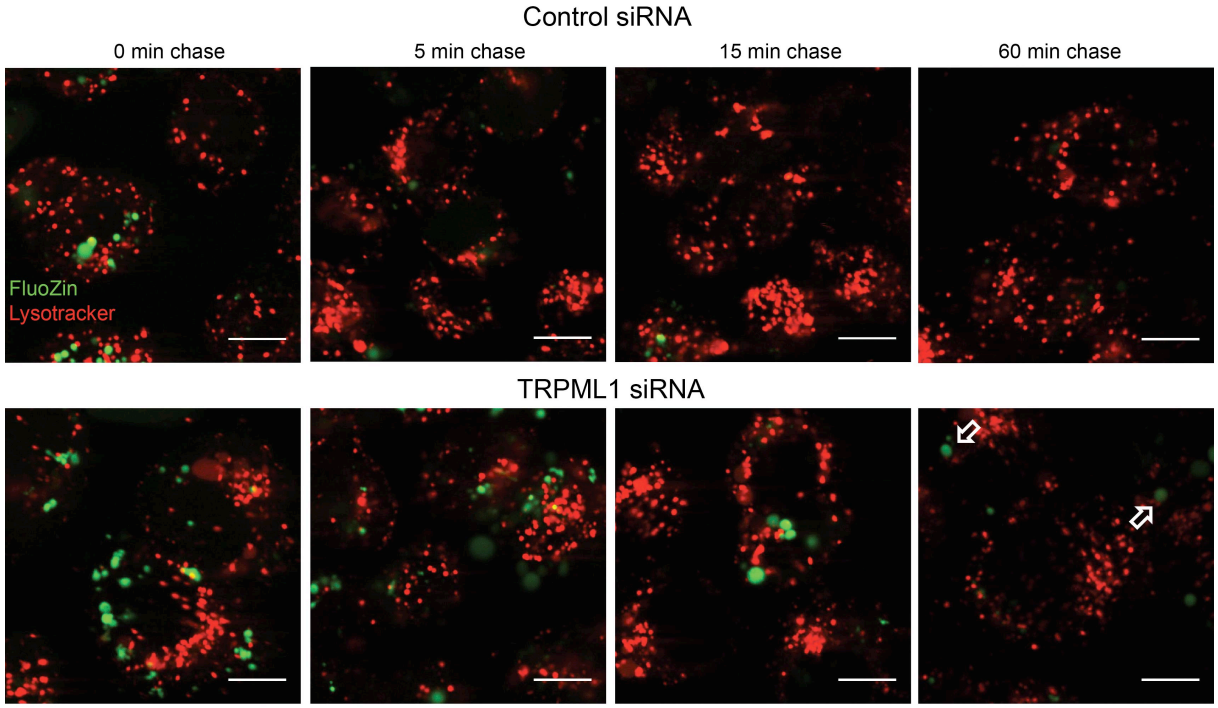

Figure 18. **Delayed clearance of Zn^{2+} from lysosomes in TRPML1-KD cells.**

HeLa cells stained with Lysotracker and FluZin-3,AM. To test whether TRPML1 is involved in Zn^{2+} we performed confocal analysis of intracellular Zn^{2+} using Zn^{2+} pulse and chase. Control and TRPML1-deficient HeLa cells were incubated with Zn^{2+} for 3 hours (pulse) and then exposed to Zn^{2+}-free medium for 0 to 60 min (chase) before confocal analysis. Cells were stained with Lysotracker and with FluoZin-3, AM as discussed before. Note that during the chase, Zn^{2+} persisted in the cytoplasmic vesicles in TRPML1-KD cells for longer period of time than it did in control cells. Scale bar is 20 μM.

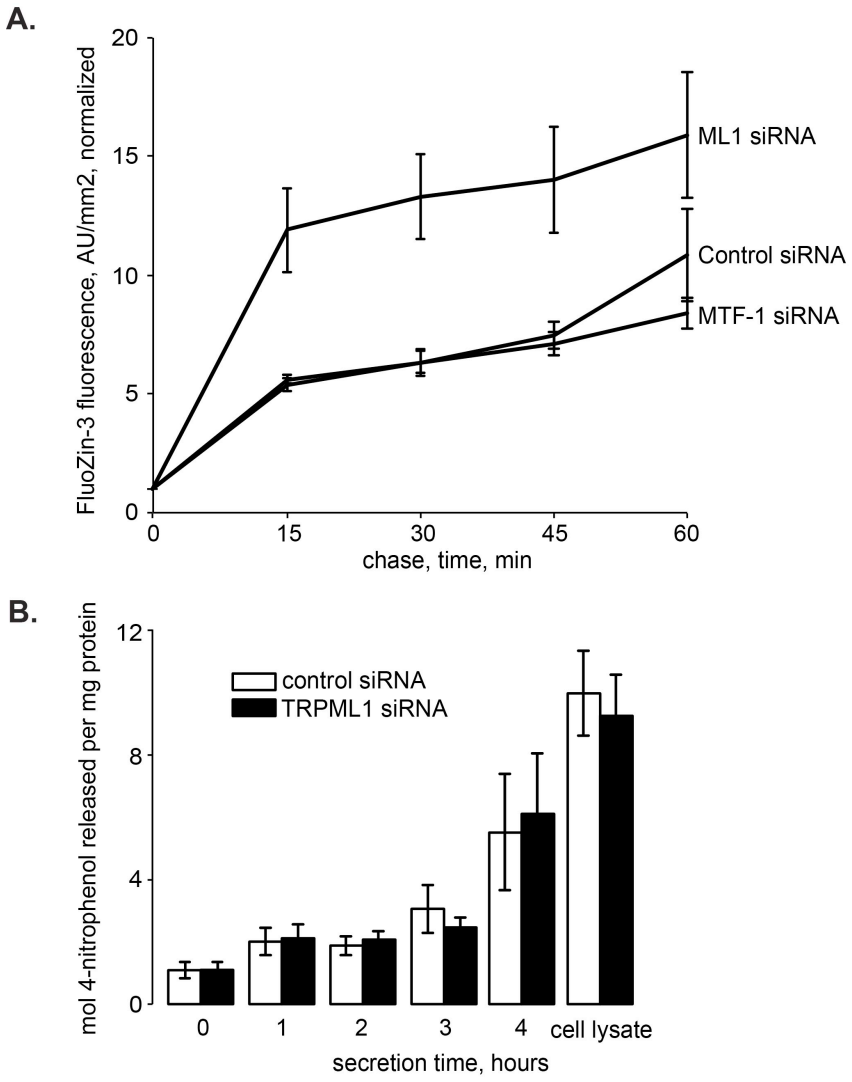

Figure 19. Zn^{2+} clearance and secretion in TRPML1-KD cells.

A. Zn^{2+} secretion in control and TRPML1-KD cells. Cells were loaded in 100 µM Zn^{2+} for 3 hours, washed and Zn^{2+} secretion was analyzed as described in the text. FluoZin-3 fluorescence was expressed in arbitrary units per illumination/light collection area and normalized to the values in control cells exposed to Zn^{2+}, which were taken as 1. Data represent 3 individual experiments, performed in duplicate. **B**. ß-hexosaminidase secretion.

between TRPML1-KD and control cells. These data are consistent with similar secretion rates, but higher lysosomal Zn^{2+} content in TRPML1-KD cells. They argue against difference in secretion being the main cause of Zn^{2+} retention in the lysosomes of TRPML1-KD cells.

2.4 DISCUSSION

In the course of these studies, we found that, in agreement with the previously published report [393], there is a significant dysregulation of Zn^{2+} handling in TRPML1-KD cells. Our findings provide further insight into this process by showing that TRPML1 loss affects processes beyond lysosomes, and by identifying some of the components of the lysosomal "Zn^{2+} sink" responsible for export of the cytoplasmic Zn^{2+} into the lysosomes.

We show that the lysosomal enlargement and Zn^{2+} buildup are alleviated by the suppression of cytoplasmic transcription factor MTF-1. These data clearly establish that a cytoplasmic step is involved in the loading of lysosomes with Zn^{2+} and their enlargement in TRPML1 KD cells exposed to Zn^{2+}. They largely rule out endocytosis as the other source of lysosomal Zn^{2+} retention. What is this step and what is the role of MTF-1 in this process?

We found that the loss of ZnT4 abolishes Zn^{2+} buildup and lysosomal enlargement in TRPML1-KD cells exposed to Zn^{2+}. The fact that ZnT2 does not appear to have an effect in our system is puzzling. It likely reflects the specifics of Zn^{2+} handling by HeLa cells. ZnT2 expression requires several factors [88]. It is possible that ZnT2 expression, or its response to Zn^{2+}, is defective in HeLa cells. Furthermore, it is possible that ZnT2 and TRPML1 do not work in the same functional space. A more exciting possibility is that TRPML1 regulates localization,

or activity of ZnTs, specifically ZnT2 (Fig 16). Accordingly, a dependence of ZnT2 activity and structural integrity on lysosomal pH was recently shown [454].

Finally, we demonstrate that Zn^{2+} leak from the lysosomes into the cytoplasm is delayed in TRPML1-KD cells. It is unlikely and that such delay is due to problems with Zn^{2+} secretion in TRPML1-KD cells, since there was no reduction in Zn^{2+} secretion in these cells, compared with control cells (Fig 18). The lack of TRPML1 effect on ß-hexosaminidase secretion in our system does not refute TRPML1's role in secretion. It is possible that TRPML1 is involved in another aspect of secretion, such as regulated secretion, which was beyond the scope of the present work.

Although MTF-1 was shown to regulate ZnT1 expression, no evidence of ZnT4 regulation by MTF-1 has been presented so far. It is important to remember that MTF-1 regulates MT expression and that MTs are indispensable for Zn^{2+} transport. Several lines of evidence show that MTs deliver and load Zn^{2+} on the transporters and that in the absence of MTs, Zn^{2+} transport is severely compromised [455, 456]. Based on this, we suggest that, in our system, MTF-1 KD affected Zn^{2+} transport into lysosomes due to the loss of MT2a, and possibly other MTs. This likely affected the loading of lysosomal Zn^{2+} transporters with Zn^{2+}. We hypothesize that, as previously suggested [457] MT2a transfers cytoplasmic Zn^{2+} onto ZnTs, such as ZnT4, promoting its export into lysosomes. Such a lysosomal "Zn^{2+} sink" may be a defense mechanism against deleterious Zn^{2+} spikes during toxic levels of Zn^{2+} exposure.

At the same time, MT2a mRNA response to Zn^{2+} in TRPML1-KD cells is dramatically increased. This is consistent with increased cytoplasmic Zn^{2+} levels in TRPML1 KD cells exposed to Zn^{2+}. What is the role of TRPML1 in this process? The fact that TRPML1 loss leads to lysosomal Zn^{2+} retention indicates that TRPML1 dissipates lysosomal Zn^{2+}. TRPML1 may transport Zn^{2+} from the lysosomes into the cytoplasm, as suggested by our data in Figure 18. It is

important to remember that the upregulation of Zn^{2+} chelation and extraction from cells persistently exposed to Zn^{2+} is likely to lead to a drop in cytoplasmic Zn^{2+} concentration after the initial spike induced by the addition of Zn^{2+}. It is possible that TRPML1 function is to dissipate Zn^{2+} accumulated in the lysosomes due to ZnT4 activity during Zn^{2+} spike. TRPML1 loss would result in weak, but prolonged Zn^{2+} leak through other transporters leading to low, but chronic Zn^{2+} elevation, perhaps sufficient to chronically activate MTF-1.

The central finding of these studies are the identification of the source of Zn^{2+} buildup in TRPML1-KD cells as cytoplasmic as well as the identification of components that are necessary for the TRPML1-deficient "Zn^{2+} sink" to function properly: ZnT4 and cytoplasmic proteins, such as the transcription factor MTF-1. These components are involved in the cellular response to exposure to Zn^{2+} against the background of the loss of a lysosomal ion channel whose function to date remains unknown. Our findings shed light on TRPML1 function and its importance for proper cell function and health. Since the loss of TRPML1 is the cause of MLIV, further studies will show whether or not dysregulation of cytoplasmic Zn^{2+} in TRPML1-KD cells is a contributing factor in the key aspects of MLIV pathogenesis, such as the buildup of storage bodies or cell death. Beyond MLIV, the fact that TRPML1 is involved in Zn^{2+} trafficking potentially impacts other neurodegenerative diseases. Zn^{2+} is an essential transition metal that needs to be highly regulated and Zn^{2+} dysregulation has been linked to neuronal death following a seizure or ischemic episode [126, 458], formation of β–amyloid plaques associated with Alzheimer's [459], and pancreatic β–cell degeneration [460]. It would be interesting to see the role of TRPML1 in those processes.

2.5 ACKNOWLEDGEMENTS

This work was supported by the National Institutes of Health grants HD058577 and ES01678 to KK and HD058614 to SLK. We thank Drs. Haoxing Xu, Shmuel Muallem, Bruce Pitt and Ora Weisz for fruitful discussion.

3.0 ZINC EFFLUX THROUGH LYSOSOMAL EXOCYTOSIS PREVENTS ZINC-INDUCED TOXICITY

The work discussed in this Chapter has been adapted from material that as of this dissertation, is in final review stages and is reprinted, with alterations, by permission from the Journal of Cell Science:

Ira Kukic, Shannon L. Kelleher, and Kirill Kiselyov, "Zinc efflux through lysosomal exocytosis prevents zinc-induced toxicity." Journal of Cell Science. 2014 © the Company of Biologists.

3.1 INTRODUCTION

Cellular Zn^{2+} dyshomeostasis has been linked to a number of human pathologies including growth defects [461], impaired immune function [462], diabetes [463], and neurodegenerative diseases [464-467]. Regulation of cellular Zn^{2+} levels involves controlling its influx, export and chelation. In general, Zn^{2+} transport is regulated by ZnT and ZIP transporters, and it is chelated by Zn^{2+} binding metallothioneins (MTs).

In addition to Zn^{2+} evacuation across the plasma membrane (PM) by the Zn^{2+} transporter ZnT1 [15], Zn^{2+} is exported from the cytoplasm into the organelles by the dedicated ZnT transporters such as ZnT6 for the Golgi [468], and ZnT2 and ZnT4 for the lysosome [431, 444, 449, 451]. This organellar Zn^{2+} export lowers potentially toxic cytoplasmic Zn^{2+} concentrations

in pathophysiological conditions such as neurodegeneration [469] and breast cancer [470]. Moreover, it provides Zn^{2+} to organellar processes that require it, such as the maturation of enzymes like the lysosomal acid sphingomyelinase [471], and the secretion of Zn^{2+} under normal physiological conditions such as synaptic transmission [115] and lactation [472].

The upregulation of Zn^{2+} chelation and transport machinery following the activation of the transcription factor MTF-1 by Zn^{2+} binding [435] requires time for transcription, translation and protein processing. It is tempting to speculate that Zn^{2+} export into organelles serves as a first line of defense to provide temporary Zn^{2+} storage, giving cells time to upregulate Zn^{2+} chelators and transporters. Our recent data on the role of lysosomes in Zn^{2+} handling, as well as some recently published results suggest that lysosomes play a role of such Zn^{2+} sinks, temporarily storing Zn^{2+} [304, 473]. In this paper, we sought to delineate the role of lysosomes in protection against Zn^{2+}-induced toxicity.

Zn^{2+} is transported from the cytoplasm into lysosomes by ZnT2 and ZnT4 [431, 449, 451]. Zn^{2+} can also be delivered to the lysosomes through endocytosis or autophagy [474, 475]. What happens to Zn^{2+} absorbed by the lysosomes? A recent series of work from several labs indicate that Zn^{2+} buildup in the lysosomes is toxic. It leads to lysosomal membrane permeabilization (LMP), to the release of the lysosomal enzymes such as Cathepsins and to cell death [476-479]. As such, the lysosomal Zn^{2+} accumulation may constitute a cell death mechanism during normal remodeling of Zn^{2+}-rich tissues, such as the mammary gland [480], as well as in pathological conditions. With this in mind, we sought to answer whether or not the accumulation of Zn^{2+} in the lysosome is the terminal depot for cellular Zn^{2+}.

Alternatively, it is possible that lysosomal Zn^{2+} dissipates and lysosomes constitute only a temporary Zn^{2+} storage site. Our recently published data suggest that the lysosomal ion channel

transient receptor potential mucolipin 1 (TRPML1) is at least partly responsible for dissipating the lysosomal Zn^{2+} into the cytoplasm [473]. It should be noted that lysosomes fuse with the PM via a process involving a specific SNARE complex, which includes the VAMP7 protein and Synaptotagmin VII (SYT7) [239, 240, 268, 481, 482]. Such secretion was recently proposed to contribute to excretion of undigested/indigestible products inside lysosomes [273]. In the course of the present studies, we used VAMP7 and SYT7 KD to suppress lysosomal secretion and assess its role in Zn^{2+} clearance from the cells.

Here we aimed to establish the functional context of the lysosomal Zn^{2+} accumulation. Our findings indicate that lysosomes actively absorb Zn^{2+} and secrete it across the PM, since suppressing the lysosomal Zn^{2+} absorption or secretion causes Zn^{2+} buildup in the cytoplasm, Golgi apparatus and mitochondria, leading to apoptosis.

3.2 EXPERIMENTAL METHODS

3.2.1 Cell Culture

HeLa cells were maintained in DMEM (Sigma-Aldrich, St Louis, MO) supplemented with 10% FBS. For siRNA and cDNA transfection, media was changed after 24 hours. 100 μM $ZnCl_2$ was added directly to the medium, containing serum, 24 hrs after transfection, for the indicated times. Bafilomycin A1 (#196000, EMD MIllipore, Darmstadt, Germany) was used at 1 μM for the indicated amount of time.

3.2.2 SiRNA-mediated KD and plasmid transfection

The VAMP7 siRNA (Cat number SASI_Hs01_00197188), SYT7 (Cat number SASI_Hs01_0047888), ZnT2 siRNA (Cat number SASI_Hs01_00055662), ZnT4 siRNA (Cat number SASI_Hs00225995), and MTF-1 siRNA (Cat number SASI_Hs01_00177112) were from Sigma (Sigma-Aldrich, St Louis, MO). Non-targeting control siRNA#1 (Sigma) was used as a negative control. Cells were transfected using Lipofectamine 2000 (Invitrogen, Carlsbag, CA) as described by manufacturer's protocol using 600 nM siRNA per 35 mm well (1200 nM siRNA per 35 mm well for efficient VAMP7 and SYT7 KD). All KDs were confirmed using SYBR-green based qPCR. For DNA transfections, 2 μg of GalT-mCherry and TFEB was transfected per 35mm dish.

3.2.3 Microscopy

Cells were seeded on glass coverslips and loaded with dyes for 15 min at 37ºC in buffer containing, in mM: 150 NaCl, 5 KCl, 1 $CaCl_2$, 1 $MgCl_2$, 10 HEPES, pH 7.4, 1 g/L glucose. The loading was followed by 15 min washout in all cases. Lysotracker Red DND-99, FluoZin-3,AM (F-24195, Invitrogen, Carlsbag, CA), were used at 0.1 μM. Confocal microscopy was performed using Leica TCS SP5 and BioRad 3000 confocal microscopes. Live cells were treated as above. Images were analyzed using ImageJ (Bethesda, MD).

3.2.4 Reverse Transcriptase and Quantitative qPCR

RNA was isolated from cells using Trizol (Invitrogen, Carlsbag, CA) according to the manufacturer's protocol. cDNA was synthesized using the GeneAmp RNA PCR system (Applied Biosystems, Carlsbad, CA) with oligo dT priming. qPCR was performed SYBR green (Fermentas, Glen Burnie, MD). The amount of cDNA loaded was normalized to starting RNA concentrations, with a final concentration of 9 ng (40 ng in ZnT experiments) of RNA loaded per experimental well. Six-point standard curves were generated for each primer using 1:2 dilutions of cDNA. cDNA for the following genes were amplified using the indicated primers (IDT, Coralville, IA). *MT2a*: forward: 5'AAGTCCCAGCGAACCCGCGT-3', reverse: 5'-CAGCAGCTGCACTTGTCCGACGC-3'. *VAMP7*: forward: 5'-CCGGACAGACTGAAGCCAT-3', reverse: 5'-ATCTGCTCTGTCACCTCCAG-3'. *SYT7*: forward: 5'-AAGCGGGTGGAGAAGAAGAA-3', reverse: 5'-CGAAGGCGAAGGACTCATTG-3'. *ZnT1 (SLC30A1)*: forward: 5'-GGGAGCAGCGACATCAACGT-3', reverse: 5'-GGGTCTGCGGGGTCCAATT-3'. *ZnT2 (SLC30A2)*: forward: 5'-GCAATCCGGTCATACACGGGAT-3', reverse: 5'-CAGCTCAATGGCCTGCAAGT-3'. *ZnT4 (SLC30A4)*: forward: 5'-CACATACAGCTAATTCCTGGAAGTTCATCT-3', reverse: 5'-GCCTGTAACTCTGAAGCTGAATAGTACAT-3'. *LAMP1:* forward: 5'-GGACAACACGACGGTGACAAG-3', reverse: 5'-GAACTTGCATTCATCCCGAACTGGA -3'. All primers were designed to span exons and negative RT controls were tested to ensure amplification of cDNA only. qPCR was performed using the Standard Curve method on the 7300 Real Time System (Applied Biosystems, Carlsbad, CA). Reactions were run on the following parameters: 2 min at 50°C, 10 min at 95°C, and 40 cycles at 95°C for 15 sec followed

by 60°C for 1 min. All experimental samples were run in triplicate and normalized to an RPL32 endogenous control.

3.2.5 β-Hexosamindase activity assay

Untreated control and transfected cells were washed with 37ºC PBS and 300 µl 37ºC PBS with 1 mM $CaCl_2$ was added to each 35mm dish. For each sample, 100 µl of the supernatant was incubated with 300 µl 3 mM 4-nitrophenyl N-acetyl-β-D-glucosaminide (N9376, Sigma-Aldrich, St Louis, MO) for 30 minutes at 37ºC in 0.1 M citrate buffer (pH 4.5) (C2488, Sigma-Aldrich, St Louis, MO). This volume was replaced with fresh 100 µl of 37ºC of PBS with 1 mM $CaCl_2$ to the culture dish. Samples were collected every after 0, 10 and 30 minutes. Reactions were stopped by adding 650 µl borate buffer (100 mM boric acid, 75 mM NaCl, 25 mM sodium borate, pH 9.8) and the absorbance was measured in a spectrophotometer at 405 nm. To determine total cellular content of β-hexosamindase, cells were lysed with 300 µl 1% Triton X-100 in PBS and after a 10,000g spin for 5 minutes at 4ºC, 10 µl of the cell extracts were used for the enzyme activity reaction. Enzyme activity was determined as the amount of 4-nitrophenol produced per mg of protein (Bradford method). Absorbance was calibrated with different amounts of 4-nitrophenol (N7660, Sigma-Aldrich, St Louis, MO) in 0.1 M citrate buffer.

3.2.6 Zinc secretion assay

Cells were plated on a 12 well plate and 48 hours after, transfection pulsed with 100 µM $ZnCl_2$ for 3 hours, washed twice with warm PBS, and chased in 1mL DMEM per well. Duplicate time-points were collected for 0, 5, 15, 30 or 60 minutes and replaced with new 50 µl of DMEM. For

each sample, 50 µl of supernatant was placed in a 96-well plate. Zn^{2+} content was measured by incubating the supernatants with 10 µM cell-impermeant FluoZin-3 tetrapotassium salt (F-24194, Molecular Probes, Invitrogen, Carlsbag, CA) for 15 minutes at 37ºC. The 96-well plate was read via a FujiFilm FLA-5100 fluorescent image analyzer. After the last time point, cells were washed with PBS, 200 µl detergent solution was added to lyse the cells and fluorescence was normalized to total protein in each sample.

3.2.7 Caspase 3 activity assay

Cells were prepared and measured using the EnzChek Caspase-3 Assay Kit #1 (E13183, Invitrogen, Carlsbag, CA) following the manufacturer's instructions. AMC substrate fluorescence was measured using a fluorometer at an excitation wavelength of 342 nm and an emission wavelength of 441 nm.

3.2.8 Western Blot Analysis

Cells were solubilized for 10 min at room temperature in either a 1X detergent solution (0.5 M EDTA, pH 8.0, 1 M Tris, pH 8.0, 0.4% deoxycholate, 1% Nonidet P-40 substitute) for (LAMP1) or a 1% CHAPS in PBS solution (for VAMP7) containing protease inhibitor mixture III (Calbiochem, Gibbstown, NJ) and centrifuged at 16,000 g for 5 min. The supernatant was collected and protein concentrations were determined using a Bradford assay. Protein was incubated at 100 °C for 5 min in sample buffer containing 14% β -mercaptoethanol. Equal amounts of protein were loaded on a 10% precast Tris-HCl polyacrylamide gel (Bio-Rad) for each experimental sample. Proteins were transferred to PVDF membrane (EMD MIllipore,

Darmstadt, Germany) and blocked in 10% nonfat dry milk for 1 hour. The following primary antibodies were used: monoclonal LAMP1 (sc-20011, Santa Cruz, Santa Cruz, CA) at 1:1,000 dilution, monoclonal VAMP7 (ab36195, Abcam, Cambridge, US) at 1:500, and monoclonal β-actin (ab6276, Abcam, Cambridge, US) at 1:5,000 dilution. HRP-conjugated goat anti-mouse secondary antibodies (Amersham Biosciences) were used at 1:20,000 dilutions. Immunodetection was performed with the Luminata Forte HRP substrate (EMD MIllipore, Darmstadt, Germany). Band densities were measured using ImageJ (Bethesda, MD).

3.2.9 Flow Cytometry

HeLa Transfected HeLa cells were treated with either 100 μM $ZnCl_2$ for 48 hours for Baf and VAMP7 experiments, or 200 μM $ZnCl_2$ for 12 hours for TFEB experiments. Cells were then washed with PBS, trypsinized, and counted. $2X10^6$ cells were pelleted for each sample, washed with PBS and then resuspended in Annexin Binding Buffer from the Vybrant Apoptosis Assay Kit #3 (V.13242, Molecular Probes). Cells were then loaded with 1 μl propidium iodide and 2 μl Annexin V 488 and sorted on the Accuri (BD) C6 at the University of Pittsburgh Cancer Institute Cytometry Facility. Cell sorting was gated to include healthy and apoptotic cells while excluding debris.

Statistical significance was calculated using a one-tailed, unpaired t-test with $p \leq 0.05$ considered significant. Data are presented as mean ± S.E.M.

3.3 RESULTS

3.3.1 Inhibition of lysosomal function through Bafilomycin increases cellular zinc

Towards testing the role of lysosomal Zn^{2+} sink in the cellular Zn^{2+} handling, we blocked the lysosomal H^+ pump in HeLa cells using 1 μM Baf and exposed cells to 100 μM $ZnCl_2$ for 3 hours. The resulting cytoplasmic Zn^{2+} spikes were measured using live-cell confocal microscopy and FluoZin-3,AM as described before [473]. Figure 20 A shows that the exposure of Baf-treated cells to Zn^{2+} caused significantly higher FlouZin-3,AM response than the exposure of untreated cells to Zn^{2+}. Although Baf has been shown to decrease cytoplasmic pH, potentially affecting Zn^{2+} binding to cytoplasmic proteins, or FlouZin-3,AM fluorescence, the magnitudes of the observed effects appear to be incompatible with the quantitative estimates of changes induced by Baf. Thus, Baf's effect on cytoplasmic pH appears to be small, within only tenths of pH units [483]. The degree of pH change necessary to cause an effect on Zn^{2+} handling, on the other hand, significantly exceeds that reported to be caused by Baf. A pH drop below 6.7 is required to trigger an increase in intracellular Zn^{2+} according to one set of studies [484], while another set showed that metallothioneins release Zn^{2+} only after cytoplasmic pH drops below 5.0 [485]. Thus, the increase in cytoplasmic Zn^{2+} caused by Baf likely correlates with the loss of lysosomal function, rather than cytosolic pH changes.

We have previously shown that Zn^{2+} transporters ZnT2 and ZnT4 colocalize with the lysosomal ion channel TRPML1 in HeLa cells [473]. We suggested that these transporters play a role in loading of the lysosomes with Zn^{2+}. In order to test this assumption, we KD ZnT2 and ZnT4 using siRNA as described before and tested the resulting changes in Zn^{2+} handling using

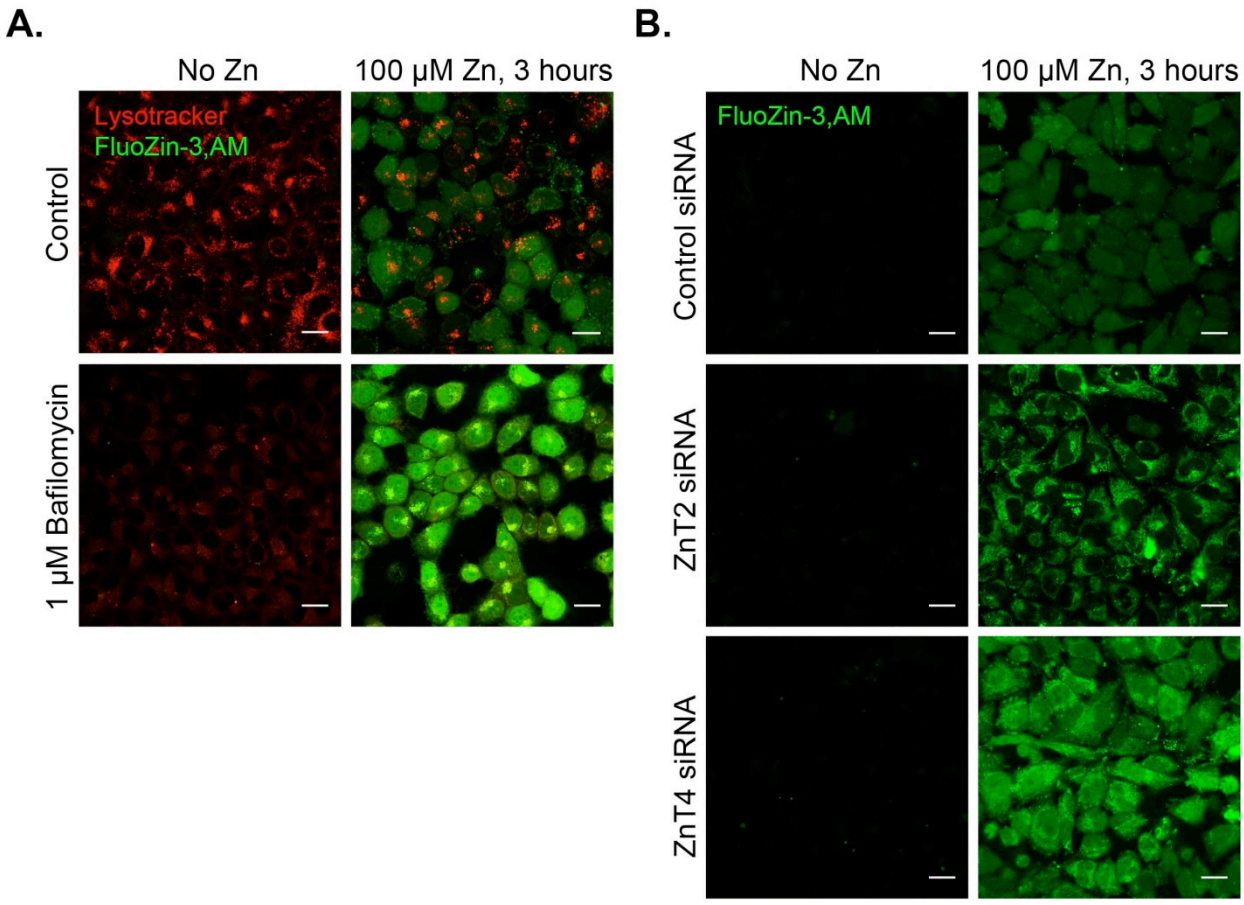

Figure 20. Inhibition of lysosomal Zn^{2+} sink function by Baf increases cytoplasmic Zn^{2+} levels.

A) Confocal images of HeLa cells treated with 100 μM Zn^{2+} and/or 1 μM Baf for 3 hours then loaded with FluoZin-3,AM and LysoTracker. Note disappearance of LysoTracker staining, indicative of lysosomal deacidification, and an increase in FluoZin-3,AM staining intensity, indicative of increased Zn^{2+}. B) Confocal images of control or ZnT siRNA transfected HeLa cells (48 hours post-transfection) treated with 100 μM Zn^{2+} for 3 hours then loaded with FluoZin-3,AM. Images represent at least 3 separate experiments, at least 3 images per condition in each experiment. Scale bars are 20 microns.

FluoZin-3,AM. Figure 20 B shows that ZnT2 and ZnT4 KD increased cytoplasmic Zn^{2+} levels observed in these cells after 3 hour long treatment with 100 μM Zn^{2+}. These results are in agreement with the previously published data on the dependence of ZnTs activity on the acidic environment of the lysosomes [24, 25] for Zn^{2+} binding and transporting activity.

3.3.2 Inhibition of lysosomal function through Bafilomycin increases the transcriptional response of zinc genes

The upregulation of MTF-1–dependent, Zn^{2+}-responsive genes such as MT2a and ZnT1 [486] indicates elevated cytoplasmic Zn^{2+}. MT2a mRNA was used previously in our studies of the role of TRPML1 in Zn^{2+} handling. We measured the expression of the mRNA of these genes using qRT-PCR (Figure 21). An increase in MT2a and ZnT1 mRNA responses to Zn^{2+} in cells treated with Baf is evident. With MT2a mRNA levels in DMSO-treated (no Zn^{2+}) cells taken for 100%, MT2a mRNA levels were 816.39±73.61% in cells treated with DMSO+Zn^{2+} (n=4; $p<0.001$), and 1174.61±94.20% (n=4; $p<0.05$ relative to DMSO-only and DMSO+Zn^{2+} controls) in cell treated with Baf+Zn^{2+} (Figure 21 A). ZnT1 mRNA increased to 323.43±23.32% (n=4; $p<0.001$) in DMSO+Zn^{2+}–treated cells, and to 552.09±40.46% (n=4; $p<0.05$ relative to DMSO-only and DMSO+Zn^{2+} controls) of control values in Baf+Zn^{2+}–treated cells (Figure 21 B). In addition to confirming the elevated cytoplasmic Zn^{2+} levels seen by FluoZin-3,AM in Figure 20 A due to Baf, these data also corroborate MTF-1 activation due to cytoplasmic Zn^{2+} buildup.

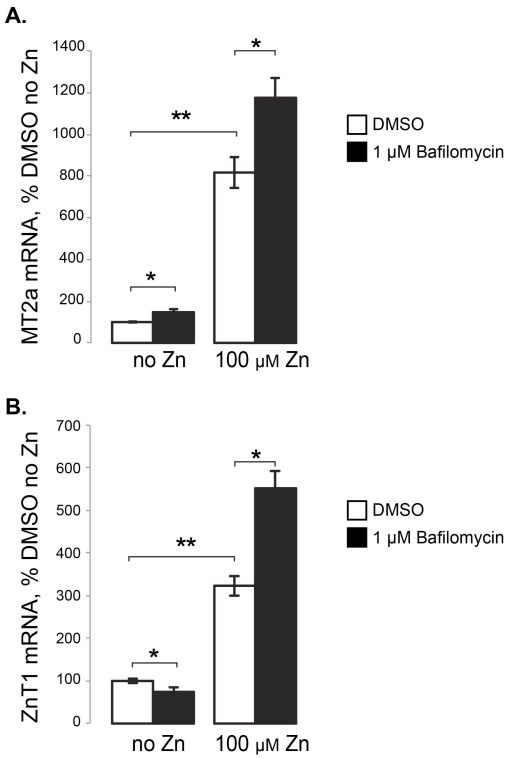

Figure 21. Inhibition of lysosomal Zn^{2+} sink function by Baf increases the transcriptional response of Zn^{2+} genes.

qRT-PCR results of MT2a (A) and ZnT1 (B) mRNA, shown as percent of DMSO-only-treated (no Zn^{2+}) cells. RNA was isolated from HeLa cells treated for 3 hours with either DMSO or 1 μM Baf alone or with 100 μM Zn^{2+}. * Represents $p<0.05$. ** Represents $p<0.001$.

3.3.3 Inhibition of the lysosomal zinc sink through Bafilomycin redistributes cellular zinc pools to the Golgi and the mitochondria

In addition to increasing cytoplasmic Zn^{2+}, suppression of the lysosomal function caused redistribution of Zn^{2+} storage pools. Concentration of FluoZin-3 fluorescence in intracellular inclusions was noted in Baf-treated cells exposed to Zn^{2+}. At least some of these inclusions were

positive for Golgi marker GalT-mCherry (Figure 22 A). Under these conditions, Zn^{2+} also accumulated in the mitochondria as well, which was shown using the mitochondrial Zn^{2+} dye RhodZin-3,AM, whose signal was brighter in Baf-treated than in control Zn^{2+}-treated cells (Figure 22 B). Therefore, suppression of the lysosomal function leads to the loss of Zn^{2+} buffering capacity and to a spike in cytoplasmic Zn^{2+} when cells are exposed to Zn^{2+}. In the absence of Zn^{2+} buffering by the lysosomes, Zn^{2+} is redirected to other organelles.

3.3.4 Inhibition of the lysosomal function and zinc exposure leads to increased cell death

As previously shown, high Zn^{2+} is toxic to the cells due to its buildup in the cytoplasm and in the organelles [487]. If the lysosomes are a Zn^{2+}-buffering sink, then inhibiting that function should result in cell death. Our findings in Figure 23 A support this: while HeLa cells were fairly resistant to the effects of 100 μM Zn^{2+} or 1 μM Baf alone, their combination caused pronounced increased Cas3 activity by 43.90± 14.25% (n=3, $p<0.05$) and exposure to 1 μM Baf increased caspase-3 (Cas3) activation, indicative of apoptosis. An exposure of cells to 100 μM Zn^{2+} for 48 hours Cas3 activity by 179.5±68.04% (n=3, $p<0.05$). A combination of Zn^{2+}- and Baf-exposure increased Cas3 activity by 387.87±36.70% (n=3, $p<0.001$ relative to untreated control), suggesting that Baf enhances the pro-apoptotic effects of Zn^{2+}. Since Baf is conventionally used to block the lysosomal H^+ pump, we think that the simplest interpretation of these data is as diminished cytoprotective capacity of the lysosomal Zn^{2+} sink in Baf-treated cells.

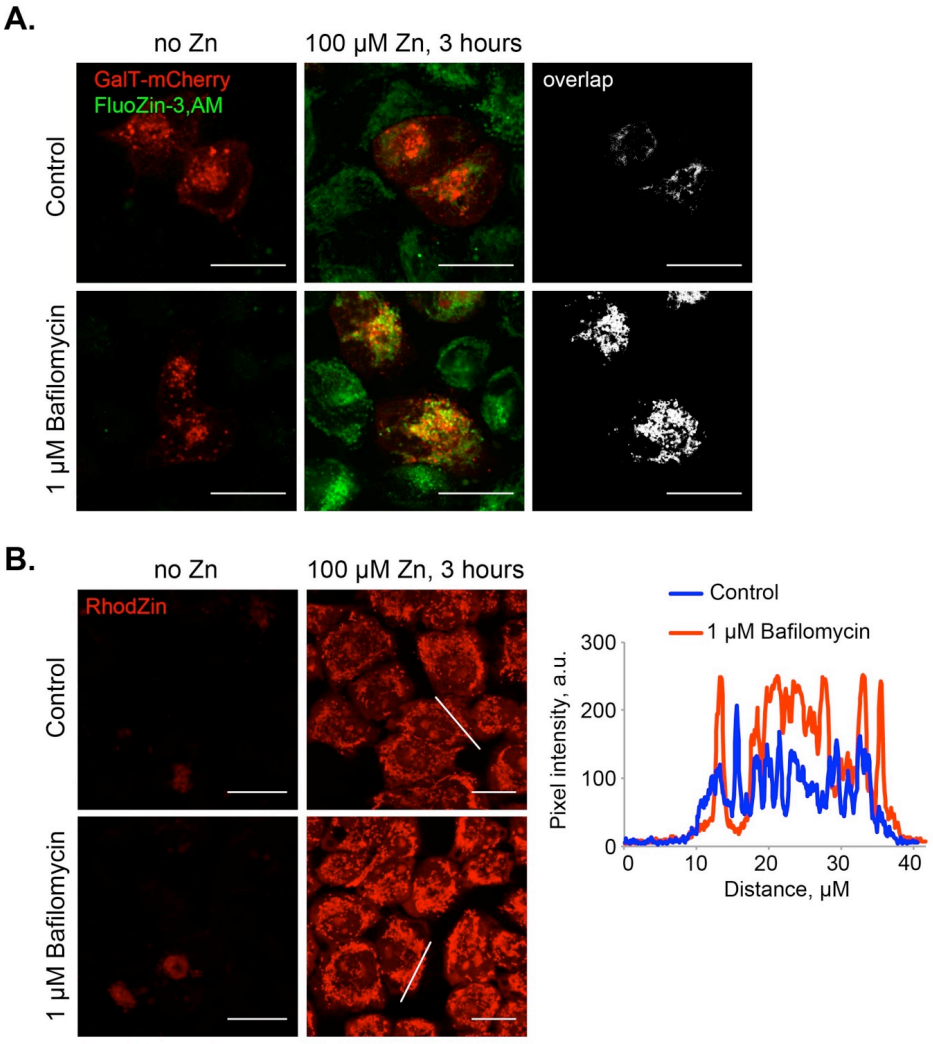

Figure 22. Inhibition of lysosomal Zn^{2+} sink function by Baf redistributes cellular Zn^{2+} pools to the Golgi and the mitochondria.

A) Confocal images of GalT-mCherry–transfected HeLa cells treated with 100 μM Zn^{2+} and/or 1 μM Baf for 3 hours, then loaded with FluoZin-3,AM. The black-and-white panes show overlap between the green and the red channels, obtained using the RG2B function of ImageJ. B) Confocal images of HeLa cells treated with 100 μM Zn^{2+} and/or 1 μM Baf for 3 hours, then loaded with RhodZin-3,AM. Plot profiles on the right show intensity profiles of RhodZin-3,AM fluorescence recorded along the lines indicated in the corresponding image. Note increased RhodZin-3,AM florescence with Baf-treated cells. Images represent at least 3 separate experiments, at least 3 images per condition in each experiment. Scale bars are 20 microns.

As a complimentary cell death assay, Annexin V (AnnV) and propidium iodide (PI) staining were analyzed using flow cytometry. Figures 23 B and 24 show an increase in the number of AnnV-positive, apoptotic cells when cells are treated for 48 hours with Zn^{2+}+Baf. Taken together, these data show that suppression of the lysosomal Zn^{2+} sink facilitates apoptotic cell death caused by Zn^{2+} exposure. They suggest that lysosomes play a crucial role in buffering cytoplasmic Zn^{2+} and in its detoxification. A loss of such a role exposes cells to the pro-apoptotic effects of Zn^{2+}.

3.3.5 A model of lysosomal zinc sink and its role in zinc detoxification

Zn^{2+} toxicity was linked to LMP resulting in cell death under some conditions [304, 477-479]. Why is the lysosomal Zn^{2+} sink cytoprotective under some, but not other conditions of Zn^{2+} exposure? We propose that the switch between pro- and anti-apoptotic effects of the Zn^{2+} sink is dictated by the rate of Zn^{2+} absorption by the lysosomes and/or the rate of its clearance from the lysosomes. If the rate of Zn^{2+} clearance exceeds the rate of its sequestration into the lysosomes, then the Zn^{2+} sink is cytoprotective. A rate of sequestration exceeding the rate of clearance leads to LMP and cell death (see Model in Figure 25). Zn^{2+} clearance may occur through a Zn^{2+} leak into the cytoplasm (as suggested by our recent publication [473]), or through its secretion via lysosomal fusion with the PM. The latter has recently gained a lot of attention as detoxification mechanism in the lysosomal storage diseases [164, 273, 488-490]. The next set of experiments tested the role of lysosomes in Zn^{2+} secretion.

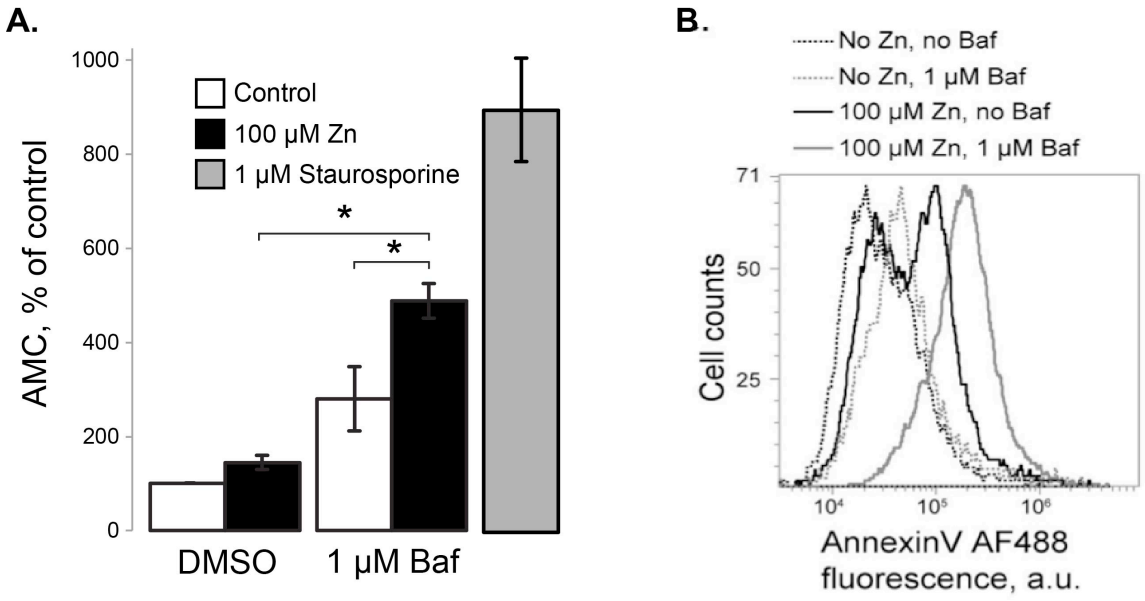

Figure 23. Inhibition of lysosomal function leads to increased cell death upon high Zn^{2+} exposure.

A) Caspase 3 activity assay showing increased Cas3 activation upon 48 hour 100 μM Zn^{2+} and 1 μM Baf treatment in HeLa cells. Three hour long exposure to 1 μM Staurosporine was used as a positive control, which increased Cas3 activity by 796.72±109.06% (n=3, p<0.001). Cas3 activity is shown as AMC fluorescence and a percentage of untreated controls. * p <0.05. B) Flow cytometry data showing increased AnnV staining of cells treated with 100 μM Zn^{2+} and/or 1 μM Baf for 48 hours. Data represent 3 experiments.

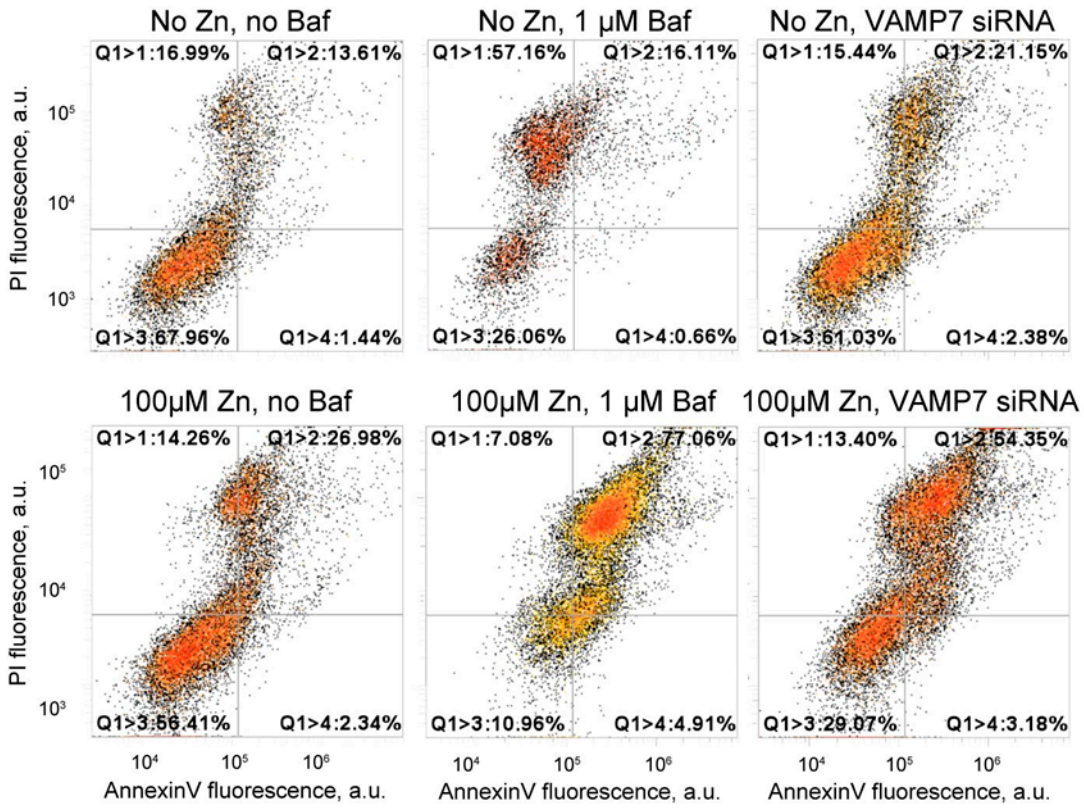

Figure 24. Baf and VAMP7 KD facilitate Zn^{2+}-dependent apoptosis.

Representative (of 3) flow cytometry experiments performed on cells stained with PI and AnnV. Note a decrease in numbers of cells with low AnnV/PI stain ("healthy" cells) and an increase in numbers of AnnV/PI-positive cells (early and late apoptotic cells) treated with Baf and Zn^{2+}, (middle panels) indicating cell death in these cells. Cells were treated with Baf and Zn^{2+} for 48 hours. Right panels show a decrease in numbers of cells with low AnnV/PI stain ("healthy" cells) and an increase in numbers of AnnV/PI-positive cells (early and late apoptotic cells) in VAMP7-KD sample, indicating cell death in these cells. Note a decrease in numbers of cells with low AnnV/PI stain ("healthy cells") and an increase in numbers of AnnV/PI-positive cells in VAMP7-KD cells ("dead or dying cells") treated with Zn^{2+}, indicating cell death in these cells.

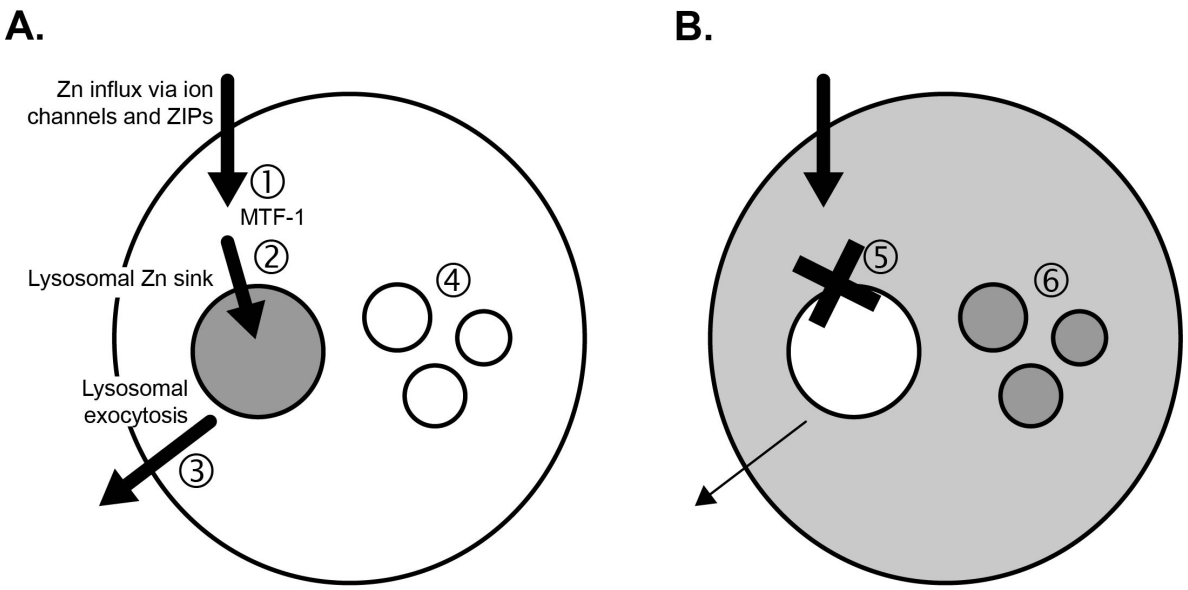

Figure 25. A model of lysosomal Zn^{2+} sink and its role in Zn^{2+} detoxification.

A) Under normal conditions, Zn^{2+} enters the cells through ion channels and ZIPs and is (1) recognized by the Zn^{2+}-sensitive transcription factor MTF-1 which once Zn^{2+}-bound, will translocate to the nucleus to upregulate ZnT1 and MT2a mRNA expression and (2), transported out of the cytoplasm and into the lysosome through ZnT2 and ZnT4. Zn^{2+} that builds up in the lysosomal Zn^{2+} sink is then secreted across the plasma membrane (3) via a VAMP7-dependent mechanism. This prevents toxic Zn^{2+} buildup in the cytoplasm and other organelles (4). B) Suppression of Zn^{2+} absorption by the lysosomal Zn^{2+} sink (5), leads to toxic levels of Zn^{2+} buildup in the cytoplasm as well as other organelles (6) such as the Golgi and mitochondria.

3.3.6 Inhibition of lysosomal exocytosis through VAMP7 and SYT7 KD inhibits zinc secretion

We suppressed lysosomal secretion by using siRNAs against two lysosomal SNARE components: VAMP7 and SYT7 [239, 240, 268, 481, 482, 491]. Figure 26 A shows that VAMP7 siRNA reduced VAMP7 mRNA to 27.76±3.99% of control siRNA levels (n=4, $p<0.001$) while Figure 27 A shows that SYT7 siRNA reduced SYT7 mRNA to 30.12±4.11% of control siRNA levels (n=3, $p<0.001$). VAMP7 mRNA levels were not altered by either 3 or 48 hour exposure to 100 μM Zn^{2+} (I.K., unpublished observation; SYT7 dependence on Zn^{2+} was not tested). VAMP7 KD was confirmed by examining protein levels through Western blot confirming that VAMP7 siRNA reduced VAMP7 protein expression to 30.21±6.82% of control siRNA levels (n=5, $p<0.001$) (Figure 26 B). VAMP7 and SYT7 KD were associated with changes in the lysosomal numbers and organization. There was an increase in the total lysosomal numbers in VAMP-7 KD cells (Figure 28), although there was a high degree of cell-to-cell variation with that metric. Both VAMP7 and SYT7 KD also caused clustering of lysosomes in large structures, which is compatible with the role of these SNARE proteins in membrane traffic. Examples of such clustering and its statistical analysis are shown in Figures 27 and 28.

VAMP7 and SYT7 KD were functionally significant as they caused a loss of secreted activity of the lysosomal enzyme β-hexosaminidase (β-hex), a common marker of lysosomal exocytosis. In these experiments, lysosomal secretion was initiated by treatment with 1 μM of the Ca^{2+} ionophore ionomycin (Ion) (Figures 26C and 27 B). After 30 minutes, control KD cells secreted 18.80±0.66% of their total β-hex content without stimulation, while VAMP7 KD cells secreted 14.09±1.60% of their total β-hex content (Figure 26C). Once stimulated with ionomycin, however, control KD cells secreted 32.57±2.36% of their total β-hex content, while

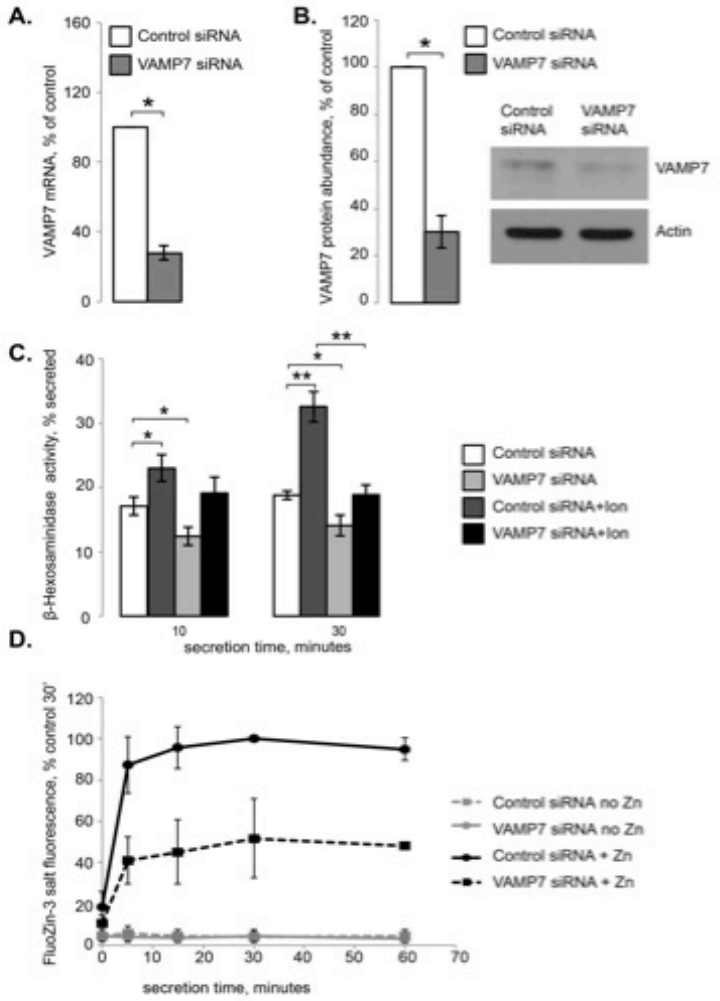

Figure 26. Inhibition of lysosomal exocytosis through VAMP7 KD inhibits Zn^{2+} secretion.

A) qRT-PCR results confirming VAMP7 KD by siRNA. **B)** Quantification of western blot results confirming VAMP7 KD. Insert shows representative blot (of 5) of endogenous VAMP7 and actin levels under with either control or VAMP7 siRNA. **C)** ß-hexosaminidase activity assay for lysosomal exocytosis. Results are shown as percent of total ß-hexosaminidase secreted after either 10 or 30 minutes. One µM ionomycin was used to stimulate lysosomal exocytosis. **D)** Zn^{2+} secretion assay using cell-impermeant FluoZin-3 tetrapotassium salt. Results are shown as percent of the maximum fluorescence value recorded in the Control+ Zn^{2+} samples, which were taken as 100%. * Represents $p<0.05$. ** Represents $p<0.001$.

VAMP7 KD cells only secreted 18.87±1.57% of their total β-hex content (n=3, $p<0.001$) (Figure 26 C). Similarly, SYT7 KD was also functionally significant, decreasing lysosomal exocytosis compared to control KD. Figure 27 B shows that after 30 minutes, ionomycin-treated control KD cells secreted 35.57±1.36% of their total β-hex content, while SYT7 KD cells secreted 20.29±1.65% of their total β-hex content (n=3, $p<0.001$).

To measure the effect of suppressing lysosomal exocytosis on Zn^{2+} secretion, we incubated control and VAMP7, or SYT7 KD cells with 100 μM Zn^{2+} for 3 hours. Next, cells were placed in normal medium (no Zn^{2+}) and Zn^{2+} secretion was analyzed using FluoZin-3 fluorescence as described before [492]. Both VAMP7 (Figure 26 D) and SYT7 (Figure 27 C) KD significantly reduced Zn^{2+} secretion. Within 30 minutes of secretion, VAMP7 KD cells were only able to secrete 51.79±19.26% (n=3, $p<0.05$) of the amount of Zn^{2+} secreted by the control KD cells (100%) (Figure 26 D), indicating that VAMP7 is necessary for Zn^{2+} secretion. Similarly, SYT7 KD cells were only able to secrete 58.90±2.87% (n=3, $p<0.05$) of the amount of Zn^{2+} secreted by the control KD cells, which was taken as 100% (Figure 27 C). This inhibition of Zn^{2+} secretion in VAMP7 and SYT7 KD cells was also corroborated by the elevated cellular Zn^{2+} levels seen by FluoZin-3,AM staining via confocal microscopy (Figure 27 D).

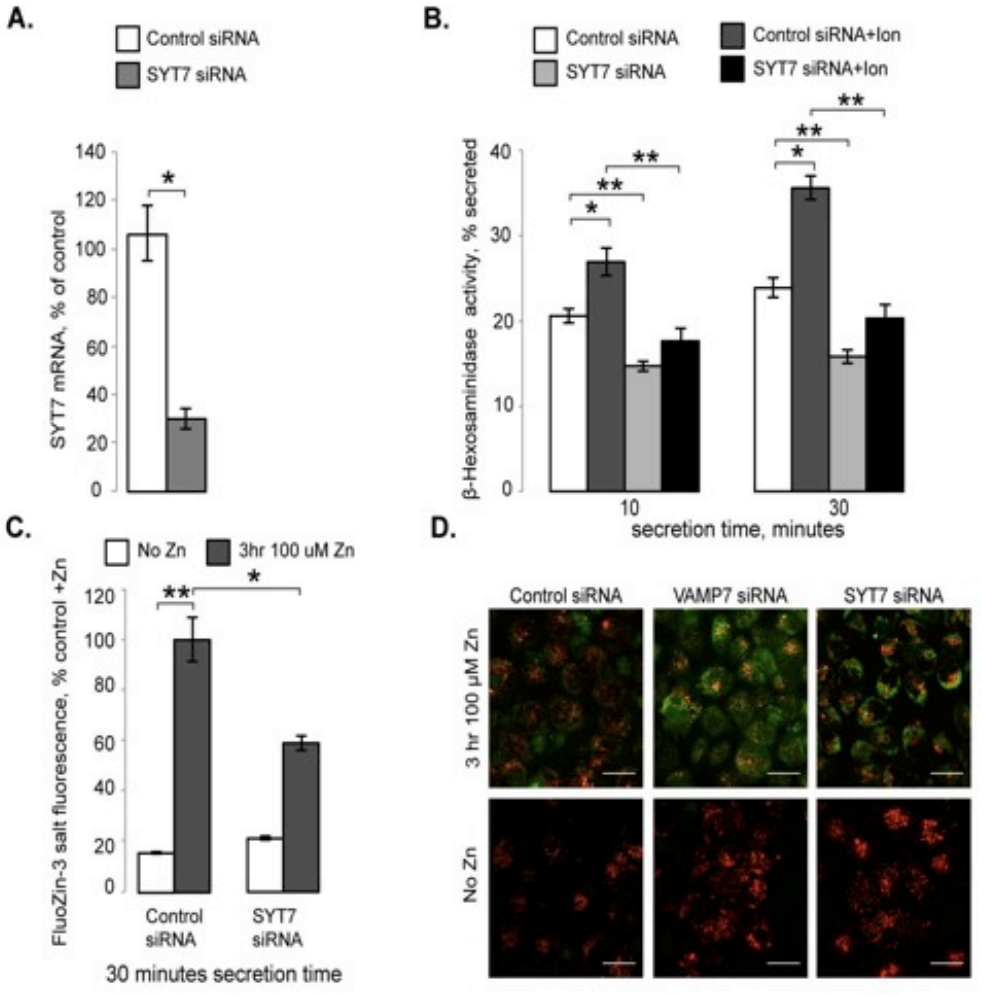

Figure 27. Inhibition of lysosomal exocytosis through SYT7 KD inhibits Zn^{2+} secretion.

A) qRT-PCR results confirming SYT7 KD by siRNA. **B)** ß-hexosaminidase activity assay for lysosomal exocytosis. Results are shown as percent of total ß-hexosaminidase secreted over 10 or 30 minutes. One μM ionomycin was used to stimulate lysosomal exocytosis. **C)** Zn^{2+} secretion assay using cell-impermeant FluoZin-3 tetrapotassium salt. Results are shown as percent of the maximum fluorescence value recorded in the Control+ Zn^{2+} samples, which were taken as 100%. * Represents $p<0.05$. ** Represents $p<0.001$. **D)** Confocal images of control, VAMP7 and SYT7 KD cells untreated or treated for 3 hours with 100 μM Zn^{2+} and loaded with FluoZin-3,AM (green) and LysoTracker (red). Scale bars are 20 microns.

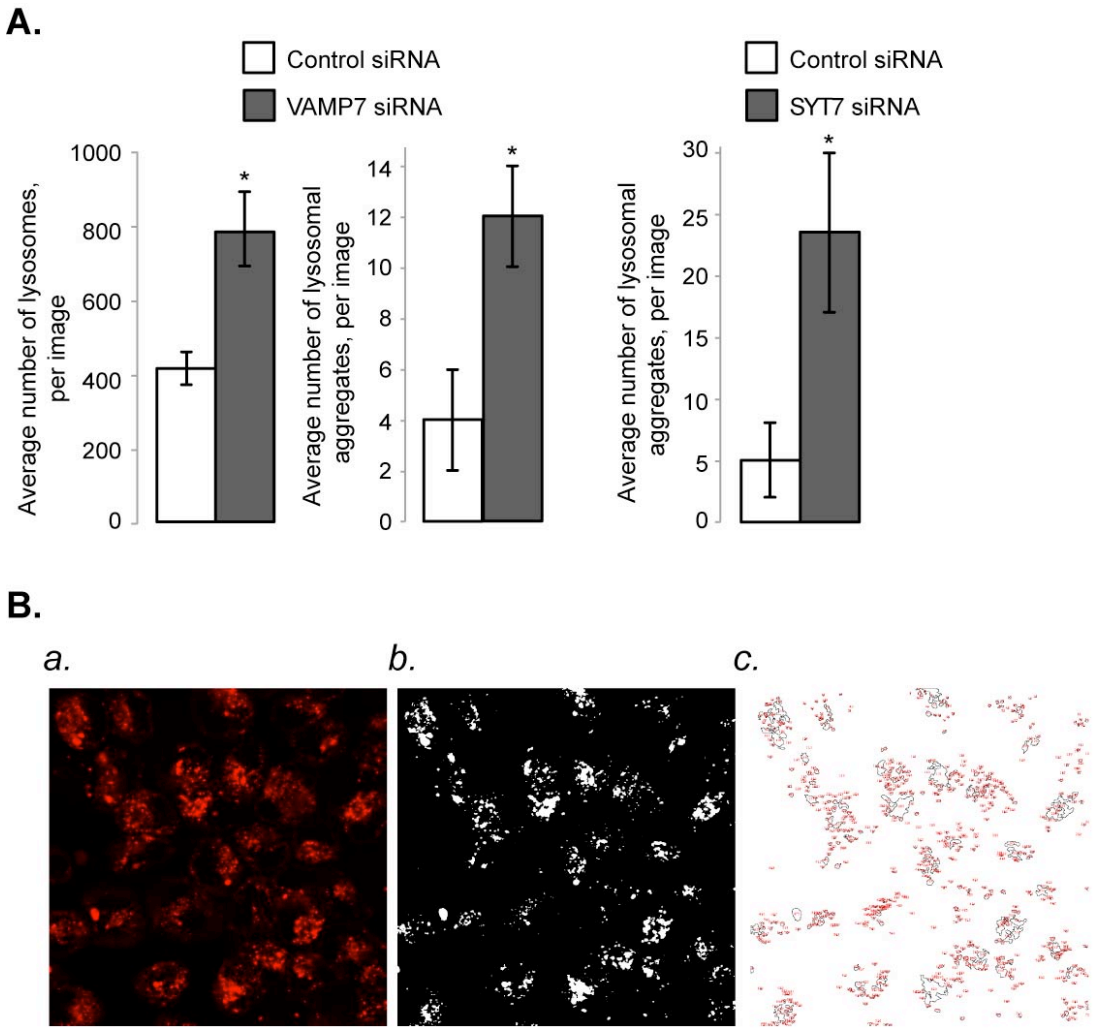

Figure 28. VAMP7 and SYT7 KD increase lysosomal numbers and aggregation.

A) Average number of lysosomes and lysosomal aggregates per image under each condition. Represents an average of 2 separate experiments, with 3 images per condition per experiment. Lysosomes were visualized using confocal microscopy with Lysotracker channel and analyzed using ImageJ. To calculate lysosomal aggregates, the same method was used, but the lower limit of particle size was set at 10 μm. * Represents $p<0.05$. **B)** Intermediate steps of calculating lysosomal sizes. Each image was thresholded at 100/255 of the maximal pixel intensity value so that most lysosomes were visible. Lysosomal size and number were then quantified using the "Analyze particle" function within ImageJ.

3.3.7 Inhibition of lysosomal exocytosis through VAMP7 KD increases cell death in zinc treated cells

The effects of suppressing lysosomal secretion on Zn^{2+}-induced cell death were analyzed using the AnnV/PI assay described above. This assay revealed significant upregulation of Zn^{2+}-induced cell death in VAMP7 KD cells treated with 100 μM Zn^{2+} for 48 hours, compared to control KD cells undergoing the same treatment (Figures 29 and 24). In summary, the data described here show that the Zn^{2+} sink integrates Zn^{2+} absorption from the cytoplasm with its secretion through lysosomal exocytosis. Both aspects of the Zn^{2+} sink function are novel and necessary for Zn^{2+} detoxification.

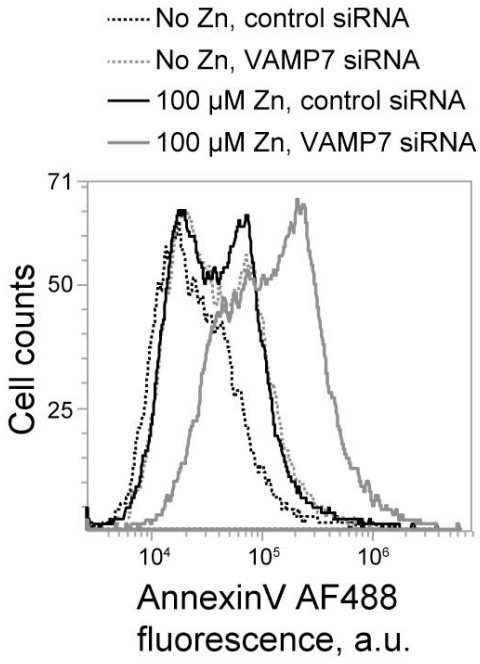

Figure 29. Inhibition of lysosomal exocytosis through VAMP7 KD increases cell death in Zn^{2+}-treated cells.

Flow cytometry data of AnnV- and PI-stained control and VAMP7-KD cells treated for 48 hours with 100 μM Zn^{2+}, showing increased Annexin V fluorescence in VAMP7- Zn^{2+} treated cells (grey solid line) compared to control-Zn^{2+} treated cells (solid black line).

3.3.8 Enhancing lysosomal exocytosis through TFEB overexpression increases zinc secretion

Since lysosomal biogenesis and exocytosis are regulated by TFEB and related factors [163, 167], TFEB should have an impact on lysosomal Zn^{2+} clearance. Indeed, Figure 30 shows that TFEB overexpression, a common protocol used to study its function, increases both lysosomal exocytosis as well as Zn^{2+} secretion. Figure 30 A shows that after 30 minutes, mock-(empty vector)-transfected cells secreted 13.95±0.67% of their total β-hex content, while TFEB-transfected cells secreted 23.11±3.75% (n=3, $p<0.05$) of their total β-hex content. Once stimulated with ionomycin, mock-transfected cells secreted 20.30±1.47% (n=3, $p<0.01$) of their total β-hex content, while TFEB-transfected cells secreted 38.65±1.98% (n=3, $p<0.001$) of their total β-hex content. TFEB also increased Zn^{2+} clearance. Figure 30 B shows that after 15 minutes, control KD cells were able to secrete 76.70±1.37% of secretable Zn^{2+} in our assay, while TFEB-transfected cells were able to secrete 104.52±10.12% (n=3, $p<0.05$) of secretable Zn^{2+}. This increase in Zn^{2+} secretion was dependent on the lysosomal fusion machinery as TFEB cDNA and SYT7 siRNA transfected cells had similar levels to control (71.70±3.09%). To our knowledge, this is the first evidence linking increased Zn^{2+} secretion by TFEB and lysosomal exocytosis.

3.3.9 Overloading the lysosomal zinc sink with 200 µM zinc leads to LMP.

Although no measureable apoptosis was detected at 100 µM Zn^{2+} alone in our system, exposure to 200 µM Zn^{2+} induced activation of the apoptosis executioner caspase 3 (Cas3), which developed between 8 and 12 hours after Zn^{2+} application (Figure 31 A). The exposure of cells to

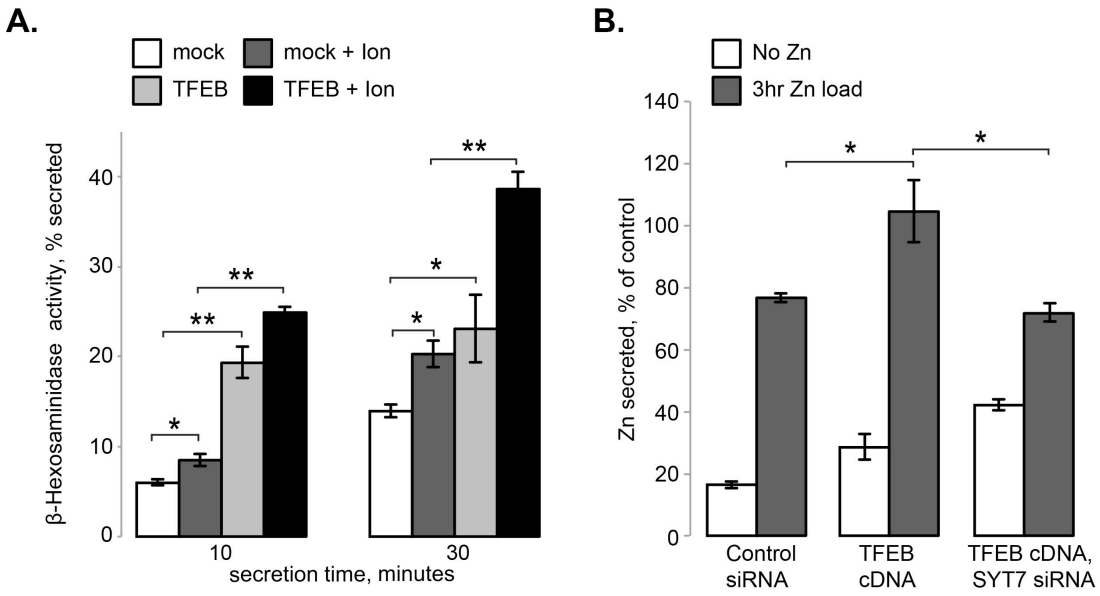

Figure 30. Enhancing lysosomal exocytosis though TFEB overexpression increases Zn^{2+} secretion.

A) ß-hexosaminidase activity assay for lysosomal exocytosis. Results are shown as percent of total ß-hexosaminidase secreted over 10 or 30 minutes. One μM ionomycin was used to stimulate lysosomal exocytosis. **B)** Zn^{2+} secretion assay using cell-impermeant FluoZin-3 tetrapotassium salt. Results are shown as percent of the maximum fluorescence value recorded in the Control+ Zn^{2+} samples at 30 minutes, which were taken as 100%. The results shown above are at 15' of secretion time. * Represents $p<0.05$. ** Represents $p<0.001$.

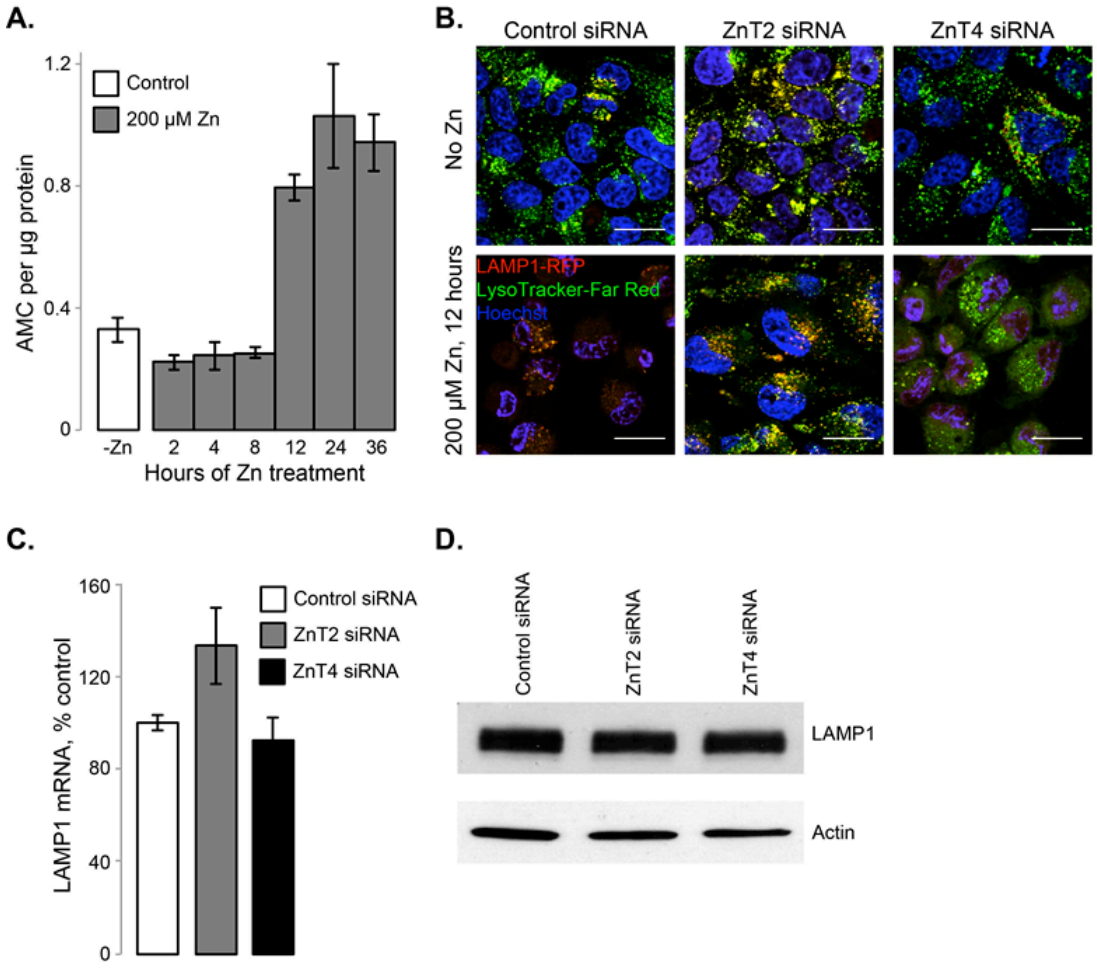

Figure 31. Exposure to 200 µM Zn^{2+} induces LMP and activates Caspase 3 activity.

A) Caspase 3 activity assay. Exposure to 200 µM Zn^{2+} over 8 hours induced Caspase 3 activation and apoptosis. B) Confocal images of control, ZnT2 or ZnT4 siRNA transfected cells, transduced with LAMP1-RFP (red) and stained with Hoechst dye (blue) and LysoTracker (green). Scale bars are 20 microns. The exposure of cells to 200 µM Zn^{2+} for up to 12 hours caused the LMP as indicated by the loss of Lysotracker stain. The Zn^{2+}-induced LMP was inhibited by ZnT2/ZnT4 KD. (C) qRT-PCR of LAMP1 mRNA levels. (D) Western blot of LAMP1 or actin levels.

200 μM Zn^{2+} for up to 12 hours caused the LMP as indicated by the loss of Lysotracker stain (Figure 31 B). The Zn^{2+}-induced LMP was inhibited by either ZnT2 or ZnT4 KD, which suggests that ZnT2 and ZnT4-mediated influx of Zn^{2+} into the lysosomes causes LMP and cell death. We suggest that normally, under the conditions of high Zn^{2+} exposure, the ZnT2- and ZnT4-dependent overload of the lysosomes with Zn^{2+} leads to LMP. The ZnT2 and ZnT4 involvement is in line with the previously published data implicating lysosomal Zn^{2+} buildup in cell death. In this system, ZnT-KD did not seem to affect lysosomal biogenesis, as neither mRNA (Figure 31C) or protein (Figure 31D) levels of the lysosomal membrane protein LAMP1, nor the levels of Lysotracker stain (Figure 31B) were significantly affected by ZnT2/ZnT4 KD under the normal conditions.

3.4 DISCUSSION

Although lysosomes are most commonly discussed in terms of their role in endocytic digestion and absorption, mounting evidence points towards their role in cell death and in signaling [493]. Recent evidence indicates that under oxidative stress conditions, Zn^{2+} accumulates in the lysosomes and can lead to LMP [304]. Furthermore, this Zn^{2+} dysregulation is mechanistically linked to autophagy [475, 478, 494]. Considering that autophagy and oxidative stress play a critical role in cell death and neurodegenerative pathologies, it is likely that Zn^{2+} represents a new target for modulating diseases and a key step in understanding neuronal cell death. The recent developments emphasize the role of lysosomes in metal toxicity. Thus, the accumulation of Zn^{2+} and other metals in lysosomes was shown to lead to LMP, to the release of lysosomal

enzymes into the cytoplasm, and to cell death. While pathological aspects of Zn^{2+} buildup in the lysosomes are undisputable, its physiological role is unclear.

Our recent data suggest that lysosomes play a role of a "Zn^{2+} sink," working in parallel with the transcriptional regulation of Zn^{2+} chelation and transport proteins. Cytoplasmic Zn^{2+} is gauged by the transcription factor MTF-1, which, upon Zn^{2+} binding, induces transcription of Zn^{2+} chelators such as metallothioneins and Zn^{2+} transporters such as ZnT (Slc30a). The ability to absorb Zn^{2+} via active transport involving ZnT transporters makes lysosomes a good candidate for absorbing rapid cytoplasmic Zn^{2+} spikes. The recently published data on the lysosomal absorption of Zn^{2+} released from metallothioneins by H_2O_2 highlight such a function of lysosomes [304, 478, 495, 496].

Although ZIP (Slc39) transporters such as ZIP8 were shown to exist in the lysosomes [497], their impact on the function of the lysosomal Zn^{2+} sink has not been shown. At the same time, the ion channel TRPML1, whose dysfunction causes the lysosomal storage disease MLIV [366], was shown to be a component of the lysosomal Zn^{2+} transport machinery. Its loss was shown to cause Zn^{2+} buildup in the lysosomes in studies by two groups [393, 473] and its permeability to Zn^{2+} by another group [376]. It seems reasonable to conclude that TRPML1 is involved in trafficking Zn^{2+} from lysosomes into the cytoplasm. We proposed that upon entering the cell, Zn^{2+} is registered by MTF-1, which leads to an eventual increase in transcription and translation of Zn^{2+} chelators and exporters. However, Zn^{2+} must be rapidly eliminated from the cytoplasm in order to protect against toxicity. Thus, in parallel, Zn^{2+} is scavenged by the lysosomes, to be later released through a TRPML1-dependent mechanism.

The data in Fig 25D, 26C and 29B show that lysosomal secretion is also involved in Zn^{2+} clearance from the cell. What is the relationship between the two mechanisms of Zn^{2+} clearance?

We think that their function reflects their ability to respond to changes in Zn^{2+} flow. Such changes can be caused by increased autophagy of Zn^{2+}-rich organelles such as mitochondria or proteins. Interestingly, TRPML1 is upregulated in response to increased endocytic load in a manner that requires the transcription factor TFEB, while VAMP7 remains unchanged (I.K., unpublished observation). Based on this, we propose that TRPML1-driven Zn^{2+} release is a dynamic response to increased Zn^{2+} load, while VAMP7- and SYT7-dependent secretion is a constitutive mechanism. We believe that our data clearly show Zn^{2+} absorption into the lysosomes followed by its secretion as an important detoxification mechanism. Furthermore, the fact that suppression of the lysosomal function caused Zn^{2+} redistribution into Golgi and mitochondria shows that the lysosomal Zn^{2+} sink has a major impact on the cellular Zn^{2+} handling.

LMP following Zn^{2+} exposure was clearly shown to be a cell death pathway [304, 477-479]. Why would cells employ a Zn^{2+} detoxification mechanism that effectively kills them? We think that the answer to this question lies in the relation between the lysosomal Zn^{2+} absorption rates and the rate of its secretion/release. Such a ratio may depend on the tissue, developmental stage and on other factors. We propose that under the normal conditions, or moderate Zn^{2+} exposure, the Zn^{2+} sink limits cytoplasmic Zn^{2+} by absorbing it (Model in Figure 25). Zn^{2+} is later released into the cytoplasm (as discussed above), or secreted across the PM. However, during the exposure to high (200 μM) levels of Zn^{2+}, Zn^{2+} extraction lags, leading to LMP and cell death (Figure 31). Our data show a role of lysosomes in transition metal toxicity and identify a novel detoxification mechanism.

3.5 ACKNOWLEDGMENTS

This project used the University of Pittsburgh Cancer Institute Cytometry Facility that is supported in part by award P30CA047904. We thank Michael Meyer and Bratislav Janjic for help with flow cytometry data analysis. The GalT mcherry construct was kindly provided by Dr. Ora Weisz and the TFEB construct was kindly provided by Dr. Rosa Puertollano. This work was supported by National Institute of Health Grants HD058577 and ES01678 to Kirill Kiselyov.

4.0 THE LYSOSOMAL ZINC SINK IS PHYSIOLOGICALY RELEVANT IN REMODELLING OF THE MAMMARY GLAND

The work discussed in this Chapter is unpublished data of which I performed all the experiments, except for the cytochrome C immunofluorescence and some of the original Mitotracker experiments, which were performed by Dr. Kirill Kiselyov and three undergraduates from our lab: Neel Andharia, Yi Wang, and Ly Li. Much of this work stems from a collaborative effort with Dr. Shannon Kelleher at Penn State.

4.1 INTRODUCTION

Zinc (Zn^{2+}) plays a critical role in many cellular functions including gene expression, cell proliferation, differentiation and apoptosis. One of the important physiological requirements for Zn^{2+} is in the mammary gland. The mammary gland depends on the coordination of processes such as cell proliferation, differentiation and apoptosis for proper development and function. For example, during lactation, the mammary gland needs to provide adequate Zn^{2+} content for cellular processes, as well as secrete substantial amounts of Zn^{2+} into milk necessary for the development of the baby. At the same time, the mammary gland undergoes one of the most profound examples of cell death as a result of apoptotic and lysosomal-mediated pathways. It has

been shown that Zn^{2+} transport plays a key role in several aspects of mammary gland development and function [498, 499].

However, Zn^{2+} dysregulation has been associated with a vast number of human diseases and pathological conditions, including impaired breast function [500] and breast cancer [501, 502]. As such, cytoplasmic Zn^{2+} levels must be carefully modulated. In fact, failure to regulate Zn^{2+} sequestration into organelles leads to defects in cell proliferation, autophagy, transcription, and apoptosis. For example, elevated cytoplasmic Zn^{2+} levels activate the mitogen-activated protein kinases (MAPKs) responsible for mediating various cellular responses to extracellular stimuli, including growth, proliferation and cell survival [503, 504]. Elevated cytoplasmic Zn^{2+} levels also activate protein kinase C (PKC), and thereby affect signal transduction pathways involved in cell growth and transcription [505, 506]. At the same time, Zn^{2+} can be cytotoxic if high levels cause Zn^{2+} buildup in the mitochondria, where it has been shown to decrease ATP production and induce apoptosis [423, 424, 507]. Thus, cytoplasmic Zn^{2+} levels are carefully modulated by two families of Zn^{2+}–specific transporters: members of the ZIP family import Zn^{2+} into the cytoplasm from the extracellular environment or from subcellular organelles, while members of the ZnT family export Zn^{2+} from the cytoplasm into organelles or out of the cell.

Lysosomes are emerging as key players in regulating cytoplasmic and organelle Zn^{2+} pools [393, 473]. Although lysosomes are critical for degradation of macromolecules, recent compelling evidence indicates that lysosomes have a much broader function and are involved in many other processes ranging from plasma membrane repair, to intracellular signaling, and secretion. Recently, the lysosomal ion channel transient receptor potential mucolipin 1 (TRPML1) has also been implicated in Zn^{2+} transport. Mutations in TRPML1 lead to mucolipidosis type IV (MLIV) [366], a disease with a neurodegenerative profile characterized by

severe mental and psychomotor delays and retinal degeneration. TRPML1 has been shown to conduct Zn^{2+} [376] and regulate the efflux of Zn^{2+} from lysosomes [393, 473]. Interestingly, while TRPML1 levels are below detection in virgin and lactating mammary glands and mouse mammary epithelial HC11 cells, TPRML1 becomes highly upregulated in the involuting mammary gland, a process associated with increased autophagy and cell death [499]. This implicates TRPML1-mediated processes in mammary gland remodeling. The other proteins implicated in lysosomal Zn^{2+} transport are ZnT2 and ZnT4. We and others have found that ZnT2 and ZnT4 import Zn^{2+} into lysosomes [431, 444, 449, 451]. Together with TRPML1, ZnT2 and ZnT4 are key elements of the lysosomal Zn^{2+} sink, which is a dynamically regulated Zn^{2+} pool that absorbs and releases cytoplasmic Zn^{2+} in response to cellular needs. Curiously, both ZnT2 and ZnT4 are required for Zn^{2+} secretion into milk [451, 508] and were found to colocalize with TRPML1 in HeLa cells [473], suggesting that ZnT2 and/or ZnT4 work with TRPML1 to regulate lysosomal Zn^{2+} pools in mammary epithelial cells. Furthermore, both ZnT2 and ZnT4 knockout mice have significant defects in mammary gland involution, while ZnT2 overexpression prematurely activates autophagic cell death (Shannon Kelleher, unpublished data).

Overall, lysosomal Zn^{2+} accumulation has not only been observed in the involuting mammary gland [499], but has also been shown to cause lysosomal membrane permeabilization (LMP) leading to cell death in neurons [304, 478], retinal pigment epithelial and photoreceptor cells [475] and breast cancer cells [477]. However, the role of Zn^{2+} and LMP in lysosomal-mediated cell death is unclear and very little information is available on lysosomal Zn^{2+} transport. Also, it is not clear what signaling pathways regulate the localization of Zn^{2+} transporters to lysosomes. Neither ZnT2 [433], nor ZnT4 [445], or TRPML1 [499] are expressed

in lysosomes of mammary epithelial cells under basal conditions. It is likely that local stimuli such as LIF, TGF-β, or TNFα produced by the mammary gland initiate involution [509] and modulate signaling pathways responsible for trafficking ZnT2 and ZnT4 to the lysosome.

Here we sought to address whether the lysosomal Zn^{2+} sink and TRPML1 are involved in mammary gland function. Our findings indicate that TRPML1 expression is regulated by involution signals such as TNFα and likely plays a vital role in mammary gland involution by dissipating lysosomal Zn^{2+} buildup. Given the vast number of Zn^{2+}–dependent processes, our findings are likely to have implications beyond lactation and MLIV pathogenesis.

4.2 EXPERIMENTAL METHODS

4.2.1 Cell Culture

HeLa cells were maintained in DMEM (Sigma-Aldrich, St Louis, MO) supplemented with 7% FBS, 100 μg/ml penicillin/streptomycin, and 5 μg/ml Plasmocin prophylactic (Invivogen, San Diego, CA) and grown at 37ºC in 5% CO_2. For siRNA and cDNA transfection, antibiotic free media was used. Zn^{2+} (100 μM) was added to antibiotic free medium, containing serum, 24 hrs after transfection, for 48 hrs.

Retinal pigmented epithelial 1 (RPE1) cells were maintained in DMEM/ Ham F12 (DMEM/F12), 1:1 mix (HyClone, Logan, UT) supplemented with 10% FBS and grown at 37ºC in 5% CO_2. TNFα was added to media containing serum, 24 hrs after transfection, for 24 hrs at a concentration of 40 ng/ml. 100 mM sucrose was pre-dissolved in media containing serum, and added to cells 24 hrs after transfection, for 48 hrs at a concentration of 100mM.

4.2.2 siRNA-mediated TRPML1 knockdown and TFEB overexpression

ON-TARGET plus siRNA were designed as described previously [387, 443] and synthesized by Dharmacon (Lafayette, CO). The TRPML1 siRNA probe targeting the sequence 5'-CCCACATCCAGGAGTGTAA-3' in *MCOLN1* was used for all TRPML1 KDs. Non-targeting control siRNA#1 (Sigma) was used as a negative control. Cells were transfected using Lipofectamine 2000 (Invitrogen, Carlsbag, CA) as described by manufacturer's protocol using 600 nM siRNA per 35 mm well. All KDs were confirmed using SYBR-green based qPCR. . For DNA transfections, 2 μg of TFEB-Flag was transfected per 35mm dish.

4.2.3 Microscopy

HeLa cells were seeded on glass coverslips and loaded with dyes for 15 min at 37ºC in buffer containing, in mM: 150 NaCl, 5 KCl, 1 $CaCl_2$, 1 $MgCl_2$, 10 HEPES, pH 7.4, 1 g/L glucose. The loading was followed by 15 min washout in all cases. Mitotracker Red CMXRos, DAPI (Invitrogen), and propidium iodide (Calbiochem) were used at 0.1, 1, 0.05 μM respectively. Confocal microscopy was performed using the BioRad 3000 confocal and Nikon microscopes. Live cells were treated as above. For Cytochrome C (CytC) experiments, cells were fixed for 5 min in 4% paraformaldehyde at room temperature and permeabilized using 0.1% Triton X100 for 5 min on ice. Following washout and blocking in BSA and goat serum, cells were treated with primary antibody overnight: CytC (Abcam, ab13575). Cells were then incubated in fluorescent-tagged secondary antibodies for 1 hr. No permeabilization or blocking was performed in DAPI experiments. Images were analyzed using ImageJ (Bethesda, MD).

4.2.4 Western Blot Analysis

For CytC experiments, cells were homogenized using a Dounce homogenizer in a buffer containing protease inhibitor cocktail mix III (Calbiochem, Gibbstown, NJ). The cytoplasmic fraction was isolated by centrifugation at 60,000 g for 20 min at 4ºC and collecting supernatant. Proteins were concentrated using Millipore 10K Ambion filters. Protein concentrations were determined using a Bradford assay. Proteins were incubated at 100°C for 5 minutes in sample buffer containing 14% β-Mercaptoethanol. Equal amounts (60 μg) of protein were loaded on a 12.5% precast Tris-HCl polyacrylamide gel (BioRad, Hercules, CA) for each experimental sample. Proteins were transferred to PVDF membrane (Millipore, Billerica MA) and blocked in 10% NFDM for 1 hr. Membranes were incubated overnight at 4ºC in primary antibody for CytC (Abcam, Cambridge MA, ab13575) or caspase 9 (Cell Signaling, #9502). HRP conjugated anti-mouse secondary antibodies (Amersham, Piscataway, NJ) were used at 1:20,000 dilution. Immunodetection was performed with the Luminata Forte HRP substrate (Millipore).

4.2.5 Seahorse assay for mitochondrial function

An XF24 Analyzer (Seahorse Biosciences, North Billerica MA) was used to determine mitochondrial function in untreated cell, cells treated with 100 μM Zn^{2+} for 48 hrs, or with 1 μM staurosporine for 4 hrs. Cells were seeded on specialized microplates so that oxygen consumption rate (OCR) and extracellular acidification rate (ECAR) or proton production rate (PPR) are monitored in real time by the XF24. Then, oligomycin (1 μg/ml), FCCP (1 μM) and antimycin A (10 μM) were injected by the cartridges in order to determine basal levels of oxygen consumption, the amount of oxygen consumption linked to ATP production, proton leak,

maximal respiration capacity and non-mitochondrial oxygen consumption. OCR and ECAR were then normalized to protein levels per well using a Bradford-based assay. Five replicates per group were analyzed.

4.2.6 Reverse Transcriptase and Quantitative qPCR

RNA was isolated from cells using Trizol (Invitrogen, Carlsbag, CA) according to the manufacturer's protocol. cDNA was synthesized using the GeneAmp RNA PCR system (Applied Biosystems, Carlsbad, CA) with oligo dT priming. qPCR was performed SYBR green (Fermentas, Glen Burnie, MD). The amount of cDNA loaded was normalized to starting RNA concentrations, with a final concentration of 9 ng of RNA loaded per experimental well. Six-point standard curves were generated for each primer using 1:2 dilutions of cDNA. cDNA for the following genes were amplified using the indicated primers (IDT, Coralville, IA). Mouse *TRPML1*: forward: 5' -GGCATTGAGGCAAAGAACCT-3', reverse: 5'-GAATGACACCGACCCAGACT-3'. Mouse *LAMP1*: forward: 5' -GCGAATGGTTCTCAGATCGT-3', reverse: 5'- AGGCTGGGGTCAGAAACATT-3'. Mouse *Cathepsin D*: forward: 5' - TACTCAAGGTATCGCAGGGTG-3', reverse: 5'-CCAATGAAGACATCGCCCAG-3'. Mouse *beta Actin*: forward: 5' -GCTCCGGCATGTGCAAAG-3', reverse: 5'- CATCACACCCTGGTGCCTA-3'. Human *LAMP1:* forward: 5'-GGACAACACGACGGTGACAAG-3', reverse: 5'-GAACTTGCATTCATCCCGAACTGGA -3'. Human *TRPML1:* forward: 5'- CAC GGT GCA GCT CAT CCT GTT T-3', reverse: 5'- CGC CAA GTT CTT GGC CTC GAT-3'. Human *RPL32:* forward: 5'- CAACATTGGTTATGGAAGCAACA-3', reverse: 5'-

TGACGTTGTGGACCAGGAACT-3'. Human *MT2a*: forward: 5'AAGTCCCAGCGAACCCGCGT-3', reverse: 5'-CAGCAGCTGCACTTGTCCGACGC-3'. All primers were designed to span exons and negative RT controls were tested to ensure amplification of cDNA only. qPCR was performed using the Standard Curve method on the 7300 Real Time System (Applied Biosystems, Carlsbad, CA). Reactions were run on the following parameters: 2 min at 50°C, 10 min at 95°C, and 40 cycles at 95°C for 15 sec followed by 60°C for 1 min. All experimental samples were run in triplicate and normalized to a β–actin endogenous control.

Statistical significance was calculated using a one-tailed, unpaired t-test with $p \leq 0.05$ considered significant. Data are presented as mean±S.E.M.

4.3 RESULTS

4.3.1 TRPML1 is a component of the lysosomal zinc sink.

Since TRPML1 has been shown to modulate Zn^{2+} efflux from the lysosomes [393], we sought to first verify that TRPML1 indeed retains Zn^{2+} in the lysosome. The upregulation of MTF-1–dependent, Zn^{2+}-responsive genes such as MT2a and ZnT1 [486] indicates elevated cytoplasmic Zn^{2+}. MT2a mRNA was used previously in our studies of the role of TRPML1 in Zn^{2+} handling. We measured the expression of the mRNA of these genes using qRT-PCR in HeLa cells (Figure 32). MT2a expression does not seem to be more sensitive to Zn^{2+} stimulation in TRPML1-deficient cells than in control cells as 2-hr long stimulation of control and TRPML1 KD cells with Zn^{2+} resulted in significant MT2a mRNA spikes, but the spikes were of similar magnitudes

in control and TRPML1 KD cells (Figure 32). When 2-hr long exposure to 100 μM Zn^{2+} was followed by a return to normal Zn^{2+} levels for 24 hours, MT2a levels in control cells fell back to pre-stimulation levels. By contrast, MT2a mRNA remained significantly higher (512±189% of control levels, n=3, $p<0.05$) in TRPML1 KD cells. These data can be explained by the protracted release of Zn^{2+} from the lysosomes into the cytoplasm in TRPML1 KD cells.

Next, we sought to explore the possible effects of TRPML1 on cell function, and to delineate mechanisms linking TRPML1 loss, Zn^{2+} dysregulation, and vacuolar enlargement in TRPML1 KD cells. MLIV is a neurodegenerative disease [441, 442, 510-513], ostensibly linked to neuronal cell death. Mitochondrial dysfunctions play a prominent role in cell death and in storage diseases [514-518]. Since mitochondrial architecture and function are directly affected by cytoplasmic ions, we first focused on the mitochondrial structure as a readout of TRPML1 effects at the cellular level. The integrity of the mitochondrial membrane and the mitochondrial network architecture are critically important determinants, as well as indicators, of cell health [519]. A number of toxic events, genetic diseases and degenerative conditions are associated with the loss of mitochondrial architecture and integrity [519]. A key step in the apoptosis program is the destabilization of the mitochondrial membrane followed by the release of cytochrome (CytC), which can be a passive outcome of chemical modification of mitochondrial lipids [520], or an active event, mediated by the pro-apoptotic Bcl-2 family members [521, 522].

Figure 33 shows that exposure of HeLa cells to 100 μM $ZnCl_2$ for 48 hours induced dramatic changes in mitochondrial structure. Cells stained with Mitotracker suggest that in Zn^{2+} treated cells mitochondrial morphology changed from a well-pronounced network of thread-like organelles to a highly fragmented punctate pattern (Figure 33A). In order to test how TRPML1 affects cells exposed to Zn^{2+}, we used siRNA to modulate TRPML1 levels. Interestingly, Figures

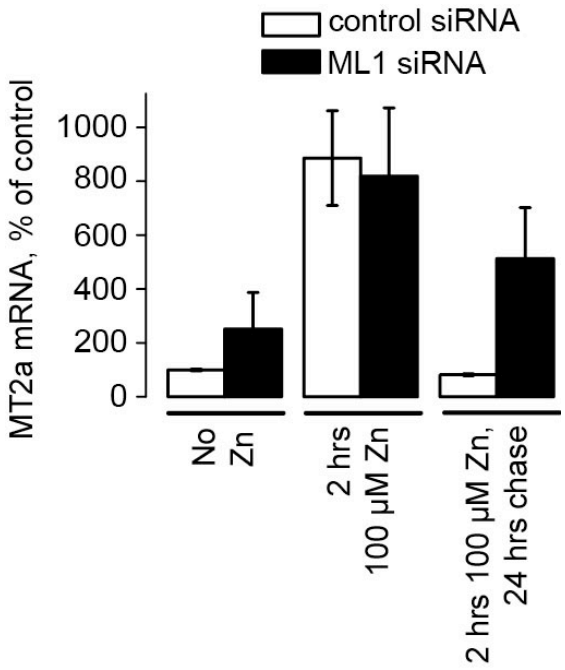

Figure 32. MT2a mRNA response to Zn in TRPML1-deficient cells persists after Zn^{2+} removal.

Pulse-chase experiments showing chronic upregulation of MT2a mRNA in TRPML1 KD cells stimulated with Zn^{2+} for 2 hours (pulse), followed by 24-hr long exposure to normal Zn^{2+} levels (chase). MT2a mRNA was measured using qPCR. Data represent 3-5 experiments. * represents $p<0.05$.

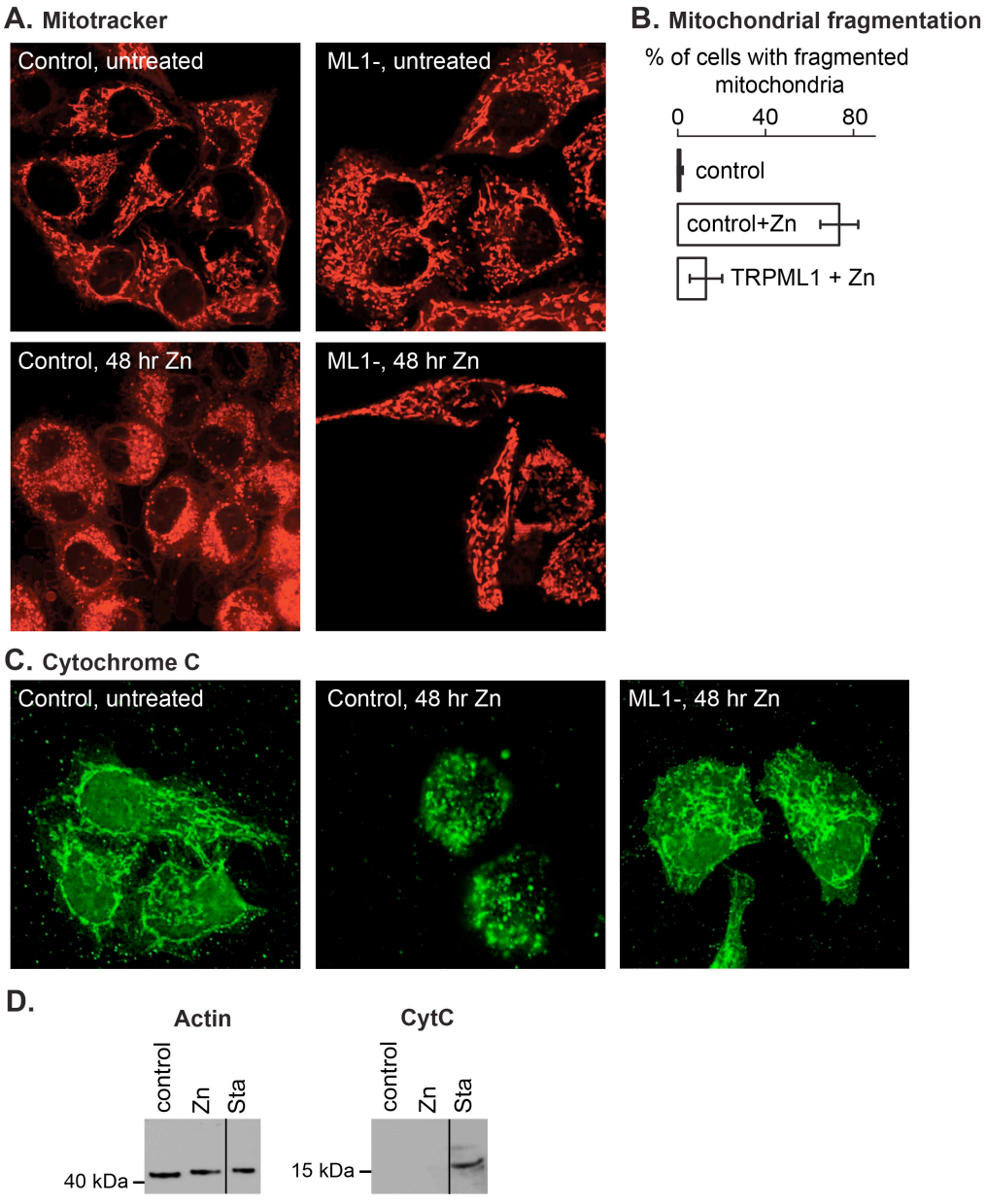

Figure 33. Mitochondrial phenotype in Zn^{2+} treated cells.

HeLa cells transfected with control and TRPML1 siRNA analyzed using confocal microscopy. **A.** Mitotracker stain. Zn^{2+} treated cells were incubated with 100 µM Zn^{2+} for 48 hrs. Panel represents 3-5 separate experiments, 5 images per experiment, per condition. **B.** Frequency of punctate mitochondrial phenotype occurrence is compared in untreated and Zn^{2+} treated control and TRPML1 KD cells. Control cells were transfected with scrambled siRNA.

Data were calculated from confocal images represented by Panel A. Images containing 3 or more cells were used. Only the cells that were completely present in the field of view were taken into account. Each column represents 3 or more experiments, 3-5 images per experiment, per condition. * represents $p<0.05$. **C.** Confocal images representing Cytochrome C stain. Zn^{2+} treated cells were incubated with 100 μM Zn^{2+} for 48 hrs. Panel represents 3-5 separate experiments, 5 images per experiment, per condition. **D.** Western blot analysis of cytoplasmic fractions from untreated and Zn^{2+} treated (48 hrs) HeLa cells probed with actin and Cytochrome C antibodies. Staurosporine (1μM) was used as positive control for Cytochrome C release into cytoplasm.

33A and B show that TRPML1 KD reversed the mitochondrial punctate phenotype induced by Zn^{2+}.

This trend persisted when mitochondrial morphology was tested using immunostaining with antibodies against CytC. This mitochondrial protein is released into the cytoplasm during apoptosis [523]. Therefore, CytC assays enabled us to monitor mitochondrial fragmentation as well as cell death as a function of TRPML1 status and Zn^{2+} exposure. Figure 33 C shows that a 48-hr treatment with Zn^{2+} induced consolidation of CytC into puncta, similar to the Mitotracker stain in cells exposed to Zn^{2+}. As with Mitotracker, TRPML1 KD reversed the punctate phenotype of CytC (Figure 33 C).

The observed effects were not directly caused by, or associated with, measureable deterioration of the mitochondrial functional status. No CytC release into the cytoplasm was observed using confocal microscopy (Figure 33 C) or Western blot (Figure 33 D) with cells treated with Zn^{2+}. Cell death assays utilizing 4',6-diamidino-2-phenylindole (DAPI) or propidium iodide did not result in a statistically significant increase in nuclear fragmentation or loss of membrane integrity (Figure 34). Experiments utilizing mitochondrial dye MitoSOX did not

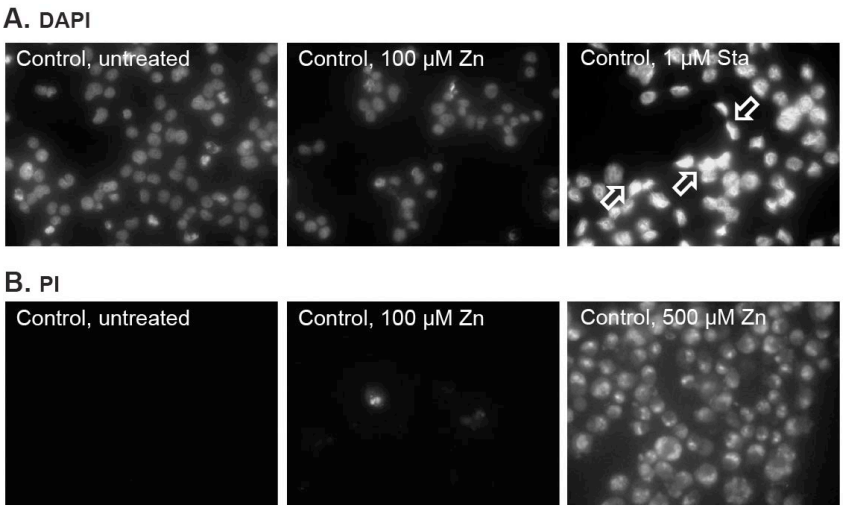

Figure 34. DAPI- and Propidium iodide-based apoptosis assays in Zn^{2+}-treated cells.

A. DAPI stain. Images were obtained using compound microscope fitted with fluorescent attachment. Arrows indicate misshapen nuclei. HeLa cells were treated with Zn^{2+} for 48 hrs, and with Staurosporine (Sta) – for 4 hours. **B.** Cells treated with various concentrations of Zn^{2+} for 48 hrs and stained with PI. No measureable PI uptake is seen in cells treated with 100 µM Zn^{2+}.

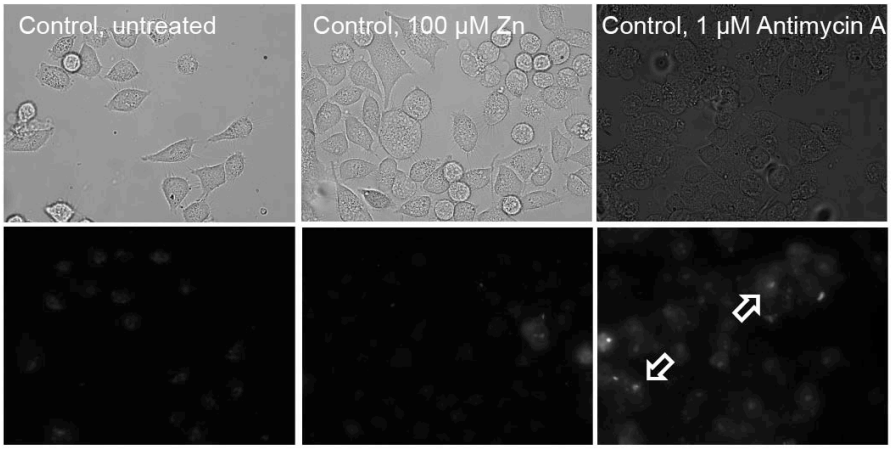

Figure 35. Mitochondrial assays in Zn^{2+}-treated cells.

Top panels show brightfield images of cells. Bottom panels - MitoSOX signal. Images were obtained using compound microscope fitted with fluorescent attachment. Zn^{2+} was applied for 48 hrs, at 100 µM concentration in HeLa cells. Antimycin A (30 min treatment at 1 µM) was used as positive control. Arrows point to cells with MitoSOX signal.

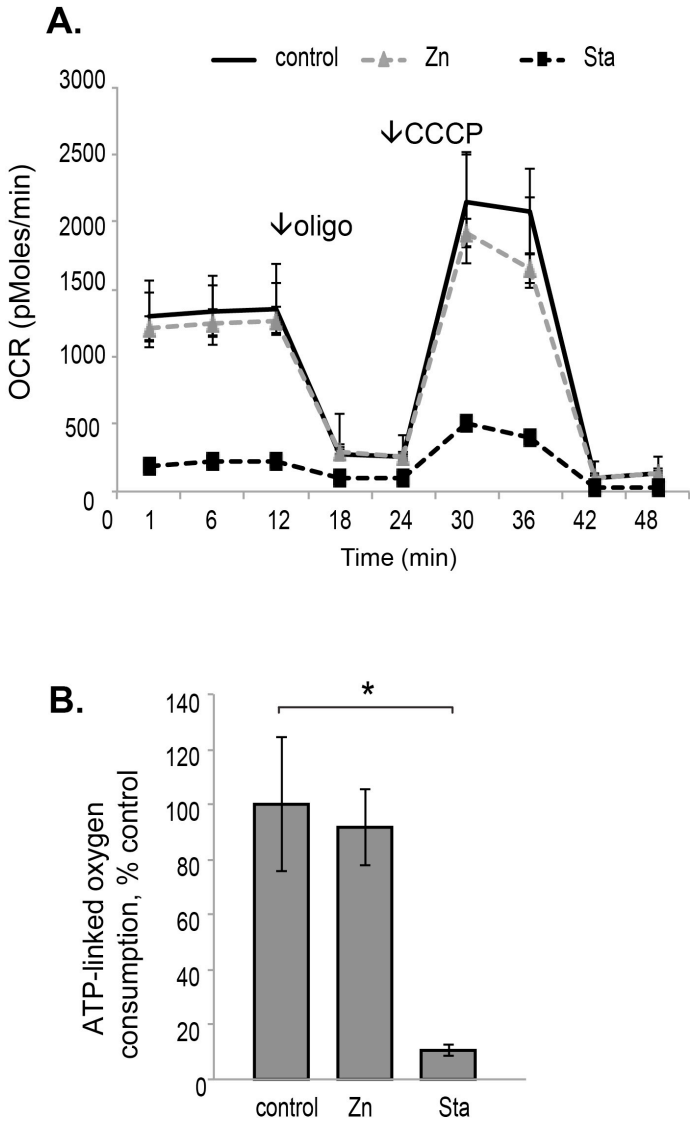

Figure 36. Functional mitochondrial health (Seahorse) assays in Zn^{2+}-treated HeLa cells.

A. Oxygen consumption rates (OCR) are shown for the basal respiration rate of untreated (solid black), Zn^{2+} treated (dashed grey), or staurosporine treated (dashed black) HeLa cells. After the basal measurements, cells were treated with oligomycin (a complex V inhibitor) at the 12 minute mark, FCCP (an uncoupler of ATP synthesis) at the 24 minute mark and Antimycin A (to disrupt the proton gradient) at the 37 minute mark. Zn^{2+} treated cells did not have a significantly reduced basal mitochondrial OCR (left side), nor a reduced ATP-linked OCR (12-24 mins). **B**. ATP-linked OCR rates were compared between untreated, Zn^{2+} treated and Sta treated cells by averaging the drop in OCR following oligomycin treatment.

reveal measurable production of reactive oxygen compound superoxide under our experimental conditions (Figure 35). Finally, the Seahorse assay did not show a statistically significant loss of basal or ATP-linked oxygen consumption in cells treated with Zn^{2+} within the time frame used in these experiments (Figure 36). Mitochondrial respiration was significantly affected and apoptosis was activated upon a 4-hr long treatment with 1 μM staurosporine, which was used as a positive control (Figure 36). These data show that prolonged Zn^{2+} treatment results in a mitochondrial punctate phenotype, which is likely an effect of Zn^{2+} and not a result of cell death. TRPML1 KD prevents mitochondrial punctate phenotype induced by Zn^{2+}.

Taken together, the data described above suggest that although TRPML1 is localized in lysosomes, its effects extend beyond lysosomes and affect other compartments. We have previously shown that TRPML1 loss affects mitochondria function and autophagy [515, 516]. This is another evidence indication that TRPML1 plays a role outside the late endocytic pathway.

4.3.2 TFEB rescues Zn^{2+}–induced LMP.

LMP following lysosomal Zn^{2+} accumulation was clearly shown to be a cell death pathway in many different cell types [304, 477-479]. We propose that the relation between the lysosomal Zn^{2+} absorption rates and the rate of its secretion/release determine whether lysosomal Zn^{2+} accumulation is protective or destructive. We have not observed a significant amount of cell death following moderate (100 μM) Zn^{2+} exposure. However, we did observe LMP with high (200 μM) Zn^{2+} (Figure 31) and show that knockdown of either ZnT2 or ZnT4 prevents LMP. Furthermore, since lysosomal biogenesis and exocytosis are regulated by TFEB and related factors [163, 167], we showed that TFEB overexpression increased lysosomal Zn^{2+} clearance and

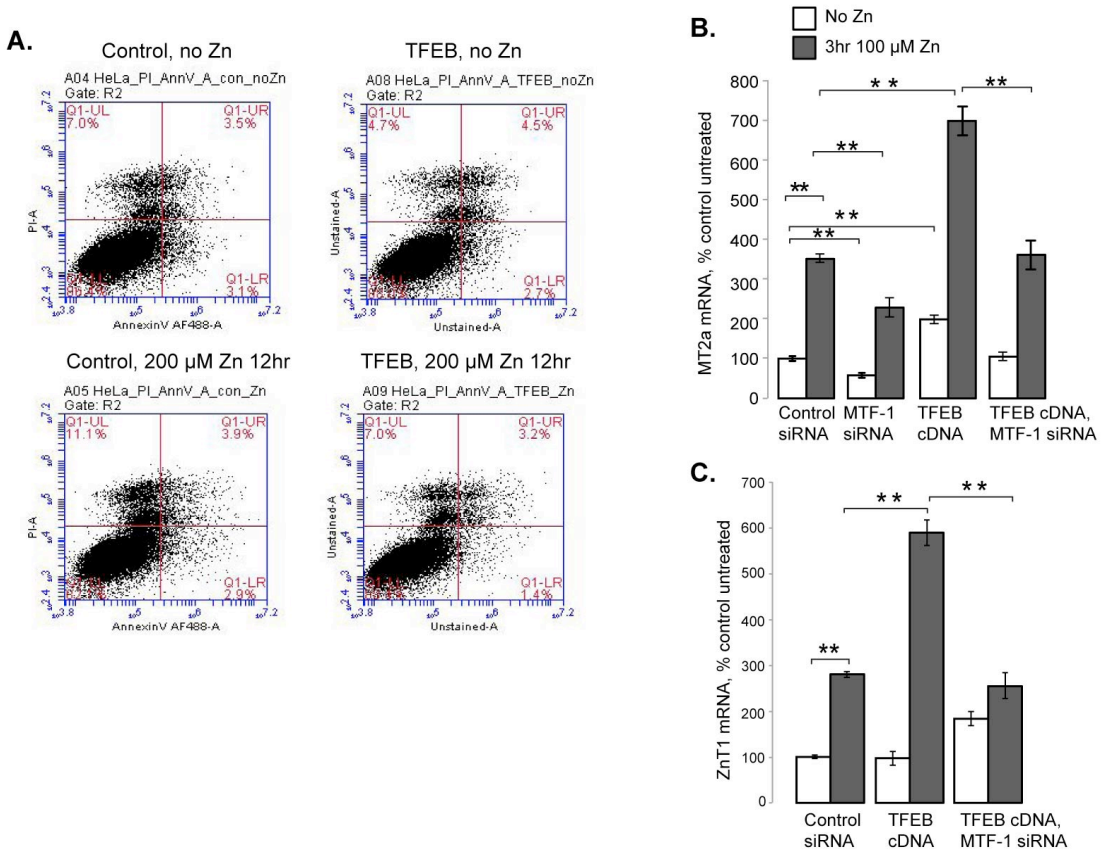

Figure 37. TFEB ameliorates cell death induced by 200 µM Zn^{2+} and LMP.

A) Flow cytometry analysis of HeLa cells stained with PI and AnnV. Mock- or TFEB-transfected cells were either untreated or treated with 200 µM $ZnCl_2$ for 12 hours. Note a decrease in number (7.0%) of cells with positive PI, negative AnnV stain ("necrotic cells") in TFEB cells treated with Zn^{2+} (lower right panel) compared to control Zn^{2+} treated cells (11.1%, lower left panel). **B** and **C)** qRT-PCR results of MT2a (B) and ZnT1 (C) mRNA, shown as percent of control untreated (no Zn^{2+}) cells. RNA was isolated from HeLa cells either untreated (no Zn), or cells treated for 3 hours with 100 µM $ZnCl_2$. * Represents $p<0.05$. ** Represents $p<0.001$.

secretion (Figure 30). If lysosomes function as Zn^{2+} sinks, then increasing lysosomal numbers through TFEB overexpression, should prevent LMP by providing additional Zn^{2+} storage sites. Indeed, Figure 37 A shows that TFEB overexpression decreased propidium iodide staining in LMP-inducing conditions compared to control cells (200 μM Zn for 12 hrs). However, TFEB overexpression, leads to increased expression of at least two genes, whose products are known to play a key role in Zn^{2+} handling. First, Figure 37 B shows that expression of the gene coding for Zn^{2+} chelating protein MT2a is increased as well. MT2a mRNA increased to 305.62±15.93% (n=3, $p<0.001$ compared to untreated control) in Zn^{2+} treated control cells, TFEB overexpression increased MT2a expression to 697.82±42.85% (n=3, $p<0.001$, compared to Zn^{2+} treated control cells). Increased MT2a expression will decrease cytoplasmic Zn^{2+} as well. It should be noted that Zn^{2+} secretion experiments in which TFEB was overexpressed in VAMP7 or SYT7 knockdown cells showed an increased fraction of Zn^{2+} export that is unaffected by VAMP7 and SYT7 knockdown (Figure 30 B). This could indicate increased ZnT1-dependent Zn^{2+} export through the plasma membrane in TFEB-overexpressing cells. Interestingly, this increase does not seem to be directly controlled by TFEB transcriptionally, as knockdown of the transcription factor MTF-1 partially reduces ZnT1 and MT2a expression (Figures 37 B and C). TFEB-cDNA and MTF-1-siRNA-transfected cells had an attenuated response where MT2a mRNA increased only to 360.94±36.86% (n=3, MTF-1 knockdown was confirmed in our previous studies [473]). Second, Figure 37 C shows that the mRNA expression of ZnT1 is increased in Zn^{2+}-treated, TFEB-overexpressing cells. ZnT1 exports Zn^{2+} from the cytoplasm across the plasma membrane. Increased ZnT1 expression itself will decrease cytoplasmic Zn^{2+}. TFEB-overexpressing cells had an elevated ZnT1 mRNA response where ZnT1 mRNA increased to 280.30±6.74% (n=3, $p<0.001$, compared to untreated control cells) in Zn^{2+} treated control cells and 589.00±27.80%

(n=3, $p<0.001$, compared to Zn^{2+} treated control cells) in TFEB-overexpressing cells. Again, this response in Zn^{2+} treated TFEB-overexpressing cells was attenuated by MTF-1 KD to 254.41±28.23%.

4.3.3 TRPML1 expression is regulated by TNFα.

The mammary gland is a highly complex and specialized tissue designed to provide nutrition for offspring. Consequently, mammary gland involution is an essential and natural process that eliminates milk-producing epithelial cells when they are no longer needed at weaning. This two-step process first involves removing the secretory epithelium through autophagic cell death and then replacing it with adipocytes [509]. For some time now, it has been recognized that certain hormones and cytokines drive the molecular mechanisms in the involution process. For example, it has been shown that weaning signals and milk stasis induce LIF, TGF-β, and TNFα signaling pathways [499, 524, 525]. However, what is not well understood are factors that modulate these processes and how they affect mammary gland remodeling and secretion. Interestingly, lysosomal Zn^{2+} accumulation has been observed in the involuting mammary gland and ZnT2 and ZnT4 have been found necessary for involution [499]. Considering that ZnT2-, ZnT4- and TRPML1-deficient cells have autophagic defects, we hypothesize that the lysosomal Zn^{2+} sink plays an important role in autophagice cell death and mammary gland remodeling. To that end, we sought to determine if TRPML1 expression can be modulated by involution signals such as TNFα. Figure 38 shows that TRPML1 expression is significantly upregulated in TNFα-treated mammary epithelial HC11 and RPE cells. Figure 38 A and B show that TNFα increased TRPML1 mRNA expression by 66.39±31.74% (n=3, $p<0.05$, compared to untreated control cells) in HC11 cells and by 38.80±7.59% (n=3, $p<0.05$, compared to untreated control cells) in

RPE cells. TNFα also increased the mRNA expression of LAMP1, a lysosomal membrane protein, by 51.84±22.27% (n=3, $p<0.01$, compared to untreated control cells) in HC11 cells and by 31.09±15.55% (n=3, $p<0.05$, compared to untreated control cells) in RPE cells (Figure 38 A and B). To our knowledge, except for TFEB, this is the only other factor shown to regulate TRPML1 expression. As expected, TFEB overexpression increased TRPML1 mRNA expression by 134.99±28.81% (n=3, $p<0.001$) in untreated RPE cells and by 326.67±47.04% (n=3, $p<0.001$, compared to TNFα–treated mock cells) in TNFα-treated RPE cells. 100mM sucrose was used for 48 hours as a positive control for TFEB as it has been shown to activate and translocate TFEB to the nucleus. 3 hour starvation was also used as a control for the activation of autophagy, another TFEB dependent process. These data support our hypothesis that TRPML1 is upregulated during involution and plays an important role in the autophagic and lysosomal-mediated cell death pathways involved in remodeling of the mammary gland.

4.4 DISCUSSION

While the channel properties of TRPML1 are only now beginning to be understood, the functional impact of TRPML1 activity on cellular processes is unclear. TRPML1 function has been implicated in Ca^{2+}–sensitive membrane fusion events within the endocytic pathway [370, 379, 380], as well as transition metal homeostasis [376, 393, 473]. These data for the first time, have implicated TRPML1 in processes outside of the lysosome. In the course of these studies, we found that, in agreement with the previously published studies, TRPML1 is a vital component of the lysosomal Zn^{2+} sink. Our findings provide further insight into this process by showing that

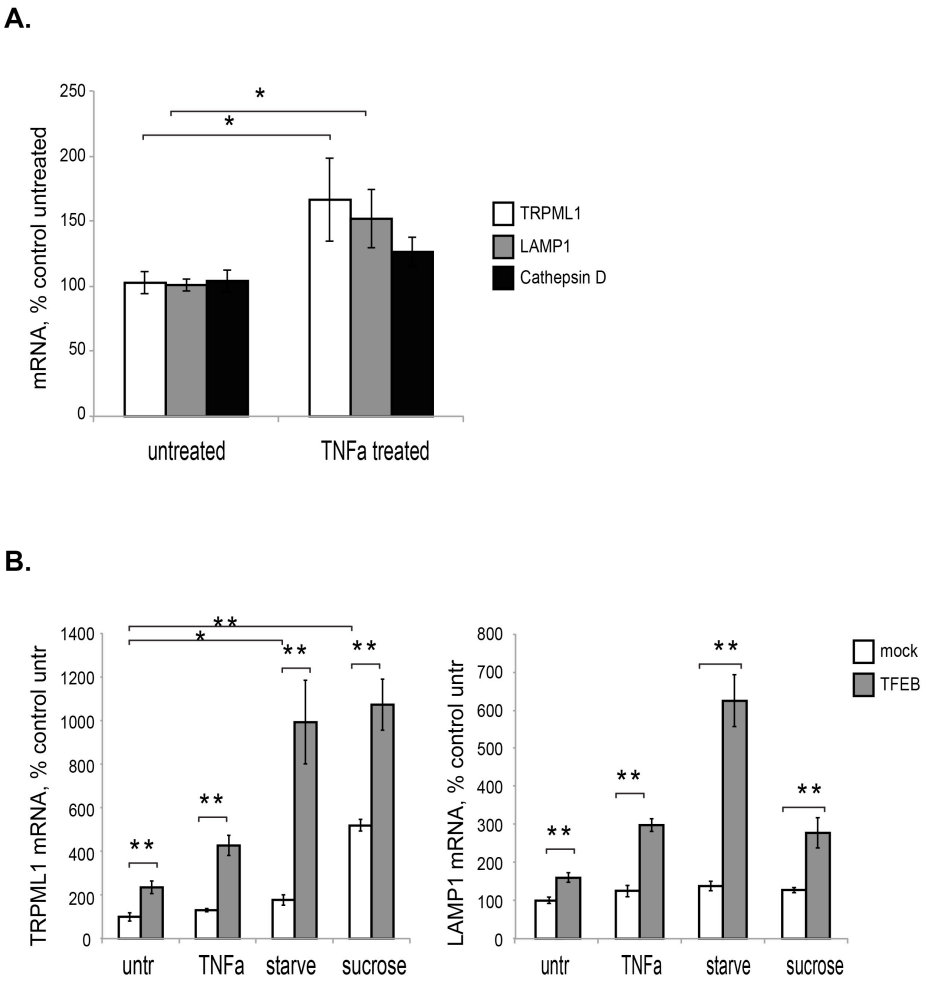

Figure 38. TRPML1 expression is regulated by mammary gland involution signals such as TNFα.

A) qRT-PCR data showing the mRNA expression of mouse TRPML1, LAMP1 and Cathepsin D in mouse mammary epithelial HC11 cells treated with 15 ng/ml TNFα. **B)** qRT-PCR of human TRPML1 (bottom, left) and LAMP1 (bottom, right) mRNA expression in RPE cells. Mock (empty vector) or TFEB overexpressing RPE cells were either untreated (untr), or 24 hours post transfection, treated with 40 ng/ml TNFα for 24 hours, 3 hour starvation, or 48 hour 100mM sucrose. RNA was isolated 48 hours post transfection. Data represents 3 independent experiments per treatment. * Represents $p<0.05$. ** Represents $p<0.001$.

TRPML1 loss affects processes beyond lysosomes, and by identifying some of the signaling pathways that regulate TRPML1 expression.

The impact of TRPML1 on Zn^{2+} regulation seems to involve the mitochondria and cytoplasmic proteins. Augmentation of the MT2a mRNA response to Zn^{2+}, as well as mitochondrial involvement strongly suggest that the effects of TRPML1 loss do not involve only lysosomal compartments; indeed such effects involve the entire cell. Although the exact mechanism and full list of components of TRPML1's mitochondrial involvement is presently unclear, these data illustrate the cell-wide role of TRPML1, beyond the lysosomal context. A role for TRPML1 in regulating cellular ionic balance may be important for understanding the mechanisms of cell death in MLIV. Overall, these data are consistent with TRPML1 as a lysosomal divalent cation channel whose function is to regulate the distribution of transition metals between the cytoplasm and lysosomes. This hypothesis is supported by previously published data on Zn^{2+} and Fe^{2+} buildup in the lysosomes of TRPML1 deficient cells [376, 393].

We have also shown that the lysosomal Zn^{2+} sink can be modulated by TFEB overexpression. TFEB overexpression rescued Zn^{2+}–induced LMP. However, even though this is a fascinating topic, it is very complicated at the moment. Our data on secretion in TFEB-overexpressing cells are in line with our main model of the lysosomal Zn^{2+} sink. However, the complexity of regulatory networks converging on, and regulated by TFEB, means that other interpretations cannot be ruled out within the context of our limited knowledge of TFEB. Our data suggest that the use of TFEB to highlight the importance of the lysosomal secretion in Zn^{2+} toxicity may be misleading since TFEB overexpression increased the mRNA expression of ZnT1 and MT2a as well. In accordance with increased ZnT1 expression, the fraction of Zn^{2+} efflux that is insensitive to VAMP7 or SYT7 KD in our assays (Figure 30) indicates that both pathways

involved in Zn^{2+} clearance under these conditions. The relative contribution of each respective pathway warrants further exploration, but has the potential to provide insights for many lysosomal, neurodegenerative and Zn^{2+} related diseases. We do not know how TFEB stimulates expression of these genes, since they do not contain CLEAR sequences required for TFEB binding. It is, however, clear that TFEB over-expression significantly changes Zn^{2+} handling by cells, and thus all interpretations of the TFEB effect on Zn^{2+} toxicity that are based on our current understanding of TFEB and Zn^{2+} regulation will have this uncertainty. At this time, we do not know any way to specifically prevent TFEB-induced ZnT1 and MT2a expression, without dramatically affecting the entire Zn^{2+} handling landscape.

More importantly, we have not only implicated TRPML1 in mammary gland remodeling, but have also identified a new signaling pathway that modulates TRPML1 expression. These data suggest that TRPML1 expression might be regulated by pro-inflammatory signals and that TRPML1 might be regulating inflammatory processes in other tissues such as the brain and eyes, which would provide novel insights into MLIV. To our knowledge, before these studies, TFEB is the only factor shown to regulate TRPML1 expression [273]. From these and our previous studies we conclude that TRPML1 releases Zn^{2+} from lysosomes into the cytoplasm. It is possible that TRPML1 also releases autophagy-derived Zn^{2+} buildup in lysosomes. For example, in lung epithelial cells, TNFα induces ZIP8 translocation to the mitochondria, and is associated with increased mitochondrial Zn^{2+} content [526]. Although ZIP8 transport activity into or out of the mitochondria has not been characterized, increased mitochondrial Zn^{2+} content has been associated with apoptosis. Yet, another study suggests that ZnT2 localizes to the mitochondria and ZnT2 overexpression leads to increased apoptosis [507]. Indeed, Zn^{2+} accumulation in the mitochondria has been demonstrated to play a major role in neuronal death [1, 527] by

decreasing mitochondrial membrane potential ($\Delta\psi_m$), and increasing the production of reactive oxygen species (ROS) [528-530]. Even though we did not observe a significant ROS signal in our experiments, cell type-specific tolerances for Zn^{2+} concentrations, and cell type-specific ZnT and ZIP expression have been shown [480]. Another possibility is that increased Zn^{2+} concentrations lead to decreased $\Delta\psi_m$ and it has been shown that TRPML1 modulates $\Delta\psi_m$ [336, 531]. It is possible that the regulation of mitochondrial Zn^{2+} pools plays a pivotal role in mammary gland involution since the mitochondria regulate cell death mechanisms leading to cytochrome C release. During autophagy, these mitochondria with high Zn^{2+} content likely accumulate in autolysosomes. We suggest that TRPML1 might be important for releasing this trapped Zn^{2+} in order to prevent LMP. In support of this hypothesis, a recent report from our lab has shown that TRPML1 loss increases the release of the lysosomal protease cathepsin B into the cytoplasm [443].

4.5 ACKNOWLEDGMENTS

This work was supported by the National Institutes of Health grants HD058577 and ES01678 to Kirill Kiselyov. We thank Drs. Shannon Kelleher, Charleen Chu, Haoxing Xu, Shmuel Muallem, Bruce Pitt and Ora Weisz for fruitful discussion. We also thank Dr. Shannon Kelleher and Stephen Hennigar for providing the RNA of TNFα-treated HC11 cells. Additionally, we thank Aaron Gusdon for help with the Seahorse assay.

5.0 CONCLUSIONS AND FUTURE DIRECTIONS

Lysosomes have long been thought of as centers for macromolecular degradation in cells due to their highly acidic environment. However, a growing body of evidence has found that many metal transporters localize to lysosomes, and has demonstrated that lysosomes are involved in many cellular processes that are crucial for regulating cellular homeostasis. Over the course of these studies, I have discovered that lysosomes act as "zinc sinks" that dynamically take up, store and expel zinc based on cellular needs. These studies have provided insights into the lysosomal regulation of zinc homeostasis, TRPML1 function, MLIV pathogenesis, and have identified a new zinc detoxification pathway. Given that over 10% of all cellular proteins bind and depend on zinc for proper function, the implication of this research extend to a large number of cellular processes and are likely to have physiological significance in many human pathologies.

5.1 TRPML1 IS A LYSOSOMAL ZINC LEAK PATHWAY

In Chapter 2, I used an siRNA-mediated approach to knockdown TRPML1 in HeLa cells to establish that TRPML1 is involved in transporting Zn^{2+} out of the lysosome and into the cytoplasm. Moreover, I have found that the source of the lysosomal Zn^{2+} buildup is ZnT4 dependent, and therefore, not autophagic or endocytic, but rather, cytoplasmic in origin.

Since very little is known about lysosomal Zn^{2+} transport mechanisms, I decided to examine whether lysosomal Zn^{2+} content was affected by TRPML1 function. It was previously shown that TRPML1 is permeable to Zn^{2+} [376], and that TRPML1 RNAi-treated HEK-293 cells have large lysosomes that accumulate chelatable Zn^{2+} [393]. The same study also showed that MLIV patient fibroblasts had increased Zn^{2+} content measured by TSQ fluorescence, and claimed (but did not show) that TRPML1 null mice had elevated levels of the $^{66}Zn^{2+}$ isotope in brain tissue. However, it was unclear where this Zn^{2+} came from. I confirmed the enlarged lysosomes and the accumulation of chelatable Zn^{2+} in TRPML1-deficient HeLa cells with two different Zn^{2+}-sensitive dyes (TSQ and FluoZin-3) and showed that knocking down either MTF-1 or ZnT4 rescued the lysosomal enlargement. MTF-1 is a cytoplasmic Zn^{2+}-sensing transcription factor that upregulates the expression of Zn^{2+}-responsive genes such as MT2a and ZnT1, while ZnT4 is a lysosomal Zn^{2+} importer. Consequently, I concluded that the accumulation in TRPML1 was due to ZnT4 importing Zn^{2+} into the lysosomes, and not due to autophagic or membrane trafficking deficits. This suggested that TRPML1 is a Zn^{2+} leak pathway, regulating Zn^{2+} transport out of lysosomes (Figure 39). Considering that lysosomes can dissipate Zn^{2+} either directly through ion channels and transporters, or indirectly through lysosomal exocytosis, I wanted to determine which mode of action was impaired in TRPML1 knockdown cells. I did not observe significant changes in lysosomal exocytosis in TRPML1 knockdown cells, so I used FluoZin-3 fluorescence to measure extracellular Zn^{2+} content to be able to monitor Zn^{2+} secretion. Interestingly, Zn^{2+} secretion assays did not show a decrease in TRPML1 knockdown cells, but rather an increase in extracellular Zn^{2+} content, suggesting that TRPML1 directly influences lysosomal Zn^{2+} release into the cytoplasm. Satisfyingly, TRPML1

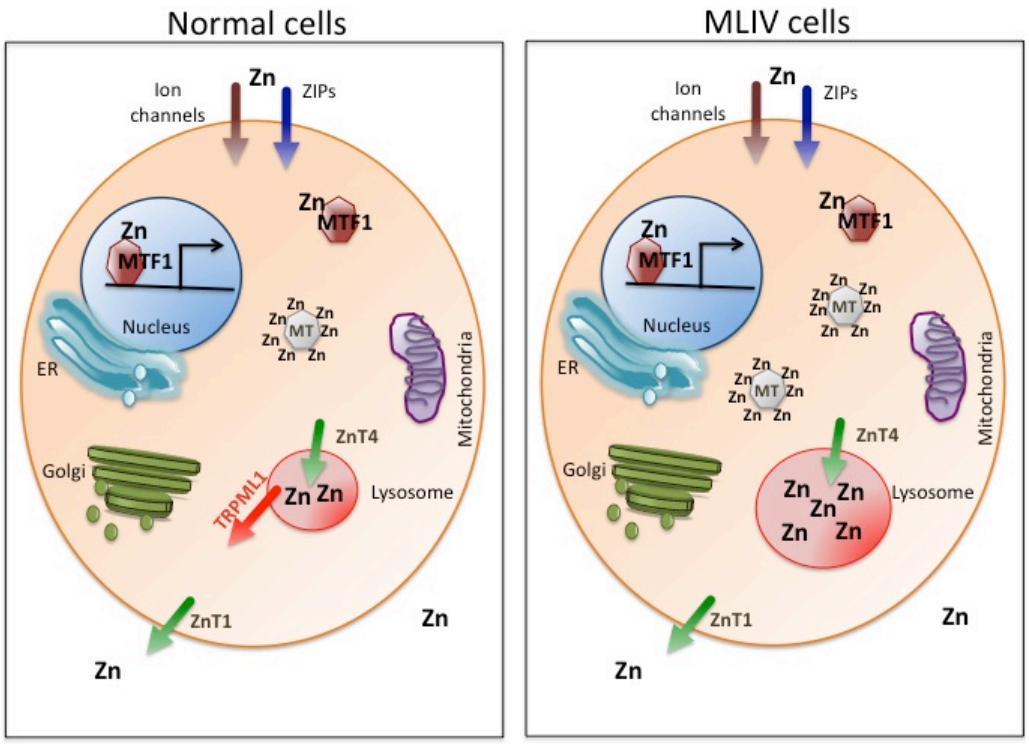

Figure 39. Loss of TRPML1 leads to zinc accumulation in and enlargement of lysosomes.

A model for TRPML1 function. In normal cells (left side), Zn^{2+} enters the cells through ion channels or ZIP transporters and is imported into the lysosome through ZnT4. TRPML1 then transports Zn^{2+} out of the lysosome and into the cytoplasm, where it can either be transported out of the cell via ZnT1, or chelated in the cytoplasm by binding to metallothionein (MT). In MLIV cells, TRPML1 loss leads to Zn^{2+} buildup in lysosomes, leading to their enlargement and an augmented MT response.

knockdown cells not only have delays in Zn^{2+} clearance, as judged by FluoZin-3 fluorescence persisting much longer than in control knockdown cells, but also have less mitochondrial fragmentation than control Zn^{2+} –treated cells (since the is Zn^{2+} trapped in lysosomes).

One of the most interesting findings of my studies was that TRPML1 knockdown cells have significantly elevated metallothionein (MT2a) mRNA expression. In search for a different

read out in addition to FluoZin-3 or TSQ fluorescence, I monitored the mRNA expression of MT2a since it is upregulated in response to elevated Zn^{2+} levels. I found that both TRPML1 knockdown in HeLa cells, as well as MLIV patient fibroblasts (Appendix A, Figure 43), have dramatically elevated MT2a mRNA levels compared to controls. This was interesting because it hints at the possibility of using MT2a mRNA expression as a biomarker for MLIV and possibly other lysosomal storage disorders, which would add a diagnostic tool for MLIV detection. Future studies will be needed to verify the sensitivity, specificity and induction level of MT2a in other cell types and *in vivo*.

Even though these studies provided great insights into TRPML1 function, they still left a lot of unanswered questions. For example, how does TRPML1 affect lysosomal Zn^{2+} release? Does it do so directly, and if so, what is the structural basis for the transport function, or does it release Zn^{2+} by modulating the function of other transporters such as ZIP8? Except for TRPML1, ZIP8 is the only Zn^{2+} transporter identified to release Zn^{2+} from lysosomes. Interestingly, ZIP8 has been shown to localize to the plasma membrane, lysosomes and mitochondria [497, 526], and to release Zn^{2+} in response to TNFα [532]. Future research will address whether TRPML1 stimulates lysosomal Zn^{2+} release by affecting ZIP8 function or localization. The other possibility is that TRPML1 affects ZnT2 or ZnT4 function by regulating the ionic environment of lysosomes, and the low lysosomal pH has been shown to be necessary for Zn^{2+} binding and transport activity of ZnTs [24, 25]. Lastly, TRPML1 has been shown to be permeable to Zn^{2+} and could directly transport Zn^{2+} out of lysosomes. Although no structural elements have been identified for TRPML1 Zn^{2+} transport, I predict that the large loop between the first and second transmembrane of TRPML1 plays a critical role. In fact, a sequence alignment of TRPML1 and TRPML3 shows a fair amount of histidine residues that localize to the loop between the 1st and

2nd transmembrane, similar to the histidine-rich domains of ZnTs and ZIPs that confer their Zn^{2+} transport activity [16, 20-22]. To date, no current TRPML1 function has been assigned to that loop.

Another area of future research is to further characterize the Zn^{2+} buildup in TRPML1 knockdown cells. Figure 8 B shows FluoZin-3,AM fluorescence within both Lysotracker positive vesicles, as well as other non-lysosomal cytoplasmic punta. At this point, it is unclear if these punta are endosomes, Golgi vesicles, or simply lysosomes that are no longer acidic. Future experiments with FluoZin-3,AM along with lysosomal constructs, such as LAMP-RFP, instead of Lysotracker, could shed light on this discrepancy. Alternatively, it would not be surprising if these were endosomes since membrane trafficking defects have been observed with TRPML1-deficient cells [218, 370, 377, 378]. Perhaps these puncta represent endocytosed Zn^{2+} trapped in endosomes en route to the lysosomes? This is actually a very interesting question within the field. Extracellular zinc ions have been shown to be taken up through the endocytic pathway and confined in vesicles termed "zincosomes' in many cell types and yeasts [17, 533-536], however, what specific proteins or Zn^{2+} transporters localize to zincosomes has remained a mystery. One report suggests that ZnT2 and protein kinase C (PKC) localize to zincosomes along with actin and possibly caspases [537]. Also, these findings should be repeated using a different TRPML1-specific siRNA to rule out any off target effects, and experiments should be done overexpressing an siRNA resistant TRPML1 construct in knockdown experiments to determine if lysosomal enlargement and Zn^{2+} buildup could be rescued.

Additionally, another possible avenue is to use TRPML1 agonists and develop lysosome-targeted genetically encoded Zn^{2+}-indicators to determine the contribution of TRPML1 lysosomal Zn^{2+} release. A genetically encoded Ca^{2+} indicator (GCaMP3) attached to TRPML1

has been successfully used to study TRPML1 lysosomal Ca^{2+} release [538]. This method could be adapted to develop a Zn^{2+} indicator using MT, for example, similar to a method developed for studying nitric oxide signaling with FRET-MT [539, 540]. Then, a TRPML1 agonist could be used to increase Zn^{2+} levels. ML-SA1 was recently identified as a TRPML1 agonist and has been shown to activate TRPML1 currents [538], along with TRPML2 and TRPML3. One way to isolate TRPML1 function would be to either use the constitutively active TRPML1-Va mutant [541] (which unfortunately, has been associated with toxicity), or to use ML-SA1 in conjunction with TRPML1 mutants. Mutations could be introduced in TRPML1 to mutate the histidine residues, the pore region, or to delete the loop between the first and second transmembrane domains, for example.

5.2 LYSOSOMES SECRETE ZINC THROUGH LYSOSOMAL EXOCYTOSIS

My work in Chapter 3 has identified a new Zn^{2+} detoxification pathway, as well as a novel lysosomal function. It was shown that lysosomal Zn^{2+} accumulation is necessary for lysosomal enzymes [471], and many processes including mammary gland remodeling, but at the same time toxic by inducing lysosomal membrane permeabilization (LMP) and cell death due to the release of the lysosomal enzymes such as cathepsins [476-479]. Since very little is known about why and how Zn^{2+} accumulates in the lysosomes, I decided to examine the role of lysosomes in Zn^{2+} homeostasis.

To begin with, I pharmacologically inhibited lysosomal function with bafilomycin, a drug that increases the lysosomal pH by inhibiting the lysosomal H^+ pump. I discovered that Zn^{2+}-exposed cells with impaired lysosomal function had elevated cytoplasmic Zn^{2+} levels, indicated

by brighter FluoZin-3 staining as well as increased mRNA expression of MT2a and ZnT1. Curiously, this elevated cytoplasmic Zn^{2+} increase correlated with a redistribution of Zn^{2+} pools to other organelles such as the Golgi and the mitochondria, as well as increased cell death. Thus, I concluded that the lysosomal "Zn^{2+} sink" was important in maintaining Zn^{2+} homeostasis (Figure 40). But this then prompted a series of other new questions: Are lysosomes the terminal depot for this Zn^{2+}, or are they temporary storage sites? How much Zn^{2+} can lysosomes store before LMP ensues? Can we increase the volume of Zn^{2+} storage by manipulating lysosomal numbers? If lysosomes are not the terminal destination for this Zn^{2+}, then where does it go and how does it get there? Lysosomes can dissipate Zn^{2+} through either lysosomal Zn^{2+} transporters, or through lysosomal exocytosis, a process where lysosomes fuse with the plasma membrane to expel their content. Considering that very limited information is available on lysosomal Zn^{2+} transporters, and that it is likely that their localization is dependent on yet unidentified signaling cascades, I decided to address these questions by inhibiting lysosomal exocytosis. Since lysosomal fusion with the plasma membrane is mediated by the vesicle SNARE (v-SNARE) TI-VAMP/VAMP7, the Ca^{2+} sensor synaptotagmin VII (SYT7) on lysosomes, the target SNAREs (t-SNAREs) SNAP23 and syntaxin 4 on the plasma membrane [268], along with many Rab proteins on the lysosomal membrane [269-271], I decided to knockdown VAMP7 and SYT7. Notably, both VAMP7 and SYT7 knockdown decreased Zn^{2+} secretion compared to control cells. VAMP7 and SYT7 knockdown cells also had increased lysosomal and cellular Zn^{2+} levels when imaged with FluoZin-3. Based on this, I concluded that lysosomes secrete Zn^{2+} through lysosomal exocytosis and thereby, are not the terminal depot for Zn^{2+}. Moreover, VAMP7 knockdown Zn^{2+}–treated cells had elevated levels of apoptosis, indicating that clearance of lysosomal Zn^{2+} content through lysosomal exocytosis was important for cell homeostasis

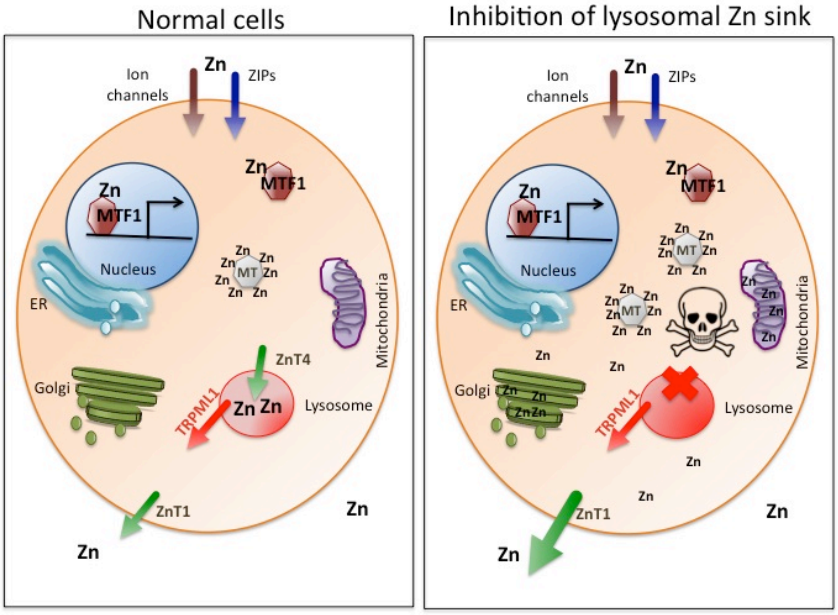

Figure 40. Inhibition of the lysosomal zinc sink leads to zinc accumulation in other organelles and cell death.

A model for the lysosomal function as a zinc sink. Lysosomes are cytoprotective and temporarily store $Zn^{2+,}$ preventing its buildup in other organelles such as the Golgi and mitochondria.

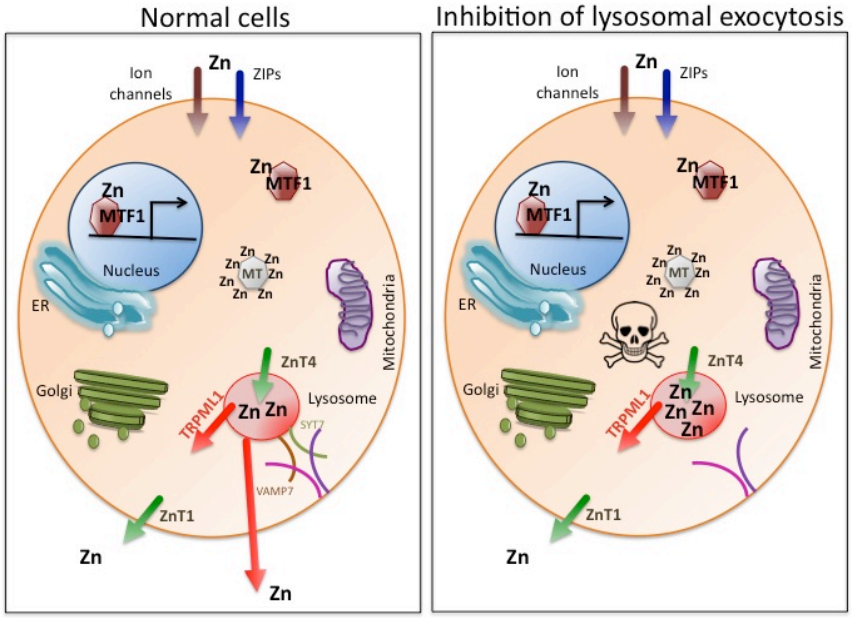

Figure 41. Inhibition of the lysosomal exocytosis in zinc treated cells leads to cell death.

Lysosomes expel sequestered Zn^{2+}, in a VAMP7 and SYT7 dependent manner through lysosomal exocytosis in order to prevent LMP and cell death.

(Figure 41). Next, I wanted to determine if this new detoxification pathway can be modulated by augmenting lysosomal biogenesis. Indeed, TFEB overexpression increased Zn^{2+} secretion, but it also unexpectedly increased ZnT1 mRNA expression as well. Consequently, without inhibiting ZnT1, it is difficult to conclude the lysosomal contribution to this observed increase in Zn^{2+} secretion. Perhaps future experiments can overexpress the recently identified transcription factor E3 (TFE3) [167] to increase lysosomal biogenesis without increasing ZnT1 expression. Nonetheless, I also wanted to determine whether LMP-inducing, higher lysosomal Zn^{2+} loads could be prevented. Indeed, I have shown that LMP can be induced in HeLa cells by increasing the Zn^{2+} concentration, and more importantly, can be prevented by ZnT2 and ZnT4 knockdown, as well as TFEB overexpression (Figure 42). These studies have identified components of the Zn^{2+} sink, shown that its function can be modulated, and transformed our perception of lysosomes into dynamic organelles that are essential for metal ion homeostasis.

Although this work has made significant progress toward understanding the role of lysosomes in Zn^{2+} trafficking, many important questions remain. For example, what is the relative contribution of lysosomal Zn^{2+} secretion to ZnT1? ZnT1 is the only Zn^{2+} detoxification pathway identified to date. This question is easily testable by performing the Zn^{2+} secretion assay with a ZnT1-specific siRNA and comparing the loss of Zn^{2+} secreted to VAMP7 or SYT7 knockdown. Also, it is possible that some Zn^{2+} is secreted through the Golgi, and as such should be analyzed with a ZIP9 knockdown. However, I would expect that a ZnT1, VAMP7 double knockdown should completely ablate Zn^{2+} secretion.

My work discussed in Chapters 3 and 4 has opened an exciting new avenue of research for the Kiselyov lab. As discussed before, while many metal transporters have been shown to localize to lysosomes, there is scarce information on lysosomal Zn^{2+} transporters, likely because

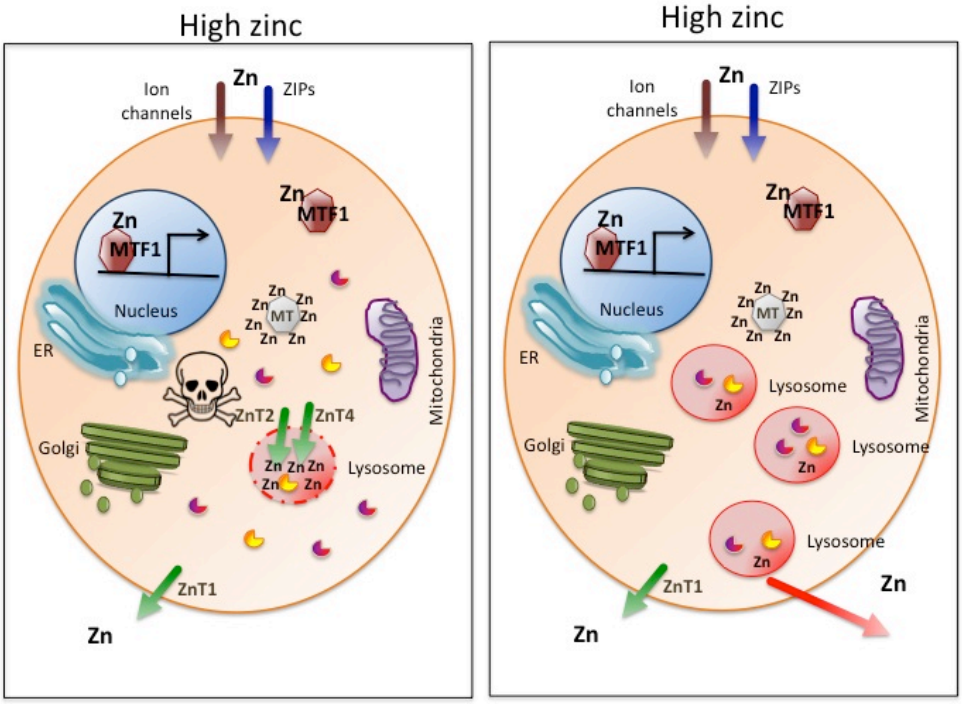

Figure 42. Inhibition of lysosomal zinc loading through ZnT2 or ZnT4 knockdown, or increasing lysosomal biogenesis through TFEB overexpression prevents LMP and cell death.

High (200 μM) zinc concentrations lead to lysosomal membrane permeabilization (LMP), which results in cell death due to the release of lysosomal enzymes such as cathepsin B and D. LMP can be rescued by reducing lysosomal loading, increasing ZnT1 function, or augmenting lysosomal biogenesis and exocytosis.

they are cell type specific and induced by yet unidentified signaling cascades. Towards that end, some Zn^{2+} transporters have been shown to be activated by transcription factors other than MTF-1, such as signal transducers and activators of transcription 3 (STAT3), STAT5 and TNFα. For example, ZIP6 localizes to the plasma membrane and has been shown to be regulated by STAT3 [87] and MAPK signaling [542]. ZIP14 also localizes to the plasma membrane and is upregulated by Interleukin-6 [96]. ZnT2 has been shown to localize to the mitochondria and lysosomes and to be regulated by STAT5 [88]. Meanwhile, ZIP8 localizes to the plasma membrane, mitochondria and lysosomes and is regulated by TNFα and NF-ϰB [497, 526, 532].

In Chapter 4, I discussed a novel pathway for TRPML1 transcriptional activation through TNFα. Future experiments will dissect the signaling pathways that regulate the lysosomal localization of Zn^{2+} transporters. I expect that the pathways that regulate lysosomal Zn^{2+} content will correlate with the physiological requirements of lysosomal Zn^{2+}, such as during development, lactation and an immune response. In most cases, I predict that these Zn^{2+} transporters will have lysosomal sorting sequences such as dileucine motifs that are revealed by the activation of the signaling pathways to allow it to re-localize to lysosomes. There is some precedence for this with the lactogenic hormone prolactin, which has been shown to change the subcellular localization of ZIP3 and ZnT2 [93, 433]. Additionally, there are bound to be genetic, dietary or environmental factors that affect lysosomal Zn^{2+} sequestration.

5.3 CLINICAL SIGNIFICANCE

There is surprisingly little information on lysosomal storage disorders (LSDs) and metal homeostasis. On the one hand, altered expression of Zn^{2+} genes and reduced Zn^{2+} serum levels have been reported in Niemann-Pick type C (NPC) disease [543-545], as well as in aspartylglycosaminuria (AGU) patients [546]. AGU is a rare LDS caused by mutations in the lysosomal enzyme aspartylglucosaminidase. AGU symptoms begin at the age of 2 and range from spine and eye deformities, behavior problems and psychomotor and intellectual disability. While on the other hand, increased Zn^{2+} concentrations have been reported in neuronal ceroid lipofuscinosis (NCL) [469, 547], and as discussed in Chapter 1, altered Zn^{2+} homeostasis has been implicated in many neurological diseases including Alzheimer's disease, amyotrophic lateral sclerosis (ALS), depression, epilepsy, ischemia, schizophrenia [14, 548], and most

recently, Parkinson's disease [549]. For example, in Parkinson's disease, ATP13A2 has been shown to maintain Zn^{2+} homeostasis and α-synuclein secretion through exosomes [550]. Thus, given the grave health consequences associated with Zn^{2+} dyshomeostasis, the implications for my research extend beyond lysosomal storage disorders and include many neuropathies.

MLIV diagnosis includes TRPML1 genetic mutations, anemia, and elevated gastrin levels [355]. There is some evidence that gastric secretion can be increased with Zn^{2+} supplementation [551, 552]. Thus, I hypothesize that some MLIV symptoms might be alleviated with Zn^{2+} chelators. Moreover, one study showed that gastrin induced the plasminogen activator inhibitor-2 (PAI-2), a protein associated with cell invasion and suppression of apoptosis, through p50 and p65 [553]. This is interesting, considering that the Kiselyov lab has found elevated p50 levels in TRPML1 knockdown cells (unpublished data, Grace Colletti 2011 dissertation). Future experiments will determine the direct correlation between gastrin levels and Zn^{2+} status.

Cumulatively, my thesis research has implicated lysosomes as "zinc sinks" that dynamically take up, store and expel zinc based on cellular needs. These studies have not only provided significant insights into TRPML1 function and MLIV pathogenesis, but have also identified a new zinc detoxification pathway. Considering the broad physiological roles of zinc, my work can be applied to study many cellular processes ranging from neurotoxicity to the immune response and wound repair. Thus, in summary, my progress on understanding the role of TRPML1 and lysosomes in zinc homeostasis will serve as a foundation for future studies to address many of the remaining unanswered questions.

APPENDIX A

ZINC DYSHOMEOSTASIS IN MLIV PATIENT FIBROBLASTS

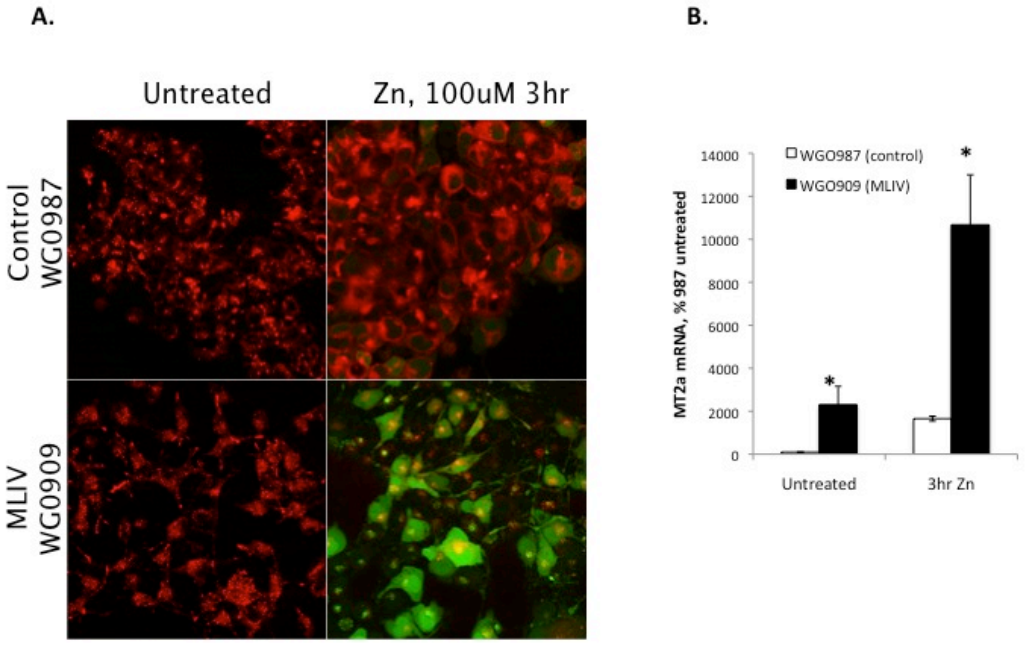

Figure 43. Elevated cellular zinc levels in MLIV patient fibroblasts.

A. Confocal images of control (WG0987) and MLIV (WG0909) patient fibroblast cells treated with 100 μM Zn^{2+} for 3 hours and loaded with FluoZin-3,AM and LysoTracker. **B.** qRT-PCR results of MT2a mRNA, shown as percent of untreated control (WG0987) cells. RNA was isolated from control (WG0987) and MLIV (WG0909) patient fibroblasts treated for 3 hours with 100 μM Zn^{2+}. * Represents $p<0.05$ compared to respective control cells.

APPENDIX B

HOMER AS A MECHANISM FOR CALCIUM SIGNALING ADAPTATION

The work discussed in this section is unpublished data of which I performed all the experiments.

B.1 INTRODUCTION

Many hormones, neurotransmitters and growth factors exert their effects on eukaryotic cells by initiating calcium (Ca^{2+}) signaling: an increase in cytoplasmic Ca^{2+} levels in target cells. Ca^{2+} signaling has both short- and long-term effects. The short-term effects include muscle contraction, vesicle fusion, fluid and electrolyte secretion, and neurotransmitter release, while prolonged exposure to intracellular Ca^{2+} spikes can have long-term, or adaptive effects and include proliferation, and gene and protein expression profile changes [554].

The major means of regulating Ca^{2+} signaling is through the proximity of key signaling elements. Scaffold proteins modulate Ca^{2+} signaling by forming molecular interactions that tether components of a signaling pathway together, allowing for more efficient signaling. Homer is a product of an immediate early gene (IEG) that is unique among scaffolds involved in Ca^{2+} signaling because it is dynamically regulated. Homers play a central role in Ca^{2+} signaling by

increasing the proximity of Ca^{2+} signaling proteins [555, 556]. As a result of alternative splicing, there are multiple Homer variants that are classified primarily into long and short forms. The long Homer forms are constitutively expressed and form protein clusters with other target proteins in order to facilitate signal transduction [557]. In neurons, cells switch in an activity-dependent manner to expressing short Homer forms that function as a natural dominant negative to long Homers, disrupting Homer clusters and Ca^{2+} signaling [556]. How this switch occurs is not known. Homer is expressed and functional in Ca^{2+} signaling in non-excitable cells [555], but the full implications of having two forms of a scaffold protein in non-neuronal cells are not fully understood. In the course of these studies, I sought to determine a) the mechanism that regulates the Homer switch and b) whether non-neuronal cells can switch Homer isoforms.

B.1.1 Ca^{2+} and GPCR signaling

When a neuron is stimulated, an influx of Ca^{2+} occurs through the activation of voltage-dependent Ca^{2+} channels in the plasma membrane [558]. This increase in cytoplasmic Ca^{2+} levels regulates a range of cellular processes including transcription, cytoskeletal structural changes, and apoptosis. Ca^{2+} also exists within the cellular compartments of all cells such as in the endoplasmic reticulum (ER), and can be released upon cell stimulation. In both neuronal and non-neuronal cells, G protein-coupled receptors (GPCRs) are the major method by which an external stimulus is translated into an intracellular Ca^{2+} signal. Upon receptor activation, Gα (the G-protein subunit containing the guanine nucleotide binding site which is GDP-bound in the inactive state) can activate effector proteins. In Ca^{2+} signaling, the effector is phospholipase C (PLC), which when activated, hydrolyzes phosphoinositides (PIP_2) to generate inositol triphosphate (IP_3) and diacylglycerol (DAG).[6] IP_3 binds to IP_3 receptors (IP_3Rs) within the ER,

facilitating Ca^{2+} release from intracellular pools such as the ER. Prolonged stimulation of IP_3Rs is associated with activation of the Ca^{2+} entry pathway [559].

GPCRs are signal interpretation, translation and amplification mechanisms for almost all hormones, growth factors and other important signaling proteins. Due to the inherent complexity of GPCR signaling, proximity of key interacting proteins is essential for efficient signaling. The major means of regulating proximity is through scaffold proteins. One of the first examples of a scaffold protein involved in Ca^{2+} signaling complex formation is the *Drosophila* photoreceptor scaffold protein INAD. INAD contains five PDZ domains that allow it to bind multiple proteins involved in visual signal transduction such as GPCRs, transient receptor potential (TRP) channels, protein kinase C (PKC) and PLC [560], bringing all of these proteins in close proximity. Mutating the PDZ domain that directly binds TRP disassembles the complex and severely handicaps signal transduction [561]. Other examples of Ca^{2+} signaling scaffold proteins include AHNAK1 [562] and IQGAP1 [563]. Thus, scaffolding proteins are well established in the formation and regulation of Ca^{2+} signaling complexes.

B.1.2 Homer in neurons

Homer is a unique scaffold protein because it is dynamically regulated. As a result of alternative splicing of the *Homer 1* gene, there are multiple Homer variants primarily classified into long and short forms. The long form of Homer 1, Homer 1 b/c (h1b/c), contains two major domains; a coiled-coil (CC) domain and an Enabled/vasodilator-stimulated phosphoprotein Homology 1 (EVH1) domain [557]. The EVH1 domain binds to proline rich sequences in target proteins such as glutamate receptors, TRP cation channel (TRPC1), or IP_3Rs, while the CC domain contains leucine zippers and is responsible for Homer multimerization (Fig. 44) [557, 564-567]. Homer

multimers hold signaling molecules together by binding plasma membrane molecules and intracellular Ca^{2+} stores to facilitate and modulate signal transduction efficiently between them [557, 568]. The short form of Homer, Homer 1 a (h1a), does not have the CC domain and thus functions as a natural dominant negative to h1b/c by disrupting the complexes formed by h1b/c (Fig. 44). In neurons, several studies have shown that h1b/c is constitutively expressed, but that h1a expression is induced during memory establishment and following specific neural activity such as seizures, learning, dopaminergic stimulation, long-term potentiation, or drug use [568-573]. Therefore, the expression of h1a might be a feedback mechanism to reduce glutamate-induced release of Ca^{2+} from intracellular pools [556].

The Homer switch has been extensively shown to occur in neuronal tissue, but little is known about the regulatory mechanism that controls this switch. Based on Homer's role in Ca^{2+} signaling and the current literature, our *main hypothesis is that the Homer switch is regulated by Ca^{2+} signaling and can be modulated by other signaling pathways such as cyclic AMP (cAMP).* In order to determine the regulatory mechanism that activates the Homer switch, we used a pheochromocytoma of the rat adrenal medulla (PC12) cell line to induce h1a upregulation in a cell culture system. Total RNA from treated cell culture samples was isolated and subjected to reverse transcription PCR (RT-PCR). Isoform specific primers were designed to span the unique last exon in rat Homer 1 a (GenBank: AJ276327.1) and to cover the unique additional exon in rat Homer 1 c (GenBank: AF093268.1). The amplified isoforms share a highly conserved sequence between the rat, mouse and human species.

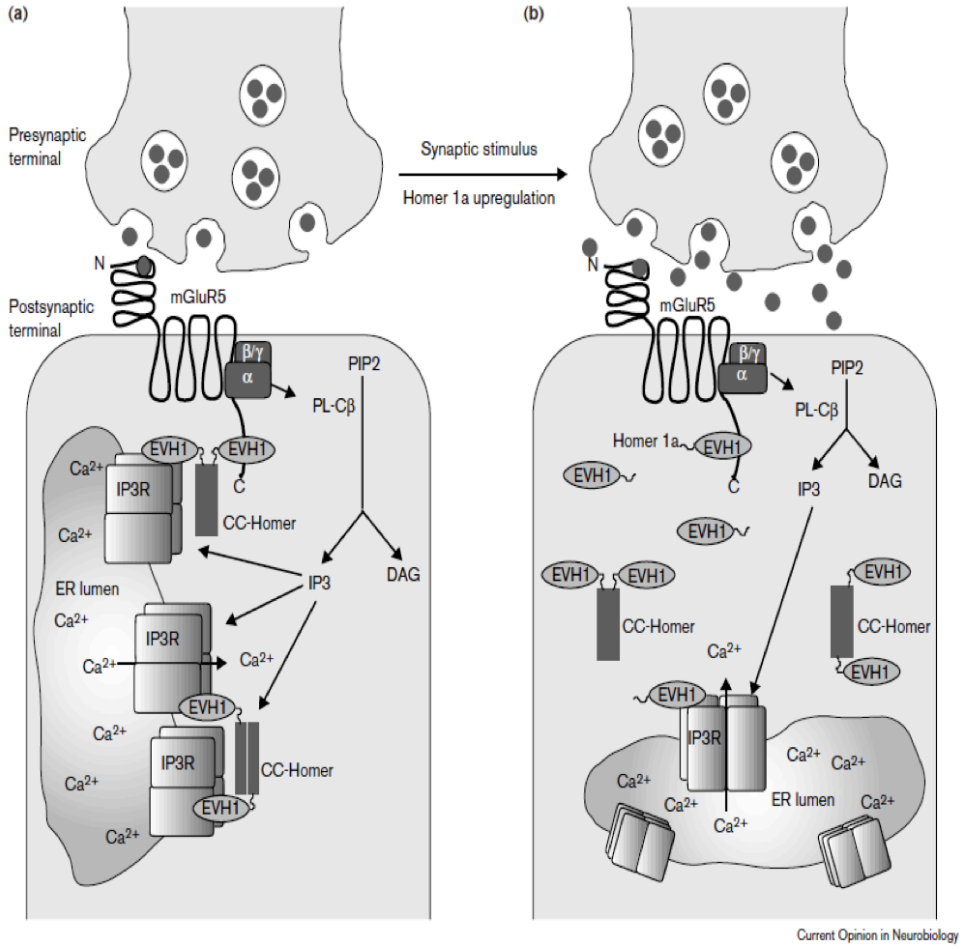

Figure 44. Homer regulates mGluR signaling.

(a) Constitutively expressed Homer proteins (CC-Homers) are localized to the postsynaptic compartment, where they bind the carboxyl terminus of group I mGluRs and IP3Rs. These receptors are physically coupled by CC-Homers to form an efficient signaling complex that generates IP3 and releases Ca^{2+} from intracellular pools. (b) In response to specific forms of neural activity, Homer 1a is rapidly upregulated. Figure adapted from [556] .

B.2 RESULTS

B.2.1 Regulation of Homer splicing

When Ca^{2+} stimulation by depolarization via 50mM potassium chloride (KCl) generates a modest increase in h1a, increasing h1a levels over 20% (21.6±0.39%, n=3, $p<0.001$) compared to control conditions. H1a was also shown to be upregulated following dopaminergic stimulation with cocaine injections [574]. Dopaminergic stimulation increases intracellular cAMP levels. To mimic this effect in cell culture, PC12 cells were stimulated with forskolin (FSK), which activates the adenylyl cyclase, raising intracellular cAMP levels. Indeed, Figure 45 shows that we successfully induced the Homer switch in a cell culture model: 3 hour stimulation with 20μM FSK and 50mM KCl upregulates h1a RNA levels by over 70% (70.57±7.48%, n=3, $p<0.001$) compared to control. This result indicates a possible synergistic effect between the Ca^{2+} pathways and cAMP pathways.

FSK alone increased h1a levels by over 50% (52.25± 12.61%, n=3, $p<0.05$). h1c levels are fairly constant across treatments with large variations, possibly reflecting the variation found in the constitutively expressed h1c levels across samples. However, because it is not known how the Homer switch occurs relative to long Homer levels, it is possible to explain these results as either a downregulation of h1c or as natural variation across samples. To answer this question, better statistical analysis with more samples is needed. In sum, we have shown that we can successfully induce the Homer switch by inducing the expression of h1a in neuronal cells.

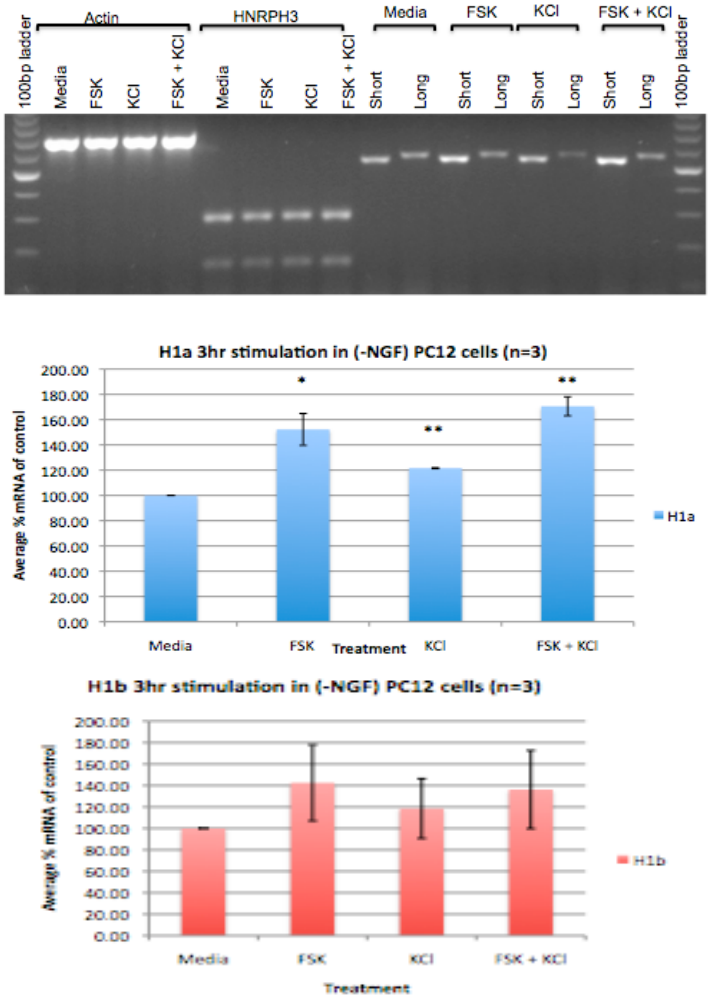

Figure 45. Forskolin and KCl activate Homer switch in neuronal cells.

Representative RT-PCR gel and quantifications of Homer levels in PC12 cells following forskolin (FSK) and KCl treatment. Short Homer increases significantly when PC12 cells are treated with both FSK and KCl, while long Homer levels do not change. * indicates $p<0.05$ and ** indicates $p<0.001$.

B.2.2 Homer in non-neuronal cells

Interestingly, Homer was shown to be expressed and functional in non-excitable cells [555, 575, 576]. A physical interaction via coimmunoprecipitation experiments between endogenous Homer 1 and TRPC1, as well as TRPC1 and the IP_3R in HEK293 cells [569] has been reported. Generally, there are two mechanisms for raising intracellular Ca^{2+} levels: receptor-activated Ca^{2+} release and store-operated Ca^{2+} entry that is activated by the depletion of intracellular Ca^{2+} stores [577]. Through their interaction with IP_3 receptors, STIM and Orai proteins [578], TRPC channels have been implicated in capacitive Ca^{2+} entry which replenishes depleted intracellular Ca^{2+} stores [577, 579]. TRPC activation is not well understood. Yuan et al. have shown that Homer 1 not only interacts with TRPC1, 2 and 5 in HEK cells, but is also involved in their gating. Thus, Homer 1 could function in activating store-depletion mechanisms in non-neuronal cells. Overall, Homer proteins help to ensure high spatial and temporal fidelity of the Ca^{2+} signal. Homer proteins are important to study because Homer knockout mice show increased spontaneous Ca^{2+} influx [569], which most certainly affects cellular functions. *If a Homer switch exists in non-neuronal cells, then this could be the first indication that the cells have Ca^{2+} signaling memory, or adaptation as a means to modulate and buffer their response to future environmental signals.* This is a novel mechanism for non-neuronal cells. Why would a postsynaptic density protein be present where there are no synapses? Can non-excitable cells actively switch between h1b/c and h1a as well and if so, how is this switch regulated? Why would a non-excitable cell need two different forms of a scaffolding protein? To answer these questions, we sought to elucidate the role of Homers in non-excitable cells by performing RT-PCR experiments in non-neuronal cell lines such as HEK293, HeLa and L cells.

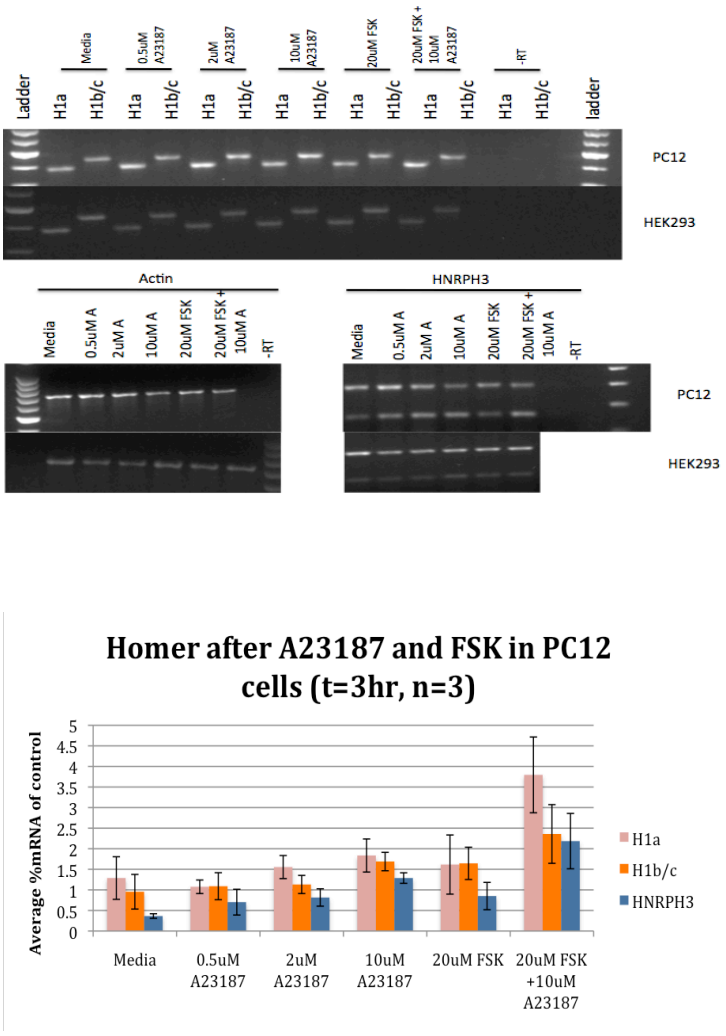

Figure 46. H1a is upregulated in neurons but not in non-neuronal cells in response to Ca^{2+} and cAMP signaling.

Representative RT-PCR of Homer levels in neuronal PC12 cells (top) and non-neuronal HEK 293 cells (bottom) following stimulation of cAMP with forskolin (FSK) and Ca^{2+} ionophore A23187 for 3 hours. H1a and the positive control gene HNRPH3 increase significantly compared to actin when PC12 cells are treated with both FSK and A23187, but do not change in HEK 293 cells. Graph indicates quantification of PC12 cell stimulations (n=3).

Figure 46 shows that H1a is upregulated in neurons (top panel, PC12 cells), but not in non-neuronal cells (bottom panels, HEK293 cells) in response to Ca^{2+} and cAMP signaling. H1a levels increase 3 fold under stimulated conditions compared to untreated cells when normalized to actin, indicating that we are successfully activating the Homer switch in neurons. Non-neuronal cells may be activated through a different mechanism, for example to replenish Ca^{2+} stores upon depletion. Interestingly, *Homer1* premRNA levels in PC12 cells also increase upon stimulation, indicating that control of the H1a transcript probably occurs at the transcriptional level, a process that is coupled with Ca^{2+} signaling pathways and the regulatory splicing machinery (Fig 47).

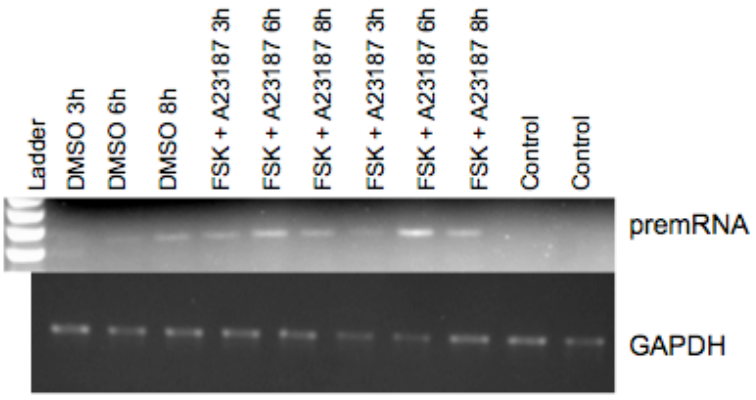

Figure 47. Homer 1 premRNA increases as H1a is induced.

RT-PCR of *Homer 1* premRNA in PC12 cells. Note the sharp increase upon stimulation with A23187 and FSK for 3 hours, peaking at 6 hours compared to control and DMSO treatments (in duplicate).

B.2.3 The Ca^{2+} -responsive splicing factor Tra2β

Changes in splicing patterns are mediated by regulatory proteins that bind the pre-mRNA and enhance or silence splice sites. Some of the best characterized positive factors of splicing are serine-arginine-rich (SR) proteins. SR proteins bind to exonic splicing enhancer elements and stimulate exon inclusion [580]. Transformer-2β (Tra2β) is an SR-like splice factor that has been shown to change in response to Ca^{2+} stimulation in neurons [581, 582]. Raising intracellular Ca^{2+} levels with thapsigargin causes hyperphosphorylation and an accumulation of Tra2β and other interacting SR proteins in the cytosol of primary neurons [582]. Once the regulatory splicing protein, Tra2β, accumulates in the cytoplasm, it changes the alternative splice-site of the ICH-1 gene, increasing levels of the ICH-1S form [582]. Upon examining the Homer RNA sequence, we observed an enrichment in Tra2β binding sequences (GAA repeats or GHVVGANR, where R indicates A or G, V indicates A, C, or G, and H indicates A, C or U) [580] compared to other splicing regulators located around a putative long Homer switch within the RNA (11 Tra2β binding sites, 4 PTB sites and 1 FOX site, Fig. 48). Moreover, a strong Tra2β exon splicing enhancer (ESE) motif (98.53% and 100% according to HSF) was identified within the Homer sequence. Known targets of Tra2β include clathrin LCB, survival of motor neuron 2 (SMN2), tau, and Tra2β itself [580]. The high enrichment of Tra2β binding sites, as well as the regulation of this splice factor by increased intracellular Ca^{2+}, made this a strong candidate for the regulation of the Homer switch.

Figure 48. Tra2β binding sites in Homer sequences.

Tra2β binding sites (in brown) are enriched around putative splice switch in the Homer sequence. Homer pre-mRNA sequence shown with known splice factor binding sites highlighted.

Towards finding how the Homer switch is regulated, we identified a candidate splice factor, Transformer 2β, based on a search for Ca^{2+} dependent splice factors that have binding motifs within the Homer sequence. Tra2β is an SR-like splice factor that has been shown to respond to Ca^{2+} stimulation in neurons and regulate the alternative splice-site. Figure 49 shows Tra2β to be phoshorylated under DMSO and H1a stimulating conditions in PC12 cells. Lambda phosphatase was used to dephosphorylate Tra2β as a control. Thus, Tra2β protein expression and phosphorylation status does not seem to correlate with H1a induction, indicating that Tra2β may not regulate Homer levels. To confirm Tra2β's involvement in the regulation of H1a, we

designed two siRNA constructs to knockdown Tra2β mRNA levels. Figure 50A shows successful knockdown of Tra2β with construct #2 in PC12 cells, which we used in following experiments. However, Tra2β knockdown does not deter H1a induction upon stimulation (Fig 50B), further confirming that Tra2β is not the only splice factor that regulates H1a. Tra2β was also successfully knocked down in HeLa cells (Fig 50C), and did not lead to H1a induction, indicating that Tra2β does not block H1a induction in non-neuronal cell types.

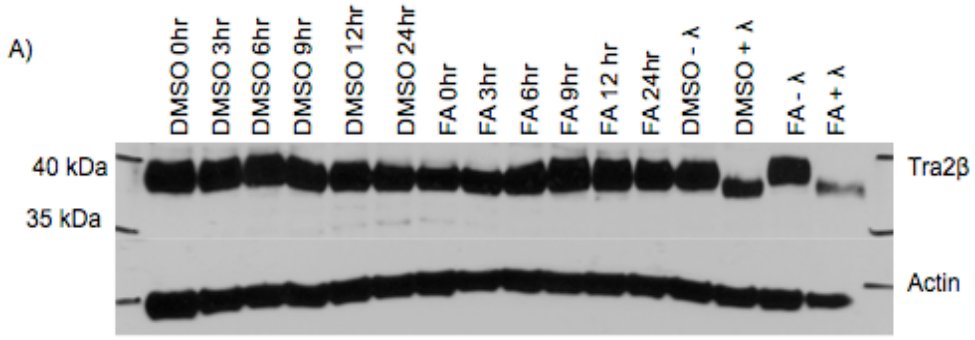

Figure 49. Tra2 Ca^{2+} and cAMP stimulation do not regulate Tra2β phosphorylation status.

Tra2β phosphorylation analysis in PC12 cells via Western blot indicates that Tra2β is phosphorylated in DMSO and FSK and A23187 stimulated cells. Tra2β phosphorylation status does not seem to correlate with H1a induction.

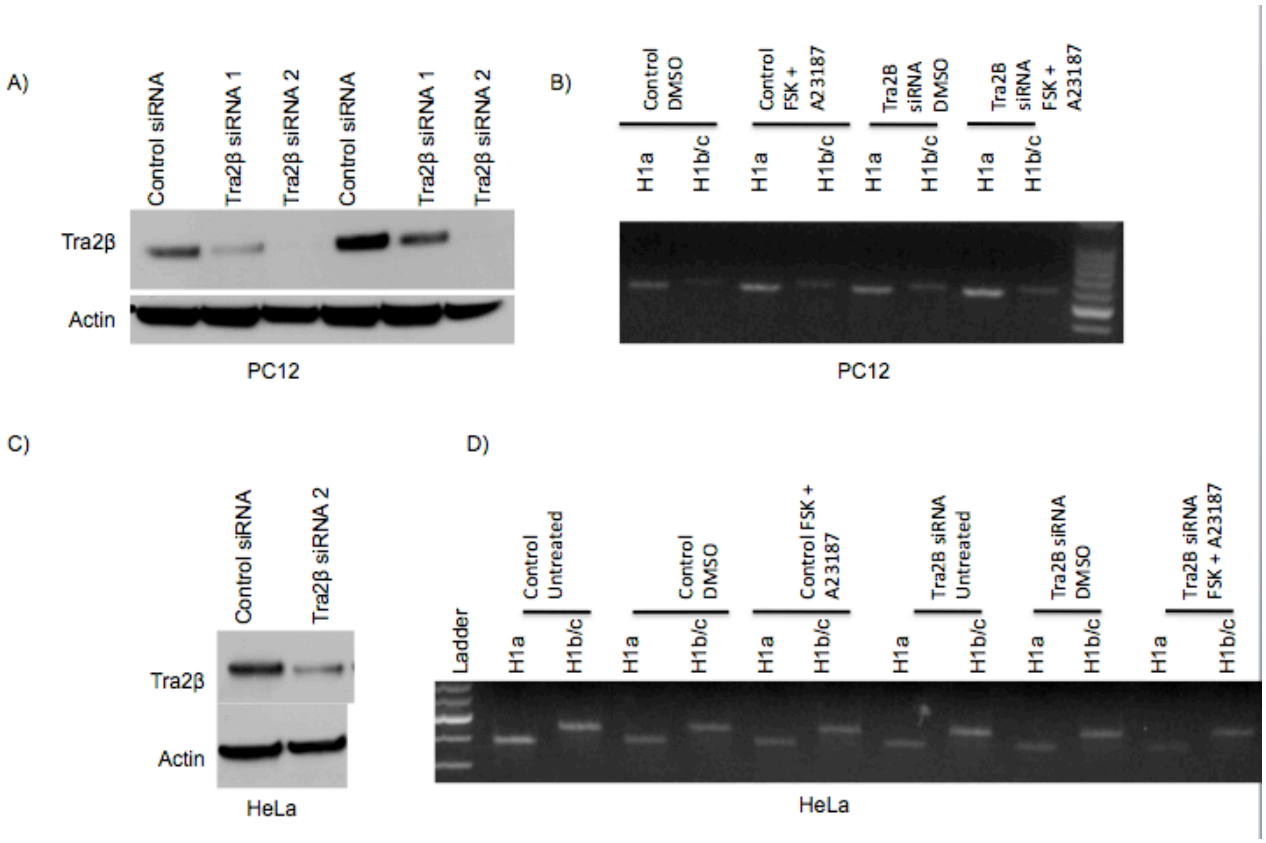

Figure 50. Tra2β siRNA knockdown of Tra2β.

Two Tra2β siRNA constructs were designed and construct #2 yielded better knockdown and was used for continued studies. Tra2β was successfully knocked down in PC12 cells as demonstrated by Western analysis (A) and HeLa cells (C). However, Tra2β knockdown does not have an effect on H1a or H1b/c levels upon stimulation in either neuronal (B, PC12) or non-neuronal cells (D, HeLa) as demonstrated by RT-PCR analysis.

B.3 DISCUSSION

My work has shown that the Homer switch in neurons is dependent on the activation of both Ca^{2+} and cAMP signaling pathways that result in the upregulation of the alternative splice variant, H1a. Furthermore, H1a mRNA induction is correlated with an increase in *Homer1* premRNA levels, suggesting an interaction between the transcriptional activation component and the regulatory splicing machinery in order to regulate H1a expression. Current data indicate that non-neuronal cells lack the ability to switch Homer isoforms. The role of Homers in non-neuronal cells remains unclear, but understanding how the Homer switch occurs in neuronal cells will provide valuable insight. It is likely that H1a functions to modulate the activity of TRPC channels in non-neurons. I have also shown through protein expression and siRNA knockout, that our putative splice factor, Tra2β, is not the definitive pathway to regulate H1a induction. However, given the poor resolution and the remaining troubleshooting associated with the experiments, we cannot confidently reach this conclusion yet.

B.3.1 Future directions.

Tra2β as a H1a regulatory factor: Confocal image analysis could be used to confirm Tra2β subcellular localization. DAPI nuclear staining could be used for controls. Additionally, subcellular fractionation can be done to determine if Tra2β accumulates in the cytoplasm. To ensure that we are not changing Tra2β's normal function with our stimulations, we could use the clathrin light chain, LCB, as our positive control since it is alternatively spliced and one of Tra2β's known targets. Alternatively, we could identify other splice factors by using published data and publicly available algorithmic tools (such as the Human Splicing Finder,

www.umd.be/HSF or SFmap, http://sfmap.technion.ac.il) to find other Ca^{2+} dependent splice factors that have binding motifs within the Homer sequence. If other Ca^{2+} dependent splice factors do not statistically correlate with h1a induction or do not have binding sites in the Homer sequence, then our alternative model might be supported; Homer may be directly activated by the cyclic AMP (cAMP) pathway, or by cAMP modulating the Ca^{2+} signal. If this is the case, then one such class of factors could potentially be PKA signaling factors.

Non-neuronal H1a regulation: It is possible that the reason for not seeing a significant upregulation of short Homer forms in non-neuronal cells is due to insufficient or too short of a stimulation with these treatments. Ca^{2+} imaging by Fura-2 could be performed to optimize treatment strength and duration. Fura-2 is a dye-molecule that binds Ca^{2+} and can be used to as an indicator, or direct readout of cytoplasmic Ca^{2+} levels. As such, different concentrations of Ca^{2+} stimulants can be used in conjunction with other treatments, until a sustained Ca^{2+} response can be detected immediately following treatment. Additionally, there might be splice factor or site specific differences in H1a induction between species. In this study, we compared rat neuronal cells with mouse and human non-neuronal cells. In the future, we could compare neuronal and non-neuronal cells from the same species. Lastly, Homer 1 coimmunoprecipitates with TRPC1 and 5, which are thought to be activated by store depletion, thus Homer could have a role in replenishing depleted stores in non-neuronal cells. We could determine if store-depletion activates the Homer switch by passively depleting Ca^{2+} stores with SERCA inhibitors such as Thapsigargin.

B.4 ACKNOWELDGEMENTS

This work was supported by National Institute of Health Grants HD058577 and ES016782 to Kirill Kiselyov. We thank Dr. Paula Grabowski for the HNRPH3 primers.

BIBLIOGRAPHY

1. Frederickson, C.J., J.Y. Koh, and A.I. Bush, *The neurobiology of zinc in health and disease*. Nature reviews. Neuroscience, 2005. **6**(6): p. 449-62.
2. Andreini, C., et al., *Counting the zinc-proteins encoded in the human genome*. Journal of proteome research, 2006. **5**(1): p. 196-201.
3. Prasad, A.S., *Zinc: an overview*. Nutrition, 1995. **11**(1 Suppl): p. 93-9.
4. Vallee, B.L. and K.H. Falchuk, *The biochemical basis of zinc physiology*. Physiological reviews, 1993. **73**(1): p. 79-118.
5. Costello, L.C., R.B. Franklin, and P. Feng, *Mitochondrial function, zinc, and intermediary metabolism relationships in normal prostate and prostate cancer*. Mitochondrion, 2005. **5**(3): p. 143-53.
6. Fukunaka, A., et al., *Demonstration and characterization of the heterodimerization of ZnT5 and ZnT6 in the early secretory pathway*. The Journal of biological chemistry, 2009. **284**(45): p. 30798-806.
7. Schissel, S.L., et al., *The cellular trafficking and zinc dependence of secretory and lysosomal sphingomyelinase, two products of the acid sphingomyelinase gene*. The Journal of biological chemistry, 1998. **273**(29): p. 18250-9.
8. Maret, W., *Zinc coordination environments in proteins as redox sensors and signal transducers*. Antioxidants & redox signaling, 2006. **8**(9-10): p. 1419-41.
9. Haase, H.a.M., W., *Cellular and Molecular Biology of Metals*, ed. R.a.K. Zalups, J. 2010, London: Taylor and Francis.
10. May, P.M. and D.R. Williams, *Computer models of metal ion-low molecular weight equilibria in plasma and the influence of D-penicillamine, triethylenetetramine and EDTA*. Proceedings of the Royal Society of Medicine, 1977. **70 Suppl 3**: p. 19-23.
11. Sutherland, D.E. and M.J. Stillman, *The "magic numbers" of metallothionein*. Metallomics : integrated biometal science, 2011. **3**(5): p. 444-63.
12. Maret, W. and Y. Li, *Coordination dynamics of zinc in proteins*. Chemical reviews, 2009. **109**(10): p. 4682-707.
13. Irving, H.a.W., R. J. P. , *Order of Stability of Metal Complexes*. Nature, 1948. **162**: p. 746-747.
14. Bitanihirwe, B.K. and M.G. Cunningham, *Zinc: the brain's dark horse*. Synapse, 2009. **63**(11): p. 1029-49.
15. Palmiter, R.D. and S.D. Findley, *Cloning and functional characterization of a mammalian zinc transporter that confers resistance to zinc*. The EMBO journal, 1995. **14**(4): p. 639-49.

16. Fukada, T. and T. Kambe, *Molecular and genetic features of zinc transporters in physiology and pathogenesis*. Metallomics : integrated biometal science, 2011. **3**(7): p. 662-74.
17. Eide, D.J., *Zinc transporters and the cellular trafficking of zinc*. Biochimica et biophysica acta, 2006. **1763**(7): p. 711-22.
18. Lu, M. and D. Fu, *Structure of the zinc transporter YiiP*. Science, 2007. **317**(5845): p. 1746-8.
19. Lu, M., J. Chai, and D. Fu, *Structural basis for autoregulation of the zinc transporter YiiP*. Nature structural & molecular biology, 2009. **16**(10): p. 1063-7.
20. Rogers, E.E., D.J. Eide, and M.L. Guerinot, *Altered selectivity in an Arabidopsis metal transporter*. Proc Natl Acad Sci U S A, 2000. **97**(22): p. 12356-60.
21. Milon, B., et al., *Histidine residues in the region between transmembrane domains III and IV of hZip1 are required for zinc transport across the plasma membrane in PC-3 cells*. Biochimica et biophysica acta, 2006. **1758**(10): p. 1696-701.
22. Hoch, E., et al., *Histidine pairing at the metal transport site of mammalian ZnT transporters controls Zn2+ over Cd2+ selectivity*. Proc Natl Acad Sci U S A, 2012. **109**(19): p. 7202-7.
23. Cousins, R.J., J.P. Liuzzi, and L.A. Lichten, *Mammalian zinc transport, trafficking, and signals*. The Journal of biological chemistry, 2006. **281**(34): p. 24085-9.
24. Chao, Y. and D. Fu, *Kinetic study of the antiport mechanism of an Escherichia coli zinc transporter, ZitB*. The Journal of biological chemistry, 2004. **279**(13): p. 12043-50.
25. Ohana, E., et al., *Identification of the Zn2+ binding site and mode of operation of a mammalian Zn2+ transporter*. The Journal of biological chemistry, 2009. **284**(26): p. 17677-86.
26. Lin, W., et al., *Selective electrodiffusion of zinc ions in a Zrt-, Irt-like protein, ZIPB*. The Journal of biological chemistry, 2010. **285**(50): p. 39013-20.
27. Margoshes, M.a.V., B. L., *A cadmium protein from equine kidney cortex*. J. Am. Chem. Soc., 1957. **79**(17): p. pp 4813-4814.
28. Karin, M., et al., *Human metallothionein genes are clustered on chromosome 16*. Proc Natl Acad Sci U S A, 1984. **81**(17): p. 5494-8.
29. Palmiter, R.D., et al., *MT-III, a brain-specific member of the metallothionein gene family*. Proc Natl Acad Sci U S A, 1992. **89**(14): p. 6333-7.
30. Quaife, C.J., et al., *Induction of a new metallothionein isoform (MT-IV) occurs during differentiation of stratified squamous epithelia*. Biochemistry, 1994. **33**(23): p. 7250-9.
31. West, A.K., et al., *Human metallothionein genes: structure of the functional locus at 16q13*. Genomics, 1990. **8**(3): p. 513-8.
32. Kramer, K.K., J.T. Zoelle, and C.D. Klaassen, *Induction of metallothionein mRNA and protein in primary murine neuron cultures*. Toxicology and applied pharmacology, 1996. **141**(1): p. 1-7.
33. Kramer, K.K., et al., *Induction of metallothionein mRNA and protein in murine astrocyte cultures*. Toxicology and applied pharmacology, 1996. **136**(1): p. 94-100.
34. Uchida, Y., et al., *The growth inhibitory factor that is deficient in the Alzheimer's disease brain is a 68 amino acid metallothionein-like protein*. Neuron, 1991. **7**(2): p. 337-47.
35. Morelock, M.M. and G.L. Tolman, *Metallothionein: a bifunctional chelator for the radiolabeling of biologically active molecules*. Experientia. Supplementum, 1987. **52**: p. 247-53.

36. Ngu, T.T., S. Krecisz, and M.J. Stillman, *Bismuth binding studies to the human metallothionein using electrospray mass spectrometry*. Biochemical and biophysical research communications, 2010. **396**(2): p. 206-12.
37. Mackay, E.A., et al., *Complete amino acid sequences of five dimeric and four monomeric forms of metallothionein from the edible mussel Mytilus edulis*. European journal of biochemistry / FEBS, 1993. **218**(1): p. 183-94.
38. Roesijadi, G., et al., *Modulation of DNA binding of a tramtrack zinc finger peptide by the metallothionein-thionein conjugate pair*. The Journal of biological chemistry, 1998. **273**(28): p. 17425-32.
39. Davis, S.R. and R.J. Cousins, *Metallothionein expression in animals: a physiological perspective on function*. The Journal of nutrition, 2000. **130**(5): p. 1085-8.
40. Kelly, E.J., et al., *Metallothionein I and II protect against zinc deficiency and zinc toxicity in mice*. The Journal of nutrition, 1996. **126**(7): p. 1782-90.
41. Kang, Y.J., G. Li, and J.T. Saari, *Metallothionein inhibits ischemia-reperfusion injury in mouse heart*. The American journal of physiology, 1999. **276**(3 Pt 2): p. H993-7.
42. Kang, Y.J., Y. Li, and X. Sun, *Antiapoptotic effect and inhibition of ischemia/reperfusion-induced myocardial injury in metallothionein-overexpressing transgenic mice*. The American journal of pathology, 2003. **163**(4): p. 1579-86.
43. Chiaverini, N. and M. De Ley, *Protective effect of metallothionein on oxidative stress-induced DNA damage*. Free radical research, 2010. **44**(6): p. 605-13.
44. Kang, Y.J., *Metallothionein redox cycle and function*. Experimental biology and medicine, 2006. **231**(9): p. 1459-67.
45. Maret, W., *Metallothionein redox biology in the cytoprotective and cytotoxic functions of zinc*. Experimental gerontology, 2008. **43**(5): p. 363-9.
46. St Croix, C.M., et al., *Nitric oxide-induced changes in intracellular zinc homeostasis are mediated by metallothionein/thionein*. American journal of physiology. Lung cellular and molecular physiology, 2002. **282**(2): p. L185-92.
47. Zhang, B., et al., *Activity of metal-responsive transcription factor 1 by toxic heavy metals and H2O2 in vitro is modulated by metallothionein*. Molecular and cellular biology, 2003. **23**(23): p. 8471-85.
48. Elgohary, W.G., et al., *Protection of DNA in HL-60 cells from damage generated by hydroxyl radicals produced by reaction of H2O2 with cell iron by zinc-metallothionein*. Chemico-biological interactions, 1998. **115**(2): p. 85-107.
49. Quesada, A.R., et al., *Direct reaction of H2O2 with sulfhydryl groups in HL-60 cells: zinc-metallothionein and other sites*. Archives of biochemistry and biophysics, 1996. **334**(2): p. 241-50.
50. Inoue, K., et al., *Role of metallothionein in antigen-related airway inflammation*. Experimental biology and medicine, 2005. **230**(1): p. 75-81.
51. Penkowa, M., et al., *Altered inflammatory response and increased neurodegeneration in metallothionein I+II deficient mice during experimental autoimmune encephalomyelitis*. Journal of neuroimmunology, 2001. **119**(2): p. 248-60.
52. Tran, C.D., et al., *Helicobacter-induced gastritis in mice not expressing metallothionein-I and II*. Helicobacter, 2003. **8**(5): p. 533-41.
53. Takano, H., et al., *Protective role of metallothionein in acute lung injury induced by bacterial endotoxin*. Thorax, 2004. **59**(12): p. 1057-62.

54. Brugnera, E., et al., *Cloning, chromosomal mapping and characterization of the human metal-regulatory transcription factor MTF-1*. Nucleic acids research, 1994. **22**(15): p. 3167-73.
55. Radtke, F., et al., *Cloned transcription factor MTF-1 activates the mouse metallothionein I promoter*. The EMBO journal, 1993. **12**(4): p. 1355-62.
56. Zhang, B., et al., *The Drosophila homolog of mammalian zinc finger factor MTF-1 activates transcription in response to heavy metals*. Molecular and cellular biology, 2001. **21**(14): p. 4505-14.
57. Langmade, S.J., et al., *The transcription factor MTF-1 mediates metal regulation of the mouse ZnT1 gene*. The Journal of biological chemistry, 2000. **275**(44): p. 34803-9.
58. Yepiskoposyan, H., et al., *Transcriptome response to heavy metal stress in Drosophila reveals a new zinc transporter that confers resistance to zinc*. Nucleic acids research, 2006. **34**(17): p. 4866-77.
59. Laity, J.H. and G.K. Andrews, *Understanding the mechanisms of zinc-sensing by metal-response element binding transcription factor-1 (MTF-1)*. Archives of biochemistry and biophysics, 2007. **463**(2): p. 201-10.
60. Guerrerio, A.L. and J.M. Berg, *Metal ion affinities of the zinc finger domains of the metal responsive element-binding transcription factor-1 (MTF1)*. Biochemistry, 2004. **43**(18): p. 5437-44.
61. Potter, B.M., et al., *The six zinc fingers of metal-responsive element binding transcription factor-1 form stable and quasi-ordered structures with relatively small differences in zinc affinities*. The Journal of biological chemistry, 2005. **280**(31): p. 28529-40.
62. Li, Y., et al., *The zinc-sensing mechanism of mouse MTF-1 involves linker peptides between the zinc fingers*. Molecular and cellular biology, 2006. **26**(15): p. 5580-7.
63. Smirnova, I.V., et al., *Zinc and cadmium can promote rapid nuclear translocation of metal response element-binding transcription factor-1*. The Journal of biological chemistry, 2000. **275**(13): p. 9377-84.
64. Jiang, H., P.J. Daniels, and G.K. Andrews, *Putative zinc-sensing zinc fingers of metal-response element-binding transcription factor-1 stabilize a metal-dependent chromatin complex on the endogenous metallothionein-I promoter*. The Journal of biological chemistry, 2003. **278**(32): p. 30394-402.
65. Dalton, T.P., et al., *Oxidative stress activates metal-responsive transcription factor-1 binding activity. Occupancy in vivo of metal response elements in the metallothionein-I gene promoter*. The Journal of biological chemistry, 1996. **271**(42): p. 26233-41.
66. Heuchel, R., et al., *The transcription factor MTF-1 is essential for basal and heavy metal-induced metallothionein gene expression*. The EMBO journal, 1994. **13**(12): p. 2870-5.
67. Gunes, C., et al., *Embryonic lethality and liver degeneration in mice lacking the metal-responsive transcriptional activator MTF-1*. The EMBO journal, 1998. **17**(10): p. 2846-54.
68. Egli, D., et al., *A family knockout of all four Drosophila metallothioneins reveals a central role in copper homeostasis and detoxification*. Molecular and cellular biology, 2006. **26**(6): p. 2286-96.
69. Bauman, J.W., et al., *Induction of metallothionein by diethyl maleate*. Toxicology and applied pharmacology, 1992. **114**(2): p. 188-96.

70. Bauman, J.W., et al., *Examination of potential mechanism(s) of metallothionein induction by diethyl maleate*. Toxicology and applied pharmacology, 1992. **117**(2): p. 226-32.
71. Bauman, J.W., et al., *Induction of hepatic metallothionein by paraquat*. Toxicology and applied pharmacology, 1992. **117**(2): p. 233-41.
72. Sawada, J., et al., *Induction of metallothionein in astrocytes by cytokines and heavy metals*. Biological signals, 1994. **3**(3): p. 157-68.
73. Dalton, T., et al., *Activation of the chicken metallothionein promoter by metals and oxidative stress in cultured cells and transgenic mice*. Comparative biochemistry and physiology. Part B, Biochemistry & molecular biology, 1997. **116**(1): p. 75-86.
74. Samson, S.L. and L. Gedamu, *Molecular analyses of metallothionein gene regulation*. Progress in nucleic acid research and molecular biology, 1998. **59**: p. 257-88.
75. Chung, M.J., C. Hogstrand, and S.J. Lee, *Cytotoxicity of nitric oxide is alleviated by zinc-mediated expression of antioxidant genes*. Experimental biology and medicine, 2006. **231**(9): p. 1555-63.
76. Stuart, G.W., et al., *A 12-base-pair DNA motif that is repeated several times in metallothionein gene promoters confers metal regulation to a heterologous gene*. Proc Natl Acad Sci U S A, 1984. **81**(23): p. 7318-22.
77. Stuart, G.W., P.F. Searle, and R.D. Palmiter, *Identification of multiple metal regulatory elements in mouse metallothionein-I promoter by assaying synthetic sequences*. Nature, 1985. **317**(6040): p. 828-31.
78. Culotta, V.C. and D.H. Hamer, *Fine mapping of a mouse metallothionein gene metal response element*. Molecular and cellular biology, 1989. **9**(3): p. 1376-80.
79. Lee, W., et al., *Activation of transcription by two factors that bind promoter and enhancer sequences of the human metallothionein gene and SV40*. Nature, 1987. **325**(6102): p. 368-72.
80. Wang, Y., et al., *Metal-responsive transcription factor-1 (MTF-1) selects different types of metal response elements at low vs. high zinc concentration*. Biological chemistry, 2004. **385**(7): p. 623-32.
81. Sims, H.I., G.W. Chirn, and M.T. Marr, 2nd, *Single nucleotide in the MTF-1 binding site can determine metal-specific transcription activation*. Proc Natl Acad Sci U S A, 2012. **109**(41): p. 16516-21.
82. Waters, B.M. and D.J. Eide, *Combinatorial control of yeast FET4 gene expression by iron, zinc, and oxygen*. The Journal of biological chemistry, 2002. **277**(37): p. 33749-57.
83. Zhao, H. and D. Eide, *The ZRT2 gene encodes the low affinity zinc transporter in Saccharomyces cerevisiae*. The Journal of biological chemistry, 1996. **271**(38): p. 23203-10.
84. Zhao, H. and D. Eide, *The yeast ZRT1 gene encodes the zinc transporter protein of a high-affinity uptake system induced by zinc limitation*. Proc Natl Acad Sci U S A, 1996. **93**(6): p. 2454-8.
85. MacDiarmid, C.W., L.A. Gaither, and D. Eide, *Zinc transporters that regulate vacuolar zinc storage in Saccharomyces cerevisiae*. The EMBO journal, 2000. **19**(12): p. 2845-55.
86. Lyons, T.J., et al., *Genome-wide characterization of the Zap1p zinc-responsive regulon in yeast*. Proc Natl Acad Sci U S A, 2000. **97**(14): p. 7957-62.
87. Yamashita, S., et al., *Zinc transporter LIVI controls epithelial-mesenchymal transition in zebrafish gastrula organizer*. Nature, 2004. **429**(6989): p. 298-302.

88. Guo, L., et al., *STAT5-glucocorticoid receptor interaction and MTF-1 regulate the expression of ZnT2 (Slc30a2) in pancreatic acinar cells*. Proc Natl Acad Sci U S A, 2010. **107**(7): p. 2818-23.
89. Koh, J.Y., et al., *The role of zinc in selective neuronal death after transient global cerebral ischemia*. Science, 1996. **272**(5264): p. 1013-6.
90. Gaither, L.A. and D.J. Eide, *The human ZIP1 transporter mediates zinc uptake in human K562 erythroleukemia cells*. The Journal of biological chemistry, 2001. **276**(25): p. 22258-64.
91. Kambe, T., *An overview of a wide range of functions of ZnT and Zip zinc transporters in the secretory pathway*. Biosci Biotechnol Biochem, 2011. **75**(6): p. 1036-43.
92. Wang, F., et al., *Zinc-stimulated endocytosis controls activity of the mouse ZIP1 and ZIP3 zinc uptake transporters*. The Journal of biological chemistry, 2004. **279**(23): p. 24631-9.
93. Kelleher, S.L. and B. Lonnerdal, *Zip3 plays a major role in zinc uptake into mammary epithelial cells and is regulated by prolactin*. Am J Physiol Cell Physiol, 2005. **288**(5): p. C1042-7.
94. Kury, S., et al., *Identification of SLC39A4, a gene involved in acrodermatitis enteropathica*. Nature genetics, 2002. **31**(3): p. 239-40.
95. Wang, F., et al., *The mammalian Zip5 protein is a zinc transporter that localizes to the basolateral surface of polarized cells*. The Journal of biological chemistry, 2004. **279**(49): p. 51433-41.
96. Liuzzi, J.P., et al., *Interleukin-6 regulates the zinc transporter Zip14 in liver and contributes to the hypozincemia of the acute-phase response*. Proc Natl Acad Sci U S A, 2005. **102**(19): p. 6843-8.
97. Mok, S.S., et al., *A novel metalloprotease in rat brain cleaves the amyloid precursor protein of Alzheimer's disease generating amyloidogenic fragments*. Biochemistry, 1997. **36**(1): p. 156-63.
98. Dodson, G. and D. Steiner, *The role of assembly in insulin's biosynthesis*. Current opinion in structural biology, 1998. **8**(2): p. 189-94.
99. Galperin, M.Y. and M.J. Jedrzejas, *Conserved core structure and active site residues in alkaline phosphatase superfamily enzymes*. Proteins, 2001. **45**(4): p. 318-24.
100. Suzuki, T., et al., *Zinc transporters, ZnT5 and ZnT7, are required for the activation of alkaline phosphatases, zinc-requiring enzymes that are glycosylphosphatidylinositol-anchored to the cytoplasmic membrane*. The Journal of biological chemistry, 2005. **280**(1): p. 637-43.
101. Kirschke, C.P. and L. Huang, *ZnT7, a novel mammalian zinc transporter, accumulates zinc in the Golgi apparatus*. The Journal of biological chemistry, 2003. **278**(6): p. 4096-102.
102. Huang, L., et al., *The ZIP7 gene (Slc39a7) encodes a zinc transporter involved in zinc homeostasis of the Golgi apparatus*. The Journal of biological chemistry, 2005. **280**(15): p. 15456-63.
103. Giunta, C., et al., *Spondylocheiro dysplastic form of the Ehlers-Danlos syndrome--an autosomal-recessive entity caused by mutations in the zinc transporter gene SLC39A13*. American journal of human genetics, 2008. **82**(6): p. 1290-305.
104. Palmiter, R.D., et al., *ZnT-3, a putative transporter of zinc into synaptic vesicles*. Proc Natl Acad Sci U S A, 1996. **93**(25): p. 14934-9.

105. Chimienti, F., A. Favier, and M. Seve, *ZnT-8, a pancreatic beta-cell-specific zinc transporter*. Biometals : an international journal on the role of metal ions in biology, biochemistry, and medicine, 2005. **18**(4): p. 313-7.
106. Piletz, J.E. and R.E. Ganschow, *Zinc deficiency in murine milk underlies expression of the lethal milk (lm) mutation*. Science, 1978. **199**(4325): p. 181-3.
107. Ackland, M.L. and J.F. Mercer, *The murine mutation, lethal milk, results in production of zinc-deficient milk*. The Journal of nutrition, 1992. **122**(6): p. 1214-8.
108. Sensi, S.L., et al., *A new mitochondrial fluorescent zinc sensor*. Cell calcium, 2003. **34**(3): p. 281-4.
109. Malaiyandi, L.M., et al., *Direct visualization of mitochondrial zinc accumulation reveals uniporter-dependent and -independent transport mechanisms*. Journal of neurochemistry, 2005. **93**(5): p. 1242-50.
110. Maske, H., *[Relation between insulin and zinc in the islands of Langerhans, with special reference to blood sugar control and insulin secretion]*. Experientia, 1955. **11**(3): p. 122-8.
111. Qian, J. and J.L. Noebels, *Visualization of transmitter release with zinc fluorescence detection at the mouse hippocampal mossy fibre synapse*. The Journal of physiology, 2005. **566**(Pt 3): p. 747-58.
112. Howell, G.A., J. Perez-Clausell, and C.J. Frederickson, *Zinc containing projections to the bed nucleus of the stria terminalis*. Brain research, 1991. **562**(2): p. 181-9.
113. Beaulieu, C., R. Dyck, and M. Cynader, *Enrichment of glutamate in zinc-containing terminals of the cat visual cortex*. Neuroreport, 1992. **3**(10): p. 861-4.
114. Frederickson, C.J., *Neurobiology of zinc and zinc-containing neurons*. International review of neurobiology, 1989. **31**: p. 145-238.
115. Frederickson, C.J. and A.I. Bush, *Synaptically released zinc: physiological functions and pathological effects*. Biometals : an international journal on the role of metal ions in biology, biochemistry, and medicine, 2001. **14**(3-4): p. 353-66.
116. Sheline, C.T., et al., *Depolarization-induced 65zinc influx into cultured cortical neurons*. Neurobiology of disease, 2002. **10**(1): p. 41-53.
117. Jia, Y., et al., *Zn2+ currents are mediated by calcium-permeable AMPA/kainate channels in cultured murine hippocampal neurones*. The Journal of physiology, 2002. **543**(Pt 1): p. 35-48.
118. Peters, S., J. Koh, and D.W. Choi, *Zinc selectively blocks the action of N-methyl-D-aspartate on cortical neurons*. Science, 1987. **236**(4801): p. 589-93.
119. Hosie, A.M., et al., *Zinc-mediated inhibition of GABA(A) receptors: discrete binding sites underlie subtype specificity*. Nature neuroscience, 2003. **6**(4): p. 362-9.
120. Lee, J.Y., et al., *Zinc released from metallothionein-iii may contribute to hippocampal CA1 and thalamic neuronal death following acute brain injury*. Experimental neurology, 2003. **184**(1): p. 337-47.
121. Maret, W., *Oxidative metal release from metallothionein via zinc-thiol/disulfide interchange*. Proc Natl Acad Sci U S A, 1994. **91**(1): p. 237-41.
122. Maret, W., *The function of zinc metallothionein: a link between cellular zinc and redox state*. The Journal of nutrition, 2000. **130**(5S Suppl): p. 1455S-8S.
123. Yokoyama, M., J. Koh, and D.W. Choi, *Brief exposure to zinc is toxic to cortical neurons*. Neuroscience letters, 1986. **71**(3): p. 351-5.

124. Weiss, J.H., et al., *AMPA receptor activation potentiates zinc neurotoxicity*. Neuron, 1993. **10**(1): p. 43-9.
125. Frederickson, C.J., M.D. Hernandez, and J.F. McGinty, *Translocation of zinc may contribute to seizure-induced death of neurons*. Brain research, 1989. **480**(1-2): p. 317-21.
126. Lee, J.M., et al., *Zinc translocation accelerates infarction after mild transient focal ischemia*. Neuroscience, 2002. **115**(3): p. 871-8.
127. Suh, S.W., et al., *Evidence that synaptically-released zinc contributes to neuronal injury after traumatic brain injury*. Brain research, 2000. **852**(2): p. 268-73.
128. Lee, J.Y., et al., *Accumulation of zinc in degenerating hippocampal neurons of ZnT3-null mice after seizures: evidence against synaptic vesicle origin*. The Journal of neuroscience : the official journal of the Society for Neuroscience, 2000. **20**(11): p. RC79.
129. Bossy-Wetzel, E., et al., *Crosstalk between nitric oxide and zinc pathways to neuronal cell death involving mitochondrial dysfunction and p38-activated K+ channels*. Neuron, 2004. **41**(3): p. 351-65.
130. Kim, E.Y., et al., *Zn2+ entry produces oxidative neuronal necrosis in cortical cell cultures*. The European journal of neuroscience, 1999. **11**(1): p. 327-34.
131. Kim, Y.H., et al., *Zinc-induced cortical neuronal death with features of apoptosis and necrosis: mediation by free radicals*. Neuroscience, 1999. **89**(1): p. 175-82.
132. Lobner, D., et al., *Zinc-induced neuronal death in cortical neurons*. Cellular and molecular biology, 2000. **46**(4): p. 797-806.
133. Park, J.A., et al., *Co-induction of p75NTR and p75NTR-associated death executor in neurons after zinc exposure in cortical culture or transient ischemia in the rat*. The Journal of neuroscience : the official journal of the Society for Neuroscience, 2000. **20**(24): p. 9096-103.
134. Jiang, D., et al., *Zn(2+) induces permeability transition pore opening and release of pro-apoptotic peptides from neuronal mitochondria*. The Journal of biological chemistry, 2001. **276**(50): p. 47524-9.
135. Sheline, C.T., et al., *Involvement of poly ADP ribosyl polymerase-1 in acute but not chronic zinc toxicity*. The European journal of neuroscience, 2003. **18**(6): p. 1402-9.
136. Greenough, M.A., et al., *Presenilins promote the cellular uptake of copper and zinc and maintain copper chaperone of SOD1-dependent copper/zinc superoxide dismutase activity*. The Journal of biological chemistry, 2011. **286**(11): p. 9776-86.
137. Duce, J.A. and A.I. Bush, *Biological metals and Alzheimer's disease: implications for therapeutics and diagnostics*. Progress in neurobiology, 2010. **92**(1): p. 1-18.
138. Corrigan, F.M., G.P. Reynolds, and N.I. Ward, *Hippocampal tin, aluminum and zinc in Alzheimer's disease*. Biometals : an international journal on the role of metal ions in biology, biochemistry, and medicine, 1993. **6**(3): p. 149-54.
139. Lovell, M.A., et al., *Copper, iron and zinc in Alzheimer's disease senile plaques*. Journal of the neurological sciences, 1998. **158**(1): p. 47-52.
140. Friedlich, A.L., et al., *Neuronal zinc exchange with the blood vessel wall promotes cerebral amyloid angiopathy in an animal model of Alzheimer's disease*. The Journal of neuroscience : the official journal of the Society for Neuroscience, 2004. **24**(13): p. 3453-9.

141. Hensley, K., et al., *Brain regional correspondence between Alzheimer's disease histopathology and biomarkers of protein oxidation*. Journal of neurochemistry, 1995. **65**(5): p. 2146-56.
142. Lee, J.Y., et al., *Contribution by synaptic zinc to the gender-disparate plaque formation in human Swedish mutant APP transgenic mice*. Proc Natl Acad Sci U S A, 2002. **99**(11): p. 7705-10.
143. Smith, A.P. and N.M. Lee, *Role of zinc in ALS*. Amyotrophic lateral sclerosis : official publication of the World Federation of Neurology Research Group on Motor Neuron Diseases, 2007. **8**(3): p. 131-43.
144. Reaume, A.G., et al., *Motor neurons in Cu/Zn superoxide dismutase-deficient mice develop normally but exhibit enhanced cell death after axonal injury*. Nature genetics, 1996. **13**(1): p. 43-7.
145. Liochev, S.I., et al., *Superoxide-dependent peroxidase activity of H48Q: a superoxide dismutase variant associated with familial amyotrophic lateral sclerosis*. Archives of biochemistry and biophysics, 1997. **346**(2): p. 263-8.
146. Crow, J.P., et al., *Decreased zinc affinity of amyotrophic lateral sclerosis-associated superoxide dismutase mutants leads to enhanced catalysis of tyrosine nitration by peroxynitrite*. Journal of neurochemistry, 1997. **69**(5): p. 1936-44.
147. Mulligan, V.K., et al., *Denaturational stress induces formation of zinc-deficient monomers of Cu,Zn superoxide dismutase: implications for pathogenesis in amyotrophic lateral sclerosis*. Journal of molecular biology, 2008. **383**(2): p. 424-36.
148. Gong, Y.H. and J.L. Elliott, *Metallothionein expression is altered in a transgenic murine model of familial amyotrophic lateral sclerosis*. Experimental neurology, 2000. **162**(1): p. 27-36.
149. Nagano, S., et al., *Reduction of metallothioneins promotes the disease expression of familial amyotrophic lateral sclerosis mice in a dose-dependent manner*. The European journal of neuroscience, 2001. **13**(7): p. 1363-70.
150. Ritchie, C.W., et al., *Metal-protein attenuation with iodochlorhydroxyquin (clioquinol) targeting Abeta amyloid deposition and toxicity in Alzheimer disease: a pilot phase 2 clinical trial*. Archives of neurology, 2003. **60**(12): p. 1685-91.
151. Kelland, E.E., M.D. Kelly, and N.J. Toms, *Pyruvate limits zinc-induced rat oligodendrocyte progenitor cell death*. The European journal of neuroscience, 2004. **19**(2): p. 287-94.
152. Lubke, T., P. Lobel, and D.E. Sleat, *Proteomics of the lysosome*. Biochimica et biophysica acta, 2009. **1793**(4): p. 625-35.
153. Bainton, D.F., *The discovery of lysosomes*. The Journal of cell biology, 1981. **91**(3 Pt 2): p. 66s-76s.
154. Appelmans, F., R. Wattiaux, and C. De Duve, *Tissue fractionation studies. 5. The association of acid phosphatase with a special class of cytoplasmic granules in rat liver*. Biochem J, 1955. **59**(3): p. 438-45.
155. De Duve, C. and R. Wattiaux, *Functions of lysosomes*. Annual review of physiology, 1966. **28**: p. 435-92.
156. de Duve, C., *The lysosome turns fifty*. Nature cell biology, 2005. **7**(9): p. 847-9.
157. Saftig, P., *Lysosomes*. Medical Intelligence Unit. 2005, Georgetown, Texas: Landes Bioscience/ Eurekah.com. 208.

158. Lullmann-Rauch, R., *History and morphology of the lysosome*. Lysosomes, ed. P. Saftig. 2005, New York: Springer.
159. Saftig, P., B. Schroder, and J. Blanz, *Lysosomal membrane proteins: life between acid and neutral conditions*. Biochemical Society transactions, 2010. **38**(6): p. 1420-3.
160. Granger, B.L., et al., *Characterization and cloning of lgp110, a lysosomal membrane glycoprotein from mouse and rat cells*. The Journal of biological chemistry, 1990. **265**(20): p. 12036-43.
161. Mellman, I., R. Fuchs, and A. Helenius, *Acidification of the endocytic and exocytic pathways*. Annual review of biochemistry, 1986. **55**: p. 663-700.
162. Kobayashi, T., et al., *A lipid associated with the antiphospholipid syndrome regulates endosome structure and function*. Nature, 1998. **392**(6672): p. 193-7.
163. Sardiello, M., et al., *A gene network regulating lysosomal biogenesis and function*. Science, 2009. **325**(5939): p. 473-7.
164. Palmieri, M., et al., *Characterization of the CLEAR network reveals an integrated control of cellular clearance pathways*. Human molecular genetics, 2011. **20**(19): p. 3852-66.
165. Settembre, C., et al., *TFEB links autophagy to lysosomal biogenesis*. Science, 2011. **332**(6036): p. 1429-33.
166. Ma, X., et al., *Enhancing lysosome biogenesis attenuates BNIP3-induced cardiomyocyte death*. Autophagy, 2012. **8**(3): p. 297-309.
167. Martina, J.A., et al., *The Nutrient-Responsive Transcription Factor TFE3 Promotes Autophagy, Lysosomal Biogenesis, and Clearance of Cellular Debris*. Science signaling, 2014. **7**(309): p. ra9.
168. Kornfeld, S. and I. Mellman, *The biogenesis of lysosomes*. Annual review of cell biology, 1989. **5**: p. 483-525.
169. Figura, N., et al., *Prevalence, species differentiation, and toxigenicity of Aeromonas strains in cases of childhood gastroenteritis and in controls*. Journal of clinical microbiology, 1986. **23**(3): p. 595-9.
170. Klumperman, J., et al., *Differences in the endosomal distributions of the two mannose 6-phosphate receptors*. The Journal of cell biology, 1993. **121**(5): p. 997-1010.
171. Waguri, S., et al., *Visualization of TGN to endosome trafficking through fluorescently labeled MPR and AP-1 in living cells*. Molecular biology of the cell, 2003. **14**(1): p. 142-55.
172. Seaman, M.N., *Cargo-selective endosomal sorting for retrieval to the Golgi requires retromer*. The Journal of cell biology, 2004. **165**(1): p. 111-22.
173. Mari, M., et al., *SNX1 defines an early endosomal recycling exit for sortilin and mannose 6-phosphate receptors*. Traffic, 2008. **9**(3): p. 380-93.
174. Doray, B., et al., *Cooperation of GGAs and AP-1 in packaging MPRs at the trans-Golgi network*. Science, 2002. **297**(5587): p. 1700-3.
175. Bonifacino, J.S., *The GGA proteins: adaptors on the move*. Nature reviews. Molecular cell biology, 2004. **5**(1): p. 23-32.
176. Peden, A.A., et al., *Localization of the AP-3 adaptor complex defines a novel endosomal exit site for lysosomal membrane proteins*. The Journal of cell biology, 2004. **164**(7): p. 1065-76.
177. van Meel, E. and J. Klumperman, *Imaging and imagination: understanding the endo-lysosomal system*. Histochemistry and cell biology, 2008. **129**(3): p. 253-66.

178. Letourneur, F. and R.D. Klausner, *A novel di-leucine motif and a tyrosine-based motif independently mediate lysosomal targeting and endocytosis of CD3 chains*. Cell, 1992. **69**(7): p. 1143-57.
179. Pond, L., et al., *A role for acidic residues in di-leucine motif-based targeting to the endocytic pathway*. The Journal of biological chemistry, 1995. **270**(34): p. 19989-97.
180. Trowbridge, I.S., J.F. Collawn, and C.R. Hopkins, *Signal-dependent membrane protein trafficking in the endocytic pathway*. Annual review of cell biology, 1993. **9**: p. 129-61.
181. Davis, C.G., et al., *The J.D. mutation in familial hypercholesterolemia: amino acid substitution in cytoplasmic domain impedes internalization of LDL receptors*. Cell, 1986. **45**(1): p. 15-24.
182. Ihrke, G., et al., *Differential use of two AP-3-mediated pathways by lysosomal membrane proteins*. Traffic, 2004. **5**(12): p. 946-62.
183. Dell'Angelica, E.C., et al., *Altered trafficking of lysosomal proteins in Hermansky-Pudlak syndrome due to mutations in the beta 3A subunit of the AP-3 adaptor*. Molecular cell, 1999. **3**(1): p. 11-21.
184. Huizing, M. and W.A. Gahl, *Disorders of vesicles of lysosomal lineage: the Hermansky-Pudlak syndromes*. Current molecular medicine, 2002. **2**(5): p. 451-67.
185. Starcevic, M., R. Nazarian, and E.C. Dell'Angelica, *The molecular machinery for the biogenesis of lysosome-related organelles: lessons from Hermansky-Pudlak syndrome*. Seminars in cell & developmental biology, 2002. **13**(4): p. 271-8.
186. Hasilik, A., A. Waheed, and K. von Figura, *Enzymatic phosphorylation of lysosomal enzymes in the presence of UDP-N-acetylglucosamine. Absence of the activity in I-cell fibroblasts*. Biochemical and biophysical research communications, 1981. **98**(3): p. 761-7.
187. Waheed, A., A. Hasilik, and K. von Figura, *UDP-N-acetylglucosamine:lysosomal enzyme precursor N-acetylglucosamine-1-phosphotransferase. Partial purification and characterization of the rat liver Golgi enzyme*. The Journal of biological chemistry, 1982. **257**(20): p. 12322-31.
188. Reitman, M.L., A. Varki, and S. Kornfeld, *Fibroblasts from patients with I-cell disease and pseudo-Hurler polydystrophy are deficient in uridine 5'-diphosphate-N-acetylglucosamine: glycoprotein N-acetylglucosaminylphosphotransferase activity*. The Journal of clinical investigation, 1981. **67**(5): p. 1574-9.
189. Saftig, P. and J. Klumperman, *Lysosome biogenesis and lysosomal membrane proteins: trafficking meets function*. Nature reviews. Molecular cell biology, 2009. **10**(9): p. 623-35.
190. Ohkuma, S., Y. Moriyama, and T. Takano, *Identification and characterization of a proton pump on lysosomes by fluorescein-isothiocyanate-dextran fluorescence*. Proc Natl Acad Sci U S A, 1982. **79**(9): p. 2758-62.
191. Mindell, J.A., *Lysosomal acidification mechanisms*. Annual review of physiology, 2012. **74**: p. 69-86.
192. Graves, A.R., et al., *The Cl-/H+ antiporter ClC-7 is the primary chloride permeation pathway in lysosomes*. Nature, 2008. **453**(7196): p. 788-92.
193. Kasper, D., et al., *Loss of the chloride channel ClC-7 leads to lysosomal storage disease and neurodegeneration*. The EMBO journal, 2005. **24**(5): p. 1079-91.
194. Weinert, S., et al., *Lysosomal pathology and osteopetrosis upon loss of H+-driven lysosomal Cl- accumulation*. Science, 2010. **328**(5984): p. 1401-3.

195. Zhang, F., et al., *TRP-ML1 functions as a lysosomal NAADP-sensitive Ca2+ release channel in coronary arterial myocytes*. Journal of cellular and molecular medicine, 2009. **13**(9B): p. 3174-85.
196. Zhang, F., et al., *Reconstitution of lysosomal NAADP-TRP-ML1 signaling pathway and its function in TRP-ML1(-/-) cells*. Am J Physiol Cell Physiol, 2011. **301**(2): p. C421-30.
197. Calcraft, P.J., et al., *NAADP mobilizes calcium from acidic organelles through two-pore channels*. Nature, 2009. **459**(7246): p. 596-600.
198. Scott, C.C. and J. Gruenberg, *Ion flux and the function of endosomes and lysosomes: pH is just the start: the flux of ions across endosomal membranes influences endosome function not only through regulation of the luminal pH*. BioEssays : news and reviews in molecular, cellular and developmental biology, 2011. **33**(2): p. 103-10.
199. Coffey, J.W. and C. De Duve, *Digestive activity of lysosomes. I. The digestion of proteins by extracts of rat liver lysosomes*. The Journal of biological chemistry, 1968. **243**(12): p. 3255-63.
200. Ohkuma, S. and B. Poole, *Fluorescence probe measurement of the intralysosomal pH in living cells and the perturbation of pH by various agents*. Proc Natl Acad Sci U S A, 1978. **75**(7): p. 3327-31.
201. Rossi, A., et al., *Comprehensive search for cysteine cathepsins in the human genome*. Biological chemistry, 2004. **385**(5): p. 363-72.
202. Bidere, N., et al., *Cathepsin D triggers Bax activation, resulting in selective apoptosis-inducing factor (AIF) relocation in T lymphocytes entering the early commitment phase to apoptosis*. The Journal of biological chemistry, 2003. **278**(33): p. 31401-11.
203. Oberle, C., et al., *Lysosomal membrane permeabilization and cathepsin release is a Bax/Bak-dependent, amplifying event of apoptosis in fibroblasts and monocytes*. Cell death and differentiation, 2010. **17**(7): p. 1167-78.
204. Michallet, M.C., et al., *Cathepsin-B-dependent apoptosis triggered by antithymocyte globulins: a novel mechanism of T-cell depletion*. Blood, 2003. **102**(10): p. 3719-26.
205. Huotari, J. and A. Helenius, *Endosome maturation*. The EMBO journal, 2011. **30**(17): p. 3481-500.
206. Stoorvogel, W., et al., *Late endosomes derive from early endosomes by maturation*. Cell, 1991. **65**(3): p. 417-27.
207. Gu, F. and J. Gruenberg, *Biogenesis of transport intermediates in the endocytic pathway*. FEBS letters, 1999. **452**(1-2): p. 61-6.
208. Mu, F.T., et al., *EEA1, an early endosome-associated protein. EEA1 is a conserved alpha-helical peripheral membrane protein flanked by cysteine "fingers" and contains a calmodulin-binding IQ motif*. The Journal of biological chemistry, 1995. **270**(22): p. 13503-11.
209. Brown, W.J., J. Goodhouse, and M.G. Farquhar, *Mannose-6-phosphate receptors for lysosomal enzymes cycle between the Golgi complex and endosomes*. The Journal of cell biology, 1986. **103**(4): p. 1235-47.
210. Mullock, B.M., et al., *Fusion of lysosomes with late endosomes produces a hybrid organelle of intermediate density and is NSF dependent*. The Journal of cell biology, 1998. **140**(3): p. 591-601.
211. Caplan, S., et al., *Human Vam6p promotes lysosome clustering and fusion in vivo*. The Journal of cell biology, 2001. **154**(1): p. 109-22.

212. Poupon, V., et al., *The role of mVps18p in clustering, fusion, and intracellular localization of late endocytic organelles*. Molecular biology of the cell, 2003. **14**(10): p. 4015-27.
213. Antonin, W., et al., *A SNARE complex mediating fusion of late endosomes defines conserved properties of SNARE structure and function*. The EMBO journal, 2000. **19**(23): p. 6453-64.
214. Antonin, W., et al., *Crystal structure of the endosomal SNARE complex reveals common structural principles of all SNAREs*. Nature structural biology, 2002. **9**(2): p. 107-11.
215. Pryor, P.R., et al., *Combinatorial SNARE complexes with VAMP7 or VAMP8 define different late endocytic fusion events*. EMBO reports, 2004. **5**(6): p. 590-5.
216. Merz, A.J. and W.T. Wickner, *Trans-SNARE interactions elicit Ca2+ efflux from the yeast vacuole lumen*. The Journal of cell biology, 2004. **164**(2): p. 195-206.
217. Pryor, P.R., et al., *The role of intraorganellar Ca(2+) in late endosome-lysosome heterotypic fusion and in the reformation of lysosomes from hybrid organelles*. The Journal of cell biology, 2000. **149**(5): p. 1053-62.
218. Treusch, S., et al., *Caenorhabditis elegans functional orthologue of human protein h-mucolipin-1 is required for lysosome biogenesis*. Proc Natl Acad Sci U S A, 2004. **101**(13): p. 4483-8.
219. Kaushik, S. and A.M. Cuervo, *Chaperone-mediated autophagy: a unique way to enter the lysosome world*. Trends in cell biology, 2012. **22**(8): p. 407-17.
220. Li, W.W., J. Li, and J.K. Bao, *Microautophagy: lesser-known self-eating*. Cellular and molecular life sciences : CMLS, 2012. **69**(7): p. 1125-36.
221. Burman, C. and N.T. Ktistakis, *Autophagosome formation in mammalian cells*. Seminars in immunopathology, 2010. **32**(4): p. 397-413.
222. Efeyan, A., R. Zoncu, and D.M. Sabatini, *Amino acids and mTORC1: from lysosomes to disease*. Trends in molecular medicine, 2012. **18**(9): p. 524-33.
223. Mizushima, N. and M. Komatsu, *Autophagy: renovation of cells and tissues*. Cell, 2011. **147**(4): p. 728-41.
224. Roczniak-Ferguson, A., et al., *The transcription factor TFEB links mTORC1 signaling to transcriptional control of lysosome homeostasis*. Science signaling, 2012. **5**(228): p. ra42.
225. Korolchuk, V.I., et al., *Lysosomal positioning coordinates cellular nutrient responses*. Nature cell biology, 2011. **13**(4): p. 453-60.
226. Rodriguez, A., et al., *Lysosomes behave as Ca2+-regulated exocytic vesicles in fibroblasts and epithelial cells*. The Journal of cell biology, 1997. **137**(1): p. 93-104.
227. Gerasimenko, J.V., O.V. Gerasimenko, and O.H. Petersen, *Membrane repair: Ca(2+)-elicited lysosomal exocytosis*. Current biology : CB, 2001. **11**(23): p. R971-4.
228. Reddy, A., E.V. Caler, and N.W. Andrews, *Plasma membrane repair is mediated by Ca(2+)-regulated exocytosis of lysosomes*. Cell, 2001. **106**(2): p. 157-69.
229. Ren, Q., S. Ye, and S.W. Whiteheart, *The platelet release reaction: just when you thought platelet secretion was simple*. Current opinion in hematology, 2008. **15**(5): p. 537-41.
230. Stinchcombe, J., G. Bossi, and G.M. Griffiths, *Linking albinism and immunity: the secrets of secretory lysosomes*. Science, 2004. **305**(5680): p. 55-9.
231. Stinchcombe, J.C. and G.M. Griffiths, *Secretory mechanisms in cell-mediated cytotoxicity*. Annual review of cell and developmental biology, 2007. **23**: p. 495-517.

232. Mostov, K. and Z. Werb, *Journey across the osteoclast*. Science, 1997. **276**(5310): p. 219-20.
233. Wesolowski, J. and F. Paumet, *The impact of bacterial infection on mast cell degranulation*. Immunologic research, 2011. **51**(2-3): p. 215-26.
234. Andrade, L.O. and N.W. Andrews, *The Trypanosoma cruzi-host-cell interplay: location, invasion, retention*. Nature reviews. Microbiology, 2005. **3**(10): p. 819-23.
235. Jaiswal, J.K., N.W. Andrews, and S.M. Simon, *Membrane proximal lysosomes are the major vesicles responsible for calcium-dependent exocytosis in nonsecretory cells*. The Journal of cell biology, 2002. **159**(4): p. 625-35.
236. Stinchcombe, J.C., et al., *Centrosome polarization delivers secretory granules to the immunological synapse*. Nature, 2006. **443**(7110): p. 462-5.
237. Feldmann, J., et al., *Munc13-4 is essential for cytolytic granules fusion and is mutated in a form of familial hemophagocytic lymphohistiocytosis (FHL3)*. Cell, 2003. **115**(4): p. 461-73.
238. Shirakawa, R., et al., *Munc13-4 is a GTP-Rab27-binding protein regulating dense core granule secretion in platelets*. The Journal of biological chemistry, 2004. **279**(11): p. 10730-7.
239. Logan, M.R., et al., *A critical role for vesicle-associated membrane protein-7 in exocytosis from human eosinophils and neutrophils*. Allergy, 2006. **61**(6): p. 777-84.
240. Mollinedo, F., et al., *Combinatorial SNARE complexes modulate the secretion of cytoplasmic granules in human neutrophils*. Journal of immunology, 2006. **177**(5): p. 2831-41.
241. Ren, Q., et al., *Endobrevin/VAMP-8 is the primary v-SNARE for the platelet release reaction*. Molecular biology of the cell, 2007. **18**(1): p. 24-33.
242. Swank, R.T., et al., *Mouse models of Hermansky Pudlak syndrome: a review*. Pigment cell research / sponsored by the European Society for Pigment Cell Research and the International Pigment Cell Society, 1998. **11**(2): p. 60-80.
243. Aridor, M. and L.A. Hannan, *Traffic jam: a compendium of human diseases that affect intracellular transport processes*. Traffic, 2000. **1**(11): p. 836-51.
244. Aridor, M. and L.A. Hannan, *Traffic jams II: an update of diseases of intracellular transport*. Traffic, 2002. **3**(11): p. 781-90.
245. Ma, Y., et al., *Autophagy and cellular immune responses*. Immunity, 2013. **39**(2): p. 211-27.
246. Galluzzi, L., et al., *Viral control of mitochondrial apoptosis*. PLoS Pathog, 2008. **4**(5): p. e1000018.
247. Galluzzi, L., et al., *To die or not to die: that is the autophagic question*. Curr Mol Med, 2008. **8**(2): p. 78-91.
248. Kuballa, P., et al., *Autophagy and the immune system*. Annu Rev Immunol, 2012. **30**: p. 611-46.
249. Levine, B., N. Mizushima, and H.W. Virgin, *Autophagy in immunity and inflammation*. Nature, 2011. **469**(7330): p. 323-35.
250. Caron, E., et al., *The MHC I immunopeptidome conveys to the cell surface an integrative view of cellular regulation*. Mol Syst Biol, 2011. **7**: p. 533.
251. Michaud, M., et al., *Autophagy-dependent anticancer immune responses induced by chemotherapeutic agents in mice*. Science, 2011. **334**(6062): p. 1573-7.

252. Pua, H.H., et al., *A critical role for the autophagy gene Atg5 in T cell survival and proliferation*. J Exp Med, 2007. **204**(1): p. 25-31.
253. Wildenberg, M.E., et al., *Autophagy attenuates the adaptive immune response by destabilizing the immunologic synapse*. Gastroenterology, 2012. **142**(7): p. 1493-503 e6.
254. Fiegl, D., et al., *Amphisomal route of MHC class I cross-presentation in bacteria-infected dendritic cells*. J Immunol, 2013. **190**(6): p. 2791-806.
255. Jia, W. and Y.W. He, *Temporal regulation of intracellular organelle homeostasis in T lymphocytes by autophagy*. J Immunol, 2011. **186**(9): p. 5313-22.
256. Bruns, C., et al., *Biogenesis of a novel compartment for autophagosome-mediated unconventional protein secretion*. J Cell Biol, 2011. **195**(6): p. 979-92.
257. Jiang, S., et al., *Secretory versus degradative autophagy: unconventional secretion of inflammatory mediators*. J Innate Immun, 2013. **5**(5): p. 471-9.
258. Nakahira, K., et al., *Autophagy proteins regulate innate immune responses by inhibiting the release of mitochondrial DNA mediated by the NALP3 inflammasome*. Nat Immunol, 2011. **12**(3): p. 222-30.
259. Thorburn, J., et al., *Autophagy regulates selective HMGB1 release in tumor cells that are destined to die*. Cell Death Differ, 2009. **16**(1): p. 175-83.
260. Kim, B.H., et al., *IFN-inducible GTPases in host cell defense*. Cell Host Microbe, 2012. **12**(4): p. 432-44.
261. Ma, Y., et al., *Anticancer chemotherapy-induced intratumoral recruitment and differentiation of antigen-presenting cells*. Immunity, 2013. **38**(4): p. 729-41.
262. Schreiber, R.D., L.J. Old, and M.J. Smyth, *Cancer immunoediting: integrating immunity's roles in cancer suppression and promotion*. Science, 2011. **331**(6024): p. 1565-70.
263. Gonzalez, M.R., et al., *Bacterial pore-forming toxins: the (w)hole story?* Cellular and molecular life sciences : CMLS, 2008. **65**(3): p. 493-507.
264. McNeil, P.L. and R. Khakee, *Disruptions of muscle fiber plasma membranes. Role in exercise-induced damage*. The American journal of pathology, 1992. **140**(5): p. 1097-109.
265. Andrews, N.W., *Lysosomes and the plasma membrane: trypanosomes reveal a secret relationship*. The Journal of cell biology, 2002. **158**(3): p. 389-94.
266. Steinhardt, R.A., G. Bi, and J.M. Alderton, *Cell membrane resealing by a vesicular mechanism similar to neurotransmitter release*. Science, 1994. **263**(5145): p. 390-3.
267. Deleze, J., *The recovery of resting potential and input resistance in sheep heart injured by knife or laser*. The Journal of physiology, 1970. **208**(3): p. 547-62.
268. Rao, S.K., et al., *Identification of SNAREs involved in synaptotagmin VII-regulated lysosomal exocytosis*. The Journal of biological chemistry, 2004. **279**(19): p. 20471-9.
269. Verhage, M. and R.F. Toonen, *Regulated exocytosis: merging ideas on fusing membranes*. Current opinion in cell biology, 2007. **19**(4): p. 402-8.
270. Jahn, R. and R.H. Scheller, *SNAREs--engines for membrane fusion*. Nature reviews. Molecular cell biology, 2006. **7**(9): p. 631-43.
271. Bossi, G. and G.M. Griffiths, *CTL secretory lysosomes: biogenesis and secretion of a harmful organelle*. Seminars in immunology, 2005. **17**(1): p. 87-94.
272. LaPlante, J.M., et al., *Lysosomal exocytosis is impaired in mucolipidosis type IV*. Molecular genetics and metabolism, 2006. **89**(4): p. 339-48.

273. Medina, D.L., et al., *Transcriptional activation of lysosomal exocytosis promotes cellular clearance*. Dev Cell, 2011. **21**(3): p. 421-30.
274. Roy, D., et al., *A process for controlling intracellular bacterial infections induced by membrane injury*. Science, 2004. **304**(5676): p. 1515-8.
275. Han, R., et al., *Dysferlin-mediated membrane repair protects the heart from stress-induced left ventricular injury*. The Journal of clinical investigation, 2007. **117**(7): p. 1805-13.
276. Ferron, M., et al., *A RANKL-PKCbeta-TFEB signaling cascade is necessary for lysosomal biogenesis in osteoclasts*. Genes & development, 2013. **27**(8): p. 955-69.
277. Idone, V., et al., *Repair of injured plasma membrane by rapid Ca2+-dependent endocytosis*. The Journal of cell biology, 2008. **180**(5): p. 905-14.
278. Tam, C., et al., *Exocytosis of acid sphingomyelinase by wounded cells promotes endocytosis and plasma membrane repair*. The Journal of cell biology, 2010. **189**(6): p. 1027-38.
279. Holopainen, J.M., M.I. Angelova, and P.K. Kinnunen, *Vectorial budding of vesicles by asymmetrical enzymatic formation of ceramide in giant liposomes*. Biophysical journal, 2000. **78**(2): p. 830-8.
280. Zhang, Z., et al., *Regulated ATP release from astrocytes through lysosome exocytosis*. Nature cell biology, 2007. **9**(8): p. 945-53.
281. Ralevic, V. and G. Burnstock, *Receptors for purines and pyrimidines*. Pharmacological reviews, 1998. **50**(3): p. 413-92.
282. Turk, B. and V. Turk, *Lysosomes as "suicide bags" in cell death: myth or reality?* The Journal of biological chemistry, 2009. **284**(33): p. 21783-7.
283. Boya, P. and G. Kroemer, *Lysosomal membrane permeabilization in cell death*. Oncogene, 2008. **27**(50): p. 6434-51.
284. Schestkowa, O., et al., *The catalytically inactive precursor of cathepsin D induces apoptosis in human fibroblasts and HeLa cells*. Journal of cellular biochemistry, 2007. **101**(6): p. 1558-66.
285. Broker, L.E., et al., *Cathepsin B mediates caspase-independent cell death induced by microtubule stabilizing agents in non-small cell lung cancer cells*. Cancer research, 2004. **64**(1): p. 27-30.
286. Guicciardi, M.E., et al., *Cathepsin B contributes to TNF-alpha-mediated hepatocyte apoptosis by promoting mitochondrial release of cytochrome c*. The Journal of clinical investigation, 2000. **106**(9): p. 1127-37.
287. Vancompernolle, K., et al., *Atractyloside-induced release of cathepsin B, a protease with caspase-processing activity*. FEBS letters, 1998. **438**(3): p. 150-8.
288. Foghsgaard, L., et al., *Cathepsin B acts as a dominant execution protease in tumor cell apoptosis induced by tumor necrosis factor*. The Journal of cell biology, 2001. **153**(5): p. 999-1010.
289. Christensen, K.A., J.T. Myers, and J.A. Swanson, *pH-dependent regulation of lysosomal calcium in macrophages*. J Cell Sci, 2002. **115**(Pt 3): p. 599-607.
290. Lloyd-Evans, E. and F.M. Platt, *Lysosomal Ca(2+) homeostasis: role in pathogenesis of lysosomal storage diseases*. Cell calcium, 2011. **50**(2): p. 200-5.
291. Churchill, G.C., et al., *NAADP mobilizes Ca(2+) from reserve granules, lysosome-related organelles, in sea urchin eggs*. Cell, 2002. **111**(5): p. 703-8.

292. Mirnikjoo, B., K. Balasubramanian, and A.J. Schroit, *Mobilization of lysosomal calcium regulates the externalization of phosphatidylserine during apoptosis*. The Journal of biological chemistry, 2009. **284**(11): p. 6918-23.
293. Roberg, K. and K. Ollinger, *Oxidative stress causes relocation of the lysosomal enzyme cathepsin D with ensuing apoptosis in neonatal rat cardiomyocytes*. The American journal of pathology, 1998. **152**(5): p. 1151-6.
294. Brunk, U.T. and I. Svensson, *Oxidative stress, growth factor starvation and Fas activation may all cause apoptosis through lysosomal leak*. Redox report : communications in free radical research, 1999. **4**(1-2): p. 3-11.
295. Bivik, C.A., et al., *UVA/B-induced apoptosis in human melanocytes involves translocation of cathepsins and Bcl-2 family members*. The Journal of investigative dermatology, 2006. **126**(5): p. 1119-27.
296. Kreuzaler, P.A., et al., *Stat3 controls lysosomal-mediated cell death in vivo*. Nature cell biology, 2011. **13**(3): p. 303-9.
297. Zuzarte-Luis, V., et al., *Lysosomal cathepsins in embryonic programmed cell death*. Developmental biology, 2007. **301**(1): p. 205-17.
298. Nylandsted, J., et al., *Heat shock protein 70 promotes cell survival by inhibiting lysosomal membrane permeabilization*. The Journal of experimental medicine, 2004. **200**(4): p. 425-35.
299. Blomgran, R., L. Zheng, and O. Stendahl, *Cathepsin-cleaved Bid promotes apoptosis in human neutrophils via oxidative stress-induced lysosomal membrane permeabilization*. Journal of leukocyte biology, 2007. **81**(5): p. 1213-23.
300. Gonzalvez, F. and A. Ashkenazi, *New insights into apoptosis signaling by Apo2L/TRAIL*. Oncogene, 2010. **29**(34): p. 4752-65.
301. Werneburg, N.W., et al., *Tumor necrosis factor-related apoptosis-inducing ligand (TRAIL) protein-induced lysosomal translocation of proapoptotic effectors is mediated by phosphofurin acidic cluster sorting protein-2 (PACS-2)*. The Journal of biological chemistry, 2012. **287**(29): p. 24427-37.
302. Appelqvist, H., et al., *Sensitivity to lysosome-dependent cell death is directly regulated by lysosomal cholesterol content*. PLoS One, 2012. **7**(11): p. e50262.
303. Persson, H.L., et al., *Prevention of oxidant-induced cell death by lysosomotropic iron chelators*. Free radical biology & medicine, 2003. **34**(10): p. 1295-305.
304. Hwang, J.J., et al., *Zinc and 4-hydroxy-2-nonenal mediate lysosomal membrane permeabilization induced by H2O2 in cultured hippocampal neurons*. The Journal of neuroscience : the official journal of the Society for Neuroscience, 2008. **28**(12): p. 3114-22.
305. Kirkegaard, T., et al., *Hsp70 stabilizes lysosomes and reverts Niemann-Pick disease-associated lysosomal pathology*. Nature, 2010. **463**(7280): p. 549-53.
306. Brzin, J., et al., *Protein inhibitors of cysteine proteinases. I. Isolation and characterization of stefin, a cytosolic protein inhibitor of cysteine proteinases from human polymorphonuclear granulocytes*. Hoppe-Seyler's Zeitschrift fur physiologische Chemie, 1983. **364**(11): p. 1475-80.
307. Kirschke, H., et al., *Cathepsin S from bovine spleen. Purification, distribution, intracellular localization and action on proteins*. Biochem J, 1989. **264**(2): p. 467-73.

308. Turk, B., et al., *Regulation of the activity of lysosomal cysteine proteinases by pH-induced inactivation and/or endogenous protein inhibitors, cystatins*. Biological chemistry Hoppe-Seyler, 1995. **376**(4): p. 225-30.
309. Lee, A.Y., S.V. Gulnik, and J.W. Erickson, *Conformational switching in an aspartic proteinase*. Nature structural biology, 1998. **5**(10): p. 866-71.
310. Cirman, T., et al., *Selective disruption of lysosomes in HeLa cells triggers apoptosis mediated by cleavage of Bid by multiple papain-like lysosomal cathepsins*. The Journal of biological chemistry, 2004. **279**(5): p. 3578-87.
311. Heinrich, M., et al., *Cathepsin D links TNF-induced acid sphingomyelinase to Bid-mediated caspase-9 and -3 activation*. Cell death and differentiation, 2004. **11**(5): p. 550-63.
312. Droga-Mazovec, G., et al., *Cysteine cathepsins trigger caspase-dependent cell death through cleavage of bid and antiapoptotic Bcl-2 homologues*. The Journal of biological chemistry, 2008. **283**(27): p. 19140-50.
313. Boya, P., et al., *Lysosomal membrane permeabilization induces cell death in a mitochondrion-dependent fashion*. The Journal of experimental medicine, 2003. **197**(10): p. 1323-34.
314. Roberg, K., K. Kagedal, and K. Ollinger, *Microinjection of cathepsin d induces caspase-dependent apoptosis in fibroblasts*. The American journal of pathology, 2002. **161**(1): p. 89-96.
315. Taha, T.A., et al., *Tumor necrosis factor induces the loss of sphingosine kinase-1 by a cathepsin B-dependent mechanism*. The Journal of biological chemistry, 2005. **280**(17): p. 17196-202.
316. Ivanova, S., et al., *MAGUKs, scaffolding proteins at cell junctions, are substrates of different proteases during apoptosis*. Cell death & disease, 2011. **2**: p. e116.
317. Zarzynska, J. and T. Motyl, *Apoptosis and autophagy in involuting bovine mammary gland*. Journal of physiology and pharmacology : an official journal of the Polish Physiological Society, 2008. **59 Suppl 9**: p. 275-88.
318. Ganley, I.G., et al., *ULK1.ATG13.FIP200 complex mediates mTOR signaling and is essential for autophagy*. The Journal of biological chemistry, 2009. **284**(18): p. 12297-305.
319. Hosokawa, N., et al., *Nutrient-dependent mTORC1 association with the ULK1-Atg13-FIP200 complex required for autophagy*. Molecular biology of the cell, 2009. **20**(7): p. 1981-91.
320. Jung, C.H., et al., *ULK-Atg13-FIP200 complexes mediate mTOR signaling to the autophagy machinery*. Molecular biology of the cell, 2009. **20**(7): p. 1992-2003.
321. Hara, T., et al., *FIP200, a ULK-interacting protein, is required for autophagosome formation in mammalian cells*. The Journal of cell biology, 2008. **181**(3): p. 497-510.
322. Zoncu, R., et al., *mTORC1 senses lysosomal amino acids through an inside-out mechanism that requires the vacuolar H(+)-ATPase*. Science, 2011. **334**(6056): p. 678-83.
323. Cang, C., et al., *mTOR regulates lysosomal ATP-sensitive two-pore Na(+) channels to adapt to metabolic state*. Cell, 2013. **152**(4): p. 778-90.
324. Sridhar, S., et al., *The lipid kinase PI4KIIIbeta preserves lysosomal identity*. The EMBO journal, 2013. **32**(3): p. 324-39.

325. Yu, L., et al., *Termination of autophagy and reformation of lysosomes regulated by mTOR*. Nature, 2010. **465**(7300): p. 942-6.
326. Rong, Y., et al., *Spinster is required for autophagic lysosome reformation and mTOR reactivation following starvation*. Proc Natl Acad Sci U S A, 2011. **108**(19): p. 7826-31.
327. Cuervo, A.M. and J.F. Dice, *When lysosomes get old*. Experimental gerontology, 2000. **35**(2): p. 119-31.
328. Rubinsztein, D.C., G. Marino, and G. Kroemer, *Autophagy and aging*. Cell, 2011. **146**(5): p. 682-95.
329. Poupetova, H., et al., *The birth prevalence of lysosomal storage disorders in the Czech Republic: comparison with data in different populations*. Journal of inherited metabolic disease, 2010. **33**(4): p. 387-96.
330. Fuller, M., P.J. Meikle, and J.J. Hopwood, *Epidemiology of lysosomal storage diseases: an overview*, in *Fabry Disease: Perspectives from 5 Years of FOS*, A. Mehta, M. Beck, and G. Sunder-Plassmann, Editors. 2006: Oxford.
331. Vitner, E.B., F.M. Platt, and A.H. Futerman, *Common and uncommon pathogenic cascades in lysosomal storage diseases*. The Journal of biological chemistry, 2010. **285**(27): p. 20423-7.
332. Futerman, A.H. and G. van Meer, *The cell biology of lysosomal storage disorders*. Nature reviews. Molecular cell biology, 2004. **5**(7): p. 554-65.
333. Takahashi, K., M. Naito, and Y. Suzuki, *Genetic mucopolysaccharidoses, mannosidosis, sialidosis, galactosialidosis, and I-cell disease. Ultrastructural analysis of cultured fibroblasts*. Acta pathologica japonica, 1987. **37**(3): p. 385-400.
334. Lubensky, I.A., et al., *Lysosomal inclusions in gastric parietal cells in mucolipidosis type IV: a novel cause of achlorhydria and hypergastrinemia*. The American journal of surgical pathology, 1999. **23**(12): p. 1527-31.
335. Beltroy, E.P., et al., *Cholesterol accumulation and liver cell death in mice with Niemann-Pick type C disease*. Hepatology, 2005. **42**(4): p. 886-93.
336. Jennings, J.J., Jr., et al., *Mitochondrial aberrations in mucolipidosis Type IV*. The Journal of biological chemistry, 2006. **281**(51): p. 39041-50.
337. Wei, H., et al., *ER and oxidative stresses are common mediators of apoptosis in both neurodegenerative and non-neurodegenerative lysosomal storage disorders and are alleviated by chemical chaperones*. Human molecular genetics, 2008. **17**(4): p. 469-77.
338. Ginzburg, L. and A.H. Futerman, *Defective calcium homeostasis in the cerebellum in a mouse model of Niemann-Pick A disease*. Journal of neurochemistry, 2005. **95**(6): p. 1619-28.
339. Platt, F.M., B. Boland, and A.C. van der Spoel, *The cell biology of disease: lysosomal storage disorders: the cellular impact of lysosomal dysfunction*. The Journal of cell biology, 2012. **199**(5): p. 723-34.
340. Brady, R.O., *Gaucher's disease: past, present and future*. Bailliere's clinical haematology, 1997. **10**(4): p. 621-34.
341. Cosma, M.P., et al., *The multiple sulfatase deficiency gene encodes an essential and limiting factor for the activity of sulfatases*. Cell, 2003. **113**(4): p. 445-56.
342. Dierks, T., et al., *Multiple sulfatase deficiency is caused by mutations in the gene encoding the human C(alpha)-formylglycine generating enzyme*. Cell, 2003. **113**(4): p. 435-44.

343. Bargal, R., et al., *When Mucolipidosis III meets Mucolipidosis II: GNPTA gene mutations in 24 patients*. Molecular genetics and metabolism, 2006. **88**(4): p. 359-63.
344. Hickman, S. and E.F. Neufeld, *A hypothesis for I-cell disease: defective hydrolases that do not enter lysosomes*. Biochemical and biophysical research communications, 1972. **49**(4): p. 992-9.
345. Lloyd-Evans, E., et al., *Niemann-Pick disease type C1 is a sphingosine storage disease that causes deregulation of lysosomal calcium*. Nature medicine, 2008. **14**(11): p. 1247-55.
346. Town, M., et al., *A novel gene encoding an integral membrane protein is mutated in nephropathic cystinosis*. Nature genetics, 1998. **18**(4): p. 319-24.
347. Berman, E.R., et al., *Congenital corneal clouding with abnormal systemic storage bodies: a new variant of mucolipidosis*. The Journal of pediatrics, 1974. **84**(4): p. 519-26.
348. Bach, G., *Mucolipidosis type IV*. Molecular genetics and metabolism, 2001. **73**(3): p. 197-203.
349. Bargal, R., et al., *Mucolipidosis type IV: novel MCOLN1 mutations in Jewish and non-Jewish patients and the frequency of the disease in the Ashkenazi Jewish population*. Human mutation, 2001. **17**(5): p. 397-402.
350. Crandall, B.F., et al., *Review article: mucolipidosis IV*. American journal of medical genetics, 1982. **12**(3): p. 301-8.
351. Goutieres, F., M.L. Arsenio-Nunes, and J. Aicardi, *Mucolipidosis IV*. Neuropadiatrie, 1979. **10**(4): p. 321-31.
352. Schiffmann, R., et al., *Mucolipidosis IV*, in *GeneReviews*, R.A. Pagon, et al., Editors. 1993: Seattle (WA).
353. Bach, G., et al., *The frequency of mucolipidosis type IV in the Ashkenazi Jewish population and the identification of 3 novel MCOLN1 mutations*. Human mutation, 2005. **26**(6): p. 591.
354. Raychowdhury, M.K., et al., *Molecular pathophysiology of mucolipidosis type IV: pH dysregulation of the mucolipin-1 cation channel*. Human molecular genetics, 2004. **13**(6): p. 617-27.
355. Altarescu, G., et al., *The neurogenetics of mucolipidosis type IV*. Neurology, 2002. **59**(3): p. 306-13.
356. Goldin, E., et al., *Transfer of a mitochondrial DNA fragment to MCOLN1 causes an inherited case of mucolipidosis IV*. Human mutation, 2004. **24**(6): p. 460-5.
357. Falardeau, J.L., et al., *Cloning and characterization of the mouse Mcoln1 gene reveals an alternatively spliced transcript not seen in humans*. BMC genomics, 2002. **3**: p. 3.
358. Goldin, E., et al., *Mucolipidosis IV consists of one complementation group*. Proc Natl Acad Sci U S A, 1999. **96**(15): p. 8562-6.
359. Riedel, K.G., et al., *Ocular abnormalities in mucolipidosis IV*. American journal of ophthalmology, 1985. **99**(2): p. 125-36.
360. Folkerth, R.D., et al., *Mucolipidosis IV: morphology and histochemistry of an autopsy case*. Journal of neuropathology and experimental neurology, 1995. **54**(2): p. 154-64.
361. Bozzato, A., S. Barlati, and G. Borsani, *Gene expression profiling of mucolipidosis type IV fibroblasts reveals deregulation of genes with relevant functions in lysosome physiology*. Biochimica et biophysica acta, 2008. **1782**(4): p. 250-8.
362. Schiffmann, R., et al., *Constitutive achlorhydria in mucolipidosis type IV*. Proc Natl Acad Sci U S A, 1998. **95**(3): p. 1207-12.

363. Sun, M., et al., *Mucolipidosis type IV is caused by mutations in a gene encoding a novel transient receptor potential channel*. Human molecular genetics, 2000. **9**(17): p. 2471-8.
364. Bassi, M.T., et al., *Cloning of the gene encoding a novel integral membrane protein, mucolipidin-and identification of the two major founder mutations causing mucolipidosis type IV*. American journal of human genetics, 2000. **67**(5): p. 1110-20.
365. Bargal, R., et al., *Identification of the gene causing mucolipidosis type IV*. Nature genetics, 2000. **26**(1): p. 118-23.
366. Slaugenhaupt, S.A., et al., *Mapping of the mucolipidosis type IV gene to chromosome 19p and definition of founder haplotypes*. American journal of human genetics, 1999. **65**(3): p. 773-8.
367. Kiselyov, K., et al., *TRP-ML1 is a lysosomal monovalent cation channel that undergoes proteolytic cleavage*. The Journal of biological chemistry, 2005. **280**(52): p. 43218-23.
368. Venkatachalam, K. and C. Montell, *TRP channels*. Annual review of biochemistry, 2007. **76**: p. 387-417.
369. Damann, N., T. Voets, and B. Nilius, *TRPs in our senses*. Current biology : CB, 2008. **18**(18): p. R880-9.
370. Pryor, P.R., et al., *Mucolipin-1 is a lysosomal membrane protein required for intracellular lactosylceramide traffic*. Traffic, 2006. **7**(10): p. 1388-98.
371. Vergarajauregui, S. and R. Puertollano, *Mucolipidosis type IV: the importance of functional lysosomes for efficient autophagy*. Autophagy, 2008. **4**(6): p. 832-4.
372. Vergarajauregui, S., et al., *Autophagic dysfunction in mucolipidosis type IV patients*. Human molecular genetics, 2008. **17**(17): p. 2723-37.
373. Curcio-Morelli, C., et al., *Functional multimerization of mucolipin channel proteins*. Journal of cellular physiology, 2010. **222**(2): p. 328-35.
374. Zeevi, D.A., et al., *Heteromultimeric TRPML channel assemblies play a crucial role in the regulation of cell viability models and starvation-induced autophagy*. J Cell Sci, 2010. **123**(Pt 18): p. 3112-24.
375. LaPlante, J.M., et al., *Identification and characterization of the single channel function of human mucolipin-1 implicated in mucolipidosis type IV, a disorder affecting the lysosomal pathway*. FEBS letters, 2002. **532**(1-2): p. 183-7.
376. Dong, X., et al., *The type IV mucolipidosis-associated protein TRPML1 is an endolysosomal iron release channel*. Nature, 2008. **455**(7215): p. 992-996.
377. Bargal, R. and G. Bach, *Mucolipidosis type IV: abnormal transport of lipids to lysosomes*. Journal of inherited metabolic disease, 1997. **20**(5): p. 625-32.
378. Fares, H. and I. Greenwald, *Regulation of endocytosis by CUP-5, the Caenorhabditis elegans mucolipin-1 homolog*. Nature genetics, 2001. **28**(1): p. 64-8.
379. Soyombo, A.A., et al., *TRP-ML1 regulates lysosomal pH and acidic lysosomal lipid hydrolytic activity*. The Journal of biological chemistry, 2006. **281**(11): p. 7294-301.
380. Chen, C.S., G. Bach, and R.E. Pagano, *Abnormal transport along the lysosomal pathway in mucolipidosis, type IV disease*. Proc Natl Acad Sci U S A, 1998. **95**(11): p. 6373-8.
381. Fares, H. and I. Greenwald, *Genetic analysis of endocytosis in Caenorhabditis elegans: coelomocyte uptake defective mutants*. Genetics, 2001. **159**(1): p. 133-45.
382. Micsenyi, M.C., et al., *Neuropathology of the Mcoln1(-/-) knockout mouse model of mucolipidosis type IV*. Journal of neuropathology and experimental neurology, 2009. **68**(2): p. 125-35.

383. Venkatachalam, K., et al., *Motor deficit in a Drosophila model of mucolipidosis type IV due to defective clearance of apoptotic cells*. Cell, 2008. **135**(5): p. 838-51.
384. Curcio-Morelli, C., et al., *Macroautophagy is defective in mucolipin-1-deficient mouse neurons*. Neurobiology of disease, 2010. **40**(2): p. 370-7.
385. Venugopal, B., et al., *Chaperone-mediated autophagy is defective in mucolipidosis type IV*. Journal of cellular physiology, 2009. **219**(2): p. 344-53.
386. Pagano, R.E., *Endocytic trafficking of glycosphingolipids in sphingolipid storage diseases*. Philosophical transactions of the Royal Society of London. Series B, Biological sciences, 2003. **358**(1433): p. 885-91.
387. Miedel, M.T., et al., *Membrane traffic and turnover in TRP-ML1-deficient cells: a revised model for mucolipidosis type IV pathogenesis*. J Exp Med, 2008. **205**(6): p. 1477-90.
388. Dong, X.P., et al., *PI(3,5)P(2) controls membrane trafficking by direct activation of mucolipin Ca(2+) release channels in the endolysosome*. Nat Commun, 2010. **1**(4): p. 38.
389. Zhang, X., X. Li, and H. Xu, *Phosphoinositide isoforms determine compartment-specific ion channel activity*. Proc Natl Acad Sci U S A, 2012. **109**(28): p. 11384-9.
390. Vergarajauregui, S., J.A. Martina, and R. Puertollano, *Identification of the penta-EF-hand protein ALG-2 as a Ca2+-dependent interactor of mucolipin-1*. The Journal of biological chemistry, 2009. **284**(52): p. 36357-66.
391. Abe, K. and R. Puertollano, *Role of TRP channels in the regulation of the endosomal pathway*. Physiology, 2011. **26**(1): p. 14-22.
392. Zhu, M.X., et al., *TPCs: Endolysosomal channels for Ca2+ mobilization from acidic organelles triggered by NAADP*. FEBS letters, 2010. **584**(10): p. 1966-74.
393. Eichelsdoerfer, J.L., et al., *Zinc dyshomeostasis is linked with the loss of mucolipidosis IV-associated TRPML1 ion channel*. J Biol Chem, 2010. **285**(45): p. 34304-8.
394. Cisternas, F.A., et al., *Early histological and functional effects of chronic copper exposure in rat liver*. Biometals : an international journal on the role of metal ions in biology, biochemistry, and medicine, 2005. **18**(5): p. 541-51.
395. Eaton, J.W. and M. Qian, *Molecular bases of cellular iron toxicity*. Free radical biology & medicine, 2002. **32**(9): p. 833-40.
396. Pourahmad, J., S. Ross, and P.J. O'Brien, *Lysosomal involvement in hepatocyte cytotoxicity induced by Cu(2+) but not Cd(2+)*. Free radical biology & medicine, 2001. **30**(1): p. 89-97.
397. Brunk, U.T., C.B. Jones, and R.S. Sohal, *A novel hypothesis of lipofuscinogenesis and cellular aging based on interactions between oxidative stress and autophagocytosis*. Mutation research, 1992. **275**(3-6): p. 395-403.
398. Terman, A. and U.T. Brunk, *Lipofuscin*. The international journal of biochemistry & cell biology, 2004. **36**(8): p. 1400-4.
399. Morgan, E.H. and P.S. Oates, *Mechanisms and regulation of intestinal iron absorption*. Blood cells, molecules & diseases, 2002. **29**(3): p. 384-99.
400. Andrews, N.C. and P.J. Schmidt, *Iron homeostasis*. Annual review of physiology, 2007. **69**: p. 69-85.
401. Bellettato, C.M. and M. Scarpa, *Pathophysiology of neuropathic lysosomal storage disorders*. Journal of inherited metabolic disease, 2010. **33**(4): p. 347-62.
402. Nixon, R.A., D.S. Yang, and J.H. Lee, *Neurodegenerative lysosomal disorders: a continuum from development to late age*. Autophagy, 2008. **4**(5): p. 590-9.

403. Ravikumar, B., et al., *Regulation of mammalian autophagy in physiology and pathophysiology*. Physiological reviews, 2010. **90**(4): p. 1383-435.
404. Hara, T., et al., *Suppression of basal autophagy in neural cells causes neurodegenerative disease in mice*. Nature, 2006. **441**(7095): p. 885-9.
405. Komatsu, M., et al., *Loss of autophagy in the central nervous system causes neurodegeneration in mice*. Nature, 2006. **441**(7095): p. 880-4.
406. Lee, S., Y. Sato, and R.A. Nixon, *Lysosomal proteolysis inhibition selectively disrupts axonal transport of degradative organelles and causes an Alzheimer's-like axonal dystrophy*. The Journal of neuroscience : the official journal of the Society for Neuroscience, 2011. **31**(21): p. 7817-30.
407. Yu, W.H., et al., *Macroautophagy--a novel Beta-amyloid peptide-generating pathway activated in Alzheimer's disease*. The Journal of cell biology, 2005. **171**(1): p. 87-98.
408. Li, J., et al., *Differential regulation of amyloid-beta endocytic trafficking and lysosomal degradation by apolipoprotein E isoforms*. The Journal of biological chemistry, 2012. **287**(53): p. 44593-601.
409. Lee, J.H., et al., *Lysosomal proteolysis and autophagy require presenilin 1 and are disrupted by Alzheimer-related PS1 mutations*. Cell, 2010. **141**(7): p. 1146-58.
410. Neely, K.M., K.N. Green, and F.M. LaFerla, *Presenilin is necessary for efficient proteolysis through the autophagy-lysosome system in a gamma-secretase-independent manner*. The Journal of neuroscience : the official journal of the Society for Neuroscience, 2011. **31**(8): p. 2781-91.
411. Wolfe, D.M., et al., *Autophagy failure in Alzheimer's disease and the role of defective lysosomal acidification*. The European journal of neuroscience, 2013. **37**(12): p. 1949-61.
412. Coen, K., et al., *Lysosomal calcium homeostasis defects, not proton pump defects, cause endo-lysosomal dysfunction in PSEN-deficient cells*. The Journal of cell biology, 2012. **198**(1): p. 23-35.
413. Yang, D.S., et al., *Reversal of autophagy dysfunction in the TgCRND8 mouse model of Alzheimer's disease ameliorates amyloid pathologies and memory deficits*. Brain : a journal of neurology, 2011. **134**(Pt 1): p. 258-77.
414. Dehay, B., et al., *Pathogenic lysosomal depletion in Parkinson's disease*. The Journal of neuroscience : the official journal of the Society for Neuroscience, 2010. **30**(37): p. 12535-44.
415. Vila, M., et al., *Lysosomal membrane permeabilization in Parkinson disease*. Autophagy, 2011. **7**(1): p. 98-100.
416. Mak, S.K., et al., *Lysosomal degradation of alpha-synuclein in vivo*. The Journal of biological chemistry, 2010. **285**(18): p. 13621-9.
417. Mazzulli, J.R., et al., *Gaucher disease glucocerebrosidase and alpha-synuclein form a bidirectional pathogenic loop in synucleinopathies*. Cell, 2011. **146**(1): p. 37-52.
418. Harris, H. and D.C. Rubinsztein, *Control of autophagy as a therapy for neurodegenerative disease*. Nature reviews. Neurology, 2012. **8**(2): p. 108-17.
419. Ravikumar, B., et al., *Inhibition of mTOR induces autophagy and reduces toxicity of polyglutamine expansions in fly and mouse models of Huntington disease*. Nature genetics, 2004. **36**(6): p. 585-95.
420. Spampanato, C., et al., *Transcription factor EB (TFEB) is a new therapeutic target for Pompe disease*. EMBO molecular medicine, 2013. **5**(5): p. 691-706.

421. Tsunemi, T., et al., *PGC-1alpha rescues Huntington's disease proteotoxicity by preventing oxidative stress and promoting TFEB function*. Science translational medicine, 2012. **4**(142): p. 142ra97.
422. Stefanidou, M., et al., *Zinc: a multipurpose trace element*. Arch Toxicol, 2006. **80**(1): p. 1-9.
423. Wright, R.O. and A. Baccarelli, *Metals and neurotoxicology*. Journal of Nutrition, 2007. **137**(12): p. 2809-13.
424. Kroncke, K.D., *Cellular stress and intracellular zinc dyshomeostasis*. Arch Biochem Biophys, 2007. **463**(2): p. 183-7.
425. Thirumoorthy, N., et al., *A review of metallothionein isoforms and their role in pathophysiology*. World J Surg Oncol, 2011. **9**: p. 54.
426. Devirgiliis, C., et al., *Zinc fluxes and zinc transporter genes in chronic diseases*. Mutat Res, 2007. **622**(1-2): p. 84-93.
427. Eide, D.J., *The SLC39 family of metal ion transporters*. Pflugers Arch, 2004. **447**(5): p. 796-800.
428. Lichten, L.A. and R.J. Cousins, *Mammalian zinc transporters: nutritional and physiologic regulation*. Annual review of nutrition, 2009. **29**: p. 153-76.
429. Hill, G.M. and J.E. Link, *Transporters in the absorption and utilization of zinc and copper*. J Anim Sci, 2009. **87**(14 Suppl): p. E85-9.
430. Maret, W. and A. Krezel, *Cellular zinc and redox buffering capacity of metallothionein/thionein in health and disease*. Molecular medicine, 2007. **13**(7-8): p. 371-5.
431. Falcon-Perez, J.M. and E.C. Dell'Angelica, *Zinc transporter 2 (SLC30A2) can suppress the vesicular zinc defect of adaptor protein 3-depleted fibroblasts by promoting zinc accumulation in lysosomes*. Exp Cell Res, 2007. **313**(7): p. 1473-83.
432. Seo, Y.A. and S.L. Kelleher, *Functional analysis of two single nucleotide polymorphisms in SLC30A2 (ZnT2): implications for mammary gland function and breast disease in women*. Physiol Genomics, 2010. **42A**(4): p. 219-27.
433. Lopez, V. and S.L. Kelleher, *Zinc transporter-2 (ZnT2) variants are localized to distinct subcellular compartments and functionally transport zinc*. Biochem J, 2009. **422**(1): p. 43-52.
434. Palmiter, R.D. and L. Huang, *Efflux and compartmentalization of zinc by members of the SLC30 family of solute carriers*. Pflugers Archiv : European journal of physiology, 2004. **447**(5): p. 744-51.
435. Andrews, G.K., *Cellular zinc sensors: MTF-1 regulation of gene expression*. Biometals : an international journal on the role of metal ions in biology, biochemistry, and medicine, 2001. **14**(3-4): p. 223-37.
436. Laity, J.H. and G.K. Andrews, *Understanding the mechanisms of zinc-sensing by metal-response element binding transcription factor-1 (MTF-1)*. Arch Biochem Biophys, 2007. **463**(2): p. 201-10.
437. Vergarajauregui, S. and R. Puertollano, *Two di-leucine motifs regulate trafficking of mucolipin-1 to lysosomes*. Traffic, 2006. **7**(3): p. 337-53.
438. Miedel, M.T., et al., *Posttranslational cleavage and adaptor protein complex-dependent trafficking of mucolipin-1*. J Biol Chem, 2006. **281**(18): p. 12751-9.
439. Slaugenhaupt, S.A., et al., *Mapping of the mucolipidosis type IV gene to chromosome 19p and definition of founder haplotypes*. Am J Hum Genet, 1999. **65**(3): p. 773-8.

440. Colletti, G.A. and K. Kiselyov, *Trpml1*. Adv Exp Med Biol, 2011. **704**: p. 209-19.
441. Venugopal, B., et al., *Neurologic, gastric, and opthalmologic pathologies in a murine model of mucolipidosis type IV*. Am J Hum Genet, 2007. **81**(5): p. 1070-83.
442. Slaugenhaupt, S.A., *The molecular basis of mucolipidosis type IV*. Curr Mol Med, 2002. **2**(5): p. 445-50.
443. Colletti, G.A., et al., *Loss of Lysosomal Ion Channel Transient Receptor Potential Channel Mucolipin-1 (TRPML1) Leads to Cathepsin B-dependent Apoptosis*. J Biol Chem, 2012. **287**(11): p. 8082-91.
444. McCormick, N.H. and S.L. Kelleher, *ZnT4 provides zinc to zinc-dependent proteins in the trans-Golgi network critical for cell function and Zn export in mammary epithelial cells*. Am J Physiol Cell Physiol, 2012. **303**(3): p. C291-7.
445. McCormick, N., et al., *X-ray fluorescence microscopy reveals accumulation and secretion of discrete intracellular zinc pools in the lactating mouse mammary gland*. PLoS One, 2010. **5**(6): p. e11078.
446. Thirumoorthy, N., et al., *A review of metallothionein isoforms and their role in pathophysiology*. World journal of surgical oncology, 2011. **9**: p. 54.
447. Meeusen, J.W., et al., *TSQ (6-methoxy-8-p-toluenesulfonamido-quinoline), a common fluorescent sensor for cellular zinc, images zinc proteins*. Inorganic chemistry, 2011. **50**(16): p. 7563-73.
448. Meeusen, J.W., A. Nowakowski, and D.H. Petering, *Reaction of Metal-Binding Ligands with the Zinc Proteome: Zinc Sensors and N,N,N',N'-Tetrakis(2-pyridylmethyl)ethylenediamine*. Inorganic chemistry, 2012. **51**(6): p. 3625-32.
449. Palmiter, R.D., T.B. Cole, and S.D. Findley, *ZnT-2, a mammalian protein that confers resistance to zinc by facilitating vesicular sequestration*. The EMBO journal, 1996. **15**(8): p. 1784-91.
450. Falcon-Perez, J.M. and E.C. Dell'Angelica, *Zinc transporter 2 (SLC30A2) can suppress the vesicular zinc defect of adaptor protein 3-depleted fibroblasts by promoting zinc accumulation in lysosomes*. Experimental cell research, 2007. **313**(7): p. 1473-83.
451. Huang, L. and J. Gitschier, *A novel gene involved in zinc transport is deficient in the lethal milk mouse*. Nature genetics, 1997. **17**(3): p. 292-7.
452. Chimienti, F., et al., *In vivo expression and functional characterization of the zinc transporter ZnT8 in glucose-induced insulin secretion*. J Cell Sci, 2006. **119**(Pt 20): p. 4199-206.
453. Marciniak, J., et al., *Optimization of an enzymatic method for the determination of lysosomal N-acetyl-beta-D-hexosaminidase and beta-glucuronidase in synovial fluid*. Clinical chemistry and laboratory medicine : CCLM / FESCC, 2006. **44**(8): p. 933-7.
454. Lasry, I., et al., *A dominant negative heterozygous G87R mutation in the zinc transporter, ZnT-2 (SLC30A2), results in transient neonatal zinc deficiency*. J Biol Chem, 2012. **287**(35): p. 29348-61.
455. Cole, T.B., et al., *Seizures and neuronal damage in mice lacking vesicular zinc*. Epilepsy research, 2000. **39**(2): p. 153-69.
456. Knipp, M., et al., *Zn7metallothionein-3 and the synaptic vesicle cycle: interaction of metallothionein-3 with the small GTPase Rab3A*. Biochemistry, 2005. **44**(9): p. 3159-65.
457. Costello, L.C., C.C. Fenselau, and R.B. Franklin, *Evidence for operation of the direct zinc ligand exchange mechanism for trafficking, transport, and reactivity of zinc in mammalian cells*. Journal of inorganic biochemistry, 2011. **105**(5): p. 589-99.

458. Choi, D.W. and J.Y. Koh, *Zinc and brain injury*. Annual review of neuroscience, 1998. **21**: p. 347-75.
459. Cherny, R.A., et al., *Treatment with a copper-zinc chelator markedly and rapidly inhibits beta-amyloid accumulation in Alzheimer's disease transgenic mice*. Neuron, 2001. **30**(3): p. 665-76.
460. Kim, B.J., et al., *Zinc as a paracrine effector in pancreatic islet cell death*. Diabetes, 2000. **49**(3): p. 367-72.
461. Prasad, A.S., *Discovery of human zinc deficiency: its impact on human health and disease*. Advances in nutrition, 2013. **4**(2): p. 176-90.
462. Rink, L. and P. Gabriel, *Zinc and the immune system*. The Proceedings of the Nutrition Society, 2000. **59**(4): p. 541-52.
463. Jansen, J., W. Karges, and L. Rink, *Zinc and diabetes--clinical links and molecular mechanisms*. The Journal of nutritional biochemistry, 2009. **20**(6): p. 399-417.
464. Lee, J.Y., et al., *Contribution by synaptic zinc to the gender-disparate plaque formation in human Swedish mutant APP transgenic mice*. Proceedings of the National Academy of Sciences of the United States of America, 2002. **99**(11): p. 7705-10.
465. Rulon, L.L., et al., *Serum zinc levels and Alzheimer's disease*. Biological trace element research, 2000. **75**(1-3): p. 79-85.
466. Vinceti, M., et al., *Erythrocyte zinc, copper, and copper/zinc superoxide dismutase and risk of sporadic amyotrophic lateral sclerosis: a population-based case-control study*. Amyotrophic lateral sclerosis and other motor neuron disorders : official publication of the World Federation of Neurology, Research Group on Motor Neuron Diseases, 2002. **3**(4): p. 208-14.
467. Forsleff, L., et al., *Evidence of functional zinc deficiency in Parkinson's disease*. Journal of alternative and complementary medicine, 1999. **5**(1): p. 57-64.
468. Huang, L., C.P. Kirschke, and J. Gitschier, *Functional characterization of a novel mammalian zinc transporter, ZnT6*. The Journal of biological chemistry, 2002. **277**(29): p. 26389-95.
469. Kanninen, K.M., et al., *Altered biometal homeostasis is associated with CLN6 mRNA loss in mouse neuronal ceroid lipofuscinosis*. Biol Open, 2013. **2**(6): p. 635-46.
470. Lopez, V., F. Foolad, and S.L. Kelleher, *ZnT2-overexpression represses the cytotoxic effects of zinc hyper-accumulation in malignant metallothionein-null T47D breast tumor cells*. Cancer letters, 2011. **304**(1): p. 41-51.
471. Schissel, S.L., et al., *Zn2+-stimulated sphingomyelinase is secreted by many cell types and is a product of the acid sphingomyelinase gene*. The Journal of biological chemistry, 1996. **271**(31): p. 18431-6.
472. Kelleher, S.L., Y.A. Seo, and V. Lopez, *Mammary gland zinc metabolism: regulation and dysregulation*. Genes & nutrition, 2009. **4**(2): p. 83-94.
473. Kukic, I., et al., *Zinc-dependent lysosomal enlargement in TRPML1-deficient cells involves MTF-1 transcription factor and ZnT4 (Slc30a4) transporter*. The Biochemical journal, 2013. **451**(2): p. 155-63.
474. Lee, S.J. and J.Y. Koh, *Roles of zinc and metallothionein-3 in oxidative stress-induced lysosomal dysfunction, cell death, and autophagy in neurons and astrocytes*. Mol Brain, 2010. **3**(1): p. 30.

475. Cho, K.S., et al., *Induction of autophagy and cell death by tamoxifen in cultured retinal pigment epithelial and photoreceptor cells*. Investigative Ophthalmology & Visual Science, 2012. **53**(9): p. 5344-53.
476. Hwang, S.R. and V. Hook, *Zinc regulation of aminopeptidase B involved in neuropeptide production*. FEBS letters, 2008. **582**(17): p. 2527-31.
477. Hwang, J.J., et al., *Zinc(II) ion mediates tamoxifen-induced autophagy and cell death in MCF-7 breast cancer cell line*. Biometals : an international journal on the role of metal ions in biology, biochemistry, and medicine, 2010. **23**(6): p. 997-1013.
478. Lee, S.J., K.S. Cho, and J.Y. Koh, *Oxidative injury triggers autophagy in astrocytes: the role of endogenous zinc*. Glia, 2009. **57**(12): p. 1351-61.
479. Chung, H., et al., *Ethambutol-induced toxicity is mediated by zinc and lysosomal membrane permeabilization in cultured retinal cells*. Toxicology and applied pharmacology, 2009. **235**(2): p. 163-70.
480. Kelleher, S.L., et al., *Zinc in specialized secretory tissues: roles in the pancreas, prostate, and mammary gland*. Advances in nutrition, 2011. **2**(2): p. 101-11.
481. Martinez-Arca, S., et al., *Role of tetanus neurotoxin insensitive vesicle-associated membrane protein (TI-VAMP) in vesicular transport mediating neurite outgrowth*. The Journal of cell biology, 2000. **149**(4): p. 889-900.
482. Braun, V., et al., *TI-VAMP/VAMP7 is required for optimal phagocytosis of opsonised particles in macrophages*. The EMBO journal, 2004. **23**(21): p. 4166-76.
483. Heming, T.A., et al., *Effects of bafilomycin A1 on cytosolic pH of sheep alveolar and peritoneal macrophages: evaluation of the pH-regulatory role of plasma membrane V-ATPases*. The Journal of experimental biology, 1995. **198**(Pt 8): p. 1711-5.
484. Kiedrowski, L., *Cytosolic acidification and intracellular zinc release in hippocampal neurons*. Journal of neurochemistry, 2012. **121**(3): p. 438-50.
485. Jiang, L.J., et al., *Zinc transfer potentials of the alpha - and beta-clusters of metallothionein are affected by domain interactions in the whole molecule*. Proceedings of the National Academy of Sciences of the United States of America, 2000. **97**(6): p. 2503-8.
486. Saydam, N., et al., *Regulation of metallothionein transcription by the metal-responsive transcription factor MTF-1: identification of signal transduction cascades that control metal-inducible transcription*. The Journal of biological chemistry, 2002. **277**(23): p. 20438-45.
487. Medvedeva, Y.V., et al., *Intracellular Zn2+ accumulation contributes to synaptic failure, mitochondrial depolarization, and cell death in an acute slice oxygen-glucose deprivation model of ischemia*. The Journal of neuroscience : the official journal of the Society for Neuroscience, 2009. **29**(4): p. 1105-14.
488. Fraldi, A., et al., *Lysosomal fusion and SNARE function are impaired by cholesterol accumulation in lysosomal storage disorders*. The EMBO journal, 2010. **29**(21): p. 3607-20.
489. Pastore, N., A. Ballabio, and N. Brunetti-Pierri, *Autophagy master regulator TFEB induces clearance of toxic SERPINA1/alpha-1-antitrypsin polymers*. Autophagy, 2013. **9**(7): p. 1094-6.
490. Decressac, M., et al., *TFEB-mediated autophagy rescues midbrain dopamine neurons from alpha-synuclein toxicity*. Proceedings of the National Academy of Sciences of the United States of America, 2013. **110**(19): p. E1817-26.

491. Flannery, A.R., C. Czibener, and N.W. Andrews, *Palmitoylation-dependent association with CD63 targets the Ca2+ sensor synaptotagmin VII to lysosomes*. The Journal of cell biology, 2010. **191**(3): p. 599-613.
492. !!! INVALID CITATION !!!
493. Settembre, C., et al., *Signals from the lysosome: a control centre for cellular clearance and energy metabolism*. Nature reviews. Molecular cell biology, 2013. **14**(5): p. 283-96.
494. Yoon, Y.H., et al., *Induction of lysosomal dilatation, arrested autophagy, and cell death by chloroquine in cultured ARPE-19 cells*. Investigative Ophthalmology & Visual Science, 2010. **51**(11): p. 6030-7.
495. Tang, Z.L., et al., *Nitric oxide decreases the sensitivity of pulmonary endothelial cells to LPS-induced apoptosis in a zinc-dependent fashion*. Molecular and cellular biochemistry, 2002. **234-235**(1-2): p. 211-7.
496. Suntres, Z.E. and E.M. Lui, *Antioxidant effect of zinc and zinc-metallothionein in the acute cytotoxicity of hydrogen peroxide in Ehrlich ascites tumour cells*. Chemico-biological interactions, 2006. **162**(1): p. 11-23.
497. Aydemir, T.B., et al., *Zinc transporter ZIP8 (SLC39A8) and zinc influence IFN-gamma expression in activated human T cells*. Journal of leukocyte biology, 2009. **86**(2): p. 337-48.
498. Berg, J.M. and Y. Shi, *The galvanization of biology: a growing appreciation for the roles of zinc*. Science, 1996. **271**(5252): p. 1081-5.
499. McCormick, N.H., et al., *The biology of zinc transport in mammary epithelial cells: implications for mammary gland development, lactation, and involution*. J Mammary Gland Biol Neoplasia, 2014. **19**(1): p. 59-71.
500. Dempsey, C., et al., *Marginal maternal zinc deficiency in lactating mice reduces secretory capacity and alters milk composition*. J Nutr, 2012. **142**(4): p. 655-60.
501. Lopez, V. and S.L. Kelleher, *Zip6-attenuation promotes epithelial-to-mesenchymal transition in ductal breast tumor (T47D) cells*. Exp Cell Res, 2010. **316**(3): p. 366-75.
502. Hogstrand, C., et al., *A mechanism for epithelial-mesenchymal transition and anoikis resistance in breast cancer triggered by zinc channel ZIP6 and STAT3 (signal transducer and activator of transcription 3)*. Biochem J, 2013. **455**(2): p. 229-37.
503. Lefebvre, D., et al., *Inhibition of insulin-like growth factor-I mitogenic action by zinc chelation is associated with a decreased mitogen-activated protein kinase activation in RAT-1 fibroblasts*. FEBS Lett, 1999. **449**(2-3): p. 284-8.
504. Hansson, A., *Extracellular zinc ions induces mitogen-activated protein kinase activity and protein tyrosine phosphorylation in bombesin-sensitive Swiss 3T3 fibroblasts*. Arch Biochem Biophys, 1996. **328**(2): p. 233-8.
505. Parker, P.J., et al., *The complete primary structure of protein kinase C--the major phorbol ester receptor*. Science, 1986. **233**(4766): p. 853-9.
506. Csermely, P., et al., *Zinc can increase the activity of protein kinase C and contributes to its binding to plasma membranes in T lymphocytes*. J Biol Chem, 1988. **263**(14): p. 6487-90.
507. Seo, Y.A., V. Lopez, and S.L. Kelleher, *A histidine-rich motif mediates mitochondrial localization of ZnT2 to modulate mitochondrial function*. Am J Physiol Cell Physiol, 2011. **300**(6): p. C1479-89.

508. Chowanadisai, W., B. Lonnerdal, and S.L. Kelleher, *Identification of a mutation in SLC30A2 (ZnT-2) in women with low milk zinc concentration that results in transient neonatal zinc deficiency*. J Biol Chem, 2006. **281**(51): p. 39699-707.
509. Watson, C.J., *Involution: apoptosis and tissue remodelling that convert the mammary gland from milk factory to a quiescent organ*. Breast Cancer Res, 2006. **8**(2): p. 203.
510. Chandra, M., et al., *A role for the Ca2+ channel TRPML1 in gastric acid secretion, based on analysis of knockout mice*. Gastroenterology, 2011. **140**(3): p. 857-67.
511. Micsenyi, M.C., Dobrenis, K., Stephney, G., Pickel, J., Vanier, M.T., Slaugenhaupt, S.A., Walkley, S.U., *Neuropathology of the Mcoln1-/- Knockout Mouse Model of Mucolipidosis Type IV*. J Neuropathol Exp Neurol, 2009. **68**(2): p. 125-135.
512. Bonavita, S., et al., *Diffuse neuroaxonal involvement in mucolipidosis IV as assessed by proton magnetic resonance spectroscopic imaging*. J Child Neurol, 2003. **18**(7): p. 443-9.
513. Smith, J.A., et al., *Noninvasive diagnosis and ophthalmic features of mucolipidosis type IV*. Ophthalmology, 2002. **109**(3): p. 588-94.
514. Kiselyov, K. and S. Muallem, *Mitochondrial Ca(2+) homeostasis in lysosomal storage diseases*. Cell Calcium, 2008. **44**(1): p. 103-11.
515. Kiselyov, K., et al., *Autophagy, mitochondria and cell death in lysosomal storage diseases*. Autophagy, 2007. **3**(3): p. 259-62.
516. Jennings, J.J., Jr., et al., *Mitochondrial aberrations in mucolipidosis Type IV*. J Biol Chem, 2006. **281**(51): p. 39041-50.
517. Takamura, A., et al., *Enhanced autophagy and mitochondrial aberrations in murine G(M1)-gangliosidosis*. Biochem Biophys Res Commun, 2008. **367**(3): p. 616-22.
518. Duchen, M.R., A. Verkhratsky, and S. Muallem, *Mitochondria and calcium in health and disease*. Cell Calcium, 2008. **44**(1): p. 1-5.
519. Knott, A.B., et al., *Mitochondrial fragmentation in neurodegeneration*. Nature reviews. Neuroscience, 2008. **9**(7): p. 505-18.
520. Kagan, V.E., et al., *The "pro-apoptotic genies" get out of mitochondria: oxidative lipidomics and redox activity of cytochrome c/cardiolipin complexes*. Chem Biol Interact, 2006. **163**(1-2): p. 15-28.
521. Orrenius, S., *Mitochondrial regulation of apoptotic cell death*. Toxicol Lett, 2004. **149**(1-3): p. 19-23.
522. Nomura, M., et al., *Apoptotic cytosol facilitates Bax translocation to mitochondria that involves cytosolic factor regulated by Bcl-2*. Cancer Research, 1999. **59**(21): p. 5542-8.
523. Polster, B.M. and G. Fiskum, *Mitochondrial mechanisms of neural cell apoptosis*. J Neurochem, 2004. **90**(6): p. 1281-9.
524. Levy, C.S., et al., *Tumor necrosis factor alpha induces LIF expression through ERK1/2 activation in mammary epithelial cells*. J Cell Biochem, 2010. **110**(4): p. 857-65.
525. Yu, T.C., et al., *Involvement of TNF-alpha and MAPK pathway in the intramammary MMP-9 release via degranulation of cow neutrophils during acute mammary gland involution*. Vet Immunol Immunopathol, 2012. **147**(3-4): p. 161-9.
526. Besecker, B., et al., *The human zinc transporter SLC39A8 (Zip8) is critical in zinc-mediated cytoprotection in lung epithelia*. Am J Physiol Lung Cell Mol Physiol, 2008. **294**(6): p. L1127-36.
527. Sensi, S.L., et al., *Zinc in the physiology and pathology of the CNS*. Nature reviews. Neuroscience, 2009. **10**(11): p. 780-91.

528. Sensi, S.L., H.Z. Yin, and J.H. Weiss, *AMPA/kainate receptor-triggered Zn2+ entry into cortical neurons induces mitochondrial Zn2+ uptake and persistent mitochondrial dysfunction*. The European journal of neuroscience, 2000. **12**(10): p. 3813-8.
529. Dineley, K.E., et al., *Zinc causes loss of membrane potential and elevates reactive oxygen species in rat brain mitochondria*. Mitochondrion, 2005. **5**(1): p. 55-65.
530. Sensi, S.L., et al., *Preferential Zn2+ influx through Ca2+-permeable AMPA/kainate channels triggers prolonged mitochondrial superoxide production*. Proc Natl Acad Sci U S A, 1999. **96**(5): p. 2414-9.
531. Coblentz, J., C. St Croix, and K. Kiselyov, *Loss of TRPML1 promotes production of reactive oxygen species: is oxidative damage a factor in mucolipidosis type IV?* Biochem J, 2014. **457**(2): p. 361-8.
532. Liu, M.J., et al., *ZIP8 regulates host defense through zinc-mediated inhibition of NF-kappaB*. Cell Rep, 2013. **3**(2): p. 386-400.
533. Beyersmann, D. and H. Haase, *Functions of zinc in signaling, proliferation and differentiation of mammalian cells*. Biometals, 2001. **14**(3-4): p. 331-41.
534. Varea, E., et al., *Capture of extracellular zinc ions by astrocytes*. Glia, 2006. **54**(4): p. 304-15.
535. Ballestin, R., et al., *Ethanol reduces zincosome formation in cultured astrocytes*. Alcohol Alcohol, 2011. **46**(1): p. 17-25.
536. Devirgiliis, C., et al., *Exchangeable zinc ions transiently accumulate in a vesicular compartment in the yeast Saccharomyces cerevisiae*. Biochem Biophys Res Commun, 2004. **323**(1): p. 58-64.
537. Chai, F., et al., *Regulation of caspase activation and apoptosis by cellular zinc fluxes and zinc deprivation: A review*. Immunol Cell Biol, 1999. **77**(3): p. 272-8.
538. Shen, D., et al., *Lipid storage disorders block lysosomal trafficking by inhibiting a TRP channel and lysosomal calcium release*. Nat Commun, 2012. **3**: p. 731.
539. St Croix, C.M., et al., *Fluorescence resonance energy transfer-based assays for the real-time detection of nitric oxide signaling*. Methods Enzymol, 2005. **396**: p. 317-26.
540. Pearce, L.L., et al., *Role of metallothionein in nitric oxide signaling as revealed by a green fluorescent fusion protein*. Proc Natl Acad Sci U S A, 2000. **97**(1): p. 477-82.
541. Dong, X.P., et al., *Activating mutations of the TRPML1 channel revealed by proline-scanning mutagenesis*. J Biol Chem, 2009. **284**(46): p. 32040-52.
542. Zhang, Y., R.M. Gonzalez, and R.C. Zangar, *Protein secretion in human mammary epithelial cells following HER1 receptor activation: influence of HER2 and HER3 expression*. BMC Cancer, 2011. **11**: p. 69.
543. Reddy, J.V., I.G. Ganley, and S.R. Pfeffer, *Clues to neuro-degeneration in Niemann-Pick type C disease from global gene expression profiling*. PLoS One, 2006. **1**: p. e19.
544. De Windt, A., et al., *Gene set enrichment analyses revealed several affected pathways in Niemann-pick disease type C fibroblasts*. DNA Cell Biol, 2007. **26**(9): p. 665-71.
545. Abe, T., et al., *Serum Zn(2+)-stimulated sphingomyelinase deficiency in type B Niemann-Pick disease*. Eur J Pediatr, 1999. **158**(11): p. 953.
546. van Langevelde, F., et al., *Copper and zinc metabolism in aspartylglycosaminuria and Salla disease*. Sci Total Environ, 1985. **42**(1-2): p. 171-80.
547. Kanninen, K.M., et al., *Increased zinc and manganese in parallel with neurodegeneration, synaptic protein changes and activation of Akt/GSK3 signaling in ovine CLN6 neuronal ceroid lipofuscinosis*. PLoS One, 2013. **8**(3): p. e58644.

548. Lee, J.Y., et al., *Alteration of the cerebral zinc pool in a mouse model of Alzheimer disease*. J Neuropathol Exp Neurol, 2012. **71**(3): p. 211-22.
549. Park, J.S., et al., *Parkinson's disease-associated human ATP13A2 (PARK9) deficiency causes zinc dyshomeostasis and mitochondrial dysfunction*. Hum Mol Genet, 2014.
550. Kong, S.M., et al., *Parkinson's disease-linked human PARK9/ATP13A2 maintains zinc homeostasis and promotes alpha-Synuclein externalization via exosomes*. Hum Mol Genet, 2014.
551. Yamaguchi, M., T. Yoshino, and S. Okada, *Effect of zinc on the acidity of gastric secretion in rats*. Toxicol Appl Pharmacol, 1980. **54**(3): p. 526-30.
552. McLeay, L.M. and B.L. Smith, *Effects of intraruminal administration of zinc on gastric acid secretion in sheep*. Res Vet Sci, 1977. **23**(2): p. 243-5.
553. Almeida-Vega, S., et al., *Gastrin activates paracrine networks leading to induction of PAI-2 via MAZ and ASC-1*. Am J Physiol Gastrointest Liver Physiol, 2009. **296**(2): p. G414-23.
554. Parekh, A.B., *Ca2+ microdomains near plasma membrane Ca2+ channels: impact on cell function*. J Physiol, 2008. **586**(13): p. 3043-54.
555. Worley, P.F., et al., *Homer proteins in Ca2+ signaling by excitable and non-excitable cells*. Cell Calcium, 2007. **42**(4-5): p. 363-71.
556. Xiao, B., J.C. Tu, and P.F. Worley, *Homer: a link between neural activity and glutamate receptor function*. Curr Opin Neurobiol, 2000. **10**(3): p. 370-4.
557. Xiao, B., et al., *Homer regulates the association of group 1 metabotropic glutamate receptors with multivalent complexes of homer-related, synaptic proteins*. Neuron, 1998. **21**(4): p. 707-16.
558. Hodgkin, A.L. and A.F. Huxley, *A quantitative description of membrane current and its application to conduction and excitation in nerve*. J Physiol, 1952. **117**(4): p. 500-44.
559. Kiselyov, K., et al., *Calcium signaling complexes in microdomains of polarized secretory cells*. Cell Calcium, 2006. **40**(5-6): p. 451-9.
560. Tsunoda, S., et al., *A multivalent PDZ-domain protein assembles signalling complexes in a G-protein-coupled cascade*. Nature, 1997. **388**(6639): p. 243-9.
561. Li, H.S. and C. Montell, *TRP and the PDZ protein, INAD, form the core complex required for retention of the signalplex in Drosophila photoreceptor cells*. J Cell Biol, 2000. **150**(6): p. 1411-22.
562. Matza, D., et al., *A scaffold protein, AHNAK1, is required for calcium signaling during T cell activation*. Immunity, 2008. **28**(1): p. 64-74.
563. Ren, J.G., Z. Li, and D.B. Sacks, *IQGAP1 integrates Ca2+/calmodulin and B-Raf signaling*. J Biol Chem, 2008. **283**(34): p. 22972-82.
564. Kim, J.Y., et al., *Homer 1 mediates store- and inositol 1,4,5-trisphosphate receptor-dependent translocation and retrieval of TRPC3 to the plasma membrane*. J Biol Chem, 2006. **281**(43): p. 32540-9.
565. Ryglewski, S., H.J. Pflueger, and C. Duch, *Expanding the neuron's calcium signaling repertoire: intracellular calcium release via voltage-induced PLC and IP3R activation*. PLoS Biol, 2007. **5**(4): p. e66.
566. Bramham, C.R., et al., *The immediate early gene arc/arg3.1: regulation, mechanisms, and function*. J Neurosci, 2008. **28**(46): p. 11760-7.
567. Brakeman, P.R., et al., *Homer: a protein that selectively binds metabotropic glutamate receptors*. Nature, 1997. **386**(6622): p. 284-8.

568. Klugmann, M., et al., *AAV-mediated hippocampal expression of short and long Homer 1 proteins differentially affect cognition and seizure activity in adult rats*. Mol Cell Neurosci, 2005. **28**(2): p. 347-60.
569. Yuan, J.P., et al., *Homer binds TRPC family channels and is required for gating of TRPC1 by IP3 receptors*. Cell, 2003. **114**(6): p. 777-89.
570. Ciruela, F., M.M. Soloviev, and R.A. McIlhinney, *Co-expression of metabotropic glutamate receptor type 1alpha with homer-1a/Vesl-1S increases the cell surface expression of the receptor*. Biochem J, 1999. **341 (Pt 3)**: p. 795-803.
571. Kato, A., et al., *Novel members of the Vesl/Homer family of PDZ proteins that bind metabotropic glutamate receptors*. J Biol Chem, 1998. **273**(37): p. 23969-75.
572. Saito, H., et al., *An N-terminal sequence specific for a novel Homer1 isoform controls trafficking of group I metabotropic glutamate receptor in mammalian cells*. Biochem Biophys Res Commun, 2002. **296**(3): p. 523-9.
573. Shiraishi-Yamaguchi, Y. and T. Furuichi, *The Homer family proteins*. Genome Biol, 2007. **8**(2): p. 206.
574. Szumlinski, K.K., et al., *Homer proteins regulate sensitivity to cocaine*. Neuron, 2004. **43**(3): p. 401-13.
575. Soloviev, M.M., et al., *Molecular characterisation of two structurally distinct groups of human homers, generated by extensive alternative splicing*. J Mol Biol, 2000. **295**(5): p. 1185-200.
576. Soloviev, M.M., et al., *Mouse brain and muscle tissues constitutively express high levels of Homer proteins*. Eur J Biochem, 2000. **267**(3): p. 634-9.
577. Putney, J.W., *Capacitative calcium entry: from concept to molecules*. Immunol Rev, 2009. **231**(1): p. 10-22.
578. Parekh, A.B., *Functional consequences of activating store-operated CRAC channels*. Cell Calcium, 2007. **42**(2): p. 111-21.
579. Liao, Y., et al., *Orai proteins interact with TRPC channels and confer responsiveness to store depletion*. Proc Natl Acad Sci U S A, 2007. **104**(11): p. 4682-7.
580. Li, Q., J.A. Lee, and D.L. Black, *Neuronal regulation of alternative pre-mRNA splicing*. Nat Rev Neurosci, 2007. **8**(11): p. 819-31.
581. Stoilov, P., et al., *Human tra2-beta1 autoregulates its protein concentration by influencing alternative splicing of its pre-mRNA*. Hum Mol Genet, 2004. **13**(5): p. 509-24.
582. Daoud, R., et al., *Ischemia induces a translocation of the splicing factor tra2-beta 1 and changes alternative splicing patterns in the brain*. J Neurosci, 2002. **22**(14): p. 5889-99.